MISSOURI S&T

CENTER FOR TRANSPORTATION INFRASTRUCTURE AND SAFETY

NONDESTRUCTIVE EVALUATION OF MODOT BRIDGE DECKS – PILOT STUDY

by

Lesley Sneed, Ph.D., PE
Assistant Professor
Department of Civil, Architectural & Environmental Engineering
Missouri University of Science and Technology

Neil Anderson Ph.D.
Professor
Department of Geological Sciences & Engineering
Missouri University of Science and Technology

Evgeniy Torgashov, Ph.D.
Research Associate
Department of Geological Sciences & Engineering
Missouri University of Science and Technology

A National University Transportation Center at Missouri University of Science and Technology

Disclaimer

The contents of this report reflect the views of the author(s), who are responsible for the facts and the accuracy of information presented herein. This document is disseminated under the sponsorship of the Department of Transportation, University Transportation Centers Program and the Center for Transportation Infrastructure and Safety NUTC program at the Missouri University of Science and Technology, in the interest of information exchange. The U.S. Government and Center for Transportation Infrastructure and Safety assumes no liability for the contents or use thereof.

Technical Report Documentation Page

1. Report No.	2. Government Accession No.	3. Recipient's Catalog No.
NUTC R311		

4. Title and Subtitle	5. Report Date
Nondestructive Evaluation Of Modot Bridge Decks – Pilot Study	March 2014
	6. Performing Organization Code

7. Author/s	8. Performing Organization Report No.
Lesley Sneed, Neil Anderson, Evgeniy Torgashov	Project #00040085

9. Performing Organization Name and Address	10. Work Unit No. (TRAIS)
Center for Transportation Infrastructure and Safety/NUTC program Missouri University of Science and Technology 220 Engineering Research Lab Rolla, MO 65409	11. Contract or Grant No. DTRT06-G-0014

12. Sponsoring Organization Name and Address	13. Type of Report and Period Covered
U.S. Department of Transportation Research and Innovative Technology Administration 1200 New Jersey Avenue, SE Washington, DC 20590	Final
	14. Sponsoring Agency Code

15. Supplementary Notes

16. Abstract

This research has examined the use of nondestructive techniques for concrete bridge deck condition assessments. The primary nondestructive testing/evaluation (NDT/NDE) technique utilized in this research was ground-coupled ground penetrating radar (GPR). The objectives of this research were to examine the utility of the nondestructive techniques in evaluating the condition of MoDOT bridge decks to enable faster, better, and more cost-effective bridge deck assessments, and to determine the accuracy of the information provided.Eleven bridge decks were investigated using detailed visual inspections, GPR, portable seismic property analyzer (PSPA), core extraction, and chloride ion concentration measurements. The cores underwent a detailed visual evaluation and testing to determine the volume of permeable pore space. Data sets were compared to determine correlations between the results. Three of the bridge decks investigated underwent rehabilitation by hydrodemolition after the initial investigation, and concrete material removal was surveyed using lidar to evaluate the NDE estimations. Good correlation was observed qualitatively. Areas of the decks where the GPR interpretations indicated evidence of extensive deterioration generally corresponded to areas with greater concrete material removal depths after hydrodemolition, and areas where the GPR interpretations indicated no evidence of deterioration generally corresponded to areas with minimal concrete removal. Findings suggest that the correlation between the GPR interpretations and concrete removal depths can be improved quantitatively by adjusting the GPR threshold values used in the interpretation, although the major challenge will be to understand how to determine the threshold values without having the benefit of the control data. Finally, recommended parameters are provided for ground-coupled GPR data acquisition, processing, and interpretation.

17. Key Words	18. Distribution Statement
Bridge Evaluation, Deck, GPR, Ground Penetrating Radar, NDE, Nondestructive evaluation, NDT, Nondestructive testing	No restrictions. This document is available to the public through the National Technical Information Service, Springfield, Virginia 22161.

19. Security Classification (of this report)	20. Security Classification (of this page)	21. No. Of Pages	22. Price
unclassified	unclassified	193	

Form DOT F 1700.7 (8-72)

EXECUTIVE SUMMARY

This study investigated the use of nondestructive techniques for bridge deck condition assessments. The primary nondestructive testing/evaluation (NDT/NDE) technique utilized in this study was ground-coupled ground penetrating radar (GPR). The use of a portable seismic property analyzer (PSPA) was also investigated. Eleven bridge decks were investigated using detailed visual inspections, GPR, PSPA, core extraction, and chloride ion concentration measurements. The cores underwent a detailed visual evaluation and testing to determine the volume of permeable pore space. Data sets were compared to determine correlations between the results.

Ground-coupled GPR responds to the presence of saline moisture in a bridge deck and can be used to identify areas of a bridge deck where there is a high probability that incipient to extensive concrete deterioration has occurred. Ground-coupled GPR is a useful tool for estimating areas of a bridge deck that are in good condition, fair condition, and poor condition. GPR interpretations of the top reinforcement reflection amplitude showed a strong correlation with visual assessment results in areas where visual deterioration was noted. A fair to good correlation was observed between the GPR data and the visual core evaluation results. A higher degree of correlation can be anticipated in areas where the concrete cores are visibly deteriorated; a lower degree of correlation can be expected in areas where the concrete cores do not exhibit signs of deterioration. Cores with higher volume of permeable core space generally had a lower visual core rating.

Three of the bridge decks investigated underwent rehabilitation by hydrodemolition after the initial investigation, and concrete material removal was surveyed using lidar to evaluate the NDE estimations. Areas of the decks where the GPR interpretations indicated evidence of extensive deterioration generally corresponded to areas with greater concrete material removal depths after hydrodemolition. Similarly, areas where the GPR interpretations indicated moderate or no evidence of deterioration generally corresponded to areas with lesser material removal depths. Apparent discrepancies between the GPR interpretations and the concrete removal depths can be attributed to several factors, including the fact that GPR responds to the presence of saline moisture in the deck, whereas rehabilitation removes weaker concrete. Also, GPR interpretations presented in this study are based on the reflection amplitude from the top transverse layer of reinforcement and do not represent the condition of the concrete below the top transverse reinforcement. Findings suggest that the correlation between the GPR interpretations and concrete removal depths can be improved by adjusting the GPR threshold values used in the interpretation, although the major challenge is to understand how to determine the threshold values a priori, without having the benefit of the control data.

This research was performed by the Missouri University of Science and Technology. The report fully documents the research

AUTHOR ACKNOWLEDGEMENTS

The research reported herein was sponsored by the Missouri Department of Transportation (MoDOT) and the National University Transportation Center (NUTC) at the Missouri University of Science and Technology (Missouri S&T). The research was performed by Missouri S&T. At Missouri S&T, the principal investigator was Lesley Sneed, and the co-principal investigators were Neil Anderson and William Schonberg. The principal investigator for the lidar work was Norbert Maerz. Major contributions to the project were made by Evgeniy Torgashov, Ken Boyko, Brandon Goodwin, Aleksey Khamzin, Mengxing Li, and Aleksandra Varnavina. The assistance of each of these individuals is gratefully acknowledged.

TABLE OF CONTENTS

LIST OF FIGURES

LIST OF TABLES

1 INTRODUCTION

1.1 Project Goal

The overarching goal of this pilot study was to demonstrate proof of concept that advanced nondestructive testing/evaluation (NDT/NDE) techniques can be rapidly, effectively, and economically implemented as part of MoDOT bridge deck surveys to improve the overall quality and cost of bridge deck evaluations.

Results of this pilot study will be used to evaluate the feasibility of a large scale, long-term program (multi-year, routine basis) that incorporates NDE techniques into MoDOT bridge deck surveys for the purpose of reducing cost of assessment and maintenance of bridge decks.

1.2 Project Objectives

The primary objectives of this project were to:

- Demonstrate the utility of the GPR tool in evaluating the condition of MoDOT bridge decks and confirm that this noninvasive method can be implemented as a part of a long-term program that enables faster, better, and more cost-effective bridge deck assessments; and
- Explore, compare, and contrast other existing and emerging noninvasive imaging technologies in terms of accuracy and information provided in evaluating the existing condition of bridge decks.

1.3 Scope of Work

Twelve field investigations of 11 different bridge decks took place as a part of this study. For each of the 11 bridge decks, the following work was performed:

- A thorough visual investigation of the top surface of the bridge deck.
- GPR scans using a GSSI 1.5 GHz antenna. GPR profile spacing varied from bridge to bridge.
- Collection of PSPA data on select regions of each bridge deck and, where possible, over core locations prior to core extraction.
- Extraction of cores from the bridge deck. The number of cores extracted from each deck varied, with limits set by MoDOT of one core per lane per span. All cores were 2 in. in diameter and varied in length.
- Careful visual evaluation of all extracted cores. Noted characteristics included length, material, location and causes of fracture planes, cracks, voids, aggregate and paste proportions, air entrainment, and discolorations.
- Chloride ion concentration measurements at select core locations.

In addition to these investigations, additional investigations were conducted on three of the bridge decks. This work included:

- Surveying of material removal depths during the rehabilitation process, which utilized hydrodemolition as a method of material removal. Light detection and ranging (lidar) was used to determine the locations and depths of material removal.

The bridges that were investigated were selected by MoDOT and researchers from Missouri S&T. Bridges investigated and dates of investigation are summarized in Table 1-1, and the locations of the bridges investigated are shown in Figure 1-1. Bridges are listed in numerical order throughout this report.

Table 1-1 Summary of Bridges Investigated

Bridge	Date of Investigation	Weather Conditions	Dates of Rehabilitation
A0569	11/26/2012	26-46° F, absence of rain	-
A1187 – 1st Scan	09/16/2012	60-76° F, absence of rain	-
A1187 – 2nd Scan	05/19/2013	69-89° F, rain	-
A1193	11/07/2012	40-50° F, absence of rain	May - September 2013
A1297	10/24/2012	68-82° F, absence of rain	May - September 2013
A1479	11/08/2012	32-64° F, absence of rain	March - May 2013
A2111	05/23/2013	53-65° F, absence of rain	-
A2966	10/17/2012	60-70° F, absence of rain	-
A3017	06/06/2013	62-75° F, absence of rain	-
A3405	11/14/2012	31-52° F, absence of rain	-
A3406	11/15/2012	30-55° F, absence of rain	-
K0197	11/28/2012	30-40° F, absence of rain	-

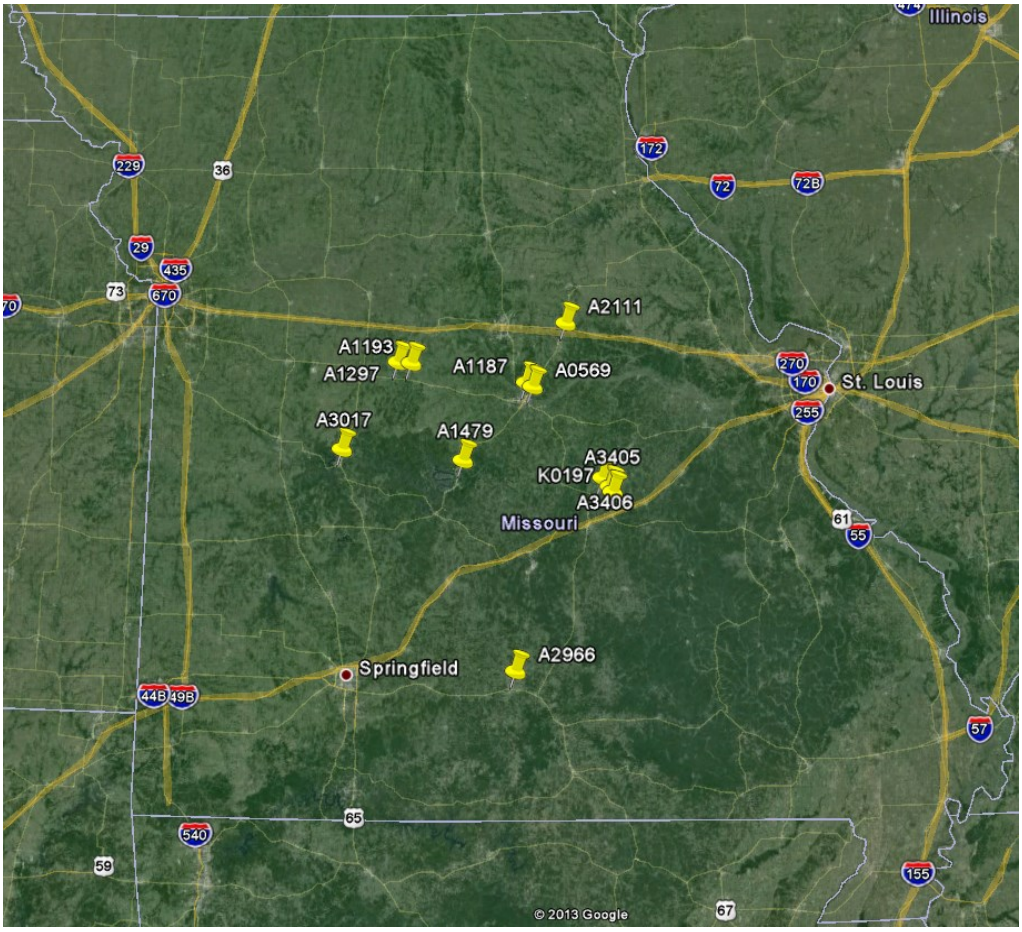

Figure 1-1 Map of Bridge Locations (Source: Google Earth)

1.4 Organization of the Report

Chapter 1 presents the goal, objectives, and scope of this project. Chapter 2 includes a description of each bridge investigated in this project. Chapter 3 summarizes the results of the visual assessments for each bridge deck. Chapters 4, 5, and 6 discuss destructive testing results, namely from core assessments, chloride ion concentration measurements, and survey of deck rehabilitation, respectively. Chapters 7 and 8 present and discuss the results of the nondestructive testing techniques utilized in this project, namely GPR and PSPA, respectively. Section 7.5 includes recommended parameters for GPR data acquisition, processing, and interpretation. Finally, Chapter 9 summarizes the results and recommendations based on the findings of this project. Maps of the results are provided in electronic format in the Digital Appendix of this report (see Appendix A).

1.5 Links to Report Sections on Individual Bridge Decks

Electronic links to specific sections in this report pertaining to individual bridge decks are included below as hyperlinks in Table 1-2.

Table 1-2 Links to Report Sections

Bridge	Bridge Deck Description	Visual Assessment Results	Core Results	Chloride Ion Concentration Results	Deck Rehabilitation Results	GPR Results	PSPA Results
A0569	2.2.1	3.2.1	4.2.1	5.2.1	-	7.3.1	-
A1187	2.2.2	3.2.2	4.2.2	5.2.2	-	7.3.2	-
A1193	2.2.3	3.2.3	4.2.3	5.2.3	6.2.1	7.3.3	8.4.1
A1297	2.2.4	3.2.4	4.2.4	5.2.4	6.2.2	7.3.4	8.4.2
A1479	2.2.5	3.2.5	4.2.5	5.2.5	6.2.3	7.3.5	8.4.3
A2111	2.2.6	3.2.6	4.2.6	5.2.6	-	7.3.6	-
A2966	2.2.7	3.2.7	4.2.7	5.2.7	-	7.3.7	-
A3017	2.2.8	3.2.8	4.2.8	5.2.8	-	7.3.8	-
A3405	2.2.9	3.2.9	4.2.9	5.2.9	-	7.3.9	-
A3406	2.2.10	3.2.10	4.2.10	5.2.10	-	7.3.10	-
K0197	2.2.11	3.2.11	4.2.11	5.2.11	-	7.3.11	-

2 BRIDGE DECK INFORMATION

2.1 Methodology

Prior to conducting the field investigations, the as-built drawings, Structural Inventory and Appraisal Sheets, and inspection history for each bridge deck were provided to the researchers by MoDOT and were reviewed. Comprehensive computer aided design (CAD) drawings of each bridge deck were created using as-built drawings provided by MoDOT. The base map drawings include important structural elements of each bridge, including bents, main support beams, deck outline, and deck reinforcement (top mat), along with the curb and barrier wall as illustrated in Figure 2-1. After the investigation of each bridge was completed, these base maps were used to display data collected during the field investigations. Information placed on these drawings included visual defects (Chapter 3), core locations (Chapter 4), GPR reflection amplitude maps based on the top reinforcing bar in the transverse bridge direction (Chapter 7), and PSPA modulus values (Chapter 8). For the three bridges that underwent rehabilitation (A1193, A1297, and A1479), the depth of material removal maps were also incorporated into the CAD drawing (Chapter 6). Parts of each drawing are presented throughout this report, however complete digital versions are available in the Digital Appendix as discussed in Appendix A. The digital version of each drawing allows for layers to be turned on or off so specific details of the bridge can be viewed.

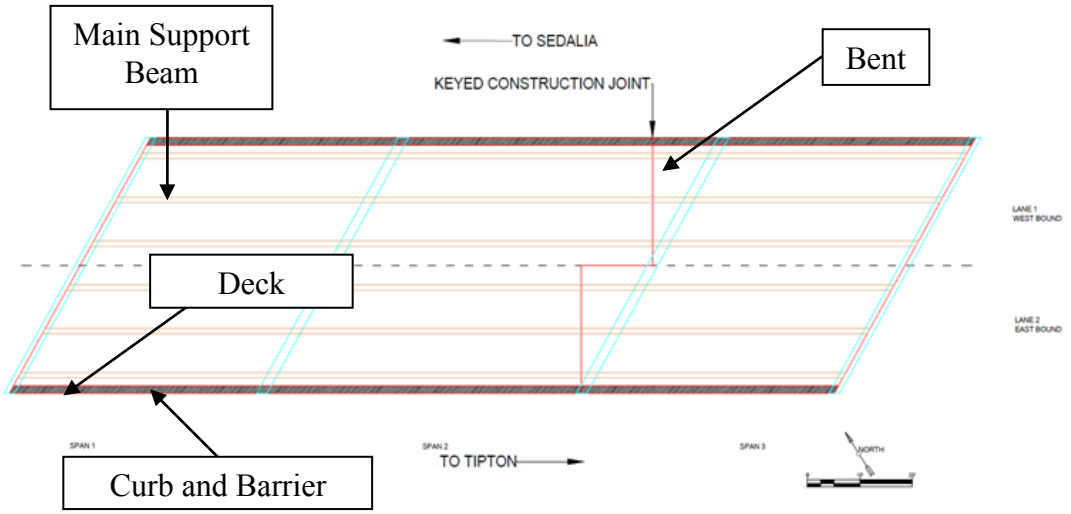

Figure 2-1 Sample Base Map CAD Drawing

2.2 Bridge Deck Descriptions

This section includes details of each bridge investigated. AADT values reported in this section are based on values recorded for 2011. Typical cross sectional drawings of each bridge deck are included. In the drawings, cross section A-A is the longitudinal cross section of the bridge deck (parallel to the orientation of GPR profiles), B-B is the cross section of the bridge deck perpendicular to traffic flow (transverse direction), and C-C is the cross section of the bridge deck perpendicular to traffic flow in areas where extra longitudinal reinforcement is provided over bents. Additional cross sections are provided where the approach slabs were scanned with the GPR. Base maps of each bridge are included in the Digital Appendix in Appendix A.

2.2.1 Bridge A0569

Table 2-1 Bridge A0569 Details

Nearest City	Jefferson City
County	Cole
Roadway Carried	Clark Avenue
Feature Intersected	U.S. 50
Year Constructed	1959
Reconstructed Year	Never Reconstructed
Number of Driving Lanes	3
Direction of Traffic	Two-Way
AADT	8,763
AADT Truck Percent	10%
Structure Length	139 ft. – 0 in.
Total Deck Width	57 ft. – 8 in.
Curb to Curb Br. Width	48 ft. – 10 in.
Main Structure Material Type	Concrete
Main Structure Construction Type	Frame
Number of Main Spans	1
Number of Approach Spans	0
Deck Material	Concrete CIP
Designed Slab Thickness	6.5 in.
Wearing Surface	Bituminous
Orientation of Top Reinforcement Layer	Transverse
Designed Depth to Top Transverse Reinforcement	1.75 in. (without asphalt overlay)
Slab Reinforcement, Transverse Direction	#5 @ 6 in. o.c. top and bottom main span, #5 @ 5 in. o.c. top and bottom abutments
Slab Reinforcement, Longitudinal Direction	#5 top and bottom main span and abutments, spacing varies
Other Information	Asphalt wearing surface was extensively deteriorated at the time of the NDE investigation. Many locations of asphalt rutting and shoving were observed, along with many cracks and potholes.

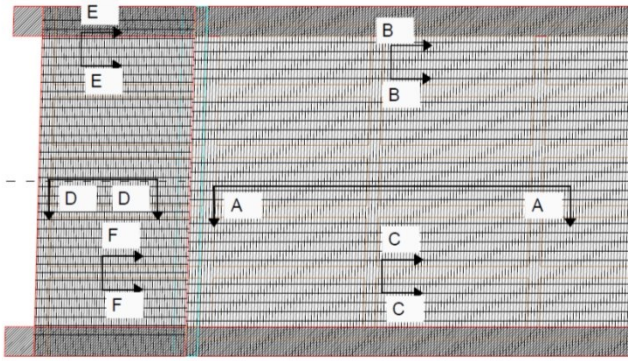

CROSS SECTION A-A

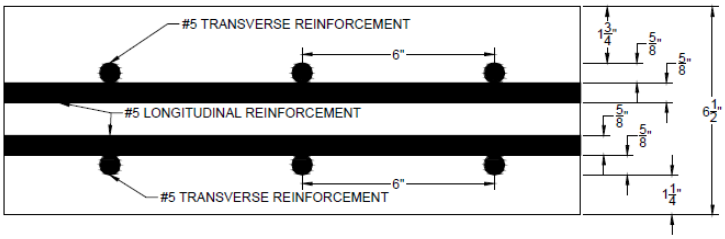

CROSS SECTION B-B

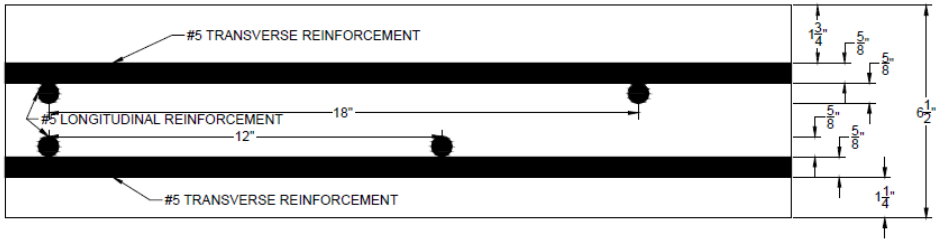

Figure 2-2 Bridge A0569 Deck Cross Sections
(Note: Deck had asphalt wearing surface that is not included in these cross section drawings)

CROSS SECTION C-C

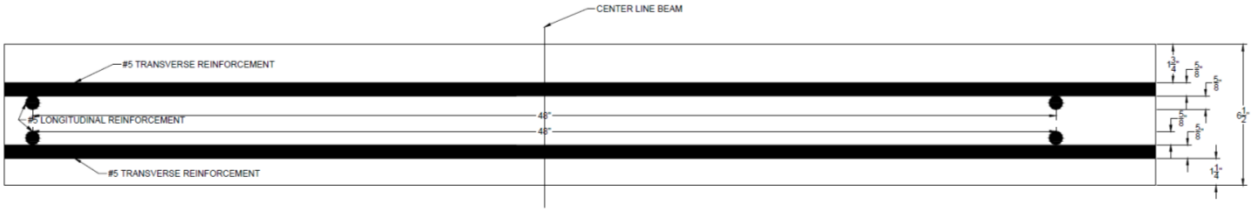

CROSS SECTION D-D

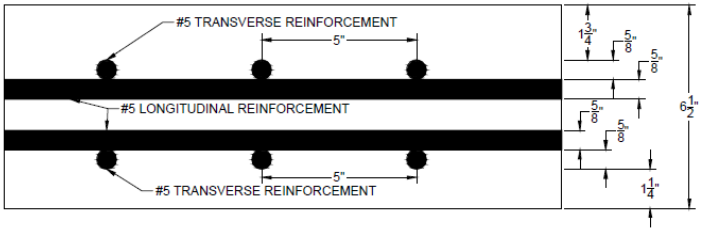

CROSS SECTION E-E

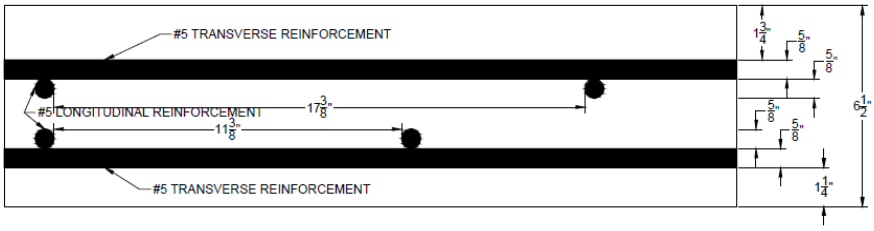

CROSS SECTION F-F

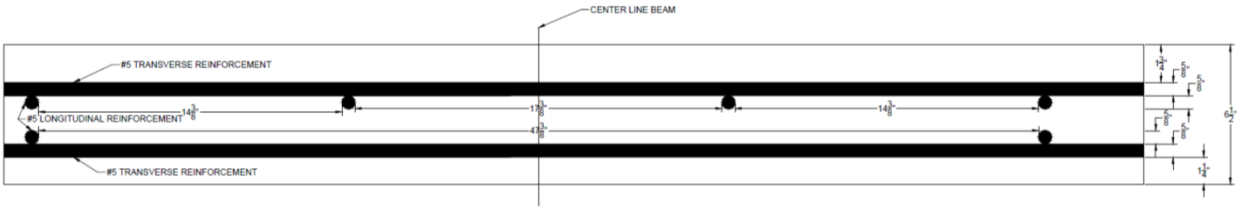

Figure 2-2 (Cont.) Bridge A0569 Deck Cross Sections
(Note: Deck had asphalt wearing surface that is not included in these cross section drawings)

2.2.2 Bridge A1187

Table 2-2 Bridge A1187 Details

Nearest City	Jefferson City
County	Cole
Roadway Carried	Dix Road
Feature Intersected	U.S. 50
Year Constructed	1964
Reconstructed Year	Never Reconstructed
Number of Driving Lanes	4
Direction of Traffic	Two-Way
AADT	13,375
AADT Truck Percent	10%
Structure Length	139 ft. – 0 in.
Total Deck Width	55 ft. – 1 in.
Curb to Curb Br. Width	47 ft. – 10 in.
Main Structure Material Type	Concrete
Main Structure Construction Type	Frame
Number of Main Spans	1
Number of Approach Spans	0
Deck Material	Concrete CIP
Designed Slab Thickness	7.0 in.
Wearing Surface	Bituminous
Orientation of Top Reinforcement Layer	Transverse
Designed Depth to Top Transverse Reinforcement	2.375 in.
Slab Reinforcement, Transverse Direction	#6 @ 6 in. o.c. top and bottom
Slab Reinforcement, Longitudinal Direction	#4 top, spacing varies; #5 bottom, spacing varies
Other Information	Bridge was scanned twice during project. First scan was performed with an extensively heavily deteriorated asphalt wearing surface, second scan was performed after deteriorated asphalt was milled off and then replaced with new asphalt wearing surface.

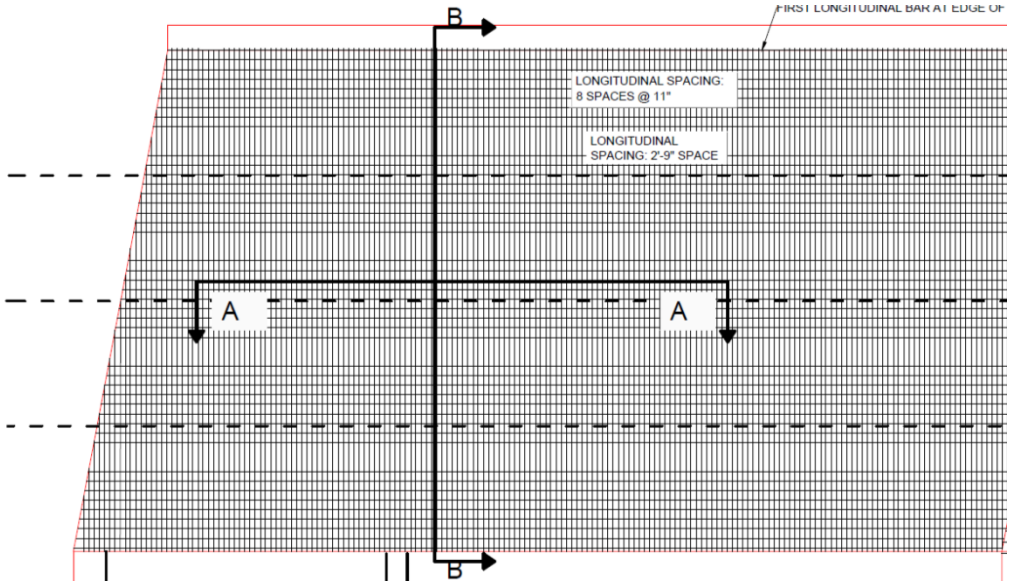

CROSS SECTION A-A

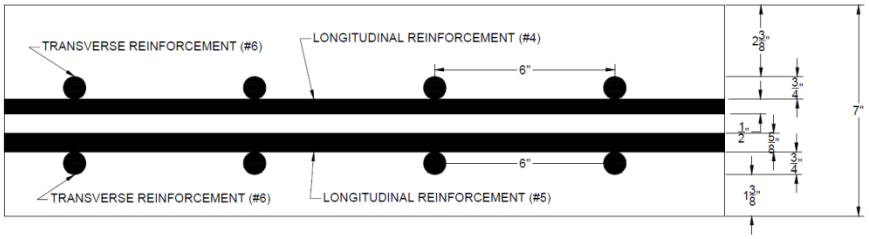

CROSS SECTION B-B

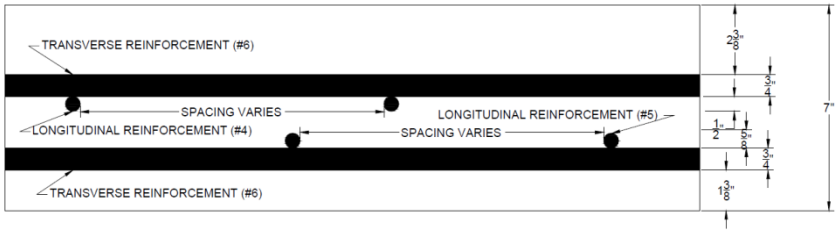

Figure 2-3 Bridge A1187 Deck Cross Sections
(Note: Deck had asphalt wearing surface that is not included in these cross section drawings)

2.2.3 Bridge A1193

Table 2-3 Bridge A1193 Details

Nearest City	Syracuse
County	Morgan
Roadway Carried	U.S. 50
Feature Intersected	Lamine River
Year Constructed	1972
Reconstructed Year	2013 (After NDE Investigation)
Number of Driving Lanes	2
Direction of Traffic	Two-Way
AADT	4,299
AADT Truck Percent	17%
Structure Length	897 ft. – 0 in.
Total Deck Width	46 ft. – 10 in.
Curb to Curb Br. Width	43 ft. – 11 in.
Main Structure Material Type	Steel Continuous
Main Structure Construction Type	Stringer/Multibeam – Grd
Number of Main Spans	4
Number of Approach Spans	8
Deck Material	Concrete CIP
Designed Slab Thickness	7.5 in.
Wearing Surface	Monolithic Concrete
Orientation of Top Reinforcement Layer	Transverse
Designed Depth to Top Transverse Reinforcement	1.875 in.
Slab Reinforcement, Transverse Direction	#5 @ 5 in. o.c. top and bottom
Slab Reinforcement, Longitudinal Direction	#4 @ 6 in. o.c. top over bents, #4 @ 12 in. o.c. top otherwise; #5 bottom, spacing varies
Other Information	Bridge deck was rehabilitated after NDE investigation in this study.

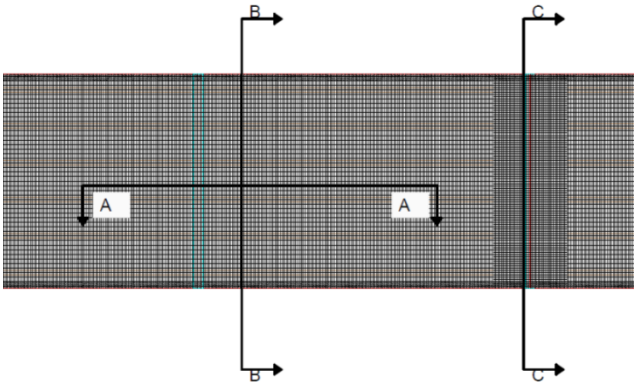

CROSS SECTION A-A

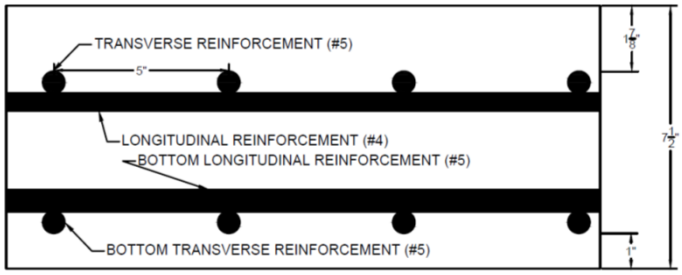

CROSS SECTION B-B

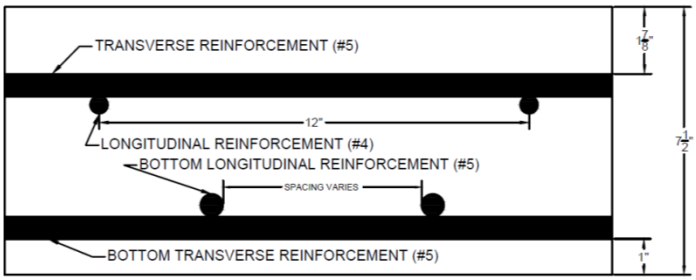

CROSS SECTION C-C

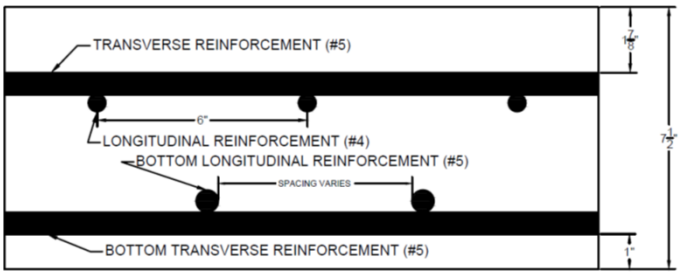

Figure 2-4 Bridge A1193 Deck Cross Sections

2.2.4 Bridge A1297

Table 2-4 Bridge A1297 Details

Nearest City	Sedalia
County	Morgan
Roadway Carried	U.S. 50
Feature Intersected	Union Pacific Railroad
Year Constructed	1972
Reconstructed Year	2013 (After NDE Investigation)
Number of Driving Lanes	2
Direction of Traffic	Two-Way
AADT	4,728
AADT Truck Percent	17%
Structure Length	157 ft. – 0 in.
Total Deck Width	46 ft. – 10 in.
Curb to Curb Br. Width	43 ft. – 11 in.
Main Structure Material Type	Steel Continuous
Main Structure Construction Type	Stringer/Multibeam – Grd
Number of Main Spans	3
Number of Approach Spans	0
Deck Material	Concrete CIP
Designed Slab Thickness	7.5 in.
Wearing Surface	Monolithic Concrete
Orientation of Top Reinforcement Layer	Transverse
Designed Depth to Top Transverse Reinforcement	1.875 in.
Slab Reinforcement, Transverse Direction	#5 @ 5 in. o.c. top and bottom
Slab Reinforcement, Longitudinal Direction	#4 @ 6 in. o.c. top over bents, #4 @ 12 in. o.c. top otherwise; #5 bottom, spacing varies
Other Information	Bridge deck was rehabilitated after NDE investigation in this study.

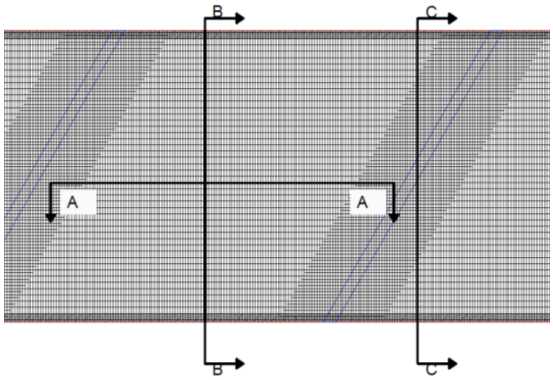

CROSS SECTION A-A

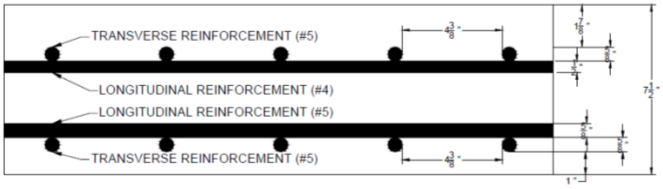

CROSS SECTION B-B

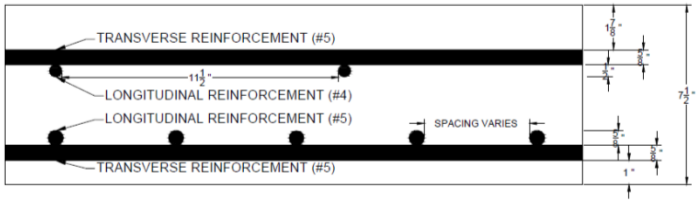

CROSS SECTION C-C

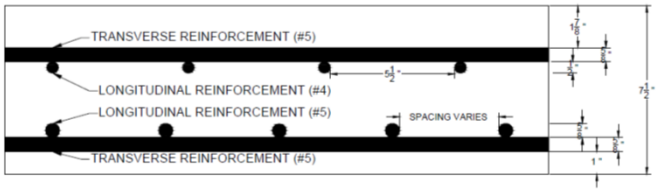

Figure 2-5 Bridge A1297 Deck Cross Sections

2.2.5 Bridge A1479

Table 2-5 Bridge A1479 Details

Nearest City	Lake Ozark
County	Miller
Roadway Carried	U.S. 54 West
Feature Intersected	Osage River
Year Constructed	1966
Reconstructed Year	2013 (After NDE Investigation)
Number of Driving Lanes	2
Direction of Traffic	One-Way
AADT	7,623
AADT Truck Percent	10%
Structure Length	868 ft. – 0 in.
Total Deck Width	34 ft. – 5 in.
Curb to Curb Br. Width	32 ft. – 1 in.
Main Structure Material Type	Steel Continuous
Main Structure Construction Type	Stringer/Multibeam - Grd
Number of Main Spans	5
Number of Approach Spans	0
Deck Material	Concrete CIP
Designed Slab Thickness	7.5 in.
Wearing Surface	Monolithic Concrete
Orientation of Top Reinforcement Layer	Longitudinal
Designed Depth to Top Transverse Reinforcement	2.5 in.
Slab Reinforcement, Transverse Direction	#6 @ 6 in. o.c. top and bottom
Slab Reinforcement, Longitudinal Direction	#4 @ 6 in. o.c. top over bents, #4 @ 12 in. o.c. top otherwise; #5 bottom, spacing varies
Other Information	Bridge deck was rehabilitated after NDE investigation in this study.

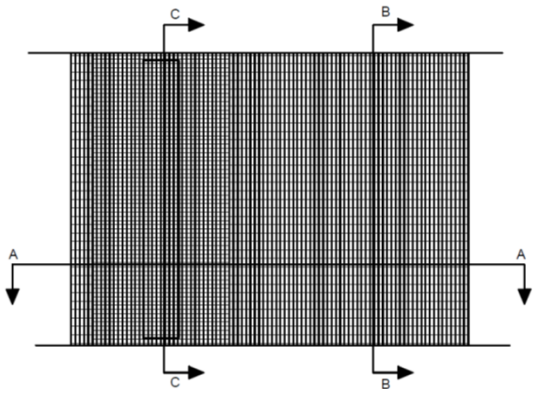

CROSS SECTION A-A

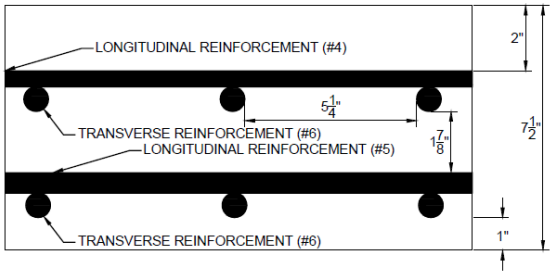

CROSS SECTION B-B

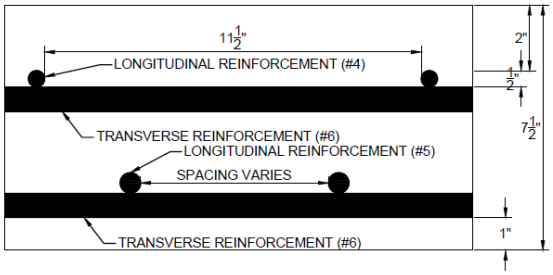

CROSS SECTION C-C

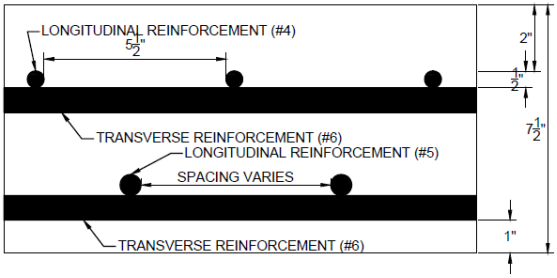

Figure 2-6 Bridge A1479 Deck Cross Sections

2.2.6 Bridge A2111

Table 2-6 Bridge A2111 Details

Nearest City	Fulton
County	Callaway
Roadway Carried	U.S. 54 East
Feature Intersected	Abandoned Railroad
Year Constructed	1968
Reconstructed Year	Never Reconstructed
Number of Driving Lanes	2
Direction of Traffic	One-Way
AADT	6,404
AADT Truck Percent	14%
Structure Length	176 ft. – 0 in.
Total Deck Width	46 ft. – 10 in.
Curb to Curb Br. Width	43 ft. – 11 in.
Main Structure Material Type	Steel Continuous
Main Structure Construction Type	Stringer/Multibeam - Grd
Number of Main Spans	3
Number of Approach Spans	0
Deck Material	Concrete CIP
Designed Slab Thickness	7.5 in.
Wearing Surface	Monolithic Concrete
Orientation of Top Reinforcement Layer	Transverse
Designed Depth to Top Transverse Reinforcement	1.875 in.
Slab Reinforcement, Transverse Direction	#5 @ 5 in. o.c. top and bottom
Slab Reinforcement, Longitudinal Direction	#4 @ 6 in. o.c. top over bents, #4 @ 12 in. o.c. top otherwise; #5 bottom, spacing varies
Other Information	-

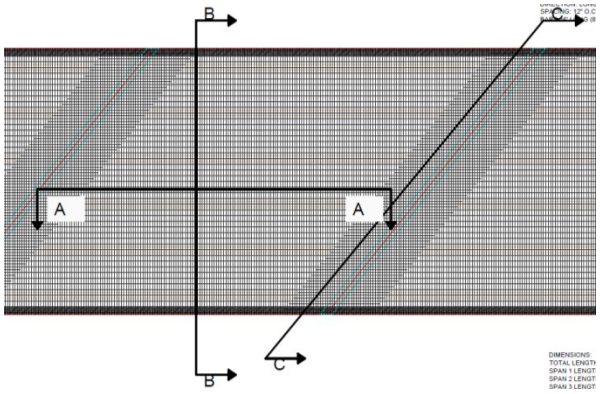

CROSS SECTION A-A

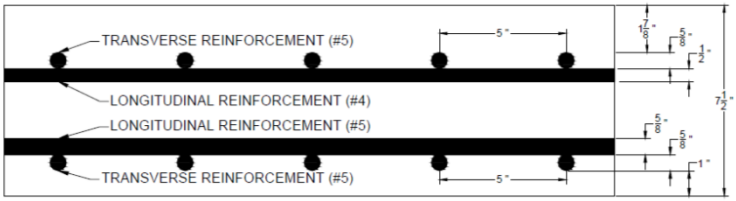

CROSS SECTION B-B

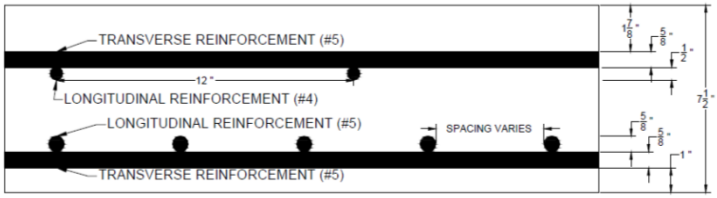

CROSS SECTION C-C

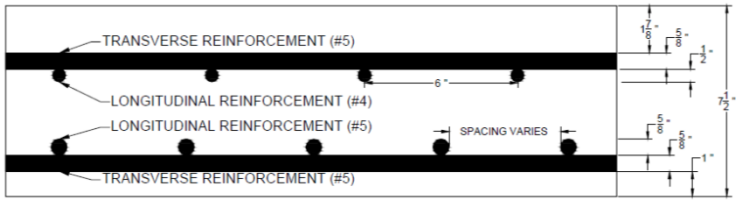

Figure 2-7 Bridge A2111 Deck Cross Sections

2.2.7 Bridge A2966

Table 2-7 Bridge A2966 Details

Nearest City	Mountain Grove
County	Wright
Roadway Carried	MO 95
Feature Intersected	U.S. 60
Year Constructed	1974
Reconstructed Year	Never Reconstructed
Number of Driving Lanes	3
Direction of Traffic	Two-Way
AADT	6,555
AADT Truck Percent	10%
Structure Length	258 ft. – 0 in.
Total Deck Width	46 ft. – 10 in.
Curb to Curb Br. Width	43 ft. – 11 in.
Main Structure Material Type	Steel Continuous
Main Structure Construction Type	Stringer/Multibeam - Grd
Number of Main Spans	2
Number of Approach Spans	0
Deck Material	Concrete CIP
Designed Slab Thickness	7.5 in.
Wearing Surface	Bituminous
Orientation of Top Reinforcement Layer	Transverse
Designed Depth to Top Transverse Reinforcement	1.875 in.
Slab Reinforcement, Transverse Direction	#5 @ 5 in. o.c. top and bottom
Slab Reinforcement, Longitudinal Direction	#4 @ 6 in. o.c. top over bents, #4 @ 12 in. o.c. top otherwise; #5 bottom, spacing varies
Other Information	Bridge deck covered by a very thin bituminous chip seal that was extensively deteriorated. Large areas (approximately 25%) of the deck exhibited bare concrete.

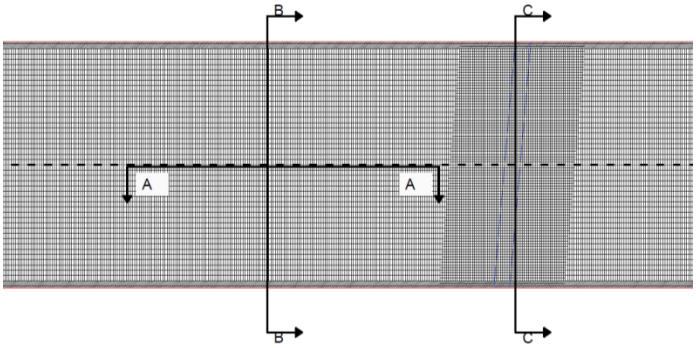

CROSS SECTION A-A

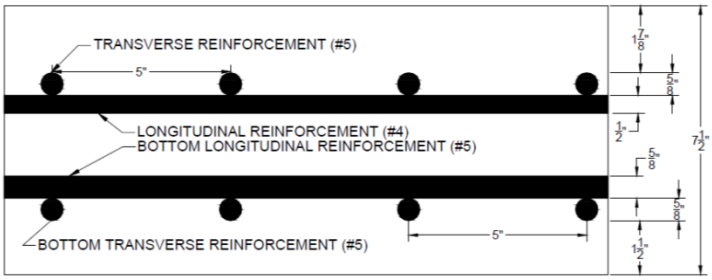

CROSS SECTION B-B

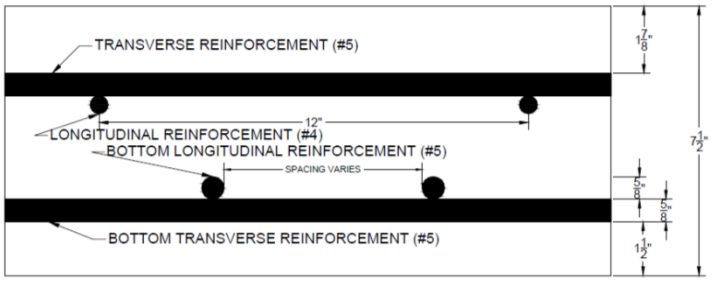

CROSS SECTION C-C

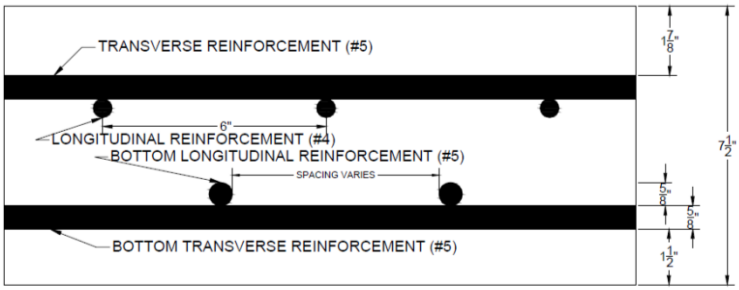

Figure 2-8 Bridge A2966 Deck Cross Sections

2.2.8 Bridge A3017

Table 2-8 Bridge A3017 Details

Nearest City	Warsaw
County	Benton
Roadway Carried	MO 7
Feature Intersected	Osage River
Year Constructed	1975
Reconstructed Year	Never Reconstructed
Number of Driving Lanes	2
Direction of Traffic	Two-Way
AADT	4,674
AADT Truck Percent	16%
Structure Length	831 ft. – 0 in.
Total Deck Width	47 ft. – 2 in.
Curb to Curb Br. Width	43 ft. – 11 in.
Main Structure Material Type	Steel Continuous and Prestressed Concrete
Main Structure Construction Type	Stringer/Multibeam - Grid
Number of Main Spans	2
Number of Approach Spans	5
Deck Material	Concrete CIP
Designed Slab Thickness	8.0 in.
Wearing Surface	Monolithic Concrete
Orientation of Top Reinforcement Layer	Longitudinal
Designed Depth to Top Transverse Reinforcement	5.875 in.
Slab Reinforcement, Transverse Direction	#5 @ 5.5 in. o.c. top and bottom
Slab Reinforcement, Longitudinal Direction	#5 @ 5 in. o.c. top over bents, #5 @ 15 in. o.c. top otherwise; #5 bottom, spacing varies
Other Information	Bridge is part of a horizontal curve

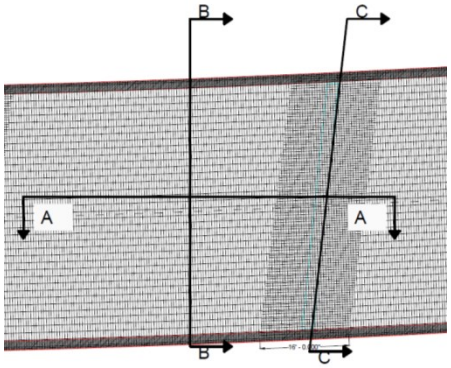

CROSS SECTION A-A

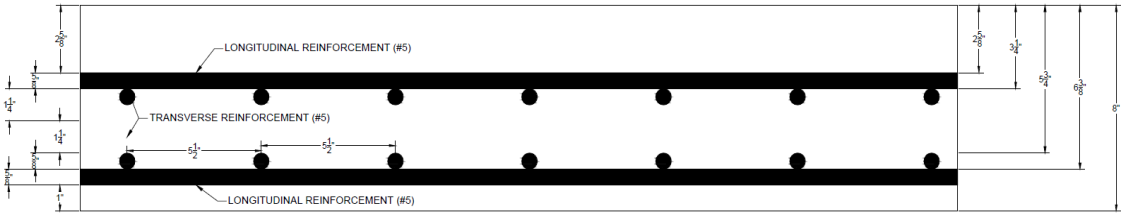

CROSS SECTION B-B

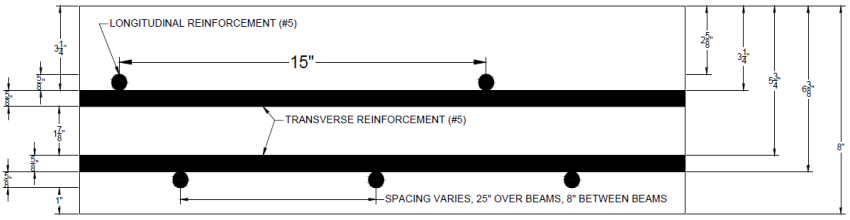

CROSS SECTION C-C

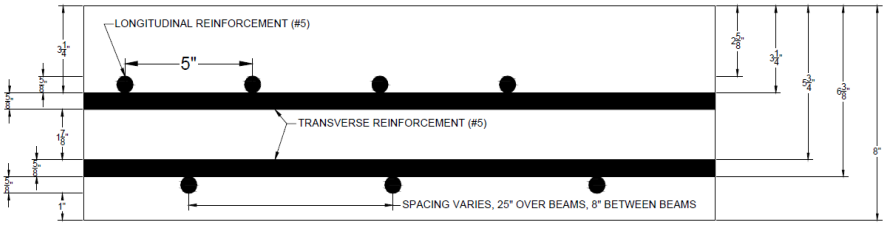

Figure 2-9 Bridge A3017 Deck Cross Sections

2.2.9 Bridge A3405

Table 2-9 Bridge A3405 Details

Nearest City	St. James
County	Maries
Roadway Carried	MO 68
Feature Intersected	Coppedge Creek
Year Constructed	1975
Reconstructed Year	Never Reconstructed
Number of Driving Lanes	2
Direction of Traffic	Two-Way
AADT	2,524
AADT Truck Percent	18%
Structure Length	144 ft. – 0 in.
Total Deck Width	46 ft. – 10 in.
Curb to Curb Br. Width	43 ft. – 11 in.
Main Structure Material Type	Concrete Continuous
Main Structure Construction Type	Slab
Number of Main Spans	4
Number of Approach Spans	0
Deck Material	Concrete CIP
Designed Slab Thickness	14.5 in.
Wearing Surface	Monolithic Concrete
Orientation of Top Reinforcement Layer	Longitudinal
Designed Depth to Top Transverse Reinforcement	3.375 in.
Slab Reinforcement, Transverse Direction	#5 @ 9 in. o.c. top and bottom
Slab Reinforcement, Longitudinal Direction	#10 @ 6 in. o.c. top over bents, #5 @ 9 in. o.c. top otherwise; #9 @ 18 in. o.c. bottom over bents, #9 & #10 @ 6 in. o.c. bottom otherwise
Other Information	-

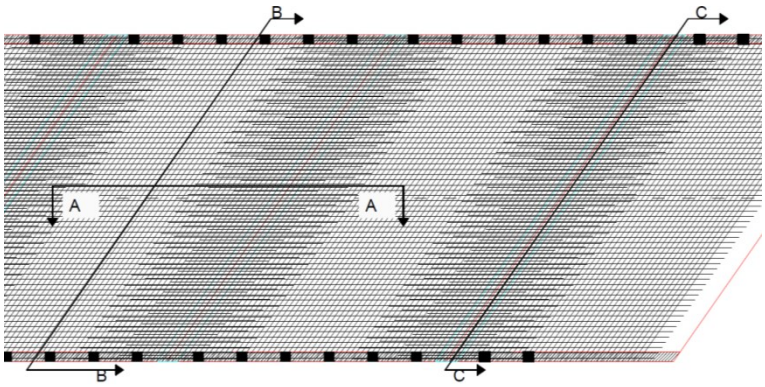

CROSS SECTION A-A

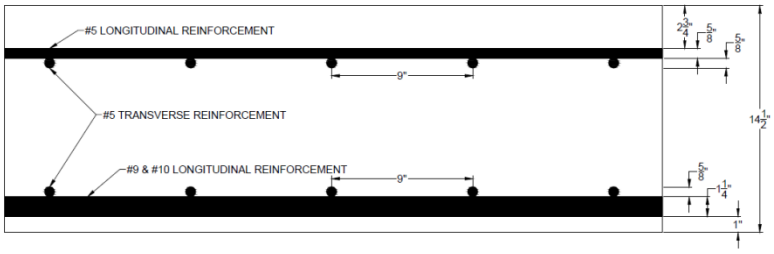

CROSS SECTION B-B

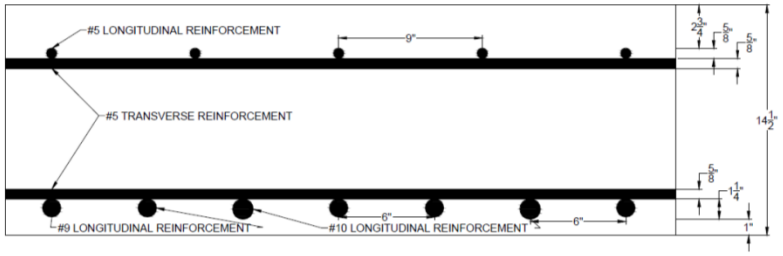

CROSS SECTION C-C

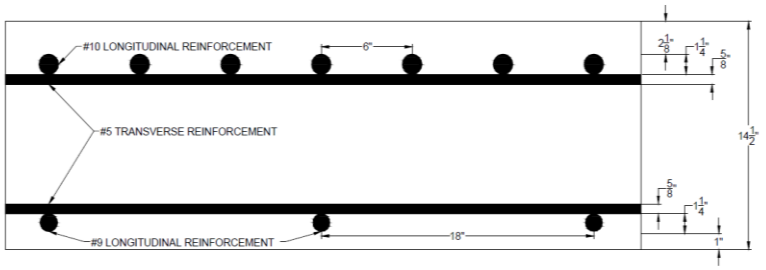

Figure 2-10 Bridge A3405 Deck Cross Sections

2.2.10 Bridge A3406

Table 2-10 Bridge A3406 Details

Nearest City	Vichy
County	Maries
Roadway Carried	MO 68
Feature Intersected	Lanes Creek
Year Constructed	1976
Reconstructed Year	Never Reconstructed
Number of Driving Lanes	2
Direction of Traffic	Two-Way
AADT	1,840
AADT Truck Percent	18%
Structure Length	163 ft. – 0 in.
Total Deck Width	46 ft. – 10 in.
Curb to Curb Br. Width	43 ft. – 11 in.
Main Structure Material Type	Prestressed Concrete Continuous
Main Structure Construction Type	Stringer/Multibeam - Grd
Number of Main Spans	3
Number of Approach Spans	0
Deck Material	Concrete CIP
Designed Slab Thickness	7.5 in.
Wearing Surface	Monolithic Concrete
Orientation of Top Reinforcement Layer	Transverse
Designed Depth to Top Transverse Reinforcement	1.875 in.
Slab Reinforcement, Transverse Direction	#5 @ 5 in. o.c. top and bottom
Slab Reinforcement, Longitudinal Direction	#4 @ 6 in. o.c. top over bents, #4 @ 12 in. o.c. top otherwise; #5 bottom, spacing varies
Other Information	-

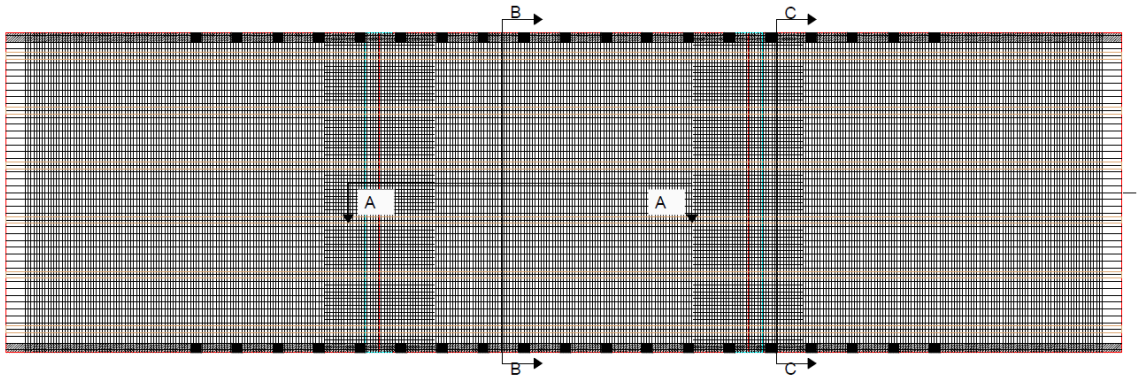

CROSS SECTION A-A

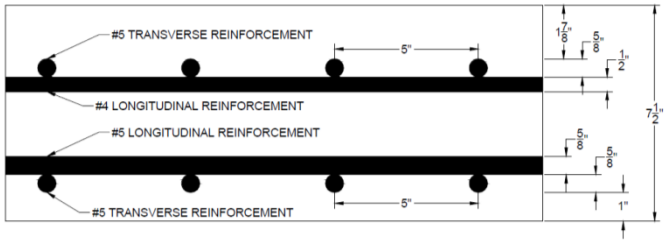

CROSS SECTION B-B

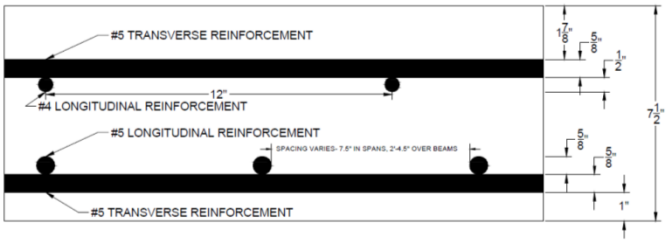

CROSS SECTION C-C

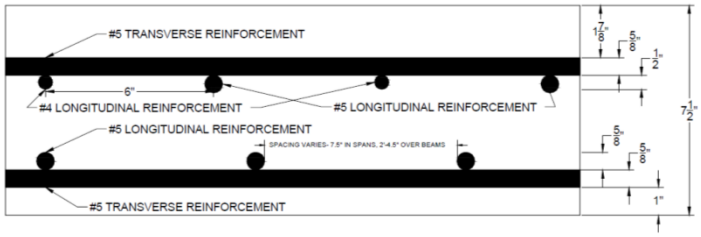

Figure 2-11 Bridge A3406 Deck Cross Sections

2.2.11 Bridge K0197

Table 2-11 Bridge K0197 Details

Nearest City	St. James
County	Phelps
Roadway Carried	MO 68
Feature Intersected	Bourbeuse River
Year Constructed	1965
Reconstructed Year	1984
Number of Driving Lanes	2
Direction of Traffic	Two-Way
AADT	2,524
AADT Truck Percent	18%
Structure Length	207 ft. – 0 in.
Total Deck Width	32 ft. – 5 in.
Curb to Curb Br. Width	29 ft. – 10 in.
Main Structure Material Type	Steel Continuous
Main Structure Construction Type	Stringer/Multibeam - Grd
Number of Main Spans	3
Number of Approach Spans	0
Deck Material	Concrete CIP
Designed Slab Thickness	7.5 in.
Wearing Surface	Bituminous
Orientation of Top Reinforcement Layer	Longitudinal
Designed Depth to Top Transverse Reinforcement	2.5 in. (without asphalt overlay)
Designed Slab Reinforcement, Transverse Direction	#6 @ 6.5 in. o.c. top and bottom
Designed Slab Reinforcement, Longitudinal Direction	#4 @ 6 in. o.c. top over bents, #4 @ 12 in. o.c. top otherwise; #4 bottom, spacing varies
Other Information	1984 reconstruction consisted of half soled and full depth repair, along with an asphalt overlay with a minimum thickness of 1.5 in. At the time of the NDE investigation, the asphalt was approximately 2.5 in. thick and appeared to be in good condition based on visual inspection.

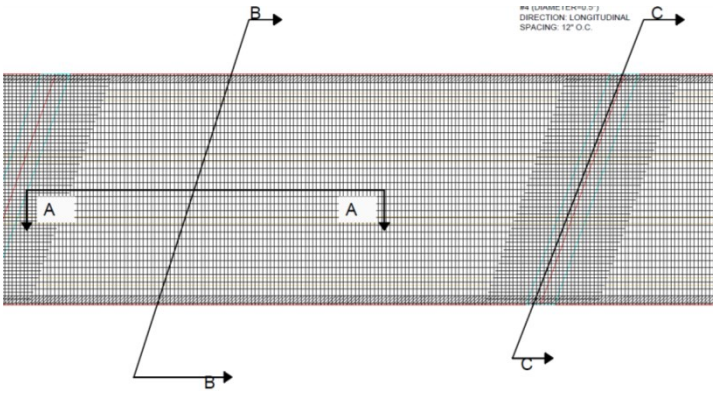

CROSS SECTION A-A

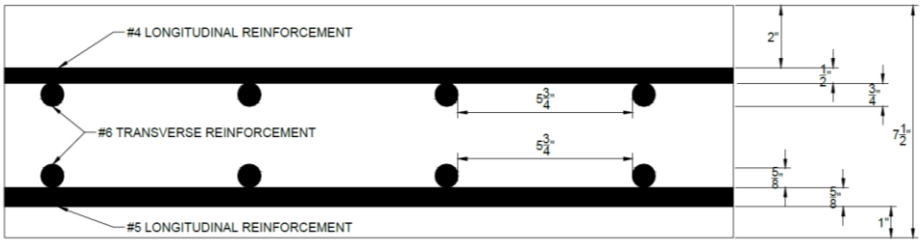

CROSS SECTION B-B

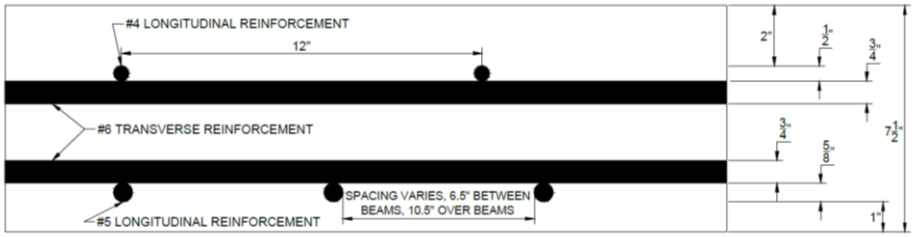

CROSS SECTION C-C

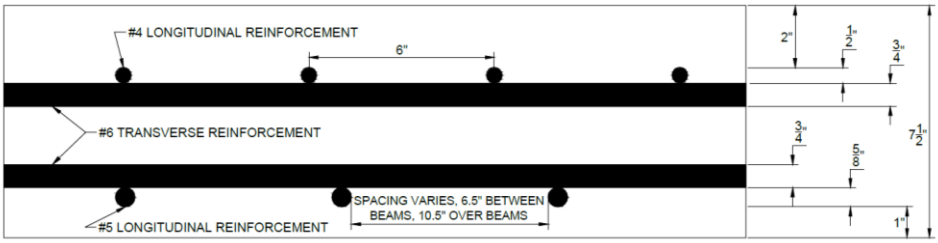

Figure 2-12 Bridge K0197 Deck Cross Sections
(Note: Deck had asphalt wearing surface that is not included in these cross section drawings)

3 VISUAL ASSESSMENTS

3.1 Methodology

A thorough visual inspection was conducted of the top surface of each bridge deck. Areas with signs of deterioration or areas that contained materials that were not the original as-built concrete were identified and mapped. The data collected during the visual evaluation were plotted on a drawing of the bridge deck using CAD software. Defects noted included concrete patches, asphalt filled potholes, unfilled concrete spalls, traverse cracks, and efflorescence. General visual condition notes are included in this section. Complete bridge drawings that display the visual assessment data are included in the Digital Appendix of this report. See Appendix A for a description of the Digital Appendix.

3.2 Visual Assessment Results

3.2.1 Bridge A0569

There were 20 defects documented during the field investigation of Bridge A0569. The deck contained an asphalt wearing surface that showed some signs of deterioration. Documented defects include concrete patches, asphalt rutting and shoving, and unfilled potholes in the concrete. Figure 3-1 below shows a concrete patch present on Bridge A0569, along with a deteriorated asphalt overlay around the patch.

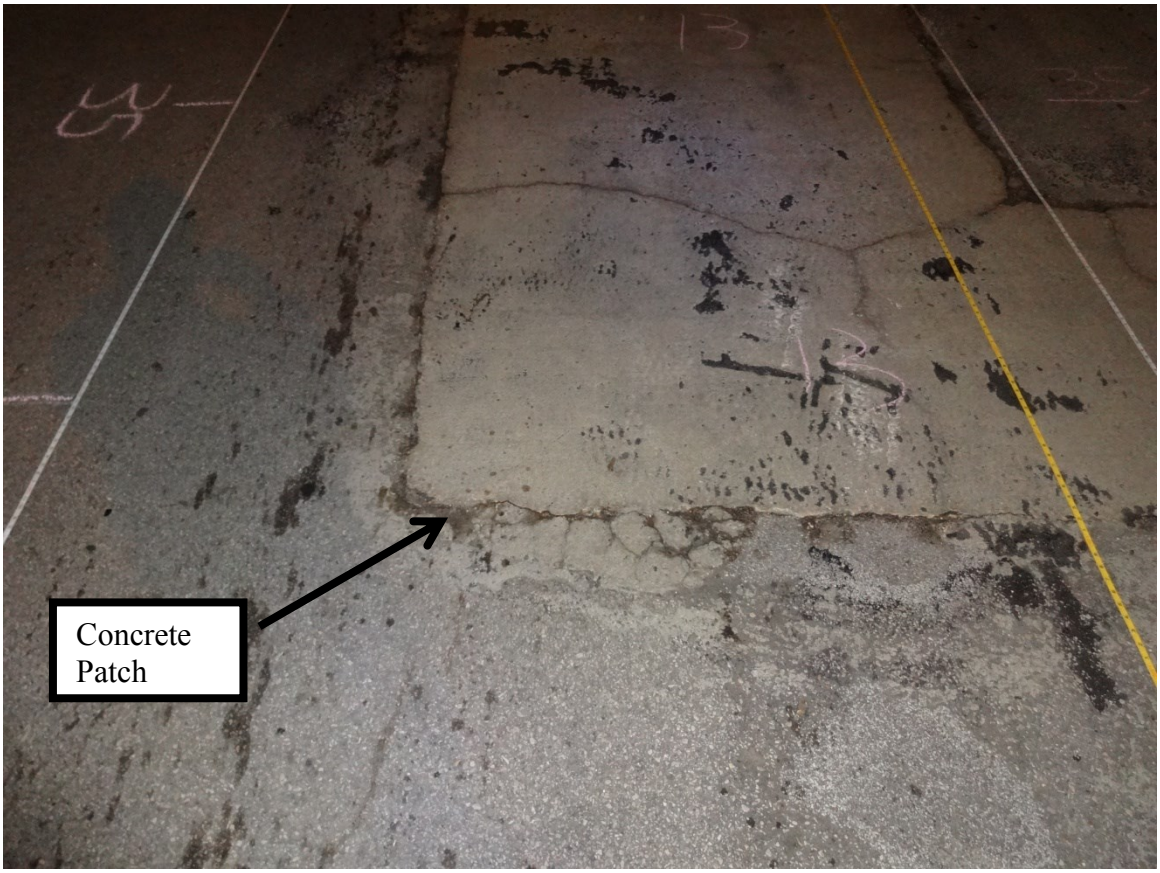

Figure 3-1 Bridge A0569 Concrete Patch and Deteriorated Asphalt Overlay Observed During Field Investigation

3.2.2 Bridge A1187

During the first investigation of Bridge A1187, the asphalt wearing surface was noted to be heavily deteriorated, and 52 individual surface defects were documented. These defects consisted mainly of concrete patches, but also included visible deterioration of the asphalt, such as rutting and shoving, as well as unfilled potholes. No defects were documented during the second visual investigation of Bridge A1187 after the wearing surface had been milled off and replaced with an approximately 1 in. thick asphalt wearing surface. Figure 3-2 shows Bridge A1187 during the first investigation. Figure 3-2 shows the deteriorated asphalt overlay and concrete patches. Figure 3-3 shows the top deck surface of the same bridge during the second investigation (approximately eight months later), with a new asphalt wearing surface.

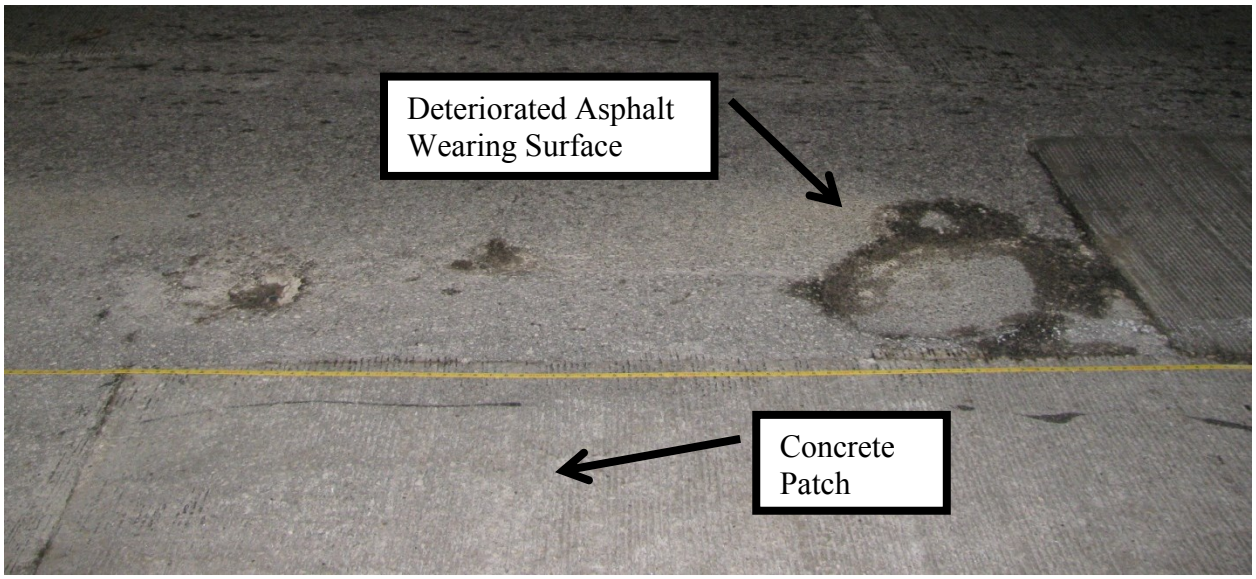

Figure 3-2 Bridge A1187 Deteriorated Asphalt Wearing Surface Observed During First Investigation

Figure 3-3 Bridge A1187 Deck Surface Observed During Second Investigation

3.2.3 Bridge A1193

There were 81 defects documented during the field investigation of Bridge A1193. Due to time constraints of the time on site, the shoulders were not examined. The bridge deck surface did not appear to be heavily deteriorated. Most of the visible defects were asphalt filled potholes, and some unfilled potholes in the concrete were noted. Figure 3-4 shows a typical asphalt filled pothole found on the deck surface of Bridge A1193. This region also had exposed reinforcing steel.

Figure 3-4 Bridge A1193 Typical Asphalt Filled Pothole Observed During Field Investigation

3.2.4 Bridge A1297

There were 69 defects documented during the field investigation of Bridge A1297. The deck had many traverse cracks, concrete patches, asphalt filled potholes, and unfilled potholes in the concrete. Figure 3-5 shows typical deterioration located during the field investigation of Bridge A1297.

Figure 3-5 Bridge A1297 Typical Deck Condition Observed During Field Investigation

3.2.5 Bridge A1479

There were 161 defects documented during the field investigation of Bridge A1479. The deck surface appeared heavily deteriorated near the middle of the beam spans. Deterioration levels appeared to be much lower near the bent supports. The researchers noticed a lot of vibration of the bridge during the investigation as large trucks passed over the bridge. The deck curb drains were also severely deteriorated with reinforcing steel visible in several areas, especially along the soffit of the deck. Documented deterioration includes concrete patches, unfilled concrete potholes, asphalt filled potholes, and transverse cracks. Figure 3-6 shows an area of the deck with multiple concrete patches and asphalt filled potholes.

Figure 3-6 Bridge A1479 Typical Deck Condition Observed During Field Investigation

3.2.6 Bridge A2111

There were 50 defects documented during the field investigation of Bridge A2111. The deck contained several concrete patches, asphalt filled potholes, and unfilled potholes. There were several areas of the deck where delaminations were suspected because tapping on the concrete surface generated a "hollow" sound. Figure 3-7 shows typical deterioration that was observed on Bridge A2111, including concrete patches and asphalt filled potholes.

Figure 3-7 Bridge A2111 Typical Deck Condition Observed During Field Investigation

3.2.7 Bridge A2966

There were 119 defects documented during the field investigation of Bridge A2966. The deck surface had many traverse cracks, along with some concrete patches, asphalt filled potholes, and some unfilled potholes in the concrete. The deck was partially covered with a chip seal, which was worn away in many areas of the deck, especially in the wheel paths. Figure 3-8 shows an overview of the deck.

Figure 3-8 Bridge A2966 Overview of Bridge Deck Observed During Field Investigation

3.2.8 Bridge A3017

There were 101 defects documented during the field investigation of Bridge A3017. The main type of visible defect noted was asphalt filled potholes. The deck also contained some concrete patches and unfilled potholes. The heaviest areas of deterioration were in the two long spans, Spans 4-5 and 5-6 (defined on the base map in Section 2.2.8). Due to time constraints, defects in the shoulders were not documented. Figure 3-9 shows multiple asphalt filled potholes, along with a region with an unfilled spall in the concrete.

Figure 3-9 Bridge A3017 Typical Deck Deterioration Observed During Field Investigation

3.2.9 Bridge A3405

There were 43 defects documented on the deck surface of Bridge A3405. The majority of the defects were cracks, in both the longitudinal and transverse directions. Most of the cracks had been filled with asphalt. Some concrete patches were also observed. The ends of the bridge had asphalt wedges to allow for a smoother ride on and off the bridge. The bridge deck appeared to be in relatively good shape considering the age at investigation (38 years old). Figure 3-10 shows an overview of Bridge A3405 during the deck investigation. Darker lines in the image are cracks that have been filled with oil or bitumen.

Figure 3-10 Bridge A3405 Overview of Bridge Deck Observed During Field Investigation

3.2.10 Bridge A3406

There were 141 defects documented during the investigation of Bridge A3406. The bridge deck surface appeared to be heavily deteriorated. Numerous transverse cracks and concrete patches were observed. The majority of the cracks were filled with oil or bitumen. Figure 3-11 shows an overview of the deck during the field investigation.

Figure 3-11 Bridge A3406 Overview of Bridge Deck Observed During Field Investigation

3.2.11 Bridge K0197

No visual defects were documented during the investigation of Bridge K0197. The deck had an asphalt wearing surface that appeared to be in good condition with no visible signs of deterioration. The asphalt overlay was approximately 2.5 in. as was visible in the deck curb drains. The soffit was deteriorated around the curb drains, with reinforcing steel visible in several areas. Figure 3-12 shows an overview of the deck.

Figure 3-12 Bridge K0197 Overview of Bridge Deck Observed During Field Investigation

3.3 Summary of Visual Assessment Results

Table 3-1 summarizes the types of defects observed on each of the bridge decks investigated in this study. Complete bridge drawings that display the visual assessment data are included in the Digital Appendix (see Appendix A of this report).

Table 3-1 Summary of Bridge Deck Defects Observed

Bridge	Type of Defect Observed in Bridge Deck					
	Concrete Patches	**Asphalt Filled Potholes**	**Unfilled Concrete Potholes**	**Deteriorated Asphalt Wearing Surface**	**Traverse Cracks**	**Random Cracks**
A0569	x		x	x		
A1187 – 1st Scan	x			x		
A1187 – 2nd Scan						
A1193		x	x			
A1297	x	x	x		x	
A1479	x	x	x		x	
A2111	x	x	x			
A2966	x	x	x		x	
A3017	x	x	x			
A3405	x				x	x
A3406	x				x	
K0197						

4 CORES

4.1 Methodology

Cores were extracted from each of the bridge decks investigated in this project. Where possible, locations of cores on each bridge deck were selected based on the visual inspection (Section 3), raw GPR data (Section 7), and USW data from the PSPA (Section 8). Core locations were chosen both from areas where the bridge deck appeared to be in good condition (based on the NDT data), and areas where the deck appeared to be deteriorated. Core locations are marked on the bridge drawings found in the Digital Appendix of this report, as discussed in Appendix A.

Six to twelve cores were extracted from each bridge deck, depending on the deck condition and the limit set by MoDOT. Cores were 2 in. diameter and were drilled to at least the bottom of the top transverse reinforcing bar where possible. MoDOT personnel extracted the cores after the locations were marked and measured by Missouri S&T researchers. The core holes were investigated, and the cores were then individually labeled, bagged, and transported back to Missouri S&T for further testing. For Bridge A1187, which was investigated twice, cores were only extracted during the first investigation.

The bridge deck cores were carefully examined and documented at Missouri S&T. Visible properties examined included diameter, length, surface material, number of pieces and the length of each piece, presence of reinforcing bar, concrete roughness, number of voids, quality of aggregate coating with the paste mixture in the concrete, the volume of paste, signs of air entrainment, flaking surfaces, discolorations, delaminations, segregation of the aggregate, and presence of cracks. Based on these properties the cores were then given a visual core rating defined for this project of either "Good," "Fair," or "Poor." A visual core rating of "Good" indicates that the core had no delaminations or visible deterioration present. "Fair" indicates that the core had some visible deterioration including delaminations, however the concrete was in a few large sections. "Poor" indicates that the core had a lot of deterioration and was in many pieces when extracted, including several small pieces. If asphalt was present on the surface of the core, only the concrete portion was rated using the visual inspection, however the bond and condition of the asphalt layer was noted in the "Other Comments" section.

Next, the volume of permeable pores was determined for each core following ASTM C642-06. The volume of permeable pores in the concrete cores indicates the amount of water that is able to enter into the pore structure of the concrete. The more permeable the concrete, the more water can enter into the pore structure and deteriorate the concrete with freeze/thaw cycles, along with allowing deicing agents to enter and accelerate the concrete degradation. In this study, it was postulated that a higher percentage of permeable pores in the concrete corresponds to a higher level of deterioration in the concrete. Figure 4-1 illustrates the process followed to obtain the volume of permeable pores. Steps taken to determine the volume of permeable pores were:

1. The mass of the cores was initially determined, and then the cores were placed into a 220°F oven for 24 hours. The cores were then cooled to room temperature, and the mass was determined again. If the percentage difference between final and initial mass was more than 0.5% then the cores were placed back into the oven for another 24 hours. If the percentage difference in mass with a 24 hour period of being in the oven was less than 0.5%, they were considered dry, and the final mass was recorded. This process was

repeated until all of the cores had a mass difference of less than 0.5% within a 24 hour drying cycle.

2. The concrete cores were immersed in room temperature water for 48 hours. The cores were then surface dried using a towel, and the mass was determined. If the mass in a 24 hour period of soaking increased by less than 0.5%, the cores were considered saturated. This process was repeated until all cores had an increase in mass of less than 0.5% in a 24 hour period. The final mass was recorded as the saturated mass after immersion.
3. A 30 qt. aluminum cylindrical container was used to boil the cores in water for 5 hours. The cores were allowed to cool to room temperature. After cooling, the surface of the cores was dried, and the saturated mass after boiling was determined.
4. The concrete cores were suspended in room temperature water, and the immersed apparent mass was determined.

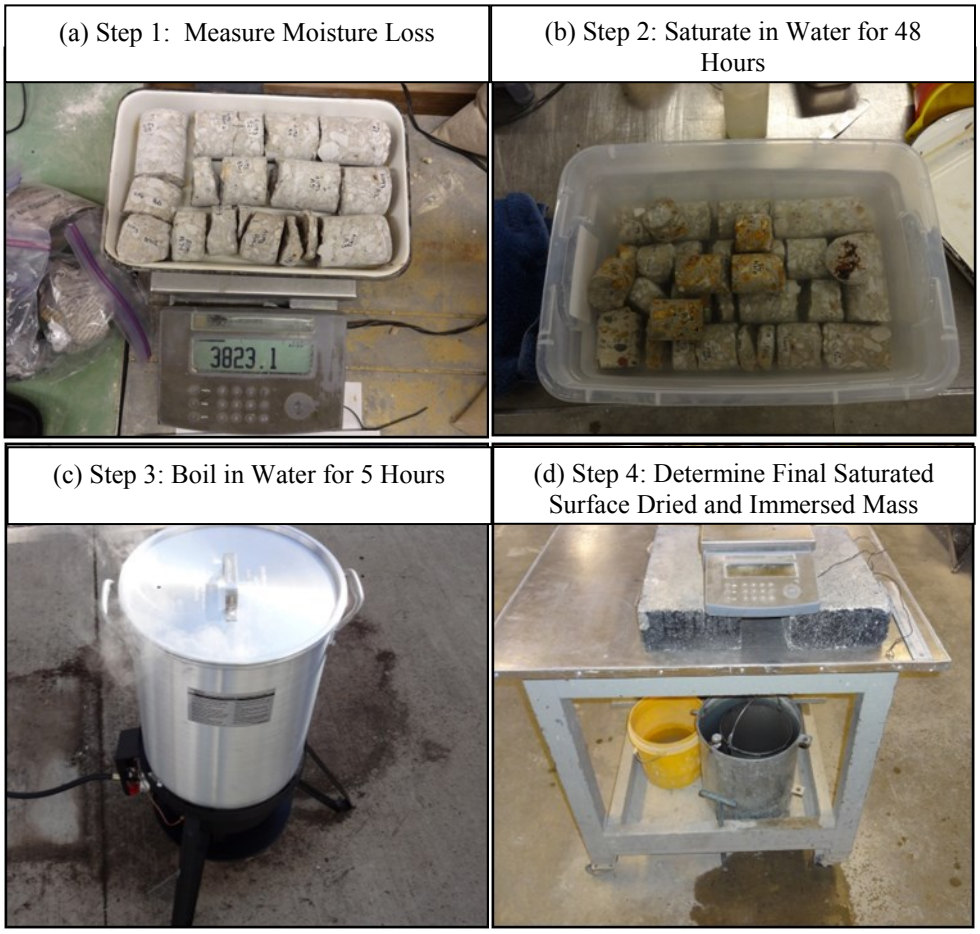

Figure 4-1 Process of Determining Volume of Permeable Pores

Section 4.2 presents the results of the visual core evaluation in tabular format and figures showing images of each core. Graphs showing volume of permeable pore space are provided for each core. Section 4.3 summarizes the core results from all bridges investigated in this project.

4.2 Core Results

4.2.1 Bridge A0569

Table 4-1 Bridge A0569 Visual Core Evaluation Results

Core	**A1**	**A2**	**A3**	**A4**
Diameter (in)	2.0	2.0	2.0	2.0
Length (in)	4.0-4.25	2.0	3.0-3.5	3.75-4.0
Surface (Asphalt: A, Concrete: C)	0.625" A	0.75" A	1.0" A in core hole	0.75" A
Number of Pieces	1	2 big, several small chunks	2 big, several small asphalt chunks	1
#1 Length (in) and failure mode [1]	4.0-4.25, CEX	0.75, PRE, asphalt debonded	0.5, PRE, asphalt debonded from concrete	3.75-4.0, CEX
#2 Length (in) and failure mode	N/A	0.75-1.25, PRE	2.25-2.75, CEX	N/A
Rebar: diameter (in), length (in), orientation [2]**, corrosion** [2]	Hit Tr. At 4.25"	None	None	None
Roughness (Smooth, Average, Very Rough)	Smooth	Average	Average	Smooth
Voids (Number >0.25 in. diameter)	0	0	0	0
Coating of the Aggregate (good or poor)	Good	Good	Good	Good
Volume of Paste (good or poor)	Good	Good	Good	Good
Air Entrained (yes or no)	Yes	Yes	Yes	Yes
Flaking surface: thickness (in)	None	None	None	None
Discoloration: color, maximum length (in)	None	None	None	None
Delaminations: depths (in)	None	0.75, 2.0	None	None
Segregation of Aggregate: depths (in)	None	None	None	None
Cracks (excluding fracture planes): number, length (in)	None	None	None	None
Other Comments	Rounded, dark colored aggregate (all cores unless noted otherwise)	Lots of material missing between pieces	Asphalt broken up by worn out bit, bit was replaced and core completed	
General Quality of Concrete[3] **(good, fair, poor)**	Good	Poor	Good	Good

[1]Preexisting Rupture (PRE), Induced during coring (IDC), Produced by shear from extracting the core (CEX), Generated during handling (HAN), Other cause (OTR)
[2]Orientation: traverse (Tr) or longitudinal (Lo); Corrosion: none (Co1), low (Co2), average (Co3), high (Co4)
[3]Good indicates no delaminations or visible deterioration, Fair indicates some visible deterioration including delaminations however concrete is in large sections, Poor indicates concrete shows a lot of deterioration and is in many pieces including several small pieces

Table 4-1 Bridge A0569 Visual Core Evaluation Results (cont.)

Core	B1	B2	C1	C2
Diameter (in)	2.0	2.0	2.0	2.0
Length (in)	3.25-3.5	3.0-3.25	3.5	4-4.25
Surface (Asphalt: A, Concrete: C)	1.25" A	C	1.5" A	1.0-1.25" A
Number of Pieces	2	1	2	2
#1 Length (in) and failure mode [1]	1.25, PRE, asphalt debonded from concrete	3.0-3.25, PRE, concrete patch debonded from original concrete	2.25-2.5, PRE	1.25-1.5, CEX
#2 Length (in) and failure mode	2-2.25, CEX	N/A	1.25-1.5, CEX	2.75-3.0, CEX
Rebar: diameter (in), length (in), orientation [2], corrosion [2]	Hit Tr. rebar at 3"	None	None	None
Roughness (Smooth, Average, Very Rough)	Average	Average	Average	Average
Voids (Number >0.25 in. diameter)	0	0	0	2
Coating of the Aggregate (good or poor)	Good	Good	Good	Good
Volume of Paste (good or poor)	Good	Good	Good	Good
Air Entrained (yes or no)	Yes	Yes	Yes	Yes
Flaking surface: thickness (in)	None	None	None	None
Discoloration: color, maximum length (in)	None	None	None	None
Delaminations: depths (in)	None	3.25 (Patch/original interface)	2.5 (Visible in core hole)	None
Segregation of Aggregate: depths (in)	None	None	None	None
Cracks (excluding fracture planes): number, length (in)	None	None	None	None
Other Comments	Hit top of rebar intentionally to determine depth	Crushed limestone coarse aggregate, 25% of bottom cross section has original concrete attached	Not much material missing between pieces, pieces fit together	Broken from extraction
General Quality of Concrete[3] (good, fair, poor)	Good	Fair	Fair	Good

[1]Preexisting Rupture (PRE), Induced during coring (IDC), Produced by shear from extracting the core (CEX), Generated during handling (HAN), Other cause (OTR)
[2]Orientation: traverse (Tr) or longitudinal (Lo); Corrosion: none (Co1), low (Co2), average (Co3), high (Co4)
[3]Good indicates no delaminations or visible deterioration, Fair indicates some visible deterioration including delaminations however concrete is in large sections, Poor indicates concrete shows a lot of deterioration and is in many pieces including several small pieces

Figure 4-2 Cores Extracted From Bridge A0569

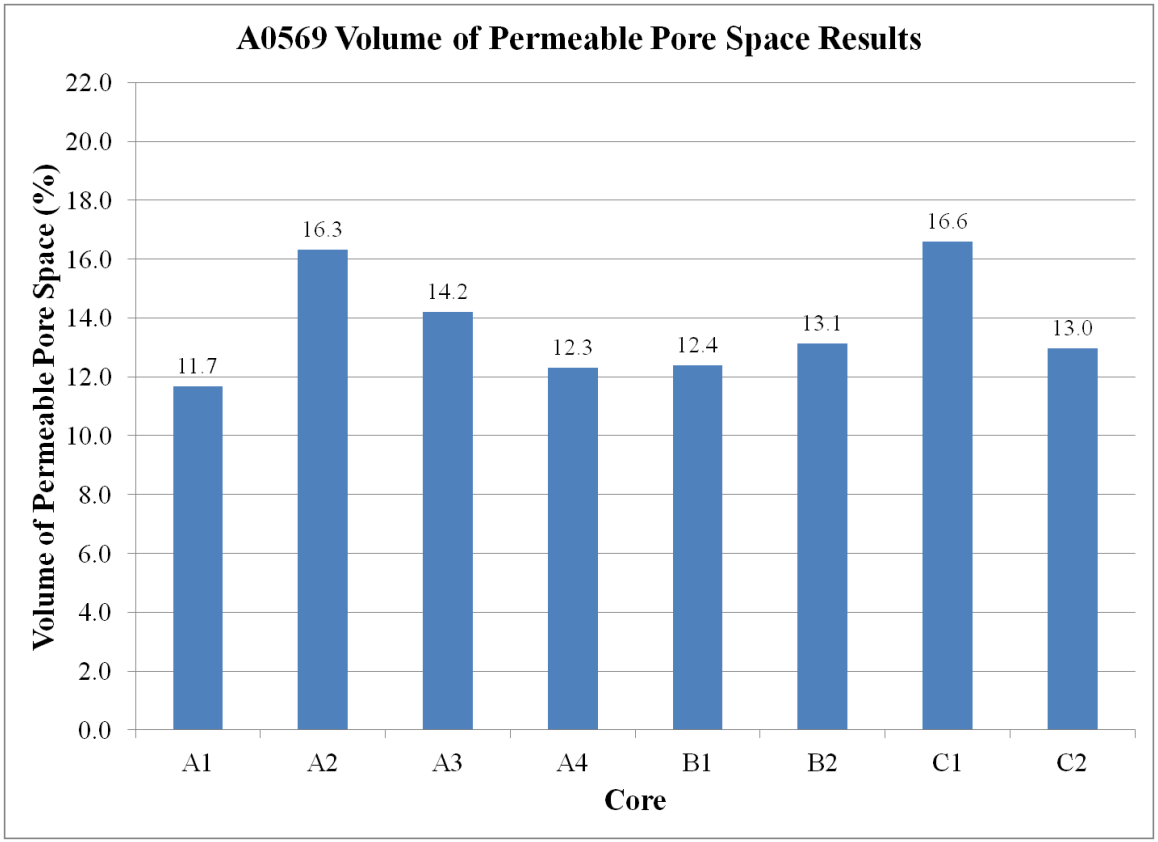

Figure 4-3 Bridge A0569 Volume of Permeable Pore Space Results

4.2.2 Bridge A1187

Table 4-2 Bridge A1187 Visual Core Evaluation Results

Core	**A1**	**A2**	**A3**	**A4**
Diameter (in)	2.0	2.0	2.0	2.0
Length (in)	3?	2.5	2.375-2.5	3-3.25
Surface (Asphalt: A, Concrete: C)	0.375" A	All A	~1" A	0.375" A
Number of Pieces	4	2	1	1
#1 Length (in) and failure mode [1]	0.375, PRE- asphalt debonded	0.75, PRE	2.375-2.5, CEX	3-3.25, CEX
#2 Length (in) and failure mode	0.5, PRE- 1/3 of cross section, very fine grey material in failure plane	1.75, CEX	N/A	N/A
#3 Length (in) and failure mode	0.5, PRE- ½ of cross section	N/A	N/A	N/A
#4 Length (in) and failure mode	0.25, PRE- ¼ of cross section	N/A	N/A	N/A
Rebar: diameter (in), length (in), orientation [2], corrosion [2]	None	None	None	None
Roughness (Smooth, Average, Very Rough)	Average	N/A	Smooth	Smooth
Voids (Number >0.25 in. diameter)	0	N/A	1	1
Coating of the Aggregate (good or poor)	Good	N/A	Good	Good
Volume of Paste (good or poor)	Good	N/A	Good	Good
Air Entrained (yes or no)	Yes	N/A	Yes	Yes
Flaking surface: thickness (in)	None	N/A	None	None
Discoloration: color, maximum length (in)	None	N/A	None	None
Delaminations: depths (in)	1.25, 2.0	N/A	None	None
Segregation of Aggregate: depths (in)	None	N/A	None	None
Cracks (excluding fracture planes): number, type, length (in)	None	N/A	None	None
Other Comments	Very deteriorated	All Asphalt	River Gravel	River Gravel
General Quality of Concrete[3] (good, fair, poor)	Poor	N/A	Good	Good

[1]Preexisting Rupture (PRE), Induced during coring (IDC), Produced by shear from extracting the core (CEX), Generated during handling (HAN), Other cause (OTR)
[2]Orientation: traverse (Tr) or longitudinal (Lo); Corrosion: none (Co1), low (Co2), average (Co3), high (Co4)
[3]Good indicates no delaminations or visible deterioration, Fair indicates some visible deterioration including delaminations however concrete is in large sections, Poor indicates concrete shows a lot of deterioration and is in many pieces including several small pieces

Table 4-2 Bridge A1187 Visual Core Evaluation Results (cont.)

Core	B1	B2	B3	B4
Diameter (in)	2.0	2.0	2.0	2.0
Length (in)	2.5-2.75	2.75-3.0	1.5-1.75	2.125-2.375
Surface (Asphalt: A, Concrete: C)	C	0.25" A	0.25" A	C
Number of Pieces	3	2	3 big, 2 small chunks	1
#1 Length (in) and failure mode [1]	0.75, PRE	0.25, PRE-asphalt debonded	0.25, PRE- asphalt debonded	2.125-2.375, CEX
#2 Length (in) and failure mode	0.75, PRE part of Piece 1	2.375, CEX	1.0, PRE	N/A
#3 Length (in) and failure mode	1.75-2.0, CEX	N/A	0.125, PRE	N/A
#4 Length (in) and failure mode	N/A	N/A	N/A	N/A
Rebar: diameter (in), length (in), orientation [2], corrosion [2]	None	None	None	None
Roughness (Smooth, Average, Very Rough)	Smooth	Smooth	Average	Smooth
Voids (Number >0.25 in. diameter)	2	3	1	1
Coating of the Aggregate (good or poor)	Good	Good	Good	Good
Volume of Paste (good or poor)	Good	Good	Good	Good
Air Entrained (yes or no)	Yes	Yes	Yes	Yes
Flaking surface: thickness (in)	None	None	None	None
Discoloration: color, maximum length (in)	None	None	None	None
Delaminations: depths (in)	0.75	None	1.0, 1.125	None
Segregation of Aggregate: depths (in)	None	None	None	None
Cracks (excluding fracture planes): number, type, length (in)	None	None	None	None
Other Comments	Mostly concrete patch, crushed limestone aggregate and fibers, bond between original concrete good-0.5" original concrete on bottom	1" Deep x 0.5" Long chunk missing from side of core	River Gravel	Concrete patch, crushed limestone aggregate
General Quality of Concrete[3] (good, fair, poor)	Fair	Fair	Poor	Good

[1]Preexisting Rupture (PRE), Induced during coring (IDC), Produced by shear from extracting the core (CEX), Generated during handling (HAN), Other cause (OTR)
[2]Orientation: traverse (Tr) or longitudinal (Lo); Corrosion: none (Co1), low (Co2), average (Co3), high (Co4)
[3]Good indicates no delaminations or visible deterioration, Fair indicates some visible deterioration including delaminations however concrete is in large sections, Poor indicates concrete shows a lot of deterioration and is in many pieces including several small pieces

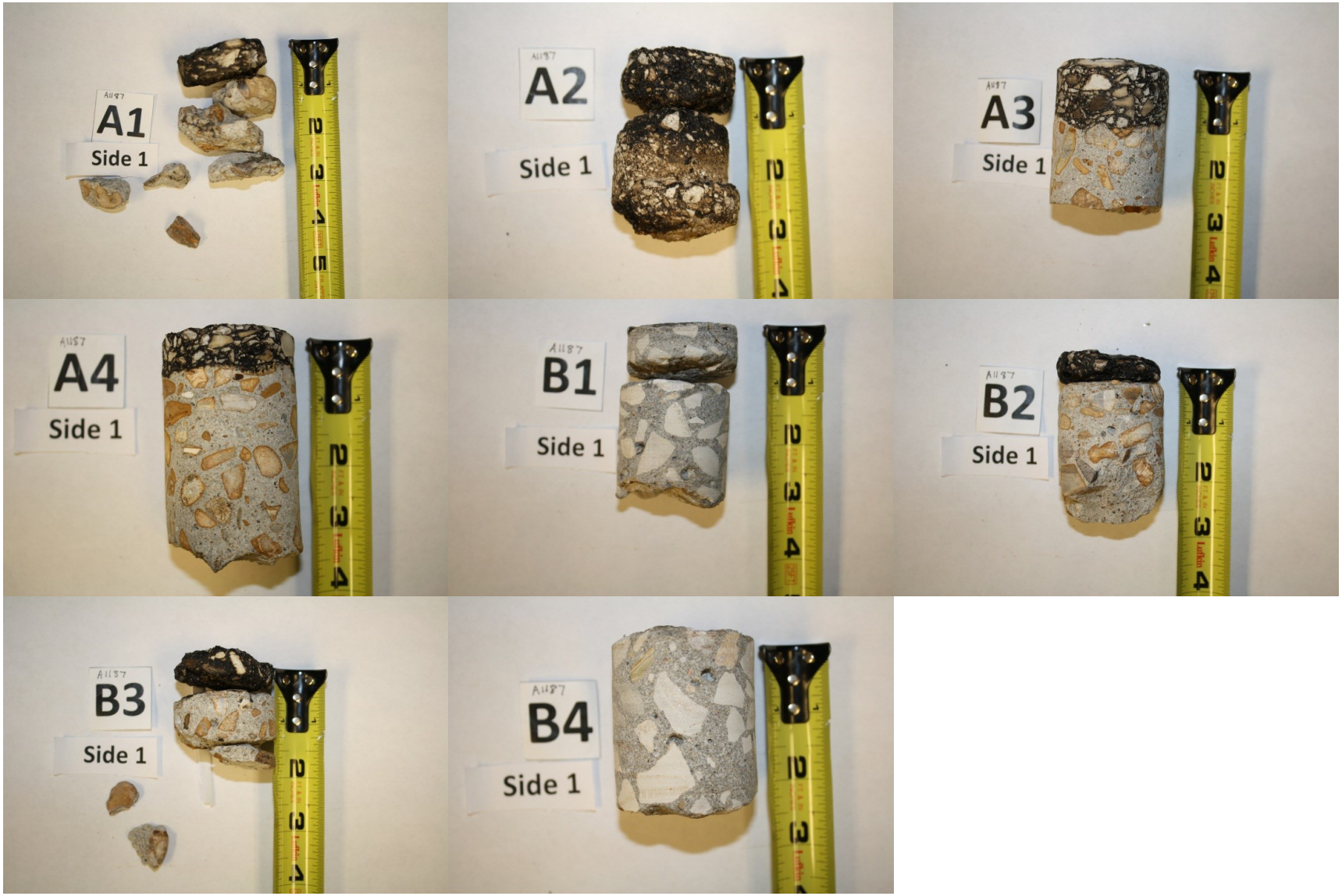

Figure 4-4 Cores Extracted From Bridge A1187

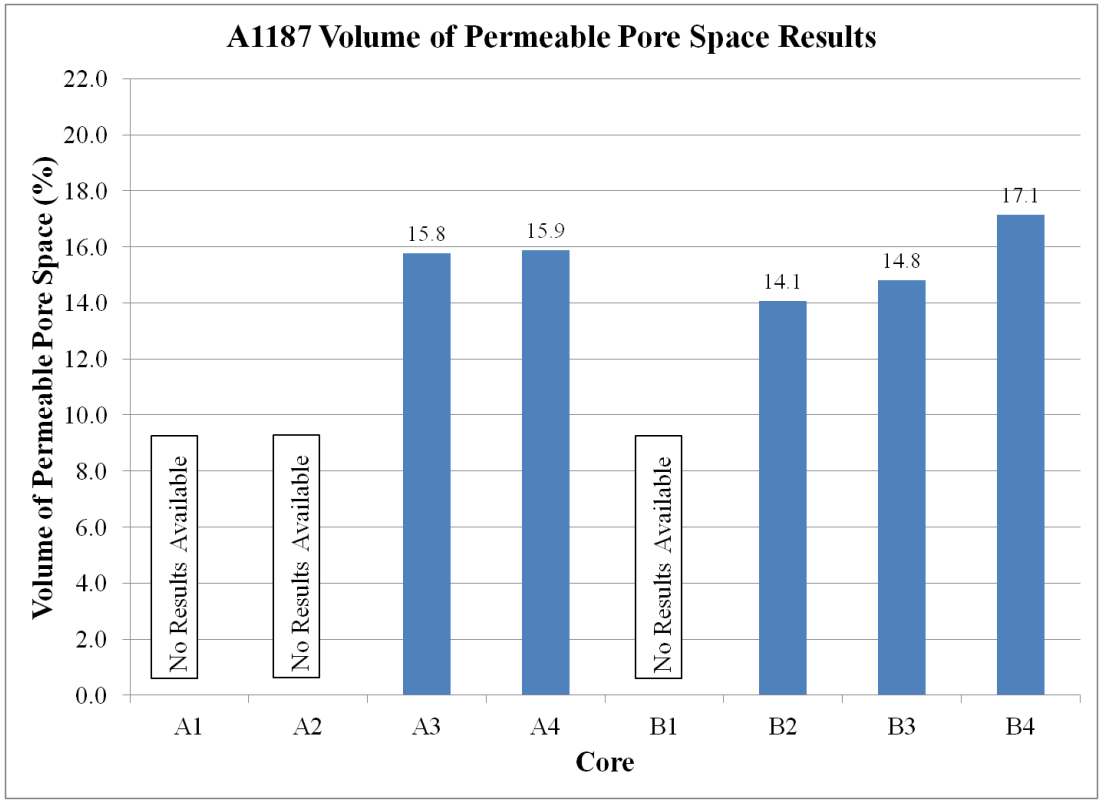

Figure 4-5 Bridge A1187 Volume of Permeable Pore Space Results

4.2.3 Bridge A1193

Table 4-3 Bridge A1193 Visual Core Evaluation Results

Core	A1	A2	A3	A4	A5
Diameter (in)	2.0	2.0	2.0	2.0	2.0
Length (in)	2.5-2.75	1.875	2.5-2.75	2.0	2.25-2.75
Surface (Asphalt: A, Concrete: C)	C	C	C	C	C
Number of Pieces	1	1	1	1	1
#1 Length (in) and failure mode [1]	2.5-2.75, CEX	1.875, PRE	2.5-2.75, CEX	2.0, CEX	2.25-2.75, CEX
#2 Length (in) and failure mode	N/A	N/A	N/A	N/A	N/A
Rebar: diameter (in), length (in), orientation [2], corrosion [2]	None	None	None	None	None
Roughness (Smooth, Average, Very Rough)	Average	Smooth	Average	Smooth	Average
Voids (Number >0.25 in. diameter)	2	0	2	2	1
Coating of the Aggregate (good or poor)	Good	Good	Good	Good	Good
Volume of Paste (good or poor)	Good	Good	Good	Good	Good
Air Entrained (yes or no)	Yes	Yes	Yes	Yes	Yes
Flaking surface: thickness (in)	None	None	None	None	None
Discoloration: color, maximum length (in)	None	None	None	None	None
Delaminations: depths (in)	None	1.875	None	None	None
Segregation of Aggregate: depths (in)	None	None	None	None	None
Cracks (excluding fracture planes): number, length (in)	None	None	None	None	None
Other Comments	Crushed Limestone Coarse Aggregate (all cores)				
General Quality of Concrete[3] (good, fair, poor)	Good	Fair	Good	Good	Good

[1]Preexisting Rupture (PRE), Induced during coring (IDC), Produced by shear from extracting the core (CEX), Generated during handling (HAN), Other cause (OTR)
[2]Orientation: traverse (Tr) or longitudinal (Lo); Corrosion: none (Co1), low (Co2), average (Co3), high (Co4)
[3]Good indicates no delaminations or visible deterioration, Fair indicates some visible deterioration including delaminations however concrete is in large sections, Poor indicates concrete shows a lot of deterioration and is in many pieces including several small pieces

Table 4-3 Bridge A1193 Visual Core Evaluation Results (cont.)

Core	B1	B2	B3	B4	B5	B6	B7
Diameter (in)	2.0	2.0	2.0	2.0	2.0	2.0	2.0
Length (in)	0.75-1.25	2.75-3.0	2.75-3.0	2.75-3.0	3.0	1.25-1.5	2.5-3.25
Surface (Asphalt: A, Concrete: C)	C	C	C	C	C	C	C
Number of Pieces	2 big, several small	2	2	3	1	1	2
#1 Length (in) and failure mode [1]	0.5, PRE	1.0-1.25, PRE	1.75, PRE	1.25-1.5, PRE	3.0, CEX	1.25-1.5, CEX	1.25, PRE
#2 Length (in) and failure mode	0.25-0.75, PRE	1.5-1.75, CEX	0.5-1.25, CEX	0-.625, PRE	N/A	N/A	1.25-2.0, CEX
#3 Length (in) and failure mode	N/A	N/A	N/A	0.75-1.125, CEX	N/A	N/A	N/A
Rebar: diameter (in), length (in), orientation [2], corrosion [2]	None	Tr. rebar hit in bottom of hole, 3" Deep, did not cut through	None	None	None	Hit Tr. rebar at 1.5" deep	None
Roughness (Smooth, Average, Very Rough)	Average	Smooth	Average	Smooth	Smooth	Average	Average
Voids (Number >0.25 in. diameter)	1	1	1	0	0	0	1
Coating of the Aggregate (good or poor)	Good	Good	Good	Good	Good	Good	Good
Volume of Paste (good or poor)	Good	Good	Good	Good	Good	Good	Good
Air Entrained (yes or no)	Yes	Yes	Yes	Yes	Yes	Yes	Yes
Flaking surface: thickness (in)	None	None	None	None	None	None	None
Discoloration: color, maximum length (in)	None	Rust, depth 2.0", less than 0.25" diameter	None	None	None	None	None
Delaminations: depths (in)	0.5, 0.75	1.0-1.25	1.75	1.25, 1.75	None	None	1.25
Segregation of Aggregate: depths (in)	None	None	None	None	None	None	None
Cracks (excluding fracture planes): number, length (in)	None	None	None	None	None	None	None
Other Comments	Material missing between pieces	Pieces fit tightly together	Material missing between pieces, delam. visible in core hole	Material missing in between pieces, delam. visible in core hole			Material missing between pieces
General Quality of Concrete[3] (good, fair, poor)	Poor	Fair	Fair	Poor	Good	Good	Fair

[1]Preexisting Rupture (PRE), Induced during coring (IDC), Produced by shear from extracting the core (CEX), Generated during handling (HAN), Other cause (OTR)
[2]Orientation: traverse (Tr) or longitudinal (Lo); Corrosion: none (Co1), low (Co2), average (Co3), high (Co4)
[3]Good indicates no delaminations or visible deterioration, Fair indicates some visible deterioration including delaminations however concrete is in large sections, Poor indicates concrete shows a lot of deterioration and is in many pieces including several small pieces

Figure 4-6 Cores Extracted From Bridge A1193

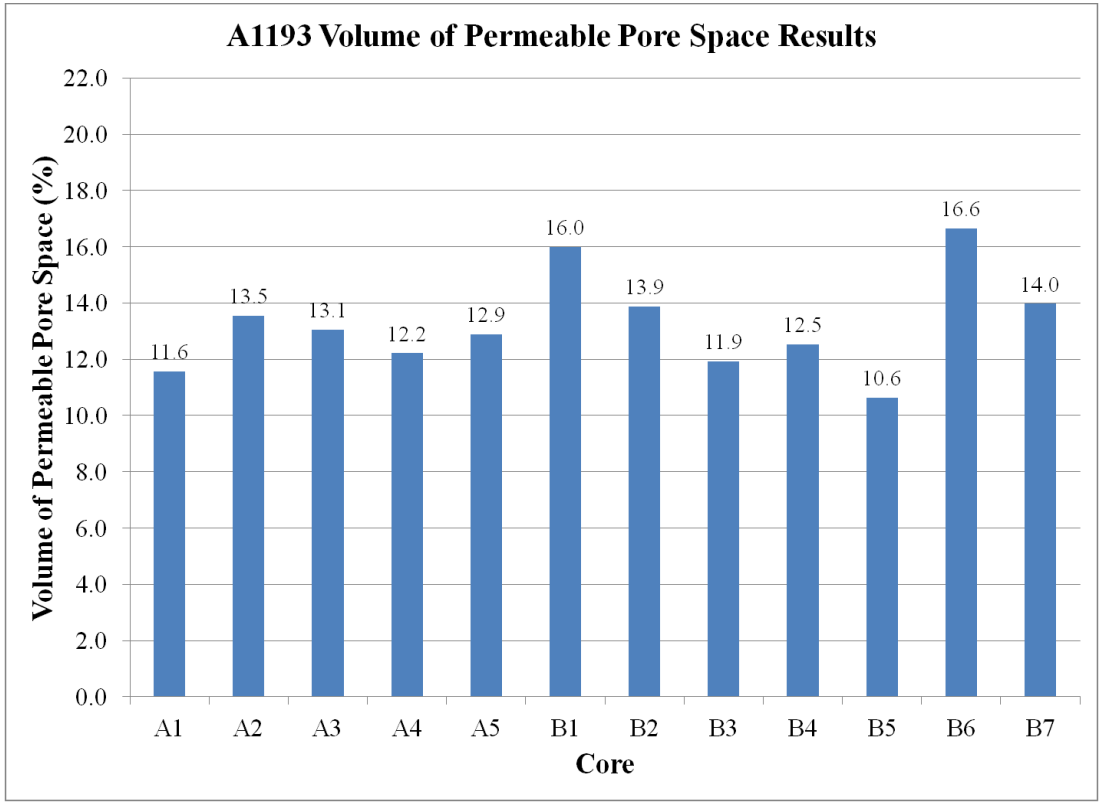

Figure 4-7 Bridge 1193 Volume of Permeable Pore Space Results

4.2.4 Bridge A1297

Table 4-4 Bridge A1297 Visual Core Evaluation Results

Core	A1	A2	A3	B1	B2	B3
Diameter (in)	2.0	2.0	2.0	2.0	2.0	2.0
Length (in)	2.5-3.0	2.75-3.375	3.125-3.75	~3.0	5.25-6.0	3.875-4.125
Surface (Asphalt: A, Concrete: C)	C	C	C	C	C	C
Number of Pieces	1	1	2	5	2	1
#1 Length (in) and failure mode [1]	2.5-3.0, CEX	2.75-3.375, CEX	1.875, PRE	1.5, PRE-Non rebar metal in core	0.25-1.0, PRE	3.875-4.125, CEX
#2 Length (in) and failure mode	N/A	N/A	1.25-1.75, CEX	0.25, PRE- Non rebar metal in core	4.25-4.75, CEX	N/A
#3 Length (in) and failure mode	N/A	N/A	N/A	0.25, PRE	N/A	N/A
#4 Length (in) and failure mode	N/A	N/A	N/A	0.25, PRE	N/A	N/A
#5 Length (in) and failure mode	N/A	N/A	N/A	0.25, CEX- Rebar marks visible on edge	N/A	N/A
Rebar: diameter (in), length (in), orientation [2], corrosion [2]	None	None	None	None	None	None
Roughness (Smooth, Average, Very Rough)	Smooth	Average	Average	Rough	Average	Average
Voids (Number >0.25 in. diameter)	1	2	0	0	5	1, 0.875" long 0.5" wide, 0.5" deep
Coating of the Aggregate (good or poor)	Good	Good	Good	Good	Good	Good
Volume of Paste (good or poor)	Good	Good	Good	Good	Good	Good
Air Entrained (yes or no)	Yes	Yes	Yes	Yes	Yes	Yes
Flaking surface: thickness (in)	None	None	None	None	None	None
Discoloration: color, maximum length (in)	None	None	None	Rust, 1.5 @ Bottom of piece 1 and 2	None	None
Delaminations: depths (in)	None	None	1.875	1.5, 1.75, 2.0	1.0	None
Segregation of Aggregate: depths (in)	None	None	None	None	None	None
Cracks (excluding fracture planes): number, type, length (in)	None	None	None	None	None	None
Other Comments						
General Quality of Concrete[3] (good, fair, poor)	Good	Good	Fair	Poor	Fair	Good

[1]Preexisting Rupture (PRE), Induced during coring (IDC), Produced by shear from extracting the core (CEX), Generated during handling (HAN), Other cause (OTR)
[2]Orientation: traverse (Tr) or longitudinal (Lo); Corrosion: none (Co1), low (Co2), average (Co3), high (Co4)
[3]Good indicates no delaminations or visible deterioration, Fair indicates some visible deterioration including delaminations however concrete is in large sections, Poor indicates concrete shows a lot of deterioration and is in many pieces including several small pieces

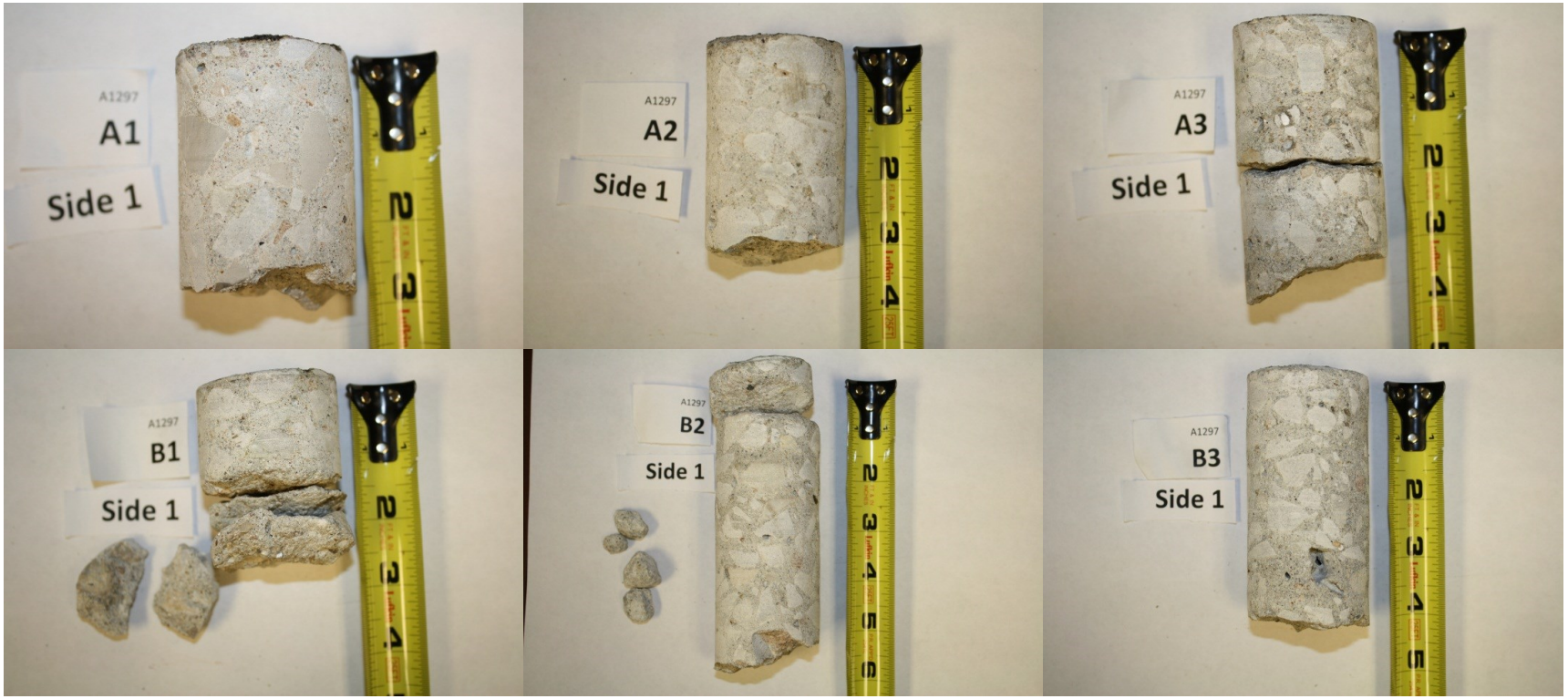

Figure 4-8 Cores Extracted From Bridge A1297

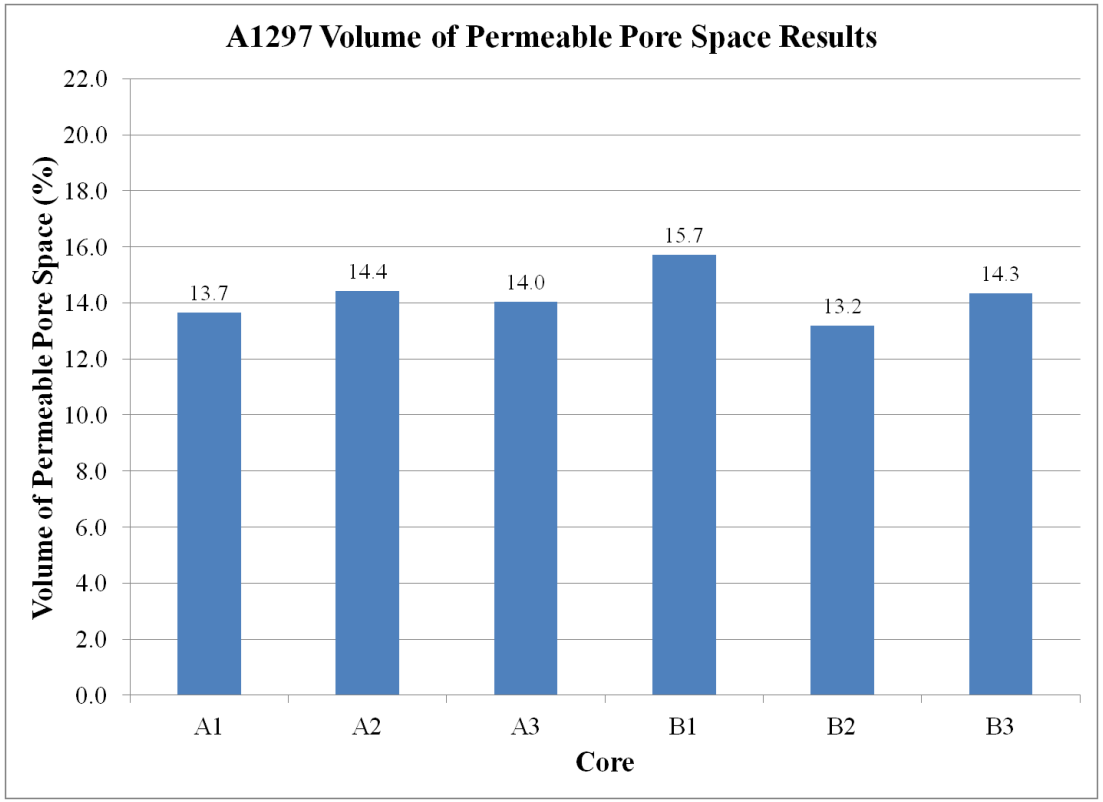

Figure 4-9 Bridge A1297 Volume of Permeable Pore Space Results

4.2.5 Bridge A1479

Table 4-5 Bridge A1479 Visual Core Evaluation Results

Core	A1	A2	A3	A4
Diameter (in)	2.0	2.0	2.0	2.0
Length (in)	1.0	2.25-2.5	2.0-2.75	2.875
Surface (Asphalt: A, Concrete: C)	C	C	C	C
Number of Pieces	1	1	2	1
#1 Length (in) and failure mode [1]	1.0, PRE	2.25-2.5, CEX	1.0, PRE	2.875, CEX
#2 Length (in) and failure mode	N/A	N/A	1.0-1.75, CEX	N/A
#3 Length (in) and failure mode	N/A	N/A	N/A	N/A
#4 Length (in) and failure mode	N/A	N/A	N/A	N/A
#5 Length (in) and failure mode	N/A	N/A	N/A	N/A
Rebar: diameter (in), length (in), orientation [2], corrosion [2]	None	Welded Wire, 0.1875 Diam., Lo, Co1	None	None
Roughness (Smooth, Average, Very Rough)	Average	Average	Average	Average
Voids (Number >0.25 in. diameter)	0	2	1	1
Coating of the Aggregate (good or poor)	Good	Good	Good	Good
Volume of Paste (good or poor)	Good	Good	Good	Good
Air Entrained (yes or no)	Yes	Yes	Yes	Yes
Flaking surface: thickness (in)	None	None	None	None
Discoloration: color, maximum length (in)	None	None	None	None
Delaminations: depths (in)	1.0	None	1.0	None
Segregation of Aggregate: depths (in)	None	None	None	None
Cracks (excluding fracture planes): number, length (in)	None	1, 2” Deep	None	None
Other Comments	Bottom Piece left in hole, would have had to break up to remove, solid in hole	Concrete patch, Rounded coarse aggregate	Material at delamination missing	
General Quality of Concrete[3] (good, fair, poor)	Fair	Good	Fair	Good

[1]Preexisting Rupture (PRE), Induced during coring (IDC), Produced by shear from extracting the core (CEX), Generated during handling (HAN), Other cause (OTR)
[2]Orientation: traverse (Tr) or longitudinal (Lo); Corrosion: none (Co1), low (Co2), average (Co3), high (Co4)
[3]Good indicates no delaminations or visible deterioration, Fair indicates some visible deterioration including delaminations however concrete is in large sections, Poor indicates concrete shows a lot of deterioration and is in many pieces including several small pieces

Table 4-5 Bridge A1479 Visual Core Evaluation Results (cont.)

Core	B1	B2	B3	B4	B5
Diameter (in)	2.0	2.0	2.0	2.0	2.0
Length (in)	2.0-2.5	2.0-2.5	2.125-2.5	1.25-1.75	2.0-2.25
Surface (Asphalt: A, Concrete: C)	C	1.75-2.0 A	C	C	C
Number of Pieces	1	2	1	1	1
#1 Length (in) and failure mode [1]	2.0-2.5, CEX	1.75-2.0, PRE asphalt debonded	2.125-2.5, CEX	1.25-1.75, PRE	2.0-2.25, CEX
#2 Length (in) and failure mode	N/A	0.75, PRE	N/A	N/A	N/A
#3 Length (in) and failure mode	N/A	N/A	N/A	N/A	N/A
#4 Length (in) and failure mode	N/A	N/A	N/A	N/A	N/A
#5 Length (in) and failure mode	N/A	N/A	N/A	N/A	N/A
Rebar: diameter (in), length (in), orientation [2], corrosion [2]	None	None	None	None	None
Roughness (Smooth, Average, Very Rough)	Average	Average	Average	Average	Average
Voids (Number >0.25 in. diameter)	5	0	2	2	1
Coating of the Aggregate (good or poor)	Good	Good	Good	Good	Good
Volume of Paste (good or poor)	Good	Good	Good	Good	Good
Air Entrained (yes or no)	Yes	Yes	Yes	Yes	Yes
Flaking surface: thickness (in)	None	None	None	None	None
Discoloration: color, maximum length (in)	None	None	None	None	None
Delaminations: depths (in)	None	2.5	None	1.75	None
Segregation of Aggregate: depths (in)	None	None	None	None	None
Cracks (excluding fracture planes): number, length (in)	None	None	1, 2.25" deep, Induced by extraction	None	None
Other Comments		Mostly asphalt, asphalt was debonded from concrete sliver		Remaining core left in hole, solid in hole, would have broken up during removal	
General Quality of Concrete[3] (good, fair, poor)	Good	Poor	Good	Fair	Good

[1]Preexisting Rupture (PRE), Induced during coring (IDC), Produced by shear from extracting the core (CEX), Generated during handling (HAN), Other cause (OTR)
[2]Orientation: traverse (Tr) or longitudinal (Lo); Corrosion: none (Co1), low (Co2), average (Co3), high (Co4)
[3]Good indicates no delaminations or visible deterioration, Fair indicates some visible deterioration including delaminations however concrete is in large sections, Poor indicates concrete shows a lot of deterioration and is in many pieces including several small pieces

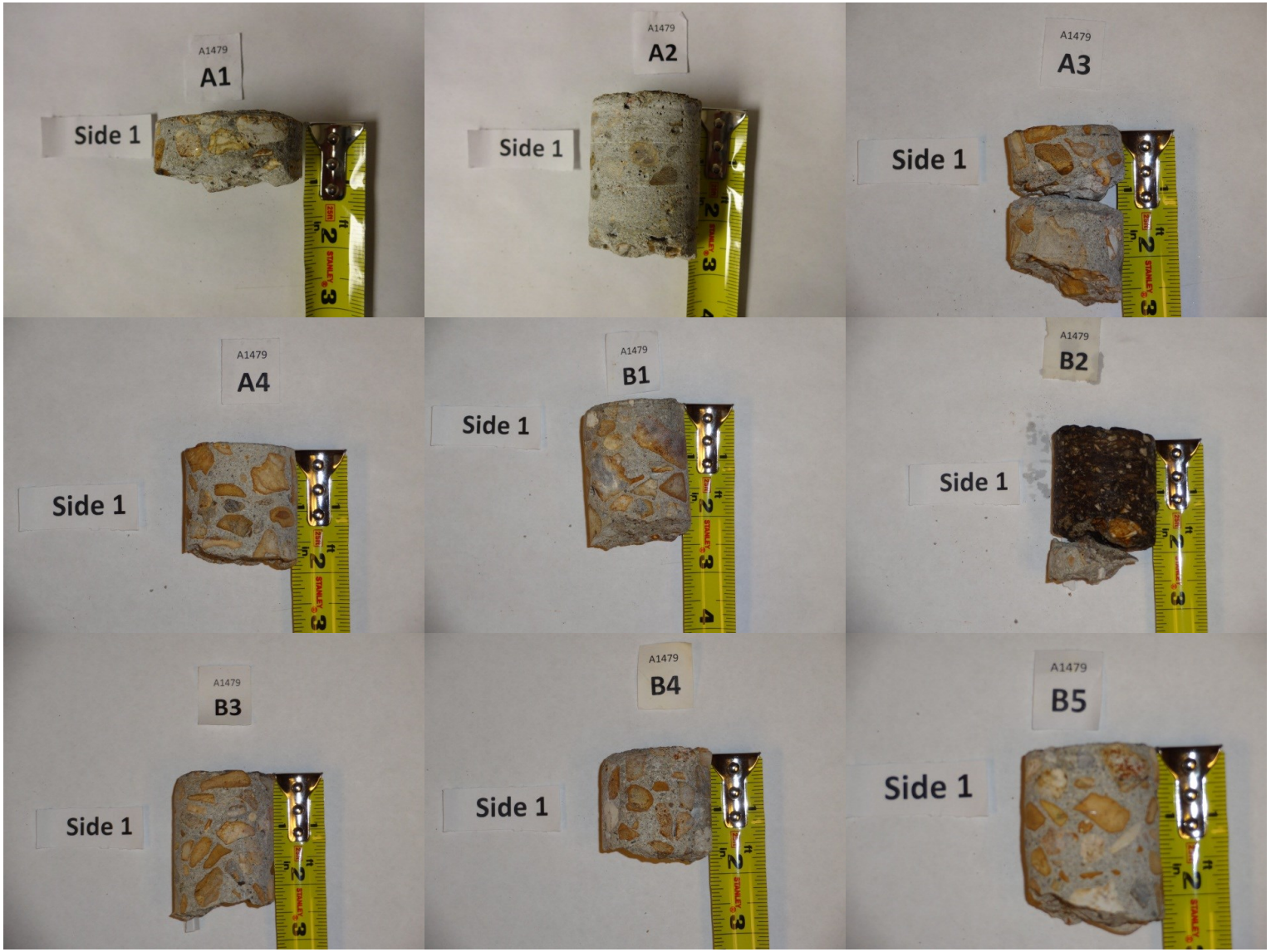

Figure 4-10 Cores Extracted From Bridge A1479

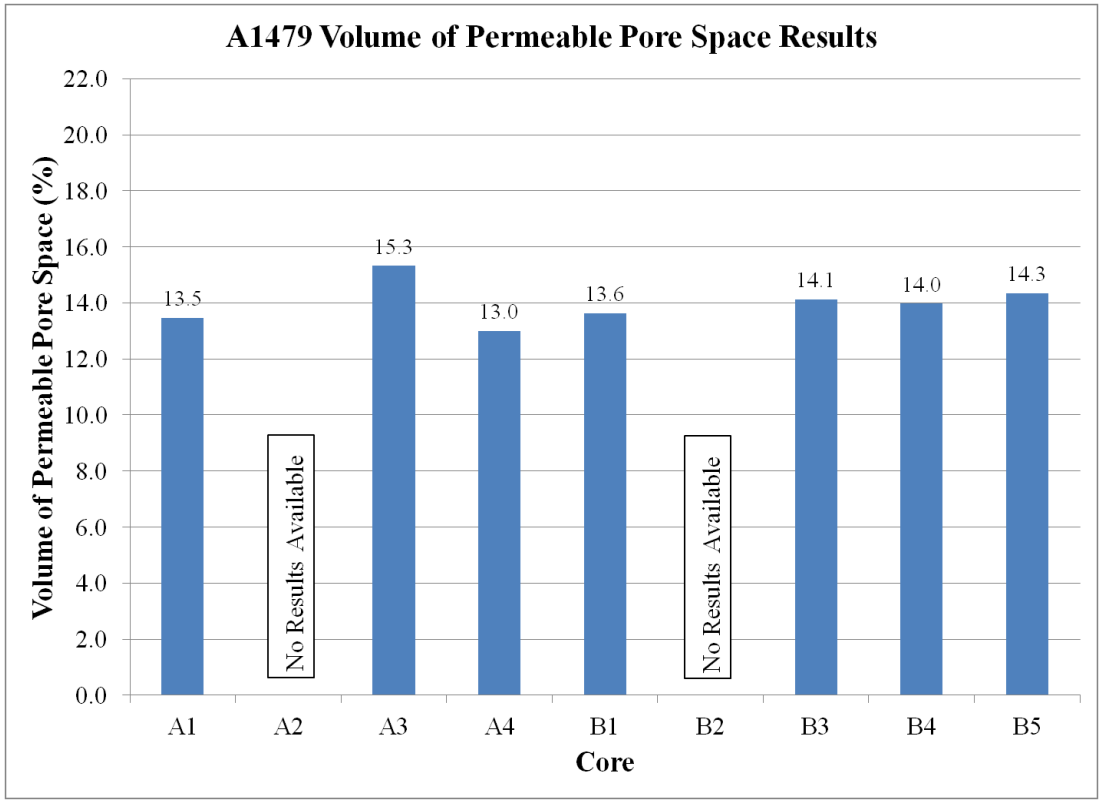

Figure 4-11 Bridge A1479 Volume of Permeable Pore Space Results

4.2.6 Bridge A2111

Table 4-6 Bridge A2111 Visual Core Evaluation Results

Core	A1	A2	A3
Diameter (in)	2.0	2.0	2.0
Length (in)	4.25	3.375-3.75	2.625-3.25
Surface (Asphalt: A, Concrete: C)	C	C	C
Number of Pieces	2	2	3
#1 Length (in) and failure mode [1]	1.0, IDC?	1.875, PRE?	1.75, PRE
#2 Length (in) and failure mode	3.25, CEX	1.5-1.875, CEX	0.5, PRE
#3 Length (in) and failure mode	N/A	N/A	0.75-1.25, CEX
Rebar: diameter (in), length (in), orientation [2], corrosion [2]	None	None	None
Roughness (Smooth, Average, Very Rough)	Rough	Smooth	Smooth
Voids (Number >0.25 in. diameter)	5	4	5
Coating of the Aggregate (good or poor)	Good	Good	Good
Volume of Paste (good or poor)	Good	Good	Good
Air Entrained (yes or no)	Yes	Yes	Yes
Flaking surface: thickness (in)	None	None	None
Discoloration: color, maximum length (in)	None	None	None
Delaminations: depths (in)	None?	1.875?	1.75, 2.25
Segregation of Aggregate: depths (in)	None	None	None
Cracks (excluding fracture planes): number, type, length (in)	None	None	None
Other Comments	No crack visible in hole, uncertain if core had preexisting rupture or it was induced during coring. Pieces fit together tight with some material missing around edges. Impact echo results show no evidence of crack.	No crack visible in hole, uncertain if core had preexisting rupture or it was induced during coring. Pieces fit together tight with some material missing around edges. Impact echo suggests preexisting crack.	Large void in core. Core hole had rust color on the sides. Cracks visible in core hole at depths of 1.75" and 2".
General Quality of Concrete[3] (good, fair, poor)	Good	Fair	Fair

[1]Preexisting Rupture (PRE), Induced during coring (IDC), Produced by shear from extracting the core (CEX), Generated during handling (HAN), Other cause (OTR)
[2]Orientation: traverse (Tr) or longitudinal (Lo); Corrosion: none (Co1), low (Co2), average (Co3), high (Co4)
[3]Good indicates no delaminations or visible deterioration, Fair indicates some visible deterioration including delaminations however concrete is in large sections, Poor indicates concrete shows a lot of deterioration and is in many pieces including several small pieces

Table 4-6 Bridge A2111 Visual Core Evaluation Results (cont.)

Core	B1	B2	B3
Diameter (in)	2.0	2.0	2.0
Length (in)	3.75	3.5	2.875-3.25
Surface (Asphalt: A, Concrete: C)	C	C	C
Number of Pieces	2	2	1
#1 Length (in) and failure mode [1]	2.25, PRE	1.75, PRE?	2.875-3.25, CEX
#2 Length (in) and failure mode	1.5, CEX	1.75, CEX	N/A
#3 Length (in) and failure mode	N/A	N/A	N/A
Rebar: diameter (in), length (in), orientation [2], corrosion [2]	None	None	None
Roughness (Smooth, Average, Very Rough)	Average	Average	None
Voids (Number >0.25 in. diameter)	4	5	5
Coating of the Aggregate (good or poor)	Good	Good	Good
Volume of Paste (good or poor)	Good	Good	Good
Air Entrained (yes or no)	Yes	Yes	Yes
Flaking surface: thickness (in)	None	None	None
Discoloration: color, maximum length (in)	None	None	None
Delaminations: depths (in)	2.25	1.75?	None
Segregation of Aggregate: depths (in)	None	None	None
Cracks (excluding fracture planes): number, type, length (in)	None	None	None
Other Comments	Crack visible in hole at depth of 2.5". Pieces lock together.	Fracture may have occurred by coring, no cracks visible in core hole. Impact echo suggests preexisting crack in core.	
General Quality of Concrete[3] (good, fair, poor)	Fair	Fair	Good

[1]Preexisting Rupture (PRE), Induced during coring (IDC), Produced by shear from extracting the core (CEX), Generated during handling (HAN), Other cause (OTR)
[2]Orientation: traverse (Tr) or longitudinal (Lo); Corrosion: none (Co1), low (Co2), average (Co3), high (Co4)
[3]Good indicates no delaminations or visible deterioration, Fair indicates some visible deterioration including delaminations however concrete is in large sections, Poor indicates concrete shows a lot of deterioration and is in many pieces including several small pieces

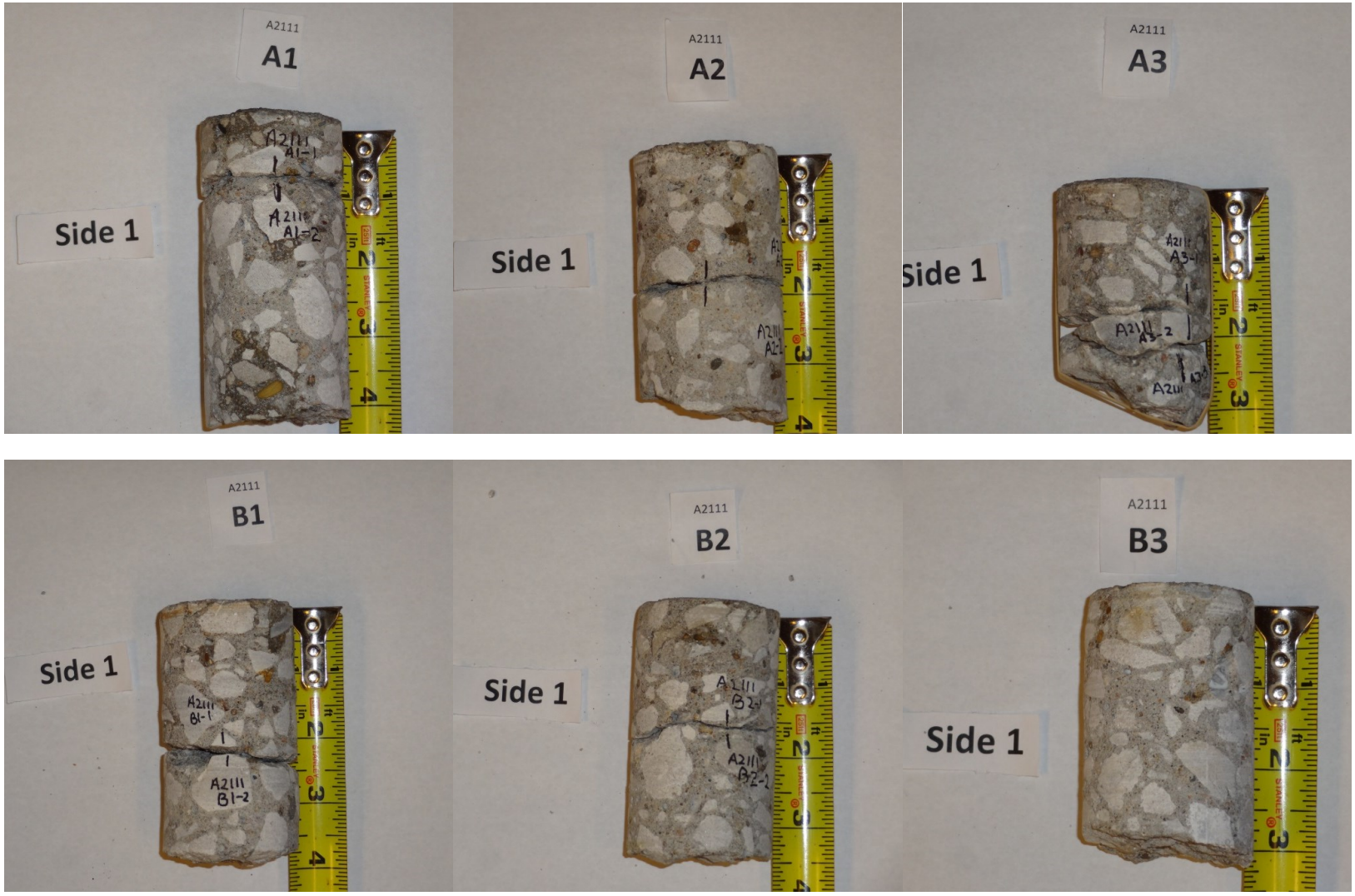

Figure 4-12 Cores Extracted From Bridge A2111

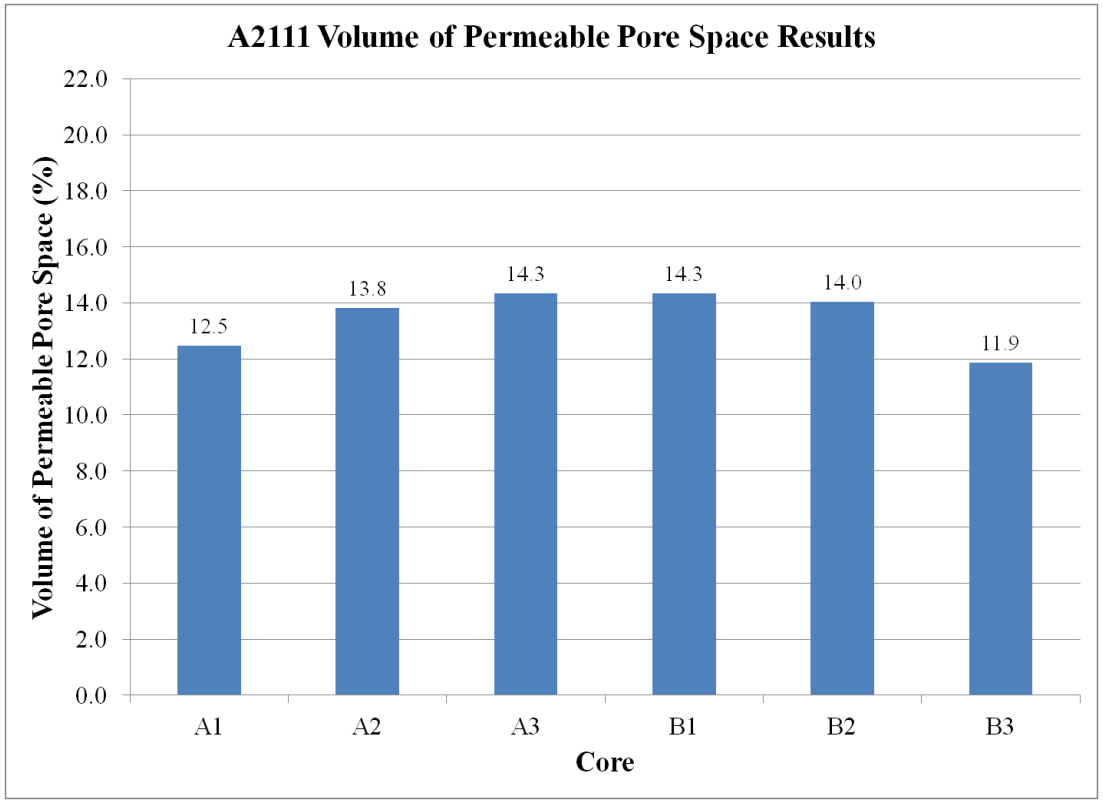

Figure 4-13 Bridge A2111 Volume of Permeable Pore Space Results

4.2.7 Bridge A2966

Table 4-7 Bridge A2966 Visual Core Evaluation Results

Core	A1	A2	A3
Diameter (in)	2.0	2.0	2.0
Length (in)	4.5	2.5-2.875	2.875
Surface (Asphalt: A, Concrete: C)	<0.1" A	<0.1" A	0.125" A
Number of Pieces	3	1	1
#1 Length (in) and failure mode [1]	1.0-1.25, PRE-locks together very tightly with piece 2	2.5-2.875, CEX fracture plane has 1 thin and elongated aggregate piece	2.875, CEX fracture plane has unbonded rebar
#2 Length (in) and failure mode	0.625-1.125, PRE-locks together with piece 3 with lots of voids around fracture 0.25" diameter rust spot on fracture plane	N/A	N/A
#3 Length (in) and failure mode	2.0-2.5, CEX	N/A	N/A
Rebar: diameter (in), length (in), orientation [2], corrosion [2]	None	None	#5, 2.0", Tr, Co1
Roughness (Smooth, Average, Very Rough)	Average	Smooth	Smooth
Voids (Number >0.25 in. diameter)	2	3	2
Coating of the Aggregate (good or poor)	Good	Good	Good
Volume of Paste (good or poor)	Good	Good	Good
Air Entrained (yes or no)	Yes	Yes	Yes
Flaking surface: thickness (in)	None	None	None
Discoloration: color, maximum length (in)	None	None	None
Delaminations: depths (in)	1.25	None	None
Segregation of Aggregate: depths (in)	None	None	None
Cracks (excluding fracture planes): number, type, length (in)	0	0	0
Other Comments			
General Quality of Concrete[3] (good, fair, poor)	Fair	Good	Good

[1]Preexisting Rupture (PRE), Induced during coring (IDC), Produced by shear from extracting the core (CEX), Generated during handling (HAN), Other cause (OTR)
[2]Orientation: traverse (Tr) or longitudinal (Lo); Corrosion: none (Co1), low (Co2), average (Co3), high (Co4)
[3]Good indicates no delaminations or visible deterioration, Fair indicates some visible deterioration including delaminations however concrete is in large sections, Poor indicates concrete shows a lot of deterioration and is in many pieces including several small pieces

Table 4-7 Bridge A2966 Visual Core Evaluation Results (cont.)

Core	B1	B2	B3
Diameter (in)	2.0	2.0	2.0
Length (in)	3?	3.125-3.5	6.25-6.5
Surface (Asphalt: A, Concrete: C)	C	25% A <.125" thick, 75% C	50% A <.125" thick, 50% C
Number of Pieces	3 Big, numerous small chunks	2 Big, 8 small chunks	2
#1 Length (in) and failure mode [1]	1.25-1.375, PRE	1.5-2.0, PRE	1.75-1.875, PRE-locks together very tightly with piece 2
#2 Length (in) and failure mode	0.375, PRE	1-1.5, CEX	4.625, CEX
#3 Length (in) and failure mode	0.25-0.75, CEX	N/A	N/A
Rebar: diameter (in), length (in), orientation [2], corrosion [2]	None	None	None
Roughness (Smooth, Average, Very Rough)	Very Rough	Smooth	Smooth
Voids (Number >0.25 in. diameter)	1	1	3
Coating of the Aggregate (good or poor)	Good	Good	Good
Volume of Paste (good or poor)	Good	Good	Good
Air Entrained (yes or no)	Yes	Yes	Yes
Flaking surface: thickness (in)	None	None	None
Discoloration: color, maximum length (in)	None	None	None
Delaminations: depths (in)	1.375, 1.75	1.875	1.875
Segregation of Aggregate: depths (in)	None	None	None
Cracks (excluding fracture planes): number, type, length (in)	0	0	0
Other Comments			
General Quality of Concrete[3] (good, fair, poor)	Poor	Poor	Fair

[1]Preexisting Rupture (PRE), Induced during coring (IDC), Produced by shear from extracting the core (CEX), Generated during handling (HAN), Other cause (OTR)
[2]Orientation: traverse (Tr) or longitudinal (Lo); Corrosion: none (Co1), low (Co2), average (Co3), high (Co4)
[3]Good indicates no delaminations or visible deterioration, Fair indicates some visible deterioration including delaminations however concrete is in large sections, Poor indicates concrete shows a lot of deterioration and is in many pieces including several small pieces

Figure 4-14 Cores Extracted From Bridge A2966

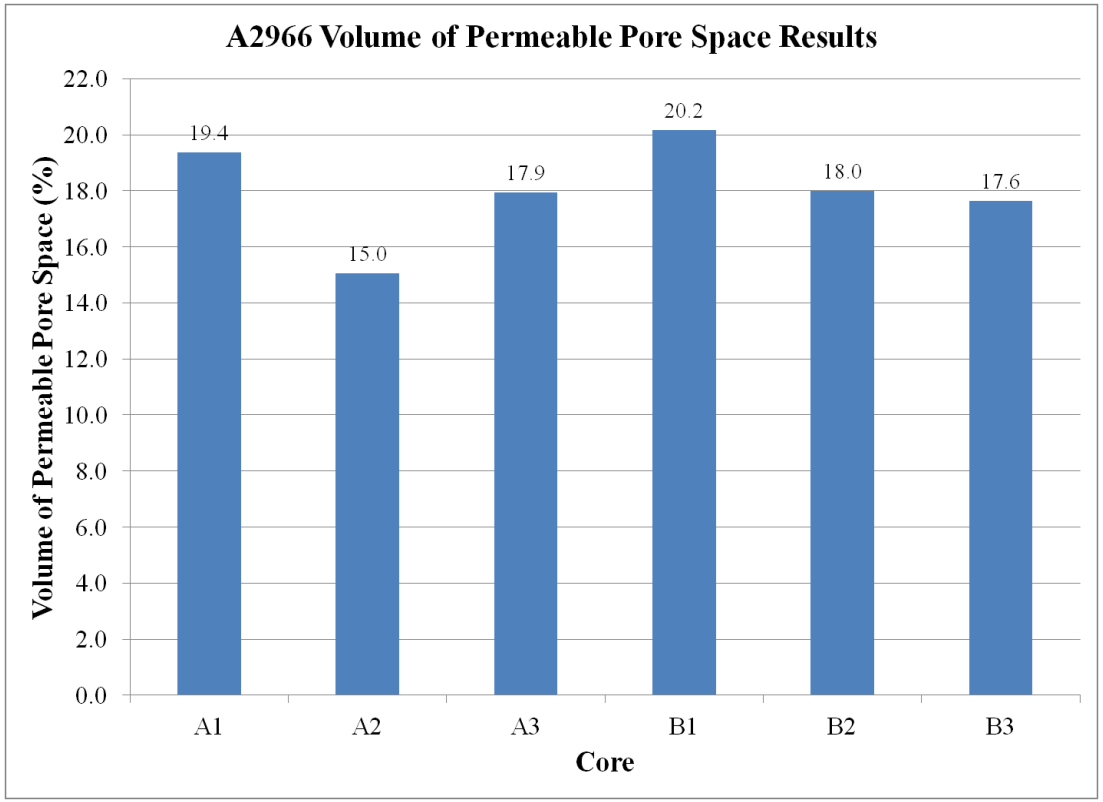

Figure 4-15 Bridge A2966 Volume of Permeable Pore Space Results

4.2.8 Bridge A3017

Table 4-8 Bridge A3017 Visual Core Evaluation Results

Core	A1	A2	A3	A4
Diameter (in)	2.0	2.0	2.0	2.0
Length (in)	3.25	3.375	3.5	2.25
Surface (Asphalt: A, Concrete: C)	C	C	C	C
Number of Pieces	1	2	2	2 large, several small
#1 Length (in) and failure mode [1]	3.25, IDC, rebar chair at bottom of hole	1.25, PRE	0.875, PRE	1.625, PRE
#2 Length (in) and failure mode	N/A	2.125, CEX	2.625, CEX	0.25, PRE
#3 Length (in) and failure mode	N/A	N/A	N/A	N/A
Rebar: diameter (in), length (in), orientation [2], corrosion [2]	Rebar chair, ¼" diameter, left in hole, Co1	None	None	None
Roughness (Smooth, Average, Very Rough)	Average	Average	Average	Smooth
Voids (Number >0.25 in. diameter)	2	8	5	3
Coating of the Aggregate (good or poor)	Good	Good	Good	Good
Volume of Paste (good or poor)	Good	Good	Good	Good
Air Entrained (yes or no)	Yes	Yes	Yes	Yes
Flaking surface: thickness (in)	None	None	None	None
Discoloration: color, maximum length (in)	None	None	None	None
Delaminations: depths (in)	None	1.25	0.875	1.625
Segregation of Aggregate: depths (in)	None	None	None	None
Cracks (excluding fracture planes): number, length (in)	None	None	None	None
Other Comments	Core came out in bit without any prying to break loose. Possible that core had horizontal crack on top of chair support.	Crack visible in hole at a depth of 1.25". Lots of small voids in core.	Crack visible in hole at a depth of 1". Rust color was noticed in hole.	Delamination visible in hole at a depth of 2.25".
General Quality of Concrete[3] (good, fair, poor)	Good	Fair	Fair	Poor

[1]Preexisting Rupture (PRE), Induced during coring (IDC), Produced by shear from extracting the core (CEX), Generated during handling (HAN), Other cause (OTR)
[2]Orientation: traverse (Tr) or longitudinal (Lo); Corrosion: none (Co1), low (Co2), average (Co3), high (Co4)
[3]Good indicates no delaminations or visible deterioration, Fair indicates some visible deterioration including delaminations however concrete is in large sections, Poor indicates concrete shows a lot of deterioration and is in many pieces including several small pieces

Table 4-8 Bridge A3017 Visual Core Evaluation Results (cont.)

Core	B1	B2	B3	B4
Diameter (in)	2.0	2.0	2.0	2.0
Length (in)	3.125	2.75	2.375	3.375
Surface (Asphalt: A, Concrete: C)	C	C	C	C
Number of Pieces	1	1	1	2
#1 Length (in) and failure mode [1]	3.125, CEX	2.75, CEX	2.375, CEX	0.5, PRE
#2 Length (in) and failure mode	N/A	N/A	N/A	2.875, CEX
#3 Length (in) and failure mode	N/A	N/A	N/A	N/A
Rebar: diameter (in), length (in), orientation [2], corrosion [2]	None	None	None	None
Roughness (Smooth, Average, Very Rough)	Average	Average	Average	Rough
Voids (Number >0.25 in. diameter)	4	4	5	2
Coating of the Aggregate (good or poor)	Good	Good	Good	Good
Volume of Paste (good or poor)	Good	Good	Good	Good
Air Entrained (yes or no)	Yes	Yes	Yes	Yes
Flaking surface: thickness (in)	None	None	None	None
Discoloration: color, maximum length (in)	None	None	None	None
Delaminations: depths (in)	None	None	None	0.5
Segregation of Aggregate: depths (in)	None	None	None	None
Cracks (excluding fracture planes): number, length (in)	None	None	None	None

[1]Preexisting Rupture (PRE), Induced during coring (IDC), Produced by shear from extracting the core (CEX), Generated during handling (HAN), Other cause (OTR)
[2]Orientation: traverse (Tr) or longitudinal (Lo); Corrosion: none (Co1), low (Co2), average (Co3), high (Co4)
[3]Good indicates no delaminations or visible deterioration, Fair indicates some visible deterioration including delaminations however concrete is in large sections, Poor indicates concrete shows a lot of deterioration and is in many pieces including several small pieces

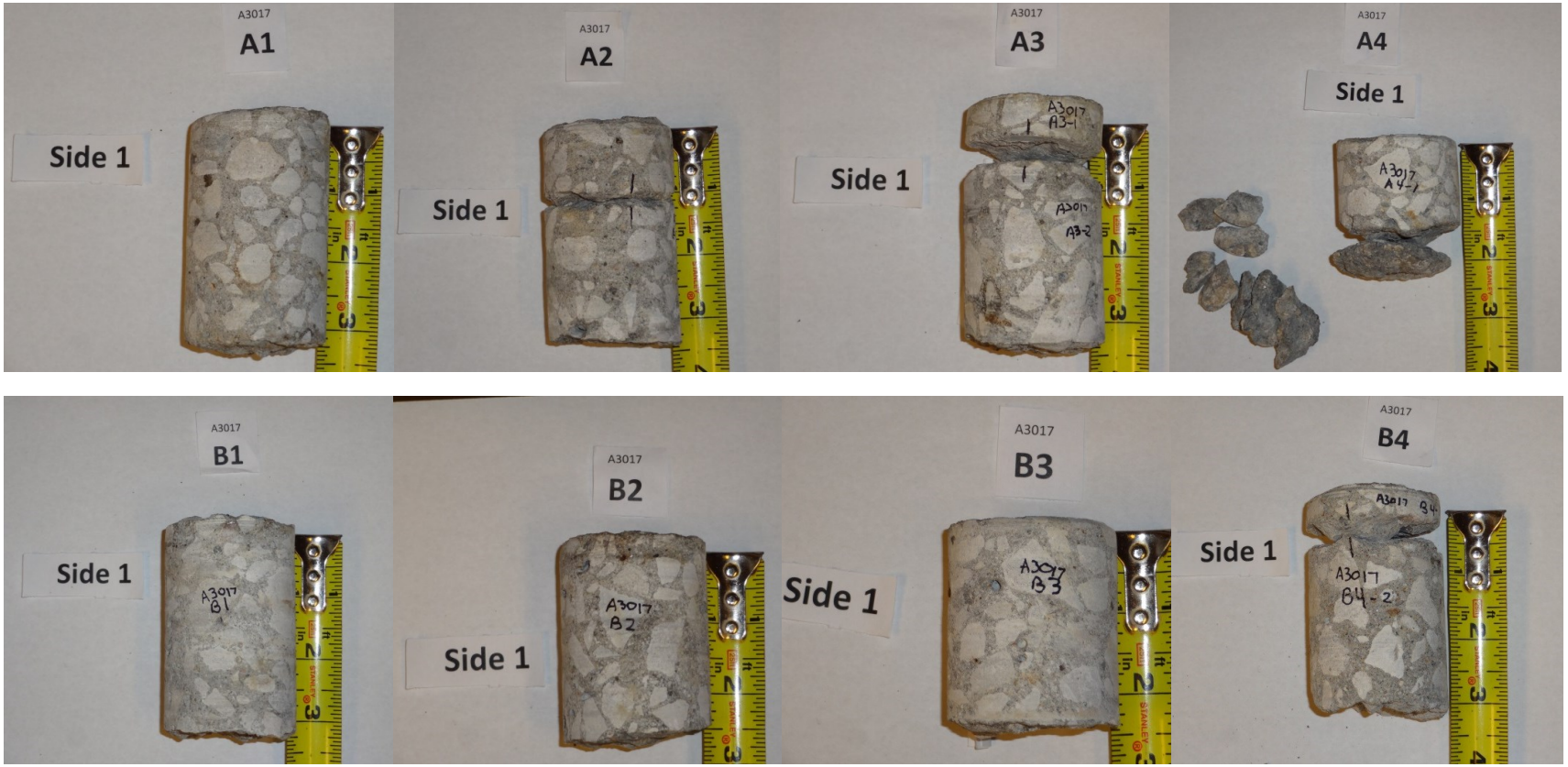

Figure 4-16 Cores Extracted From Bridge A3017

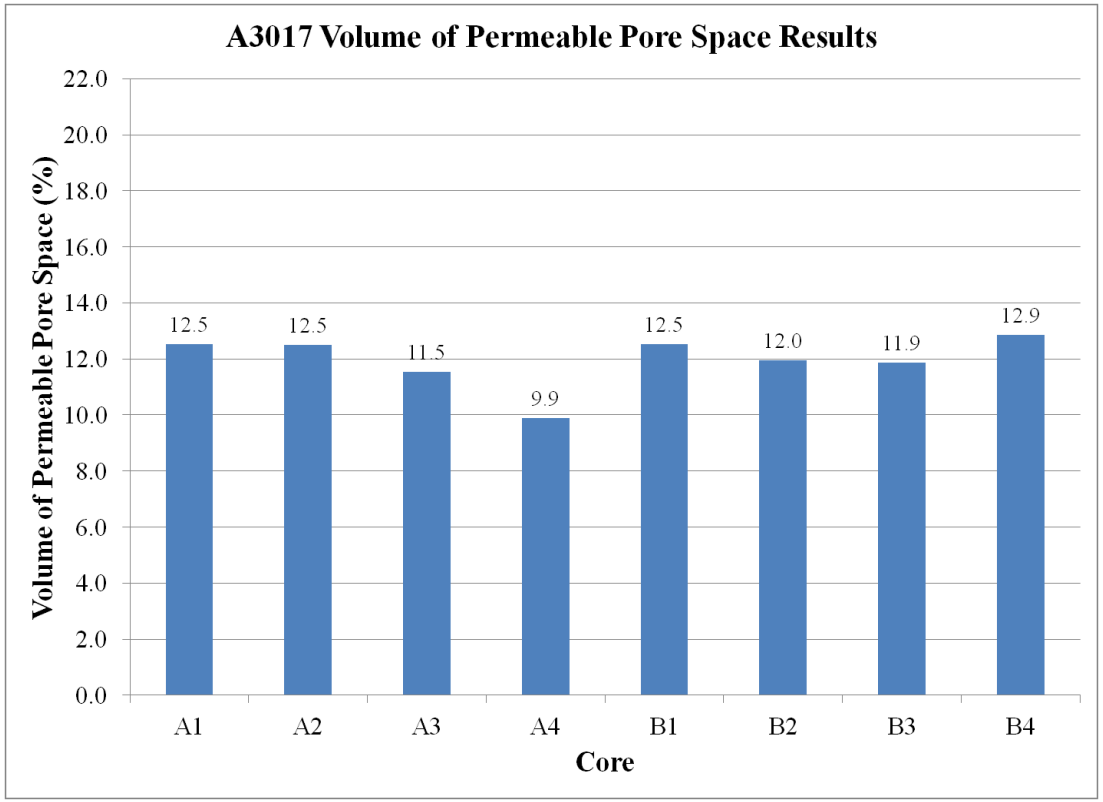

Figure 4-17 Bridge A3017 Volume of Permeable Pore Space Results

4.2.9 Bridge A3405

Table 4-9 Bridge A3405 Visual Core Evaluation Results

Core	A1	A2	A3	A4
Diameter (in)	2.0	2.0	2.0	2.0
Length (in)	3.0-3.5	3-3.25	2.375	3.5-3.875
Surface (Asphalt: A, Concrete: C)	C	C	C	C
Number of Pieces	1	3	1	1
#1 Length (in) and failure mode [1]	3.0-3.5, CEX	1.5, PRE	2.375, CEX	3.5-3.875, CEX
#2 Length (in) and failure mode	N/A	0.5, PRE	N/A	N/A
#3 Length (in) and failure mode	N/A	1-1.25, CEX	N/A	N/A
Rebar: diameter (in), length (in), orientation [2], corrosion [2]	Hit rebar at 3.375”	None	Hit rebar at 2.25”	None
Roughness (Smooth, Average, Very Rough)	Smooth	Smooth	Smooth	Smooth
Voids (Number >0.25 in. diameter)	3	0	0	1
Coating of the Aggregate (good or poor)	Good	Good	Good	Good
Volume of Paste (good or poor)	Good	Good	Good	Good
Air Entrained (yes or no)	Yes	Yes	Yes	Yes
Flaking surface: thickness (in)	None	None	None	None
Discoloration: color, maximum length (in)	None	None	None	None
Delaminations: depths (in)	None	1.5, 2.0	None	None
Segregation of Aggregate: depths (in)	None	None	None	None
Cracks (excluding fracture planes): number, length (in)	None	None	None	None
Other Comments	Angular coarse aggregate (all cores unless noted)	Some material missing between pieces, crack visible in core hole at 1.75”		
General Quality of Concrete[3] (good, fair, poor)	Good	Fair	Good	Good

[1]Preexisting Rupture (PRE), Induced during coring (IDC), Produced by shear from extracting the core (CEX), Generated during handling (HAN), Other cause (OTR)
[2]Orientation: traverse (Tr) or longitudinal (Lo); Corrosion: none (Co1), low (Co2), average (Co3), high (Co4)
[3]Good indicates no delaminations or visible deterioration, Fair indicates some visible deterioration including delaminations however concrete is in large sections, Poor indicates concrete shows a lot of deterioration and is in many pieces including several small pieces

Table 4-9 Bridge A3405 Visual Core Evaluation Results (cont.)

Core	B1	B2	B3	B4
Diameter (in)	2.0	2.0	2.0	2.0
Length (in)	2.75-3.375	3.5-4.0	2.25-2.5	2.75-3.25
Surface (Asphalt: A, Concrete: C)	C	C	C	C
Number of Pieces	2	1	1	1
#1 Length (in) and failure mode [1]	3.375, PRE	3.5-4.0, CEX	2.25-2.5, CEX	2.75-3.25, CEX
#2 Length (in) and failure mode	2.5, PRE	N/A	N/A	N/A
#3 Length (in) and failure mode	N/A	N/A	N/A	N/A
Rebar: diameter (in), length (in), orientation [2], corrosion [2]	Hit rebar at 3.25"	None	None	None
Roughness (Smooth, Average, Very Rough)	Average	Smooth	Smooth	Average
Voids (Number >0.25 in. diameter)	3	3	0	0
Coating of the Aggregate (good or poor)	Good	Good	Good	Good
Volume of Paste (good or poor)	Good	Good	Good	Good
Air Entrained (yes or no)	Yes	Yes	Yes	Yes
Flaking surface: thickness (in)	None	None	None	None
Discoloration: color, maximum length (in)	None	None	None	None
Delaminations: depths (in)	None	None	None	None
Segregation of Aggregate: depths (in)	None	None	None	None
Cracks (excluding fracture planes): number, length (in)	None	None	None	None
Other Comments	Fracture plane vertical, between patch material and original concrete. Patch has crushed limestone aggregate. Pieces fit together tight.			
General Quality of Concrete[3] (good, fair, poor)	Fair	Good	Good	Good

[1]Preexisting Rupture (PRE), Induced during coring (IDC), Produced by shear from extracting the core (CEX), Generated during handling (HAN), Other cause (OTR)
[2]Orientation: traverse (Tr) or longitudinal (Lo); Corrosion: none (Co1), low (Co2), average (Co3), high (Co4)
[3]Good indicates no delaminations or visible deterioration, Fair indicates some visible deterioration including delaminations however concrete is in large sections, Poor indicates concrete shows a lot of deterioration and is in many pieces including several small pieces

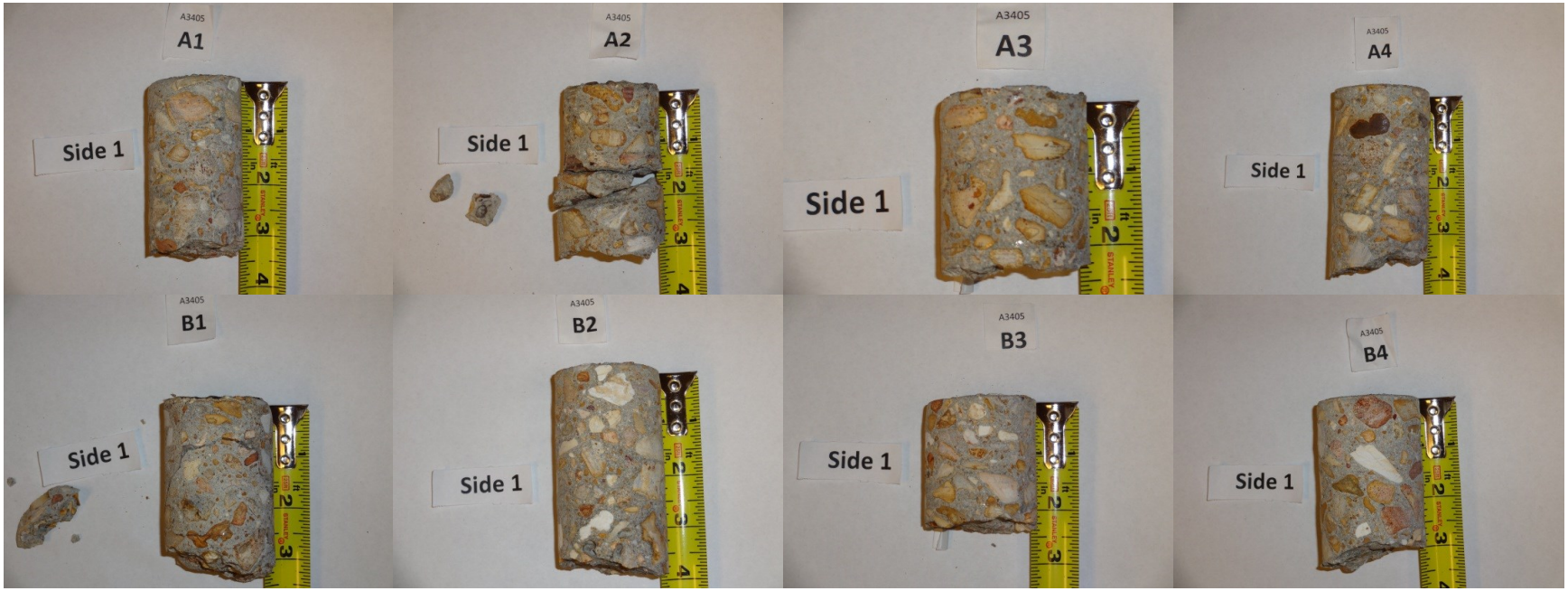

Figure 4-18 Cores Extracted From Bridge A3405

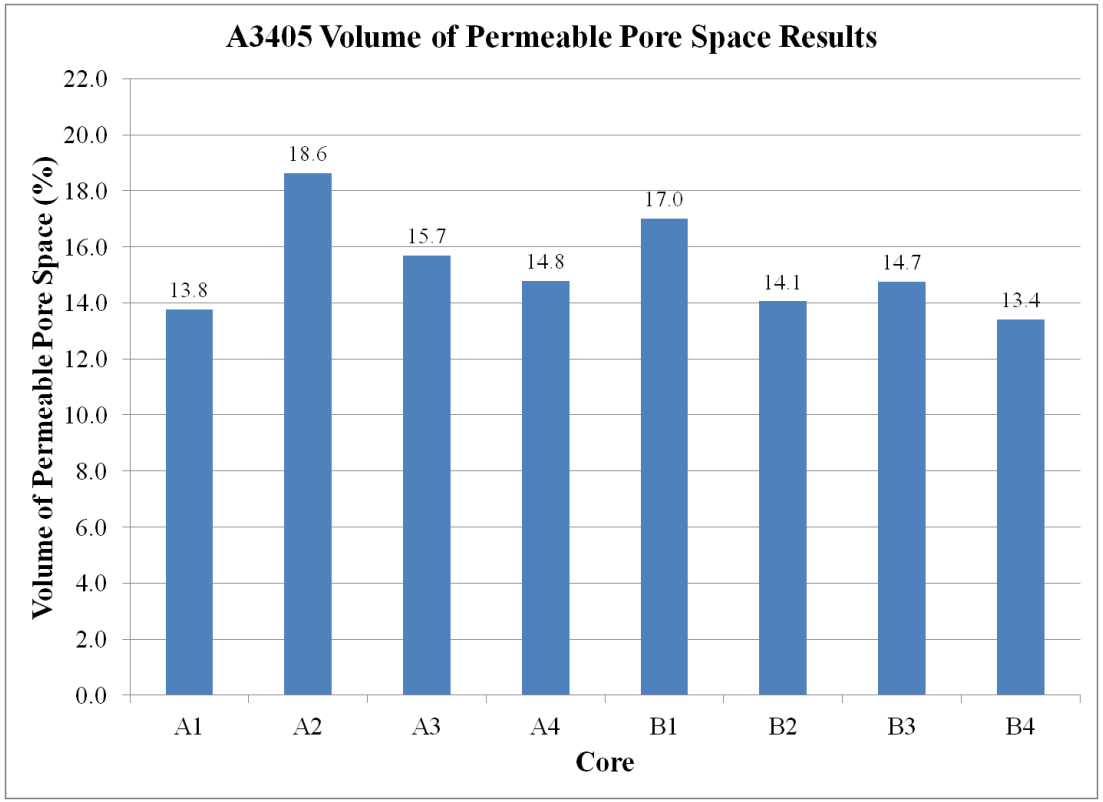

Figure 4-19 Bridge A3405 Volume of Permeable Pore Space Results

4.2.10 Bridge A3406

Table 4-10 Bridge A3406 Visual Core Evaluation Results

Core	A1	A2	A3
Diameter (in)	2.0	2.0	2.0
Length (in)	3.75	3.0	2.375
Surface (Asphalt: A, Concrete: C)	C	C	C
Number of Pieces	2	3	1
#1 Length (in) and failure mode [1]	2.375-2.5, PRE, Concrete patch	1.625-1.75, PRE	2.375, CEX
#2 Length (in) and failure mode	1.125-1.25, CEX, Original concrete	0.25-.625, PRE	N/A
#3 Length (in) and failure mode	N/A	0.5, CEX	N/A
Rebar: diameter (in), length (in), orientation [2], corrosion [2]	None	None	Hit longitudinal rebar while drilling with top of rebar at 2.375" deep
Roughness (Smooth, Average, Very Rough)	Piece 1: Average, Piece 2: Smooth	Smooth	Average
Voids (Number >0.25 in. diameter)	Piece 1: 2, Piece 2: 1	3	2
Coating of the Aggregate (good or poor)	Good	Good	Good
Volume of Paste (good or poor)	Good	Good	Good
Air Entrained (yes or no)	Yes	Yes	Yes
Flaking surface: thickness (in)	None	None	None
Discoloration: color, maximum length (in)	None	None	None
Delaminations: depths (in)	2.35-2.5	1.625-1.75, 2.0 In core hole visible at 1.0, 1.25, 2.0	None
Segregation of Aggregate: depths (in)	None	None	None
Cracks (excluding fracture planes): number, length (in)	1 at 2" below surface	None	None
Other Comments	Piece 1 concrete patch material with fibers and different aggregate versus Piece 2. Minimal material missing between pieces. Pieces lock together.	Delaminations visible in core hole. Some material missing in between pieces, but the pieces lock together enough to determine orientation.	Stopped drilling when rebar was hit, with rebar left in deck.
General Quality of Concrete[3] (good, fair, poor)	Fair	Fair	Good

[1]Preexisting Rupture (PRE), Induced during coring (IDC), Produced by shear from extracting the core (CEX), Generated during handling (HAN), Other cause (OTR)
[2]Orientation: traverse (Tr) or longitudinal (Lo); Corrosion: none (Co1), low (Co2), average (Co3), high (Co4)
[3]Good indicates no delaminations or visible deterioration, Fair indicates some visible deterioration including delaminations however concrete is in large sections, Poor indicates concrete shows a lot of deterioration and is in many pieces including several small pieces

Table 4-10 Bridge A3406 Visual Core Evaluation Results (cont.)

Core	B1	B2	B3
Diameter (in)	2.0	2.0	2.0
Length (in)	2.5	3.0	1.375-1.625
Surface (Asphalt: A, Concrete: C)	C	C	C
Number of Pieces	3 big, numerous small	3 big, numerous small	1
#1 Length (in) and failure mode [1]	1.0, PRE	1.5, PRE	1.375-1.625, PRE
#2 Length (in) and failure mode	0.25, PRE	0.5, PRE	N/A
#3 Length (in) and failure mode	1.0, CEX	1.0, PRE	N/A
Rebar: diameter (in), length (in), orientation [2], corrosion [2]	None	None	Hit top of traverse rebar while drilling at 1.75". Drilling stopped when rebar was hit.
Roughness (Smooth, Average, Very Rough)	Average	Smooth	Average
Voids (Number >0.25 in. diameter)	0	1	0
Coating of the Aggregate (good or poor)	Good	Good	Good
Volume of Paste (good or poor)	Good	Good	Good
Air Entrained (yes or no)	Yes	Yes	Yes
Flaking surface: thickness (in)	None	None	None
Discoloration: color, maximum length (in)	None	None	None
Delaminations: depths (in)	1.0, 1.25, 2.25	1.5, 2.0, 3.0	1.375-1.625
Segregation of Aggregate: depths (in)	None	None	None
Cracks (excluding fracture planes): number, length (in)	None	None	None
Other Comments	Delamination visible in core hole, measuring 1/8" thick. Total depth of hole after core removal was 2.875".	Delaminations visible in core hole at depths of 1.75" and 3.0".	Delamination visible in core hole.
General Quality of Concrete[3] (good, fair, poor)	Poor	Poor	Fair

[1]Preexisting Rupture (PRE), Induced during coring (IDC), Produced by shear from extracting the core (CEX), Generated during handling (HAN), Other cause (OTR)
[2]Orientation: traverse (Tr) or longitudinal (Lo); Corrosion: none (Co1), low (Co2), average (Co3), high (Co4)
[3]Good indicates no delaminations or visible deterioration, Fair indicates some visible deterioration including delaminations however concrete is in large sections, Poor indicates concrete shows a lot of deterioration and is in many pieces including several small pieces

Figure 4-20 Cores Extracted From Bridge A3406

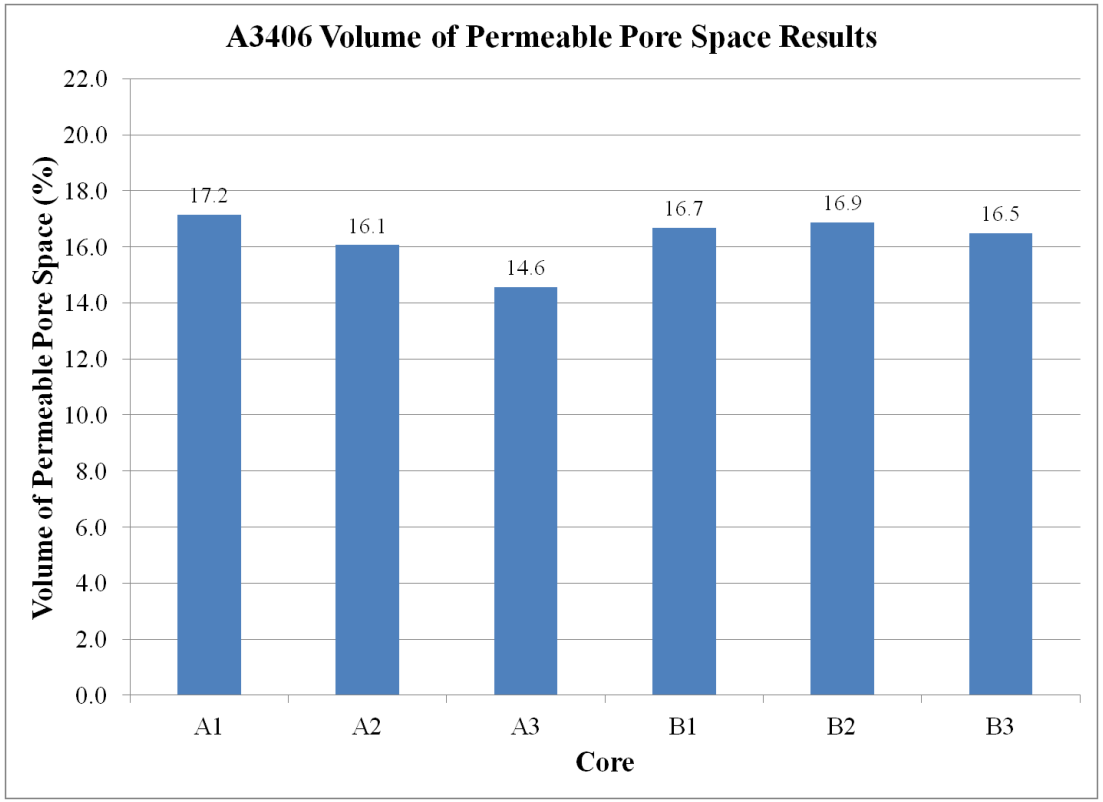

Figure 4-21 Bridge A3406 Volume of Permeable Pore Space Results

4.2.11 Bridge K0197

Table 4-11 Bridge K0197 Visual Core Evaluation Results

Core	A1	A2	A3	B1	B2	B3
Diameter (in)	2.0	2.0	2.0	2.0	2.0	2.0
Length (in)	4.25-4.75	6.25	4.75-5.0	5" drilled	5.25-5.625	4-4.625
Surface (Asphalt: A, Concrete: C)	1.75-2.0 A	2.0 A	2.0 A	1.75 A	2.375 A	1.5 A
Number of Pieces	3	2	2	1 big, Several small	2	1
#1 Length (in) and failure mode [1]	2.5, PRE	2.0, CEX	2.125, PRE	2.5-3.0, PRE	2.375, CEX	4-4.625, CEX
#2 Length (in) and failure mode	0.5, PRE	4.25, CEX	2.625, CEX	N/A	2.875-3.25, CEX	N/A
#3 Length (in) and failure mode	1.5, CEX	N/A	N/A	N/A	N/A	N/A
Rebar: diameter (in), length (in), orientation [2], corrosion [2]	None	None	1/4" Welded Wire, Lo, Co1	None	None	None
Roughness (Smooth, Average, Very Rough)	Average	Smooth	Average	Rough	Average	Smooth
Voids (Number >0.25 in. diameter)	2	4	1	0	0	0
Coating of the Aggregate (good or poor)	Good	Good	Good	Good	Good	Good
Volume of Paste (good or poor)	Good	Good	Good	Good	Good	Good
Air Entrained (yes or no)	Yes	Yes	Yes	Yes	Yes	Yes
Flaking surface: thickness (in)	None	None	None	None	None	None
Discoloration: color, maximum length (in)	None	None	None	None	None	None
Delaminations: depths (in)	2.5, 3.0	None	None	2.75	None	None
Segregation of Aggregate: depths (in)	None	None	None	None	None	None
Cracks (excluding fracture planes): number, length (in)	2.25" depth, half of core	None	None	2.25" depth, half of core	None	None
Other Comments	Asphalt bonded to concrete, material missing between pieces, dark colored rounded coarse aggregate (all K0197 cores unless noted)		Reinforcement in core, failure in concrete near surface	Remaining 5" of drilled hole had loose material that was left in place		2" of concrete patch-Smaller, angular coarse aggregate, Up to 1" of original concrete on bottom
General Quality of Concrete[3] (good, fair, poor)	Poor	Good	Good	Poor	Good	Good

[1]Preexisting Rupture (PRE), Induced during coring (IDC), Produced by shear from extracting the core (CEX), Generated during handling (HAN), Other cause (OTR)
[2]Orientation: traverse (Tr) or longitudinal (Lo); Corrosion: none (Co1), low (Co2), average (Co3), high (Co4)
[3]Good indicates no delaminations or visible deterioration, Fair indicates some visible deterioration including delaminations however concrete is in large sections, Poor indicates concrete shows a lot of deterioration and is in many pieces including several small pieces

Figure 4-22 Cores Extracted From Bridge K0197

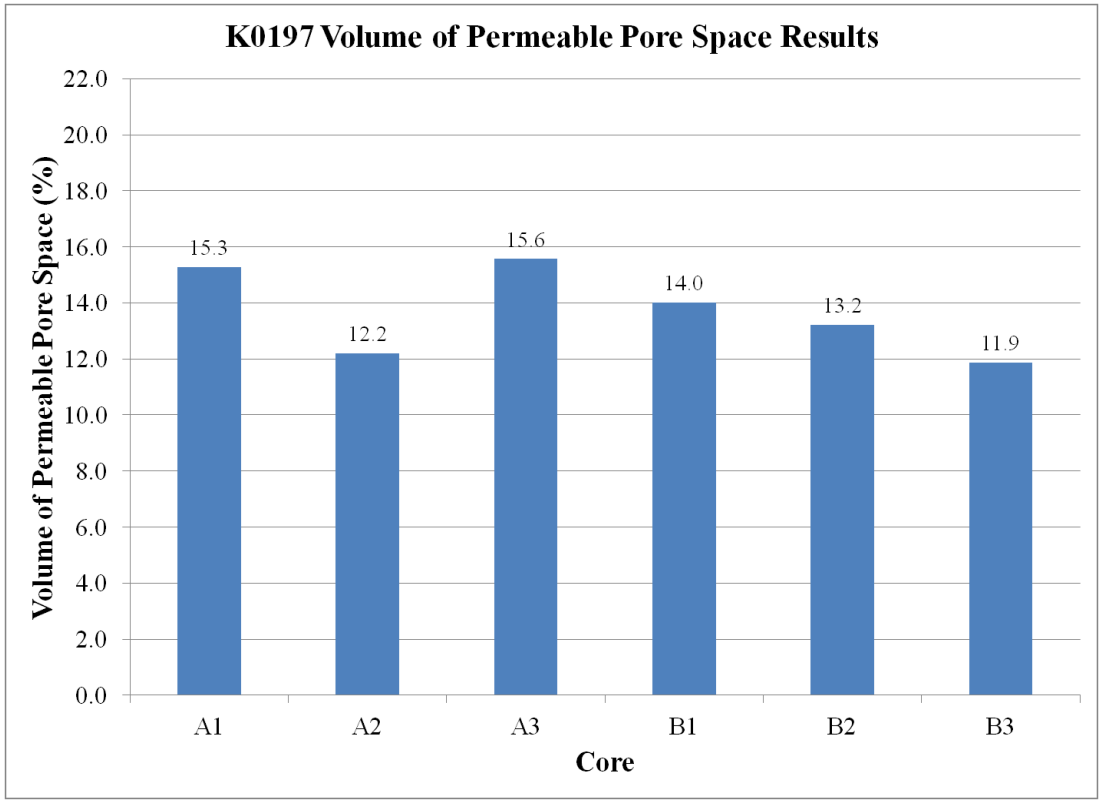

Figure 4-23 Bridge K0197 Volume of Permeable Pore Space Results

4.3 Summary of Core Results

A total of 83 cores were extracted from the 11 bridges investigated. Of those cores, 40 were rated as Good, 26 were rated as Fair, and 12 were rated as Poor using the classification system discussed in Section 4.1. The volume of permeable pore space was determined for 78 of the 83 extracted cores. Cores with no results available either consisted completely of asphalt or were too heavily deteriorated for the testing procedure. Figure 4-24 shows the average volume of permeable pore space for those cores that were assigned a visual core rating of either Good, Fair, or Poor. Figure 4-24 shows that on average, cores with higher volume of permeable core space tended to have a lower visual core rating.

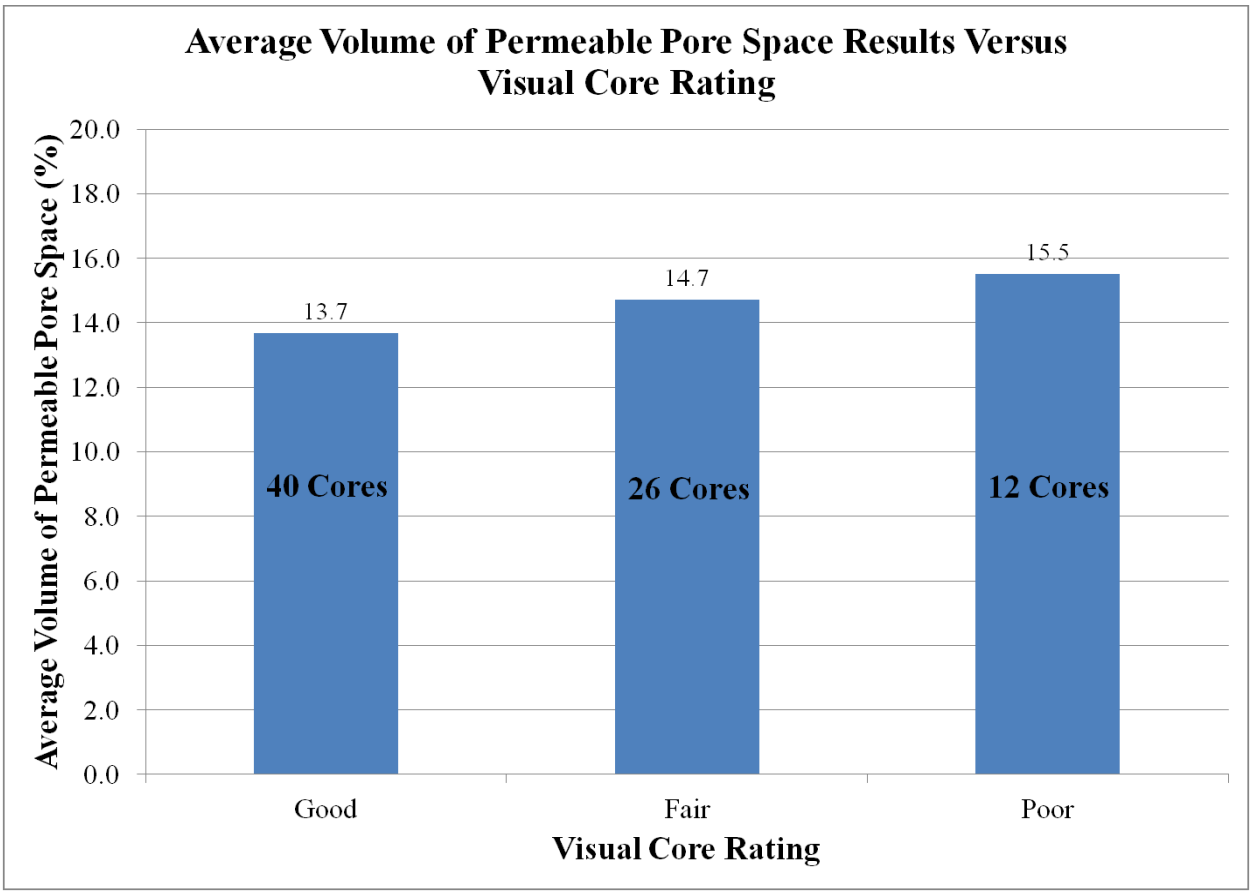

Figure 4-24 Average Volume of Permeable Pore Space Results Based on Visual Core Rating

5 CHLORIDE ION CONCENTRATION

5.1 Methodology

Chloride ion concentration levels measured in the concrete indicate the likelihood for corrosion of embedded reinforcement steel at that location. Once corrosion of the reinforcing steel is initiated, further deterioration of the surrounding concrete will occur and eventually lead to delamination of the concrete from the steel. GPR also responds to the presence of saline moisture, therefore the chloride ion concentration levels were expected to correlate with GPR results. Regions with higher chloride ion concentration levels were expected to correlate to lower reflection amplitudes in the GPR data, indicating higher likelihood of deterioration.

Tests to determine the chloride ion concentration of the concrete cores were conducted by MoDOT. MoDOT followed ASTM C1218/ C1218M-99 to determine the water soluble chloride ion concentration at different depths of the concrete (ASTM 1999). Chloride ion concentration measurements were obtained for three to five cores per bridge, depending on the length of the bridge.

Samples used to determination of chloride ion concentration were collected using two different methods in this project. For six of the 11 bridges, samples were extracted from the cores after they had been visually examined at Missouri S&T. Those bridges were A0569, A1187, A1193, A1297, A1479, and A2966. Many of the cores were in multiple pieces after being extracted from the deck. Furthermore, due to the size of the core (2 in. diameter), it was difficult to obtain samples to conduct the tests. To help facilitate sample collection from the cores, MoDOT personnel embedded the cores in fresh concrete. Even with the 2 in. diameter cores encased in concrete, damage occurred to the cores upon sampling. Therefore, chloride ion concentration measurements are only available for a few of the cores extracted from these six bridges.

In order to obtain additional chloride ion concentration measurements and allow for more effective sampling, MoDOT personnel collected samples from a separate drill hole near the core hole on Bridge A2111, A3017, A3405, A3406, and K0197. The drill hole was within 6 in. from the core hole. Figure 5-1 shows the location of the chloride ion sample hole in relation to the core location. Chloride ion concentration samples on Bridges A2111 and A3017 were obtained minutes before the cores were extracted. Chloride ion concentration samples for Bridges A3405, A3406, and K0197 were obtained almost a year after the NDE investigation took place.

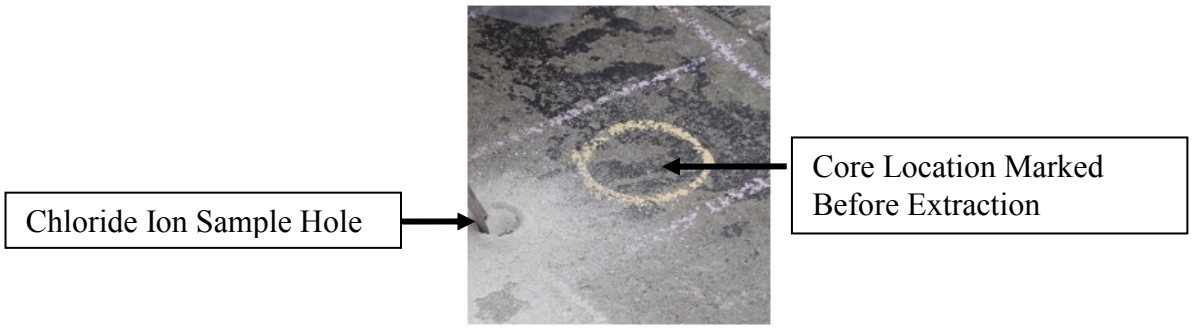

Figure 5-1 Cores Extracted From Bridge K0197

The Federal Highway Administration (FHWA) indicates that the threshold value for water-soluble chloride for corrosion to initiate is 0.15% by weight of cement (PCA 2013). It is important to note that several factors affect the corrosion of steel, including the amount of oxygen, electrical resistivity, and relative humidity of the concrete, as well as pH and temperature, therefore this threshold value is considered only as a guide.

Chloride ion concentration results are shown in the sections that follow for bridges A1187, A1193, A1297, A1479, A2111, and A3017. At the time of this report, data from Bridges A3405, A3406, and K0197 were being tested by MoDOT, and results were not yet available. The specified top clear cover for each bridge deck is noted on each figure. However, it should be noted that the actual clear cover could be more or less than specified.

5.2 Chloride Ion Concentration Results

5.2.1 Bridge A0569

Chloride ion concentration results are not available for this bridge deck.

5.2.2 Bridge A1187

Figure 5-2 shows the chloride ion concentration results for Cores A4 and B4 from Bridge A1187. Results were not available at the design depth of top reinforcing bar, but projection of the trends in the figure suggest that chloride ion concentration levels would be slightly below the threshold limit for both cores.

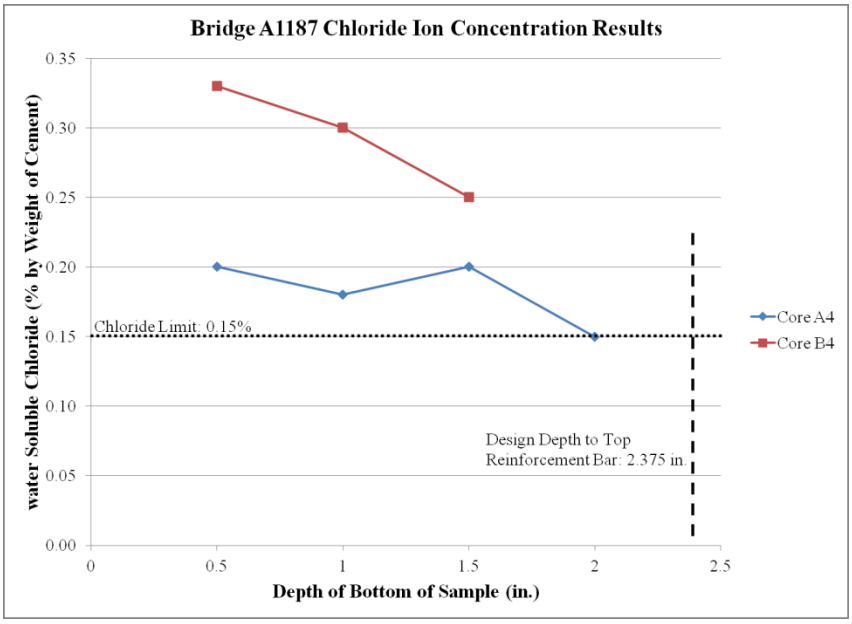

Figure 5-2 Bridge A1187 Chloride Ion Concentration Results

5.2.3 Bridge A1193

Figure 5-3 shows the chloride ion concentration results for Cores A1, A3, and A5 from Bridge A1193. Results indicate that chloride ion concentration levels are less than the threshold limit for each core.

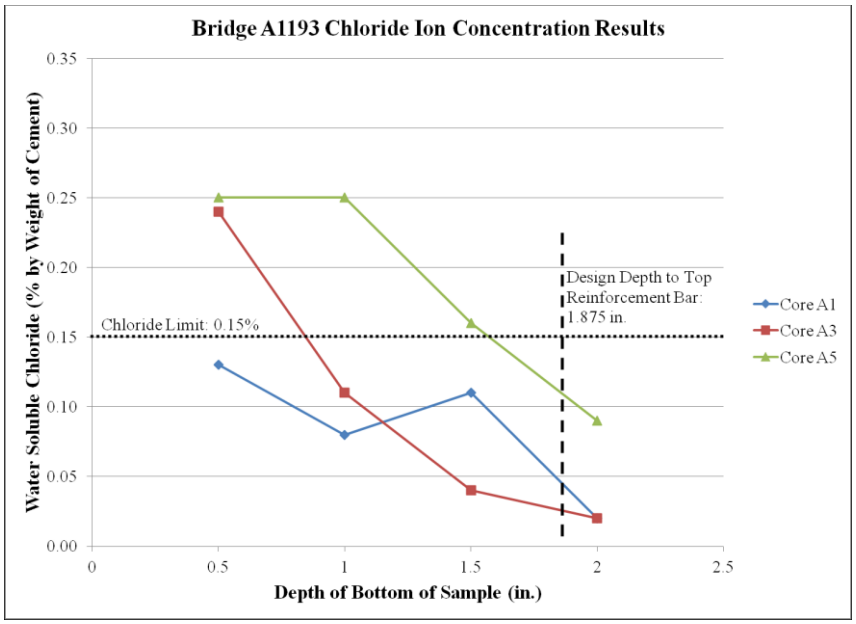

Figure 5-3 Bridge A1193 Chloride Ion Concentration Results

5.2.4 Bridge A1297

Figure 5-4 shows the chloride ion concentration results for Cores A1 and A2 from Bridge A1297. Results indicate that chloride ion concentration levels are less than the threshold limit for both cores.

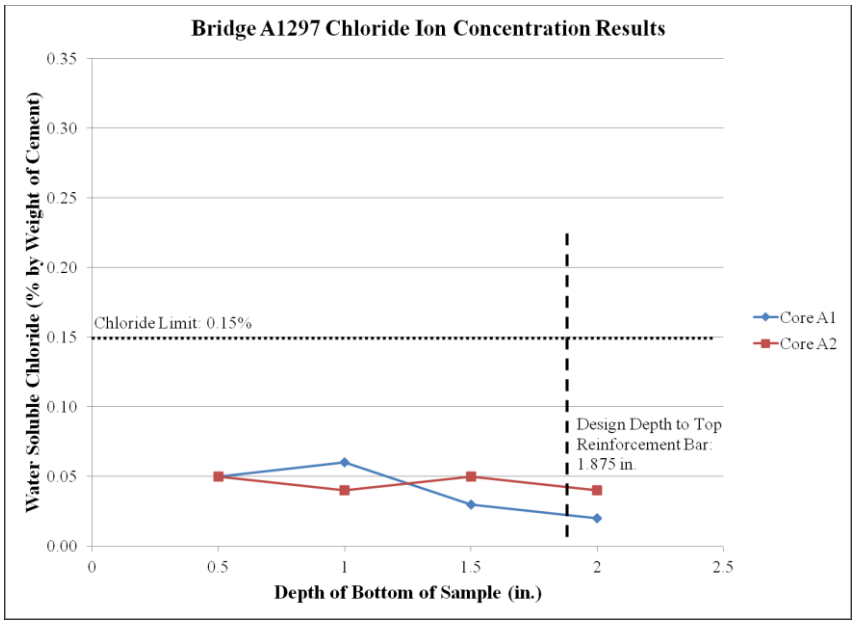

Figure 5-4 Bridge A1297 Chloride Ion Concentration Results

5.2.5 Bridge A1479

Figure 5-5 shows the chloride ion concentration results for Cores B1 and B3 from Bridge A1479. Results were not available at the design depth of top reinforcing bar, but projection of the trends in the figure suggest that chloride ion concentration levels would be below the threshold limit for both cores.

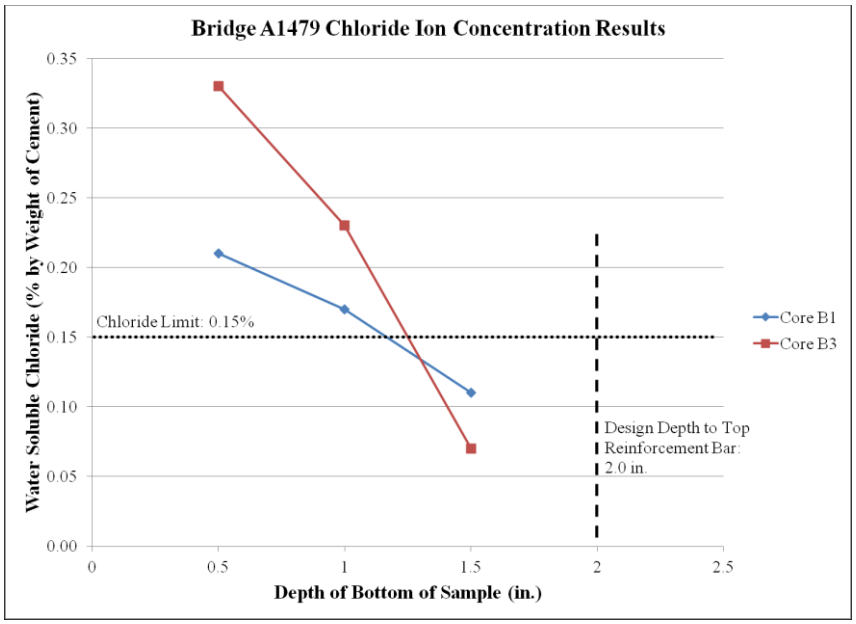

Figure 5-5 Bridge A1479 Chloride Ion Concentration Results

5.2.6 Bridge A2111

Figure 5-6 shows the chloride ion concentration results for Cores A1, A2, A3, B1, B2, and B3 from Bridge A2111. Results indicate that chloride ion concentration levels are less than the threshold limit for each core with the exception of Core B1, which had a measured chloride ion concentration above the threshold limit.

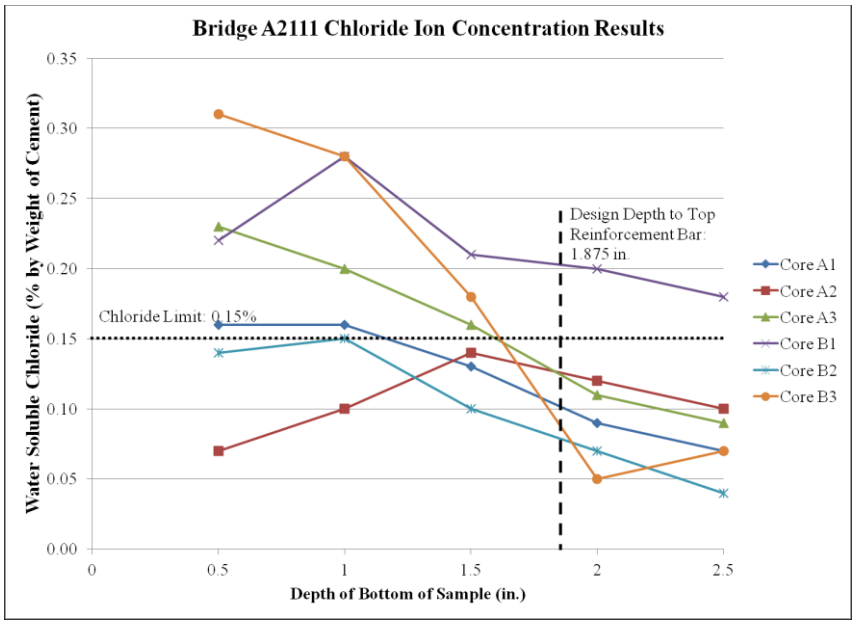

Figure 5-6 Bridge A2111 Chloride Ion Concentration Results

5.2.7 Bridge A2966

Chloride ion concentration results are not available for this bridge deck.

5.2.8 Bridge A3017

Figure 5-7 shows the chloride ion concentration results for Cores A1, A2, A3, A4, B1, B2, B3, and B4 from Bridge A3017. Results were not available at the design depth of top reinforcing bar, but projection of the trends in the figure suggest that chloride ion concentration levels would be below the threshold limit for each core.

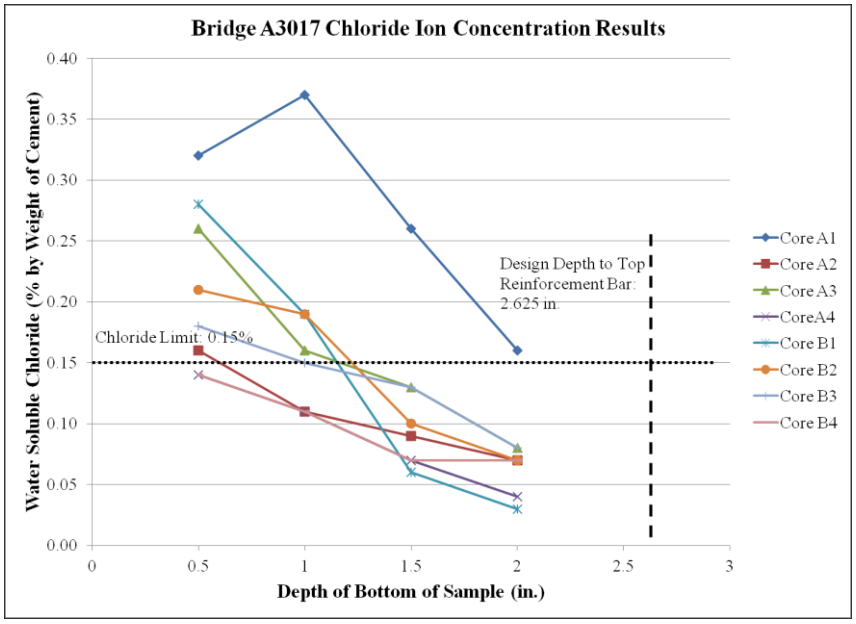

Figure 5-7 Bridge A3017 Chloride Ion Concentration Results

5.2.9 Bridge A3405

Chloride ion concentration results were not available for this bridge deck at the time of this report.

5.2.10 Bridge A3406

Figure 5-8 shows the chloride ion concentration results for Cores A2, A3, and B2 from Bridge A3406. Results indicate that chloride ion concentration levels are less than the threshold limit for each core.

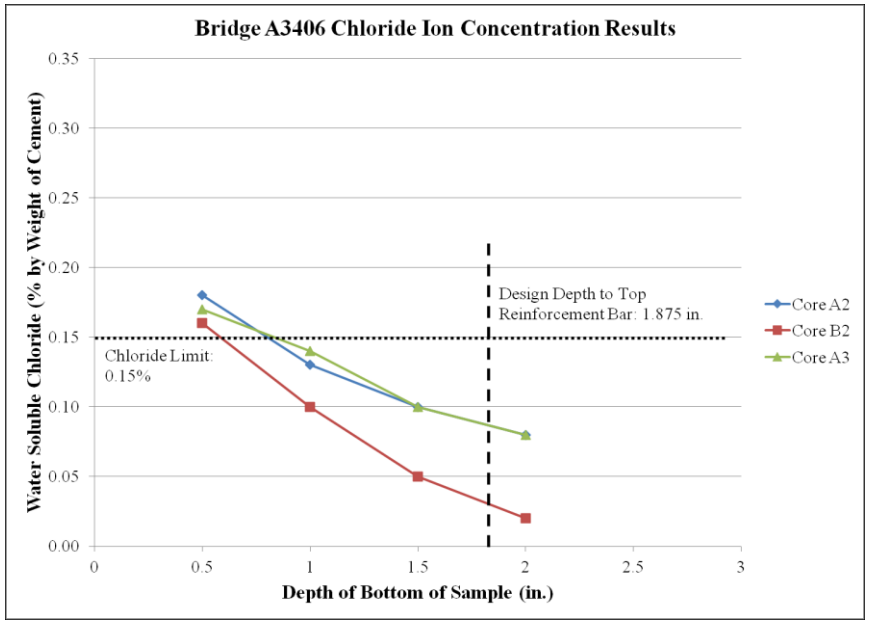

Figure 5-8 Bridge A3406 Chloride Ion Concentration Results

5.2.11 Bridge K0197

Figure 5-9 shows the chloride ion concentration results for Cores A1, B2, and B3 from Bridge K0197. Results indicate that chloride ion concentration levels are less than the threshold limit for each core.

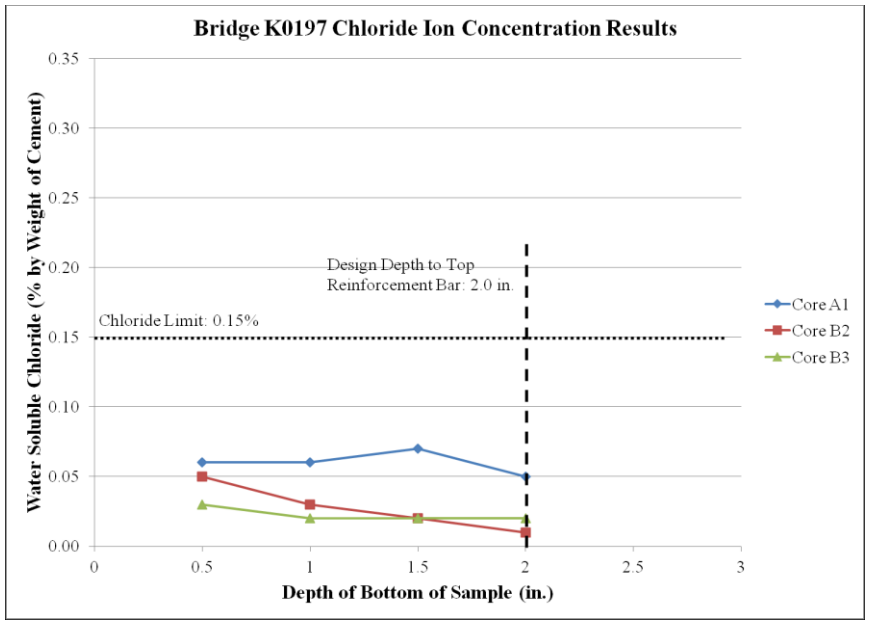

Figure 5-9 Bridge K0197 Chloride Ion Concentration Results

6 DECK REHABILITATION

6.1 Overview and Methodology

MoDOT awarded contracts for the rehabilitation of three of the 11 bridge decks that were investigated in this project (Bridges A1193, A1297, and A1479) during the project duration. All of the construction to complete the three rehabilitations was completed by the same prime contractor within one year of the bridge deck investigation. Rehabilitation included removing deteriorated concrete via hydrodemolition. The same subcontractor conducted the hydrodemolition for all three bridges decks.

Hydrodemolition can be used to remove loose and deteriorated concrete from bridge decks, including concrete below the top mat of reinforcement. Using hydrodemolition instead of traditional impact type removal methods such as milling or jack hammering is expected to prolong the life of the bridge deck because micro cracking is not induced into the surrounding concrete. The hydrodemolition machine is calibrated individually for each bridge deck to remove all unsound concrete and an additional 0.25 to 0.5 in. of sound concrete (MoDOT 2002). The material removed by the hydrodemolition process has lower tensile strength than the sound concrete that is left in place. The hydrodemolition process also removes corrosion from reinforcing steel and roughens the deck surface to provide adequate adhesion to the new overlay.

For the three decks that were rehabilitated, the top 0.75 in. of concrete was removed using a mill prior to the hydrodemolition. Milling the concrete left behind a rough and grooved surface as shown in Figure 6-1. After the milling process was complete, the contractor used a machine with high pressure water jets to remove loose and deteriorated concrete, which exposed corroded reinforcement bars as shown in Figure 6-2. A constant water pressure between 14,000 and 20,000 psi is typically used to perform hydrodemolition of bridge decks (MoDOT 2002). Following the hydrodemolition, traditional hammer and chain sounding techniques were used to identify any areas of the deck that required further concrete removal.

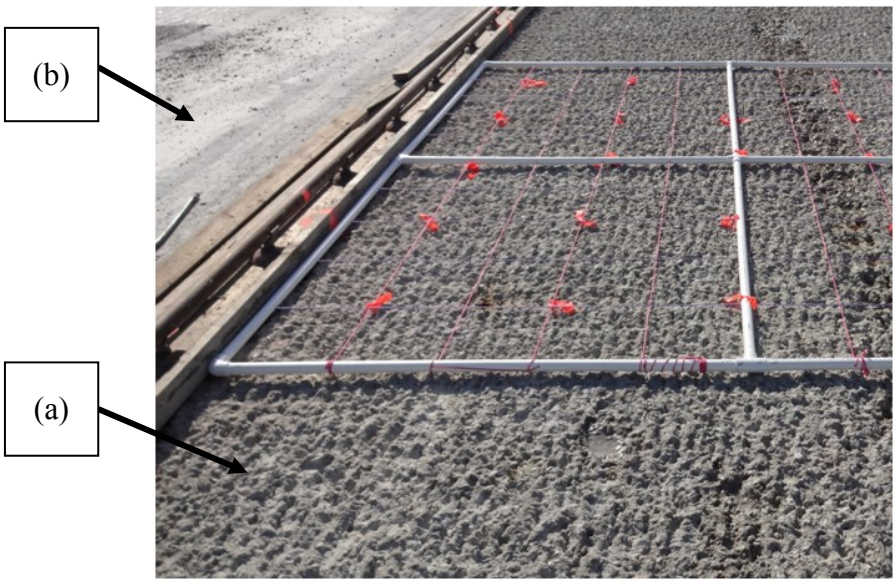

Figure 6-1 Rough Grooved Concrete Surface Caused by Milling (a) and Original As-Built Concrete Surface (b)

Figure 6-2 Corroded Rebar Exposed After Removal of Loose and Deteriorated Concrete by Hydro Demolition

Missouri S&T's Lidar Applications Team was contracted by MoDOT to obtain depth measurements of concrete removal for the three bridge decks being rehabilitated. Lidar is a form of laser imaging that can be used to map surfaces, in this study the bridge deck surface. The lidar team performed two scans per lane on each bridge deck undergoing rehabilitation. The first scan was completed less than a week prior to the milling of the concrete bridge deck. The second scan was conducted after concrete removal by hydrodemolition but prior to placement of the new concrete overlay. Using these two sets of lidar data, the lidar team was able to compare the pre-rehabilitation lidar data with the post-hydrodemolition data to obtain the location and depth (thickness) of material removal. Testing verified the lidar depth estimates are accurate to within 0.4 in. (1 cm.). Figure 6-3 shows the image generated by subtracting the second scan from the first scan. The reinforcement is visible in the figure, as well as the rough, grooved surface created by the milling of the deck surface.

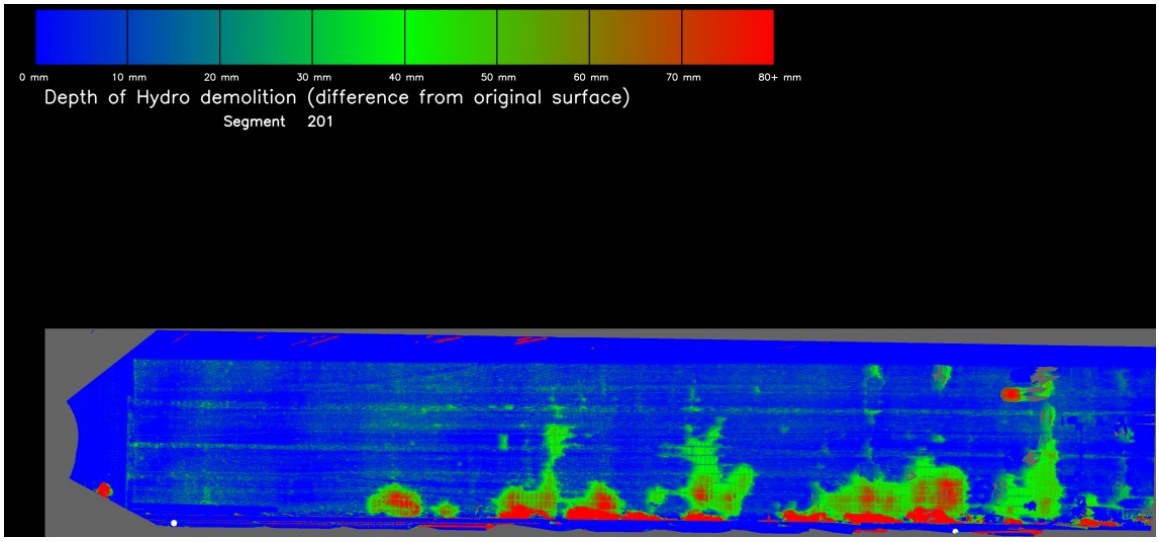

Figure 6-3 Lidar Image of Bridge Deck Showing Depth Difference Between Pre-Rehabilitation and Post-Hydrodemolition

Since MoDOT's bridge deck rehabilitation projects are usually bid based on different categories, the depth of material removal during the rehabilitation process was divided into three similar categories. The first category is a depth of removal less than 0.75 in., which is the depth of material removed by milling and hydrodemolition. The second category is material removal depths between 0.75 in. and the depth to the top of topmost layer of reinforcing bars. The third category is material removal depths greater than the depth to the top of the topmost layer of reinforcing bars. These three categories are illustrated in Figure 6-4.

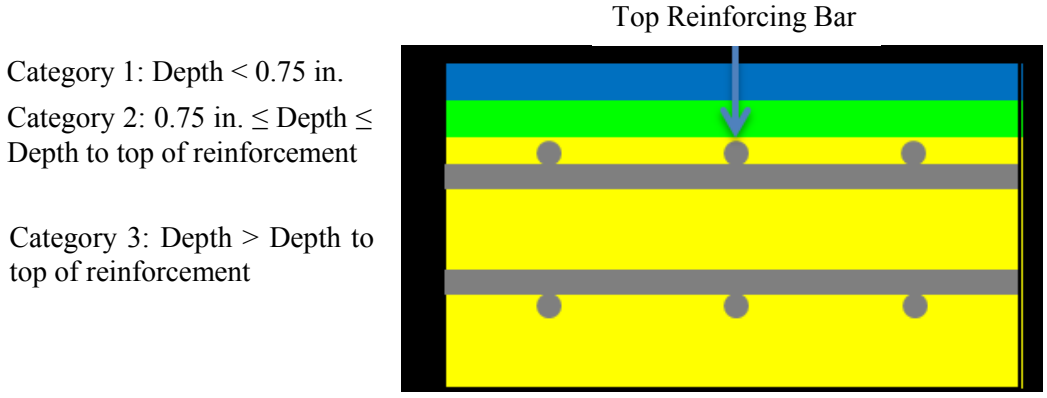

Figure 6-4 Categories of Material Depth Removal during Rehabilitation

6.2 Results

6.2.1 Bridge A1193

Figure 6-5 shows the lidar scan results for Bridge A1193 in 125 ft. long segments. The scale for depth difference (corresponding to thickness of material removal) for the lidar results in Figure 6-5 is shown in Figure 6-6. It should be noted that data were not captured in certain areas of the deck, therefore these segments were omitted and are not plotted in Figure 6-5. The amount (percentage of surface area surveyed) of concrete removed in each of the three categories defined in Section 6.1 is shown in Figure 6-7.

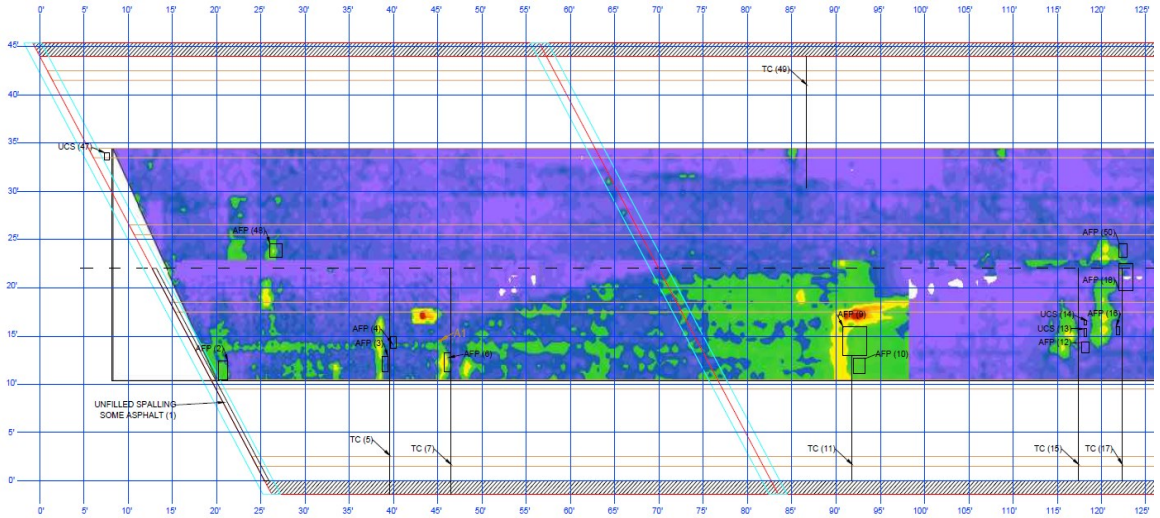

Figure 6-5 Bridge A1193 Drawing Including Lidar Rehabilitation Survey and Visual Investigation Results

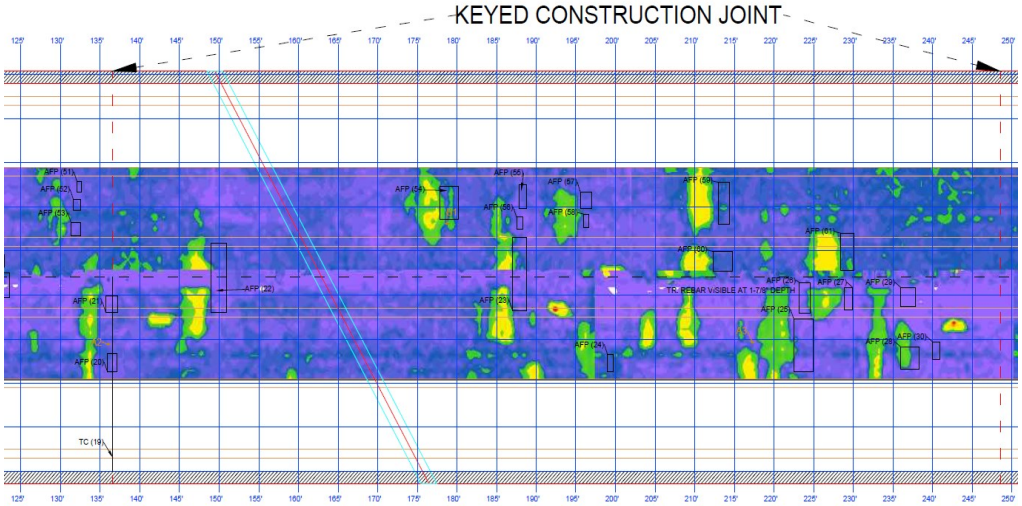

Figure 6-5 Bridge A1193 Drawing Including Lidar Rehabilitation Survey and Visual Investigation Results (Cont.)

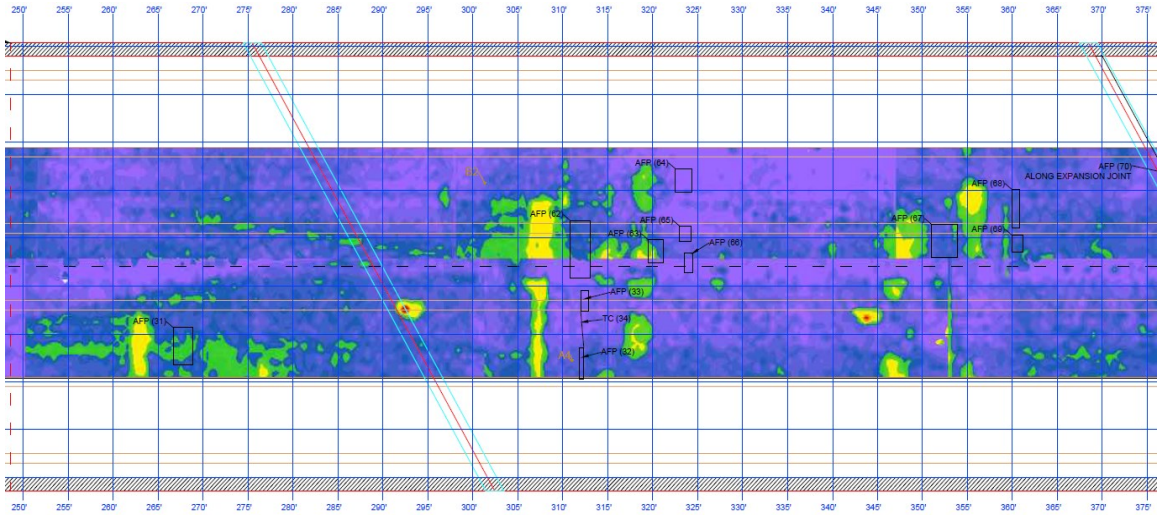

Figure 6-5 Bridge A1193 Drawing Including Lidar Rehabilitation Survey and Visual Investigation Results (Cont.)

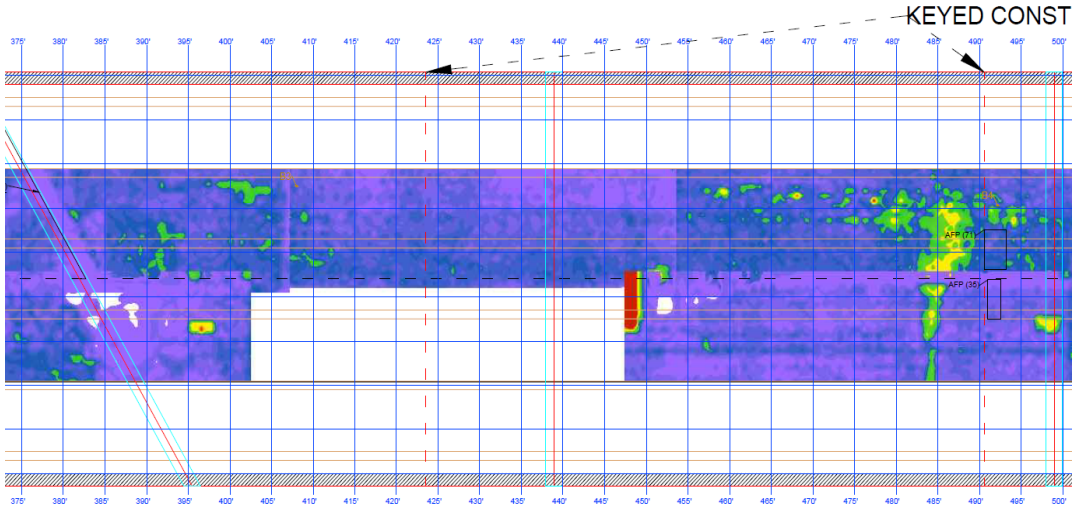

Figure 6-5 Bridge A1193 Drawing Including Lidar Rehabilitation Survey and Visual Investigation Results (Cont.)

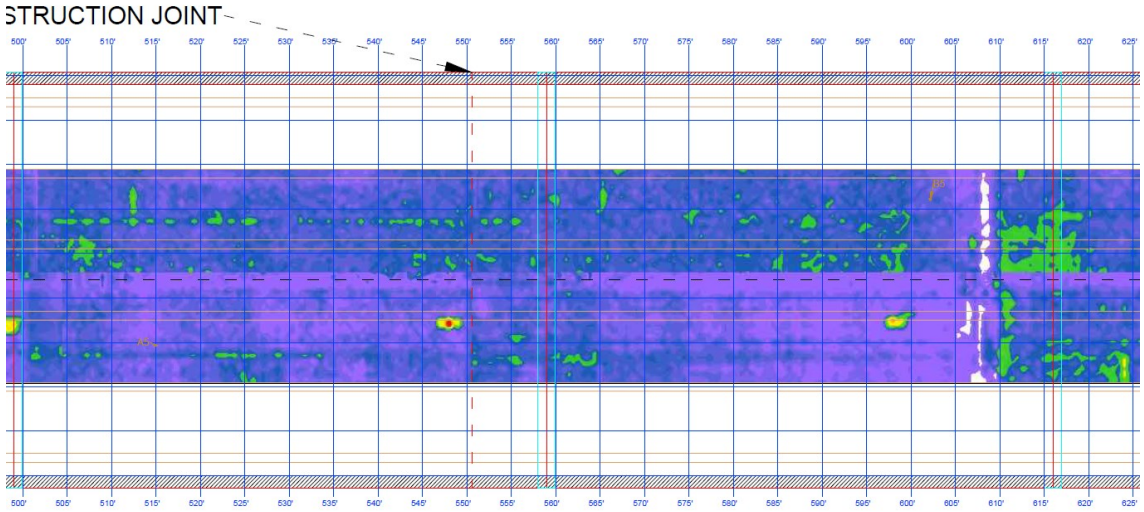

Figure 6-5 Bridge A1193 Drawing Including Lidar Rehabilitation Survey and Visual Investigation Results (Cont.)

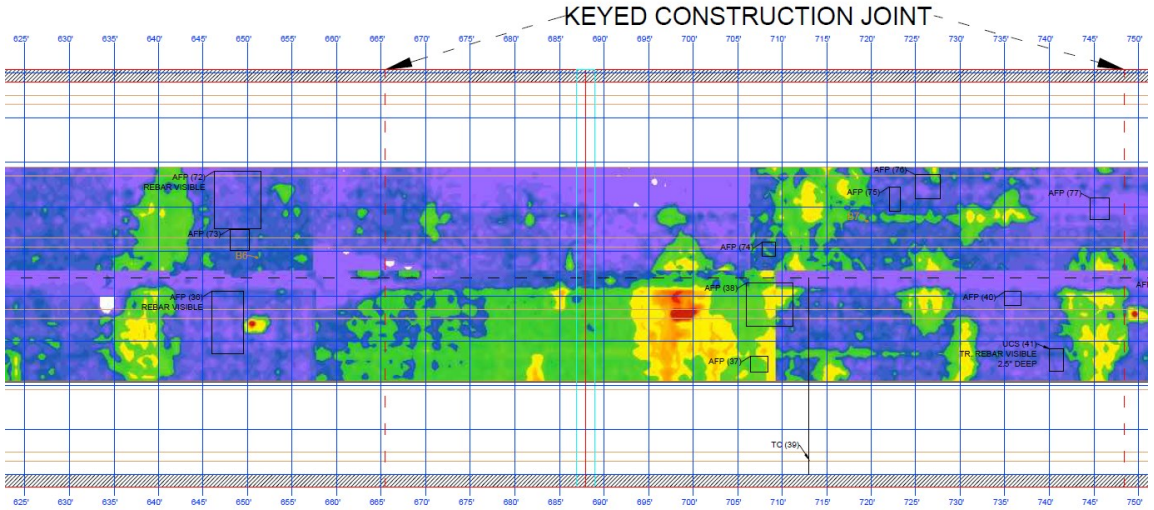

Figure 6-5 Bridge A1193 Drawing Including Lidar Rehabilitation Survey and Visual Investigation Results (Cont.)

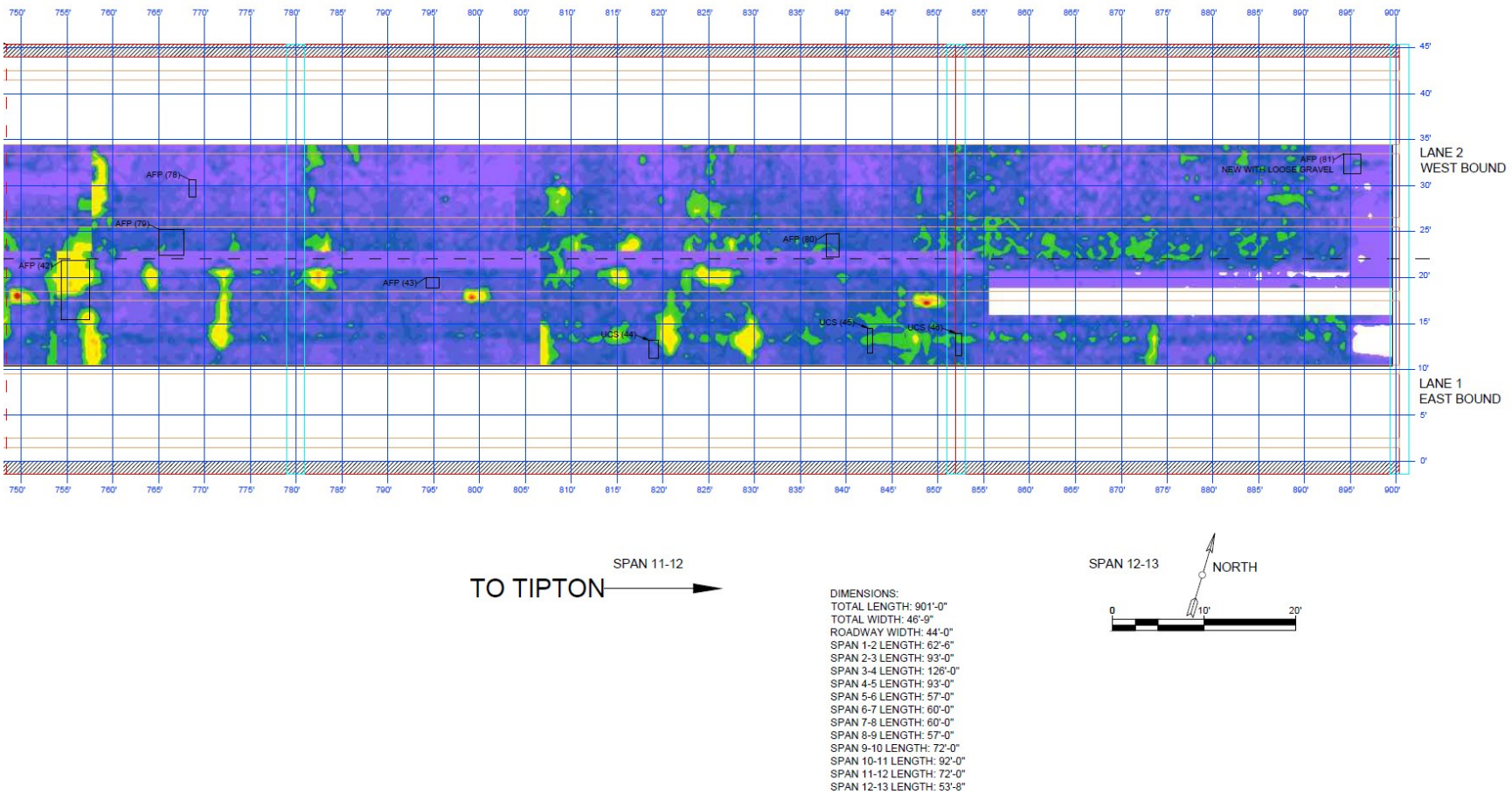

Figure 6-5 Bridge A1193 Drawing Including Lidar Rehabilitation Survey and Visual Investigation Results (Cont.)

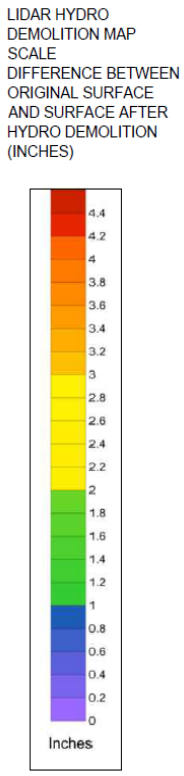

Figure 6-6 Bridge A1193 Lidar Scan Scale

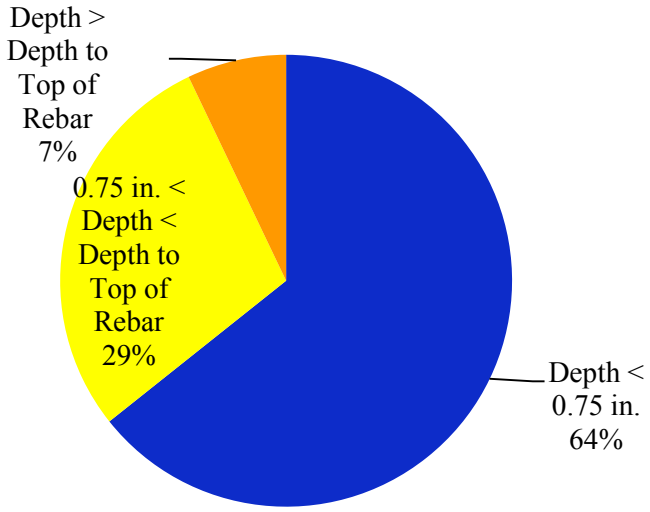

Figure 6-7 Bridge A1193 Lidar Depth of Concrete Removal Results

6.2.2 Bridge A1297

Figure 6-8 shows the lidar scan results for Bridge A1297 in 95 ft. long segments. The scale for depth difference (corresponding to thickness of material removal) for the lidar results in Figure 6-8 is shown in Figure 6-9. The amount (percentage of surface area surveyed) of concrete removed in each of the three categories defined in Section 6.1 is shown in Figure 6-10.

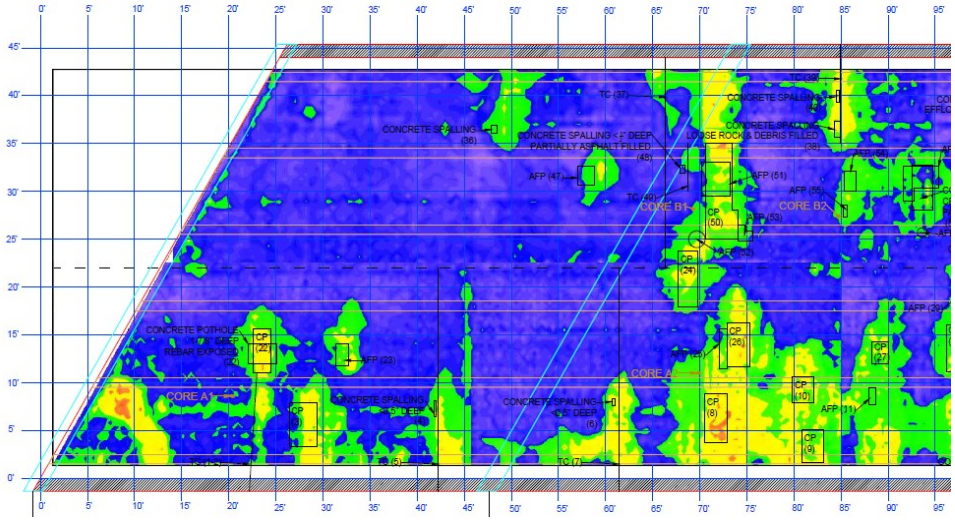

Figure 6-8 Bridge A1297 Drawing Including Lidar Rehabilitation Survey and Visual Investigation Results

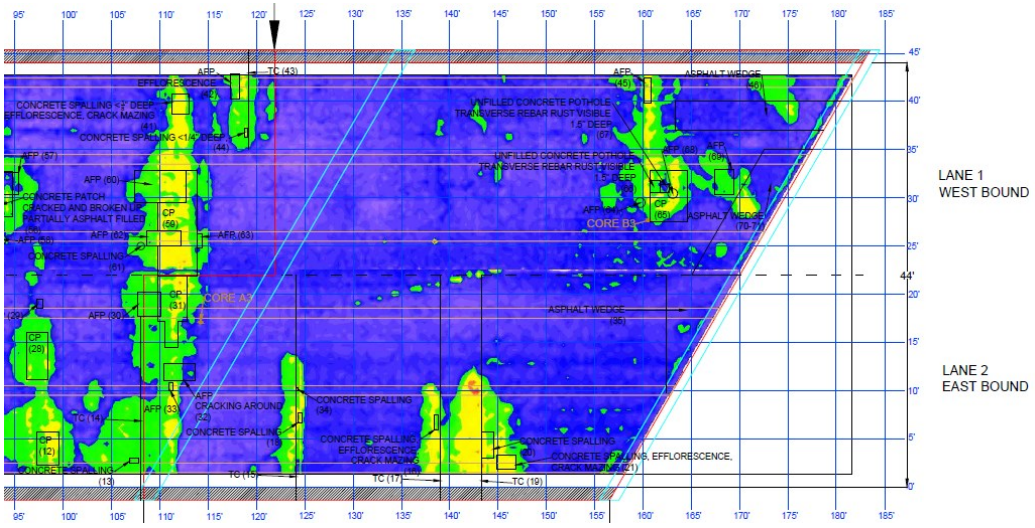

Figure 6-8 Bridge A1297 Drawing Including Lidar Rehabilitation Survey and Visual Investigation Results (Cont.)

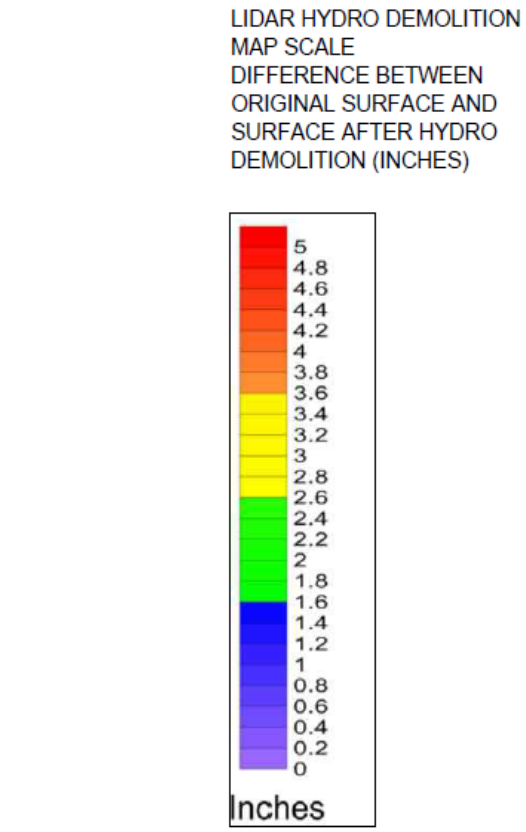

Figure 6-9 Bridge A1297 Lidar Scan Scale

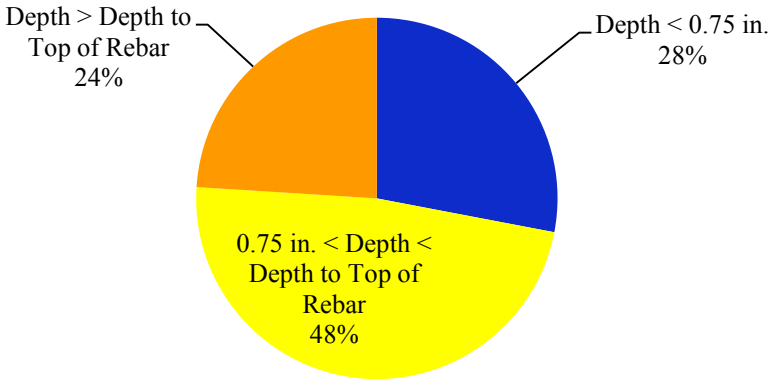

Figure 6-10 Bridge A1297 Lidar Depth of Concrete Removal Results

6.2.3 Bridge A1479

Figure 6-11 shows the lidar scan results for Bridge A1479 in 125 ft. long segments. The scale for depth difference (corresponding to thickness of material removal) for the lidar results in Figure 6-11 is shown in Figure 6-12. The amount (percentage of surface area surveyed) of concrete removed in each of the three categories defined in Section 6.1 is shown in Figure 6-13.

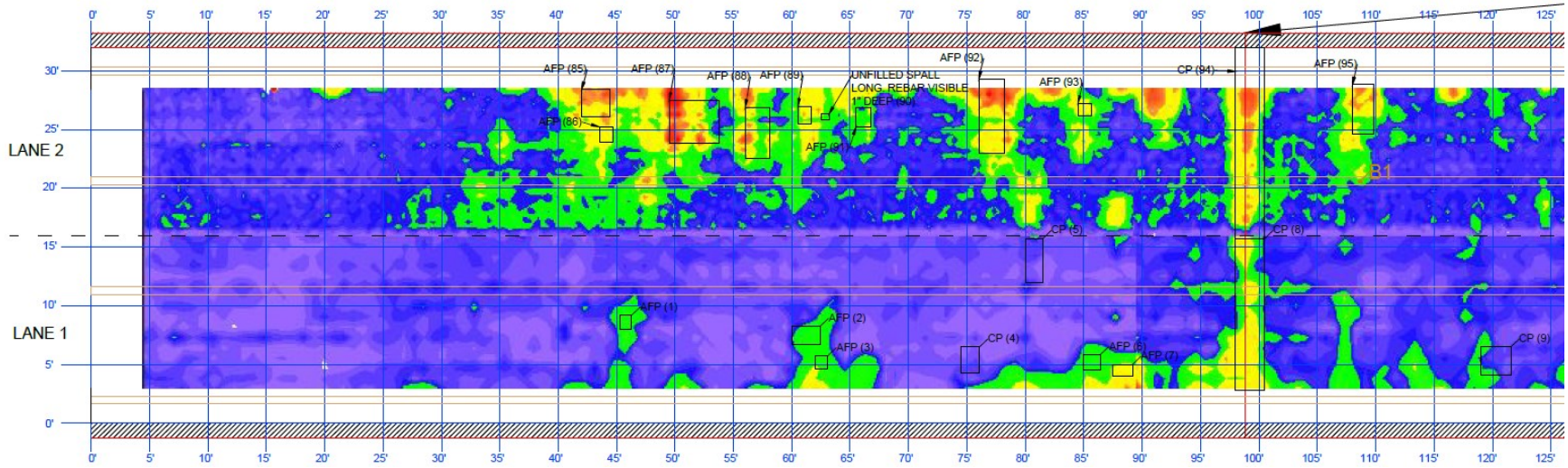

Figure 6-11 Bridge A1479 Drawing Including Lidar Rehabilitation Survey and Visual Investigation Results

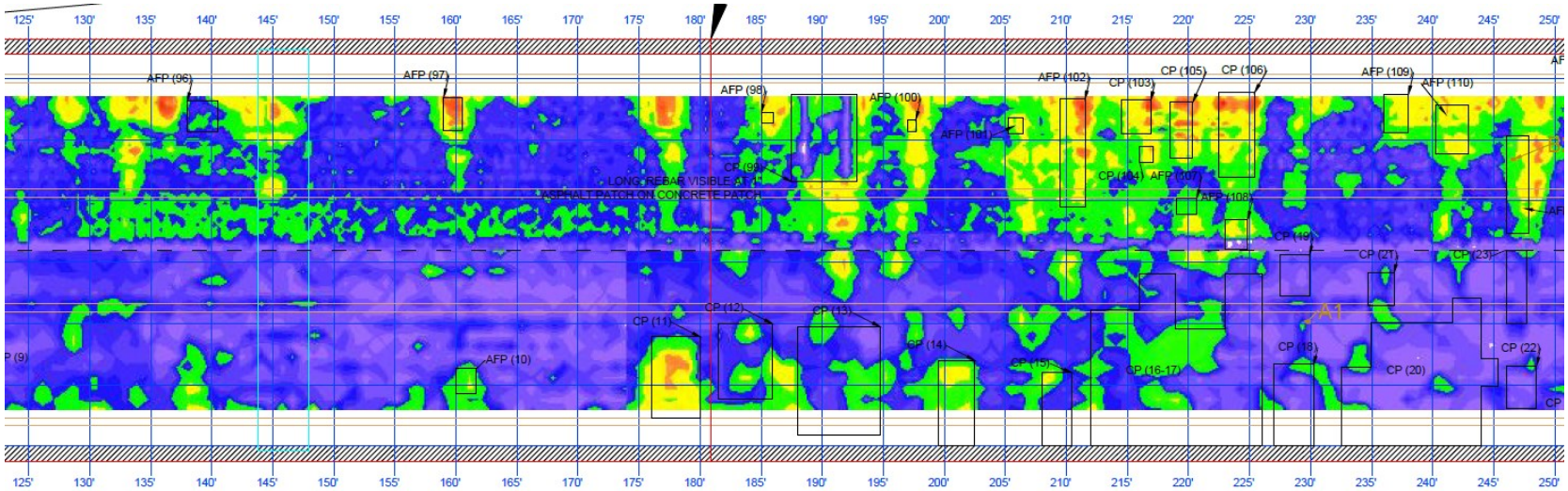

Figure 6-11 Bridge A1479 Drawing Including Lidar Rehabilitation Survey and Visual Investigation Results (Cont.)

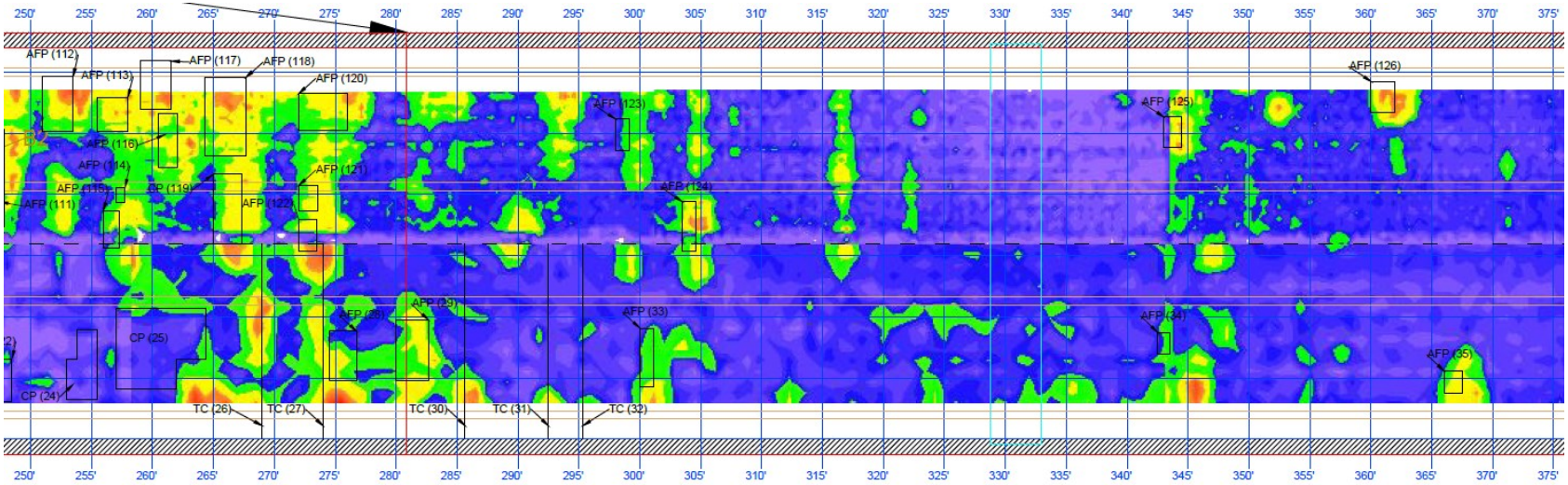

Figure 6-11 Bridge A1479 Drawing Including Lidar Rehabilitation Survey and Visual Investigation Results (Cont.)

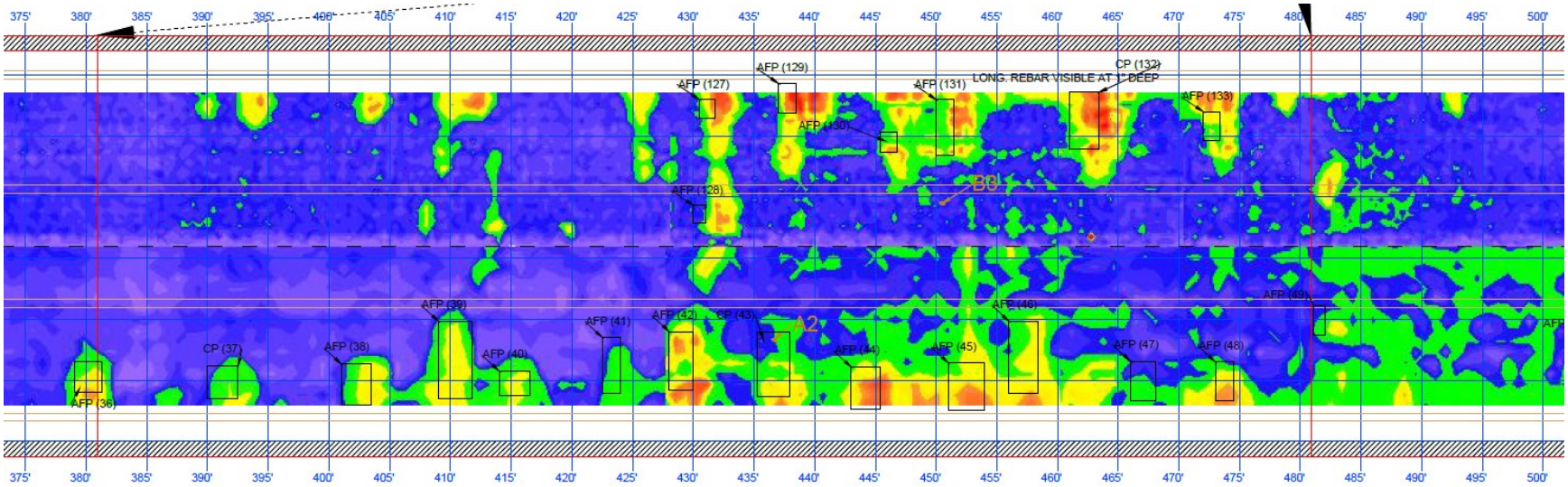

Figure 6-11 Bridge A1479 Drawing Including Lidar Rehabilitation Survey and Visual Investigation Results (Cont.)

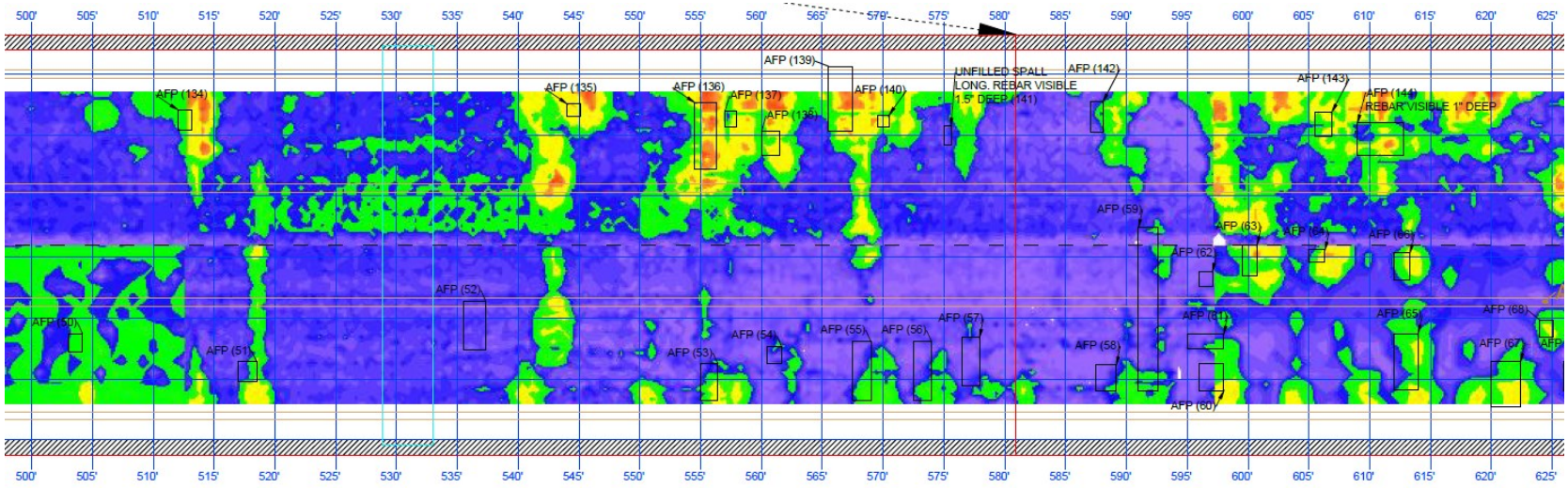

Figure 6-11 Bridge A1479 Drawing Including Lidar Rehabilitation Survey and Visual Investigation Results (Cont.)

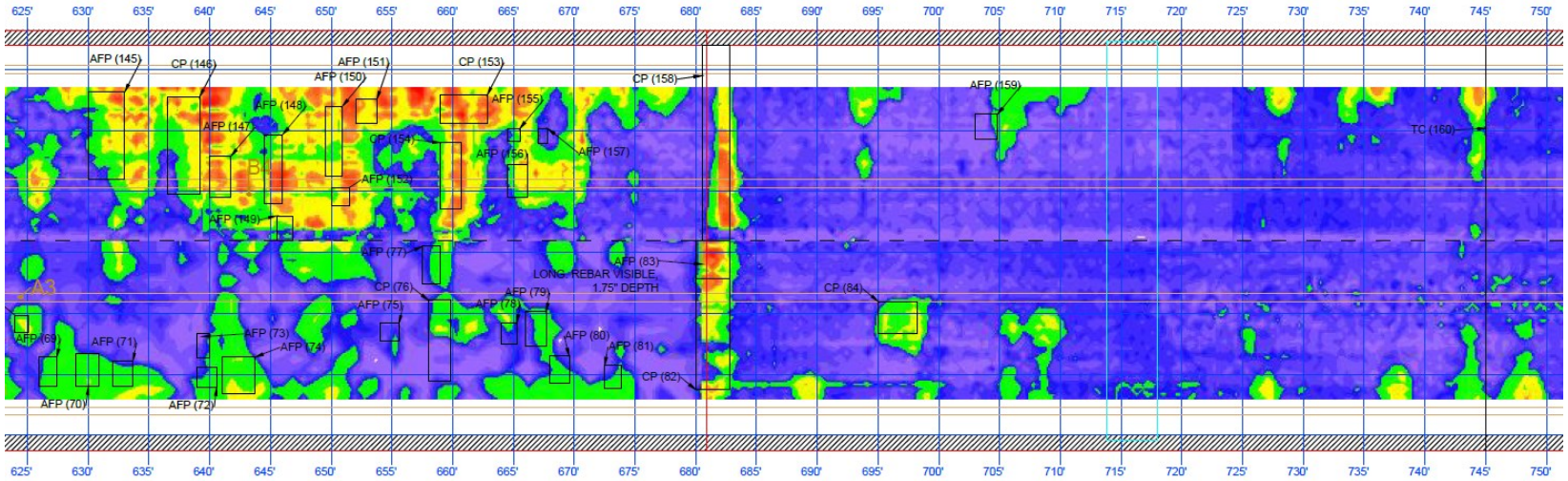

Figure 6-11 Bridge A1479 Drawing Including Lidar Rehabilitation Survey and Visual Investigation Results (Cont.)

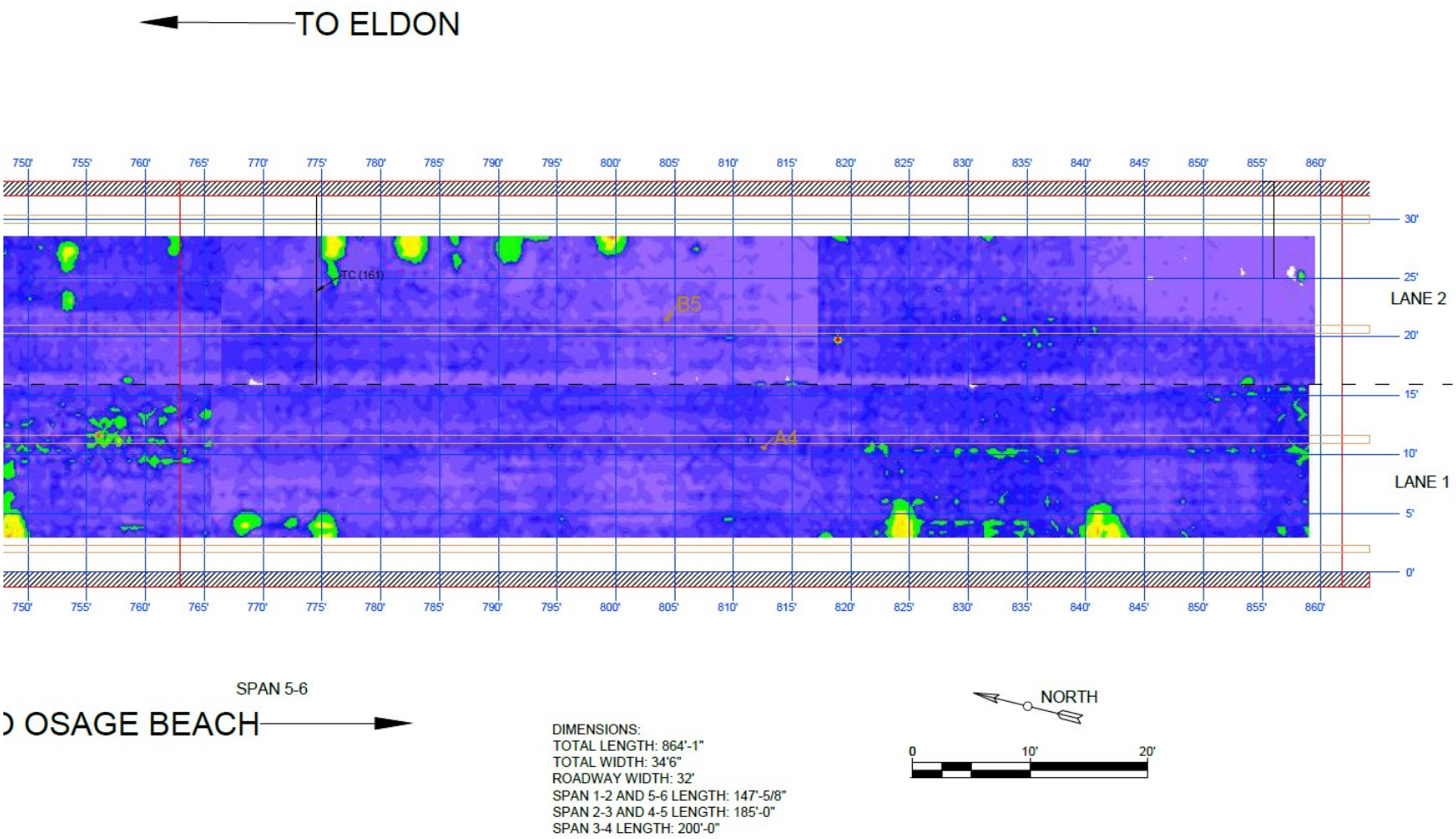

Figure 6-11 Bridge A1479 Drawing Including Lidar Rehabilitation Survey and Visual Investigation Results (Cont.)

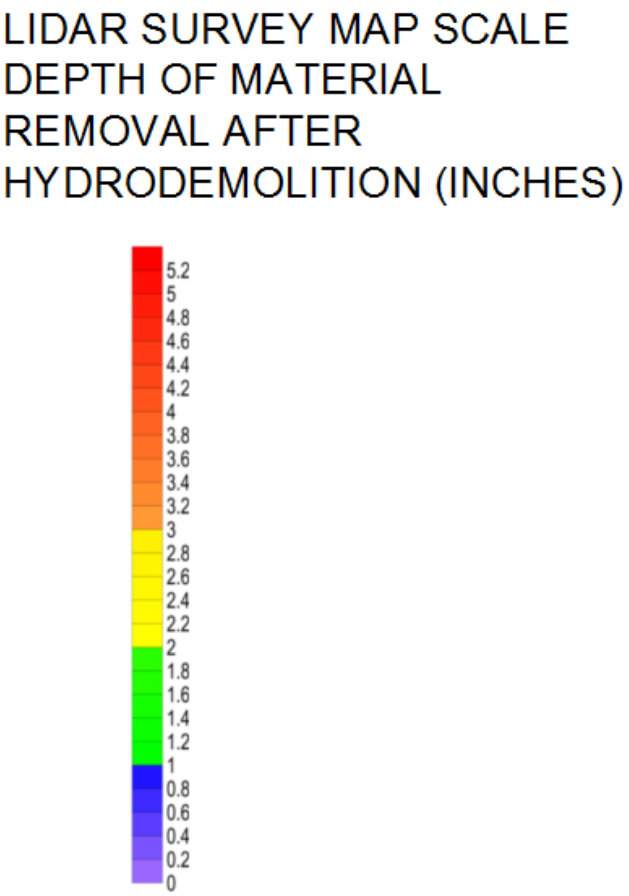

Figure 6-12 Bridge A1479 Lidar Scan Scale

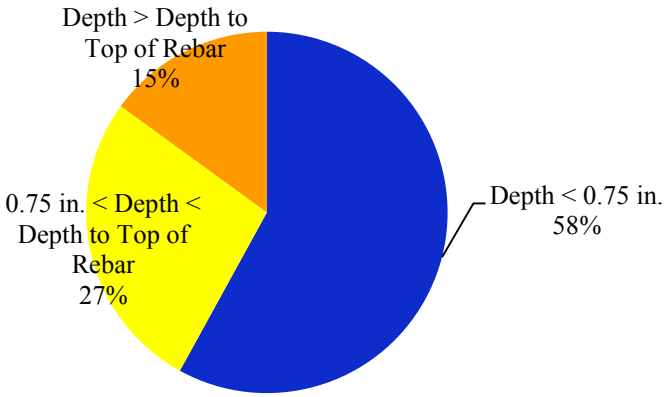

Figure 6-13 Bridge A1479 Lidar Depth of Concrete Removal Results

7 GROUND PENETRATING RADAR

7.1 Overview

Ground penetrating radar (GPR) is a non-destructive geophysical tool that uses pulsed electromagnetic radiation to image the top, base, and interior of a bridge deck. With respect to this project, the pulses of electromagnetic radiation that are emitted are partially reflected by the top of the bridge deck, the base of the deck, and from features such as embedded reinforcing steel bar (rebar) and delaminations. The principles of the GPR tool operation are shown in Figure 7.1. Analysis of the reflected signal (magnitude and arrival time) enables the operator to estimate the depth to each reflector and to assess the overall condition of the bridge deck. The most significant output of the GPR investigation is a map depicting variations in the amplitude of the reflection from the top of the transverse layer of rebar. Based on the interpretation of the amplitude map, the interpreter is able to identify areas of the bridge deck where there is no evidence of deterioration, evidence of moderate deterioration, or evidence of extensive deterioration.

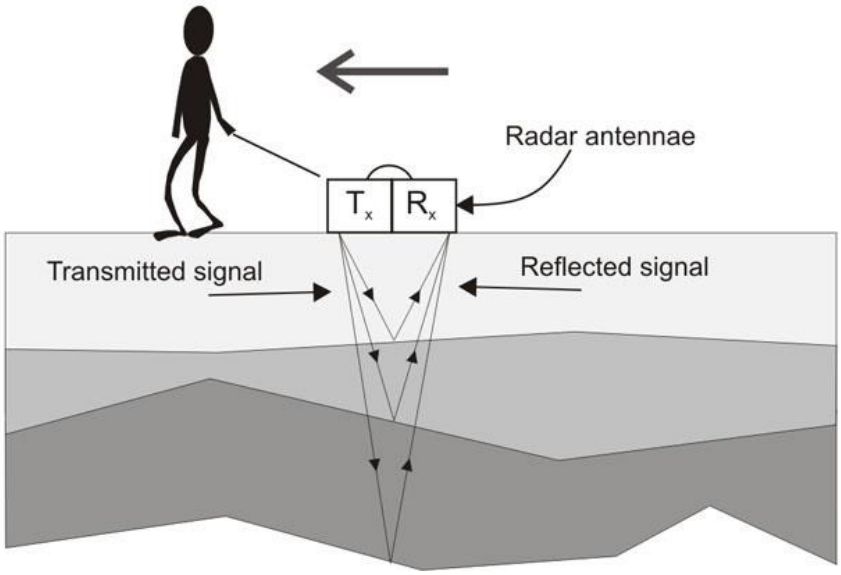

Figure 7-1 GPR Operating Principle (Maser, 2009)

A ground coupled 1.5 GHz GPR antenna was used to investigate each bridge deck. The primary objective the GPR investigations was to evaluate the capability of the GPR tool to rapidly and reliably assess the condition of the bridge deck. Section 7-2 is a discussion of the methodology. Section 7-3 is a presentation of the GPR results for each bridge deck. Section 7-4 is a summary of the results.

7.2 Methodology

The ground penetrating radar data were acquired using a GSSI SIR-3000 system and a GSSI 1.5 GHz ground coupled antenna mounted to a push-cart (Figure 7.2). The GPR data were acquired on the top surface of the bridge deck along parallel traverses variably spaced at 0.75 to 2 ft. intervals (depending on bridge deck and time constraints). Traverses were marked with chalk on the deck surface prior to the start the survey, and the cart was pushed along each traverse to

acquire data. The GPR traverses were oriented parallel to the direction of traffic flow (i.e., longitudinal direction of the bridge). The intent was to image was the uppermost layer of transverse rebar.

Figure 7-2 A MS&T Researcher Acquiring GPR Data with GSSI SIR-3000 GPR System with a GSSI 1.5 GHz Ground Coupled Antenna Along a Roadway Segment

For analyses purposes, the material within the bridge deck, and therefore the dielectric constant of that material, was assumed to be uniform. The GPR data were processed using GSSI RADAN 6.6 and RADAN 7 processing software. Initial processing steps included time-zero correction and filtering to eliminate noise. The arrival times and amplitudes of the reflections from each imaged segment of transverse reinforcement were calculated ("picked"). The output of processing was an Excel spreadsheet that included reflection amplitudes (in units of normalized decibels, NdB) and two-way travel times (in units of nanoseconds, ns) for each imaged segment of transverse rebar. Post-processing included combining the Excel spreadsheet information from individual GPR profiles into one Excel file with assigned coordinates for each GPR profile. Finally, a contour map depicting the reflection amplitude from the top of each imaged segment of transverse layer of rebar was generated using the software program Surfer (by Golden Software) for each bridge deck. It should be noted that it was necessary to interpolate between control points on adjacent GPR profiles (across 2 ft. intervals in some instances). This could be the cause of poor apparent correlation between some data sets (e.g. condition of cores extracted between GPR traverses and the GPR interpretations themselves).

During the preliminary phase of data interpretation, the processed, individual GPR profiles were visually examined to identify features such as the reflection from the uppermost transverse layer of rebar (Figure 7-3) and reflection from the base of the bridge deck (Figure 7-4). Also variations

in the apparent embedment depth of the top layer of rebar were noted since greater apparent embedment depth is usually indicative of greater concrete deterioration (Figure 7-5). After correlating the GPR results with the visual evaluation of the cores (discussed in Section 4), reflection amplitude ranges for three deterioration categories were defined. The three categories defined are: "no evidence of deterioration," "evidence of moderate deterioration," and "evidence of extensive deterioration," corresponding to relatively high reflection amplitude, moderate reflection amplitude, and low reflection amplitude, respectively. The amplitude range for each category was determined by the researchers for each individual bridge deck, and graphs were developed to show the predicted distribution of deterioration of each bridge deck in terms of deck surface area investigated.

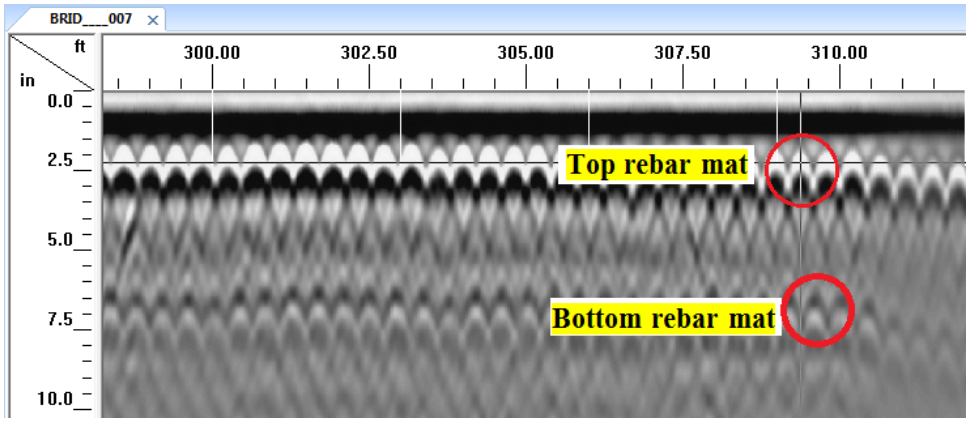

Figure 7-3 Example of GPR Data Showing Reflections from Top and Bottom Transverse Rebar. Lower Reflection Amplitudes (Top Layer of Rebar) are Normally Indicative of Deterioration.

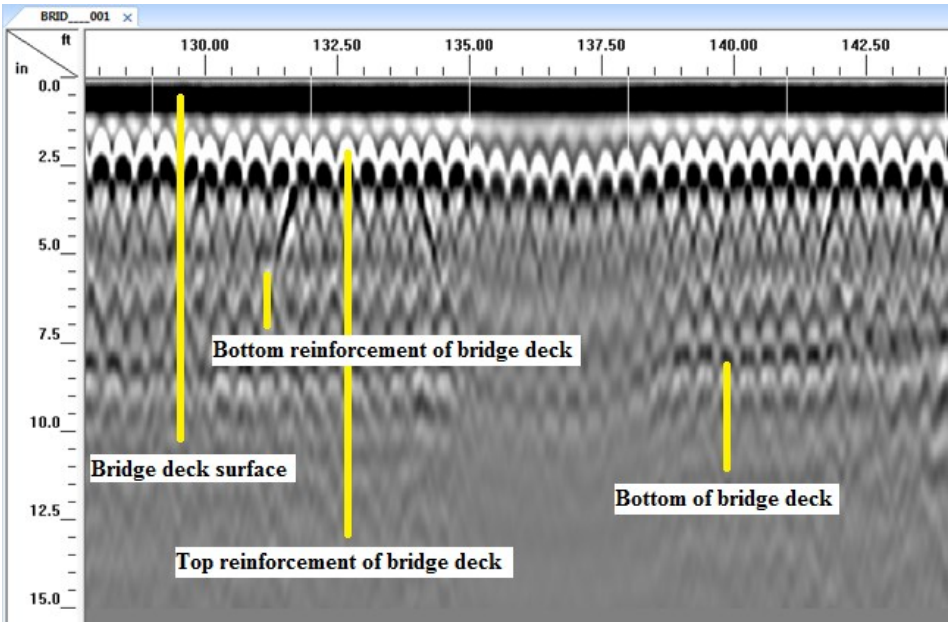

Figure 7-4 Example of GPR Data Showing Reflection from Interpreted Bottom of Bridge Deck

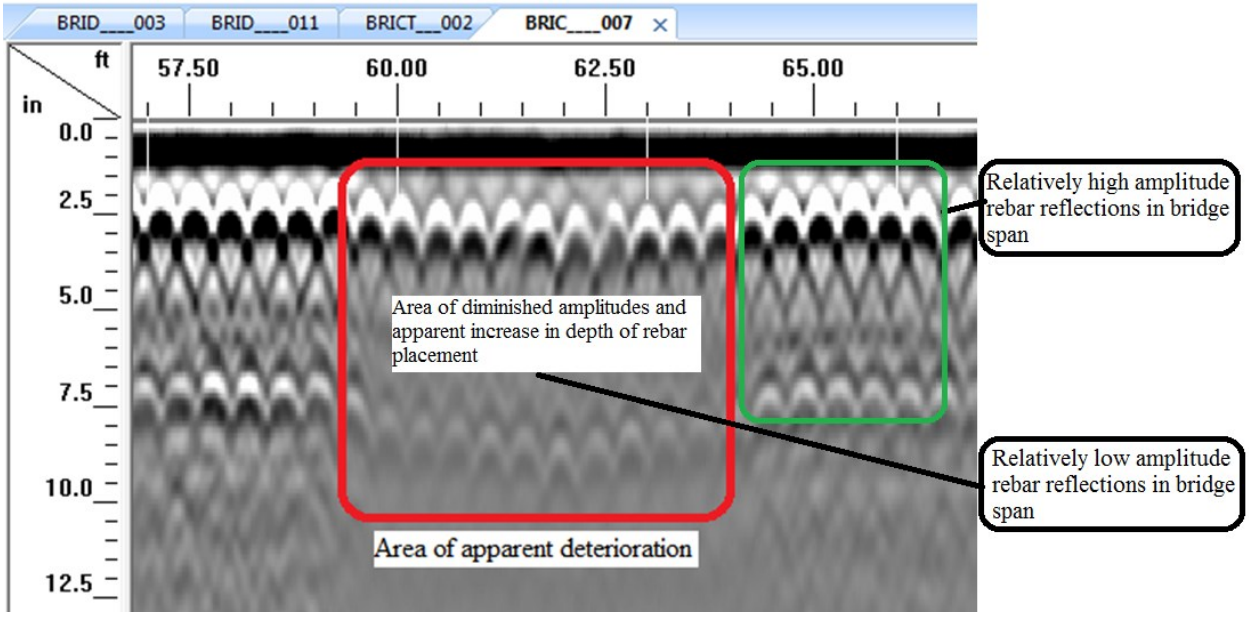

Figure 7-5 Example of GPR Data Showing Variation of the Apparent Embedment Depth of Top and Bottom Layers of Rebar. Greater Apparent Embedment Depths are Normally an Indication of Deterioration.

GPR results were compared with results from the visual core evaluation (Section 4) and chloride ion concentration (Section 5). The approach used to evaluate the correlation between the GPR results and the visual evaluation of cores is illustrated below in Table 7-1. The cores are compared in terms of the visual core rating to the GPR deterioration level estimated for the location the core was extracted. For this evaluation, ideal matches would be a core rated "Good" during the visual evaluation to be extracted from an area with "no evidence of deterioration" based on the GPR interpretation, a core rated "Fair" to be extracted from an area with "evidence of moderate deterioration," and a core rated "Poor" to be extracted from an area with "evidence of extensive deterioration." Cells indicating the ideal match are shaded in Table 7-1. Additionally, cores that were within 6 in. of a different GPR deterioration level were identified as "border line." As mentioned previously, the software used to generate the GPR contour maps interpolates between adjacent GPR profiles. The interpolation could cause slight errors in the GPR results, especially when the results are being compared to small diameter cores such as those extracted in this project (2 in. diameter).

Finally, Bridges A1193, A1297, and A1479 underwent rehabilitation during the project duration, which allowed the researchers to compare the GPR interpretations to hydrodemolition results. The lidar maps from Section 6 showing the material removed during hydrodemolition were compared with the GPR amplitude maps to evaluation the degree of correlation.

Table 7-1 Example Correlation Determination Between GPR and Visual Core Evaluation (Bridge A1479 Shown)

	Bridge A1479	VISUAL CORE RATING		
		Good	**Fair**	**Poor**
GPR MAP CLASSIFICATION	**No Evidence of Deterioration**	A2, A4, B3	A1 (Border Line Moderate)	
	Moderately Deteriorated	B1, B5 (Border Line No Deterioration)	A3, B4	B2 (asphalt core)
	Extensively Deteriorated			
	% Ideal Match	**% Ideal Match with Border Line Correct**		
	56%	**78%**		

7.3 Results

7.3.1 Bridge A0569

The GPR data were acquired along parallel traverses spaced at intervals of approximately 2 ft. The acquisition parameters employed were 512 samples/scan, 120 scans/second, and 60 scans/ft. The dielectric constant was assumed to be 10.0. A map of reflection amplitudes from the top layer of transverse rebar is shown in Figure 7-6. Amplitude ranges for three deterioration categories shown in Figure 7-6 were defined based on correlation of the GPR data with the visual evaluation of the cores. Area and percentage distribution of all three deterioration categories were calculated for the investigated bridge deck area and are shown in Figure 7-7.

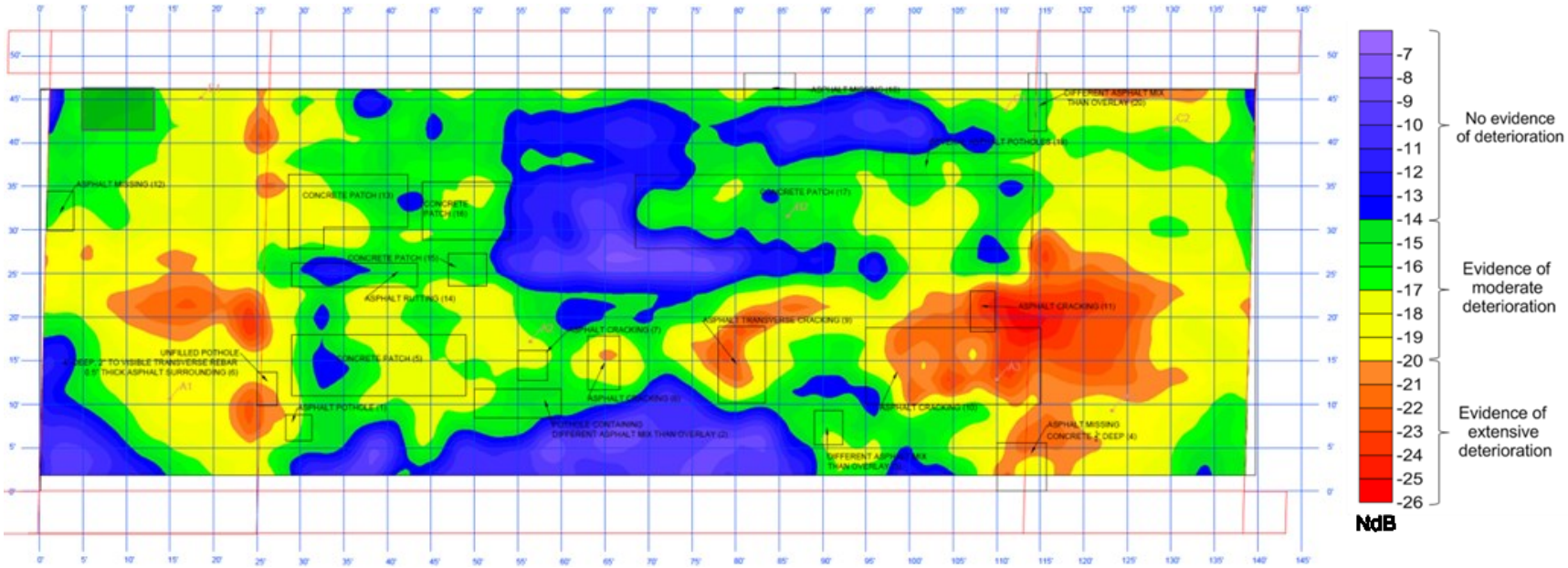

Figure 7-6 GPR Amplitude Map Based on Top Bar Reflection for Bridge Deck A0569 with Superposed Core Locations and Visual Surface Condition Features

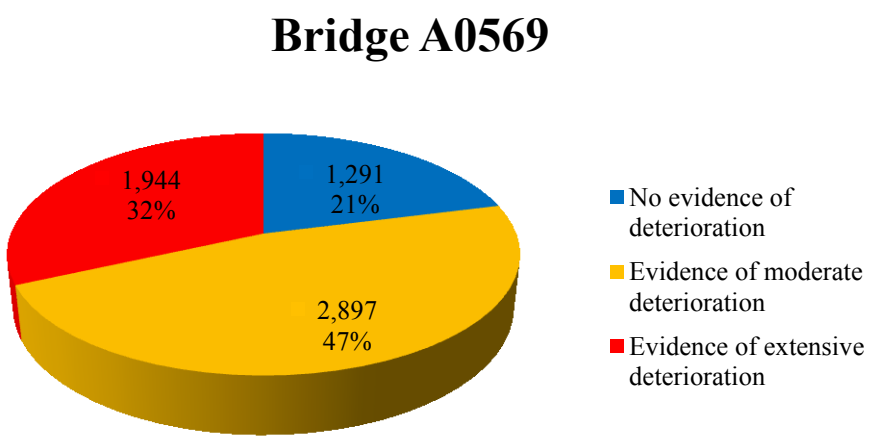

Figure 7-7 Graph Showing Predicted Distribution of Deterioration of the Bridge Deck for Bridge A0569 (investigated area) in Each Category (Based on Amplitude of the Reflection From the Top Layer of Rebar). Total Area Investigated - 6,132 ft²; No Evidence of Deterioration - 1,291 ft²; Evidence of Moderate Deterioration - 2,897 ft²; Evidence of Extensive Deterioration 1,944 ft².

Figure 7-7 shows that 21% of the area investigated on the bridge deck of Bridge A0596 exhibited no evidence of deterioration, 47% exhibited evidence of moderate deterioration, and 32% exhibited evidence of extensive deterioration based on the deterioration categories defined for the GPR amplitude results.

Table 7-2 summarizes the GPR results at the core locations so that the GPR, and visual core evaluation, and chloride ion concentration results can be compared. Results of the visual core evaluations (from Table 4-1) and the chloride ion concentration results (from Section 5) are also included in Table 7-2. The visual core evaluation and GPR estimated deterioration level comparison show a fair correlation. Bridge A0569 had 25% of the cores with an ideal match with GPR estimated deterioration levels. If the border line cores are considered to fall into a different GPR estimated deterioration level, Bridge A0569 had 90% of the cores with an ideal match.

Table 7-2 Bridge A0569 GPR Results at Core Locations

Core	Grade Classification Based on GPR Scale	Visual Core Evaluation Results	Chloride Ion Concentration
A1	Evidence of moderate deterioration	Good	Not available
A2	Evidence of moderate deterioration	Poor	Not available
A3	Evidence of extensive deterioration	Good	Not available
A4	Evidence of moderate deterioration	Good	Not available
B1	Evidence of moderate deterioration	Good	Not available
B2	Evidence of moderate deterioration	Fair	Not available
C1	Evidence of moderate deterioration	Fair	Not available
C2	Evidence of moderate deterioration	Good	Not available

7.3.2 Bridge A1187

The GPR data were acquired along parallel traverses spaced at 1 ft intervals. The acquisition parameters employed were 512 samples/scan,120 scans/second, and 90 scans/ft. The dielectric constant was assumed to be 10.0. Map of reflection amplitudes from the top layer of transverse rebar are shown in Figures 7-8 and 7-9, before and after resurfacing, respectively. Amplitude ranges for three deterioration categories shown in Figure 7-8 were defined based on correlation of the GPR data with the visual evaluation of the cores. Area and percentage distribution of all three deterioration categories were calculated for the bridge deck area, before and after resurfacing, are shown in Figure 7-10 and 7-11, respectively.

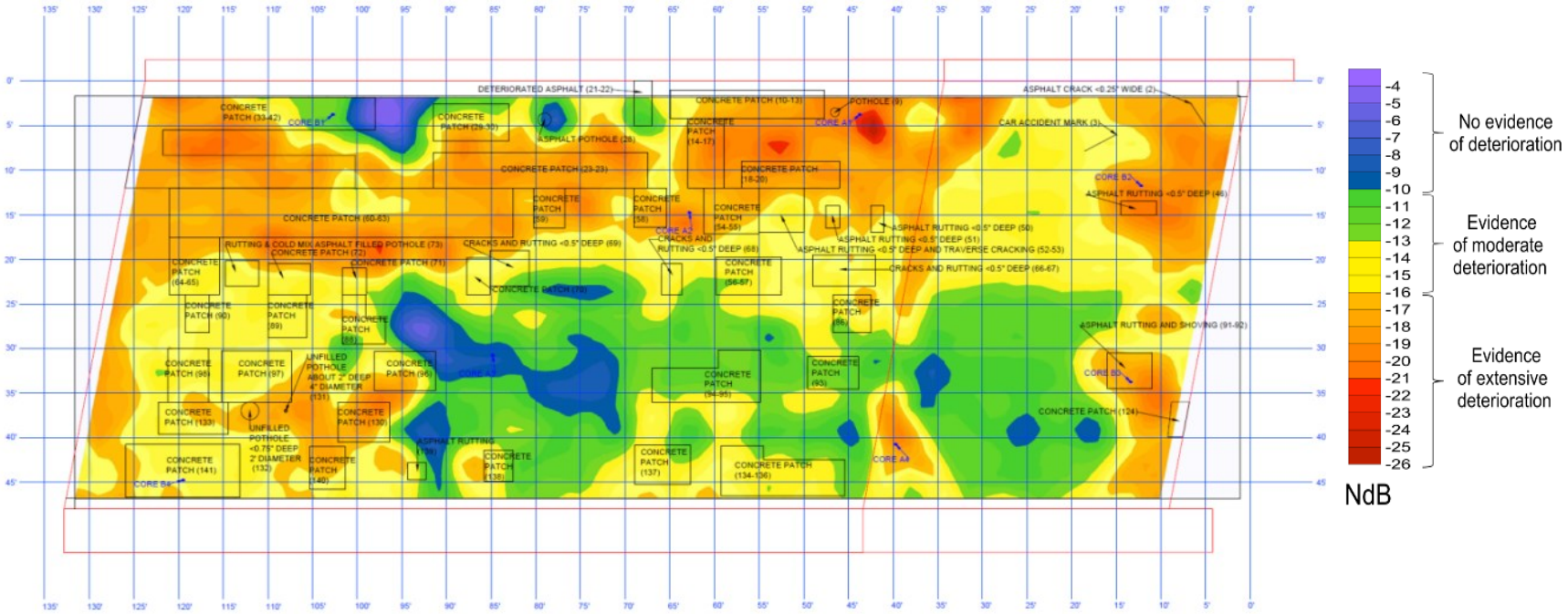

Figure 7-8 GPR Amplitude Map Based on Top Bar Reflection for Bridge Deck A1187 with Superposed Core Locations and Visual Surface Condition Features, Prior to Resurfacing

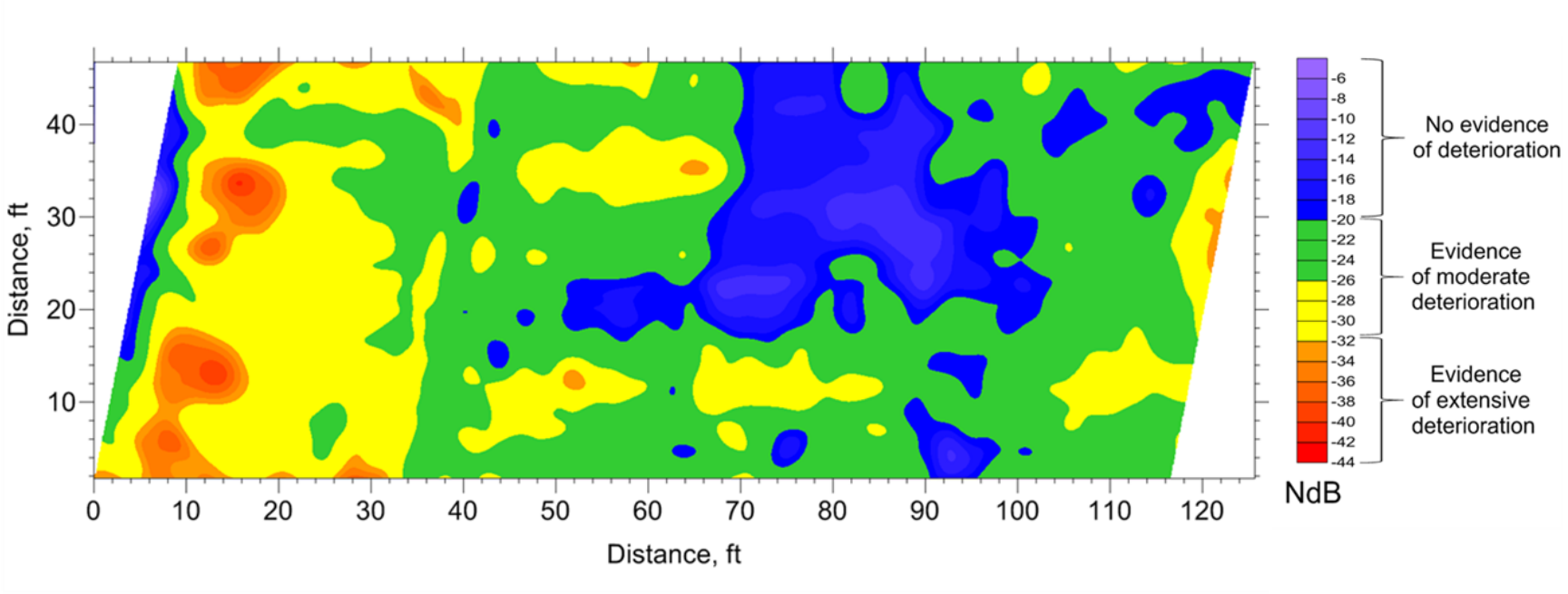

Figure 7-9 GPR Amplitude Map Based on Top Bar Reflection for Bridge Deck A1187 with Superposed Core Locations and Visual Surface Condition Features, After Resurfacing

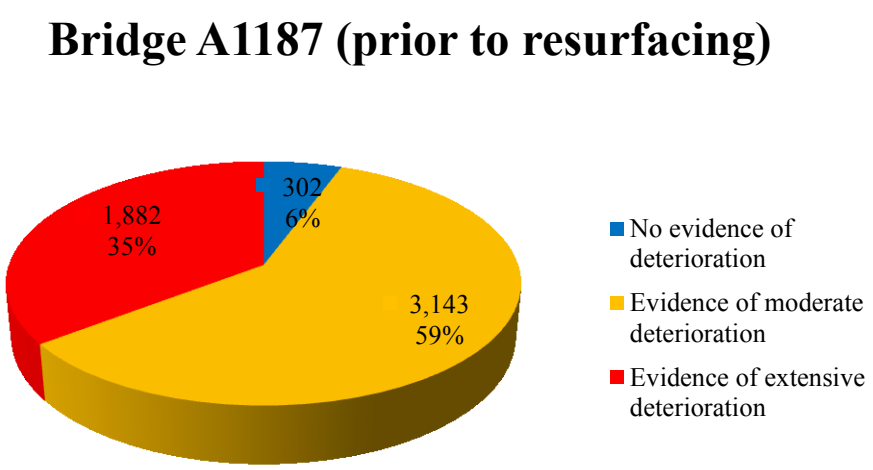

Figure 7-10 Graph Showing Predicted Distribution of Deterioration of the Bridge Deck A1187 (Investigated Area; Prior to Resurfacing) in Each Category (Based on the Amplitude of the Reflection from the Top Layer of Rebar). Total Area Investigated - 5,327 ft²; No Evidence of Deterioration - 302 ft²; Evidence of Moderate Deterioration - 3,143 ft²; Evidence of Extensive Deterioration 1,882 ft².

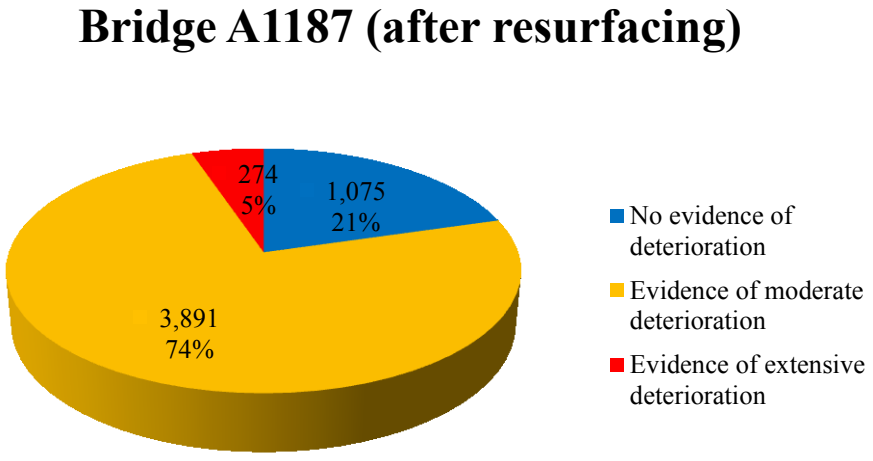

Figure 7-11 Graph Showing Predicted Distribution of Deterioration of the Bridge Deck A1187 (Investigated Area; After Resurfacing) in Each Category (Based on the Amplitude of the Reflection from the Top Layer of Rebar). Total Area Investigated - 5,240 ft²; No Evidence of Deterioration – 1,075 ft²; Evidence of Moderate Deterioration - 3,891 ft²; Evidence of Extensive Deterioration 274 ft².

Figure 7-10 shows that 6% of the area investigated on the bridge deck of Bridge A1187 exhibited no evidence of deterioration, 59% exhibited evidence of moderate deterioration, and 35% exhibited evidence of extensive deterioration based on the deterioration categories defined for the GPR amplitude results.

Table 7-3 summarizes the GPR results at the core locations so that the GPR, and visual core evaluation, and chloride ion concentration results can be compared. Results of the visual core evaluations (from Table 4-2) and the chloride ion concentration results (from Section 5) are also included in Table 7-3. The visual core evaluation and GPR estimated deterioration level comparison show a fair correlation. Bridge A1187 had 63% of the cores with an ideal match with GPR estimated deterioration levels. If the border line cores are considered to fall into a different GPR estimated deterioration level, Bridge A1187 had 88% of the cores with an ideal match.

Chloride ion concentration test results were determined for two of the eight total cores extracted from Bridge A1187, Cores A4 and B4. Both cores were rated Good in the visual examination, Core A4 showed evidence of extensive deterioration based on the GPR results, and Core B4 showed evidence of moderate deterioration based on the GPR results. Both cores had chloride ion concentrations slightly below the threshold of 0.15% by weight of cement.

Table 7-3 Bridge A1187 GPR Results at Core Locations

Core	Grade Classification Based on GPR Scale	Visual Core Evaluation Results	Chloride Ion Concentration
A1	Evidence of extensive deterioration	Poor	Not available
A2	Evidence of extensive deterioration	N/A (asphalt)	Not available
A3	No evidence of deterioration	Good	Not available
A4	Evidence of extensive deterioration	Good	<0.15%
B1	Evidence of moderate deterioration	Fair	Not available
B2	Evidence of extensive deterioration	Fair	Not available
B3	Evidence of extensive deterioration	Poor	Not available
B4	Evidence of moderate deterioration	Good	<0.15%

7.3.3 Bridge A1193

The GPR data were acquired along parallel traverses spaced at 2 ft intervals. The acquisition parameters employed were 512 samples/scan, 120 scans/second, and 48 scans/ft. The dielectric constant was assumed to be 10.0. A map of reflection amplitudes from the top layer of transverse rebar is shown in Figure 7-12. Amplitude ranges for three deterioration categories shown in Figure 7-12 were defined based on correlation of the GPR data with the visual evaluation of the cores. Bridge A1193 underwent deck rehabilitation after the NDT investigation. The lidar map from Section 6 showing the material removal during the deck rehabilitation is reproduced in Figure 7-13 for comparison with the GPR results. Area and percentage distribution of the three deterioration categories defined for the GPR data were calculated for the investigated bridge deck area and are shown in Figure 7-14.

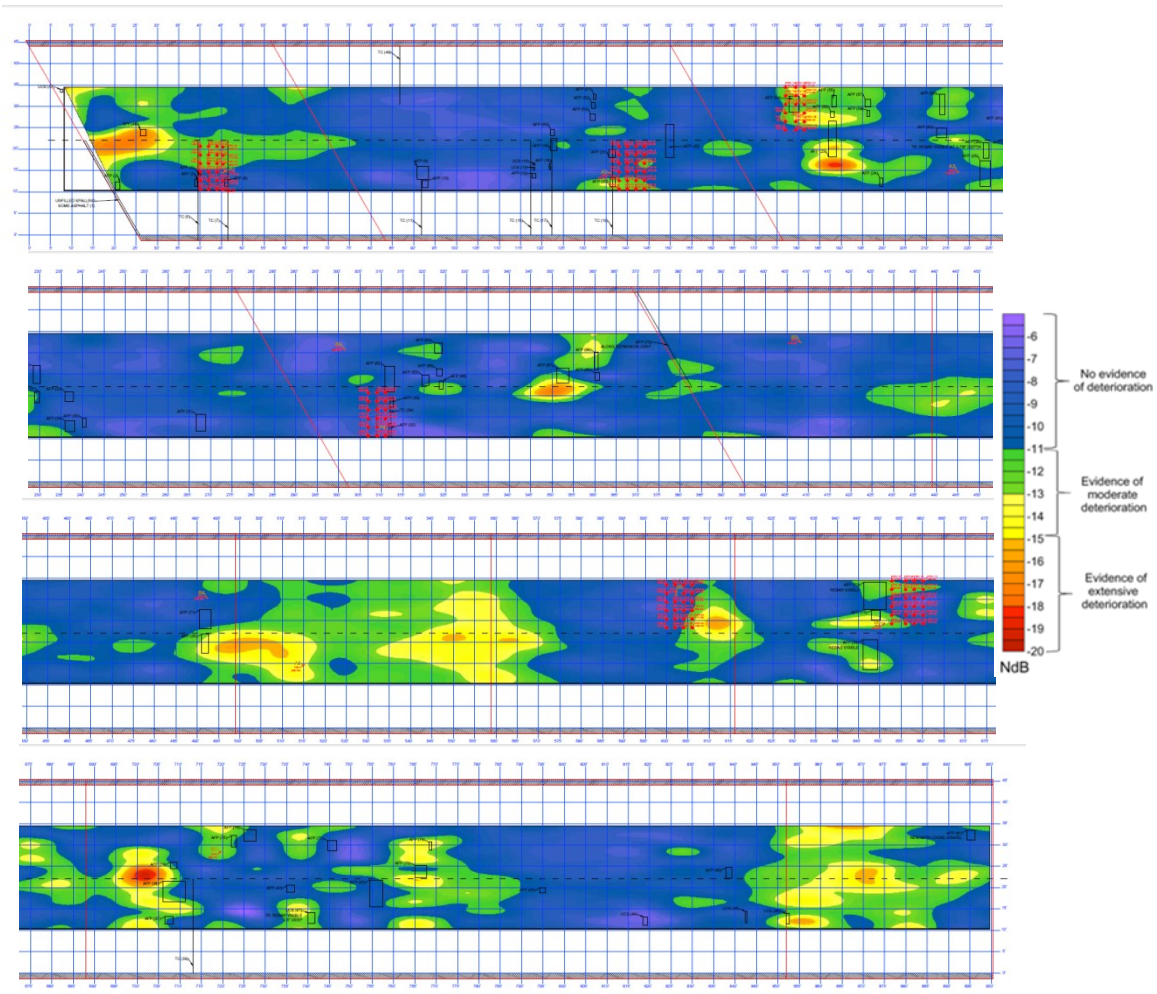

Figure 7-12 GPR Amplitude Map Based on Top Bar Reflection for Bridge Deck A1193 with Superposed Core Locations and Visual Surface Condition Features. Map Sections are Illustrated from Top to Bottom: 0-225 ft., 225-450 ft., 450-675 ft., 675-900 ft.

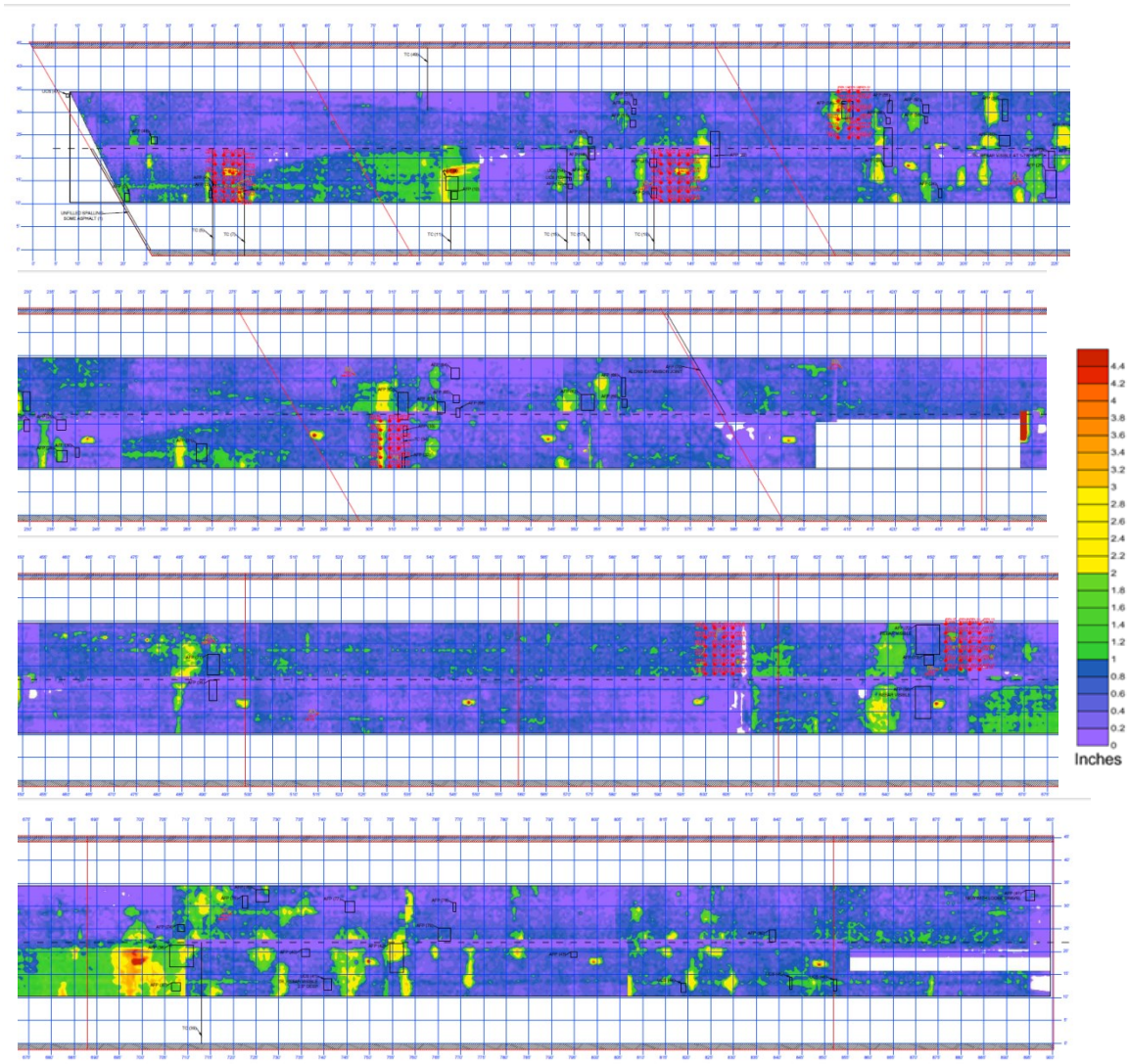

Figure 7-13 Lidar Map Showing Depth of Material Removed After the Hydro Demolition on Bridge Deck A1193. Depth Difference Between Lidar Scan Prior to Hydrodemolition and After Hydrodemolition is Shown in Inches. Map Sections are Illustrated from Top to Bottom: 0-225 ft., 225-450 ft., 450-675 ft., 675-900 ft.

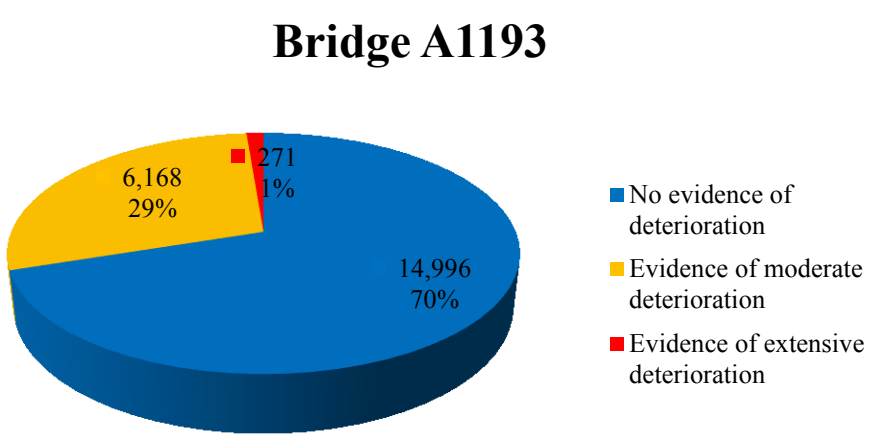

Figure 7-14 Graph Showing Predicted Distribution of Deterioration of the Bridge Deck A1193 in Each Category (Based on the Amplitude of the Reflection from the Top Layer of Rebar). Total Area Investigated - 21,435 ft²; No Evidence of Deterioration – 14,996 ft²; Evidence of Moderate Deterioration - 6,168 ft²; Evidence of Extensive Deterioration 271 ft².

Figure 7-14 shows that 70% of the area investigated on the bridge deck of Bridge A1193 exhibited no evidence of deterioration, 29% exhibited evidence of moderate deterioration, and 1% exhibited evidence of extensive deterioration based on the deterioration categories defined for the GPR amplitude results.

Table 7-4 summarizes the GPR results at the core locations so that the GPR, visual core evaluation, and chloride ion concentration results can be compared. Results of the visual core evaluations (from Table 4-3) and the chloride ion concentration results (from Section 5) are also included in Table 7-4. The visual core evaluation and GPR estimated deterioration level comparison show a good correlation. Bridge A1193 had 42% of the cores with an ideal match with GPR estimated deterioration levels. If the border line cores are considered to fall into a different GPR estimated deterioration level, Bridge A1193 had 92% of the cores with an ideal match.

Chloride ion concentration test results were determined for three of the 12 total cores extracted from Bridge A1193, Cores A1, A2, and A5. These cores were rated Good in the visual examination. Cores A1 and A3 showed no evidence of deterioration, and Core A5 showed evidence of moderate deterioration based on the GPR results. All three cores had chloride ion concentrations lower than the threshold of 0.15% by weight of cement.

Table 7-4 Bridge A1193 GPR Results at Core Locations

Core	Grade Classification Based on GPR Scale	Visual Core Evaluation Results	Chloride Ion Concentration
A1	No evidence of deterioration	Good	<0.15%
A2	No evidence of deterioration	Fair	Not available
A3	No evidence of deterioration	Good	<0.15%
A4	No evidence of deterioration	Good	Not available
A5	Evidence of moderate deterioration	Good	<0.15%
B1	Evidence of moderate deterioration	Poor	Not available
B2	No evidence of deterioration	Fair	Not available
B3	No evidence of deterioration	Fair	Not available
B4	No evidence of deterioration	Poor	Not available
B5	No evidence of deterioration	Good	Not available
B6	Evidence of moderate deterioration	Good	Not available
B7	Evidence of moderate deterioration	Fair	Not available

Comparing Figures 7-12 and 7-13, it can be seen that areas of the bridge deck where the GPR amplitude map indicates evidence of extensive deterioration generally correspond to areas with greater concrete material removal depths based on the lidar survey after hydrodemolition. Similarly, areas where the GPR amplitude map indicates moderate or no evidence of deterioration generally correspond to areas with lesser concrete material removal depths. Figure 7-1 compares the percentage of the bridge deck within each of the three categories defined for the GPR grade classification with three categories defined for depth of concrete material removed. It should be noted that a perfect correlation was not expected because the GPR grade classifications and the material removal depth categories have different meanings; see Section 7.4.2 for further discussion.

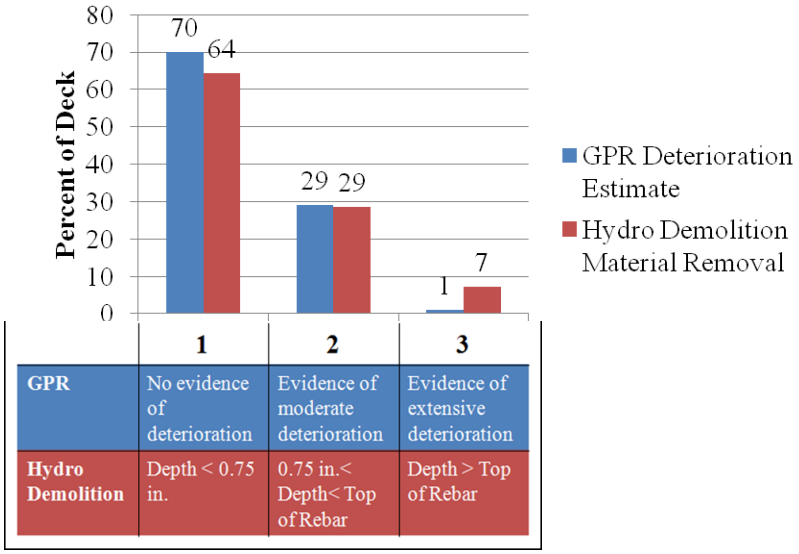

Figure 7-15 Percentage of Bridge Deck Area for Bridge A1193 Categorized by GPR Results and Rehabilitation Lidar Survey

7.3.4 Bridge A1297

The GPR data were acquired along parallel traverses spaced at 1 ft intervals. The acquisition parameters employed were 256 samples/scan, 120 scans/second, and 48 scans/ft. The dielectric constant was assumed to be 10.0. A map of reflection amplitudes from the top layer of transverse rebar is shown in Figure 7-16. Amplitude ranges for three deterioration categories shown in Figure 7-16 were defined based on correlation of the GPR data with the visual evaluation of the cores. Bridge A1297 underwent deck rehabilitation after the NDT investigation. The lidar map from Section 6 showing the material removal during the deck rehabilitation is reproduced in Figure 7-17 for comparison with the GPR results. Area and percentage distribution of all three deterioration categories were calculated for the investigated bridge deck area and are shown in Figure 7-18.

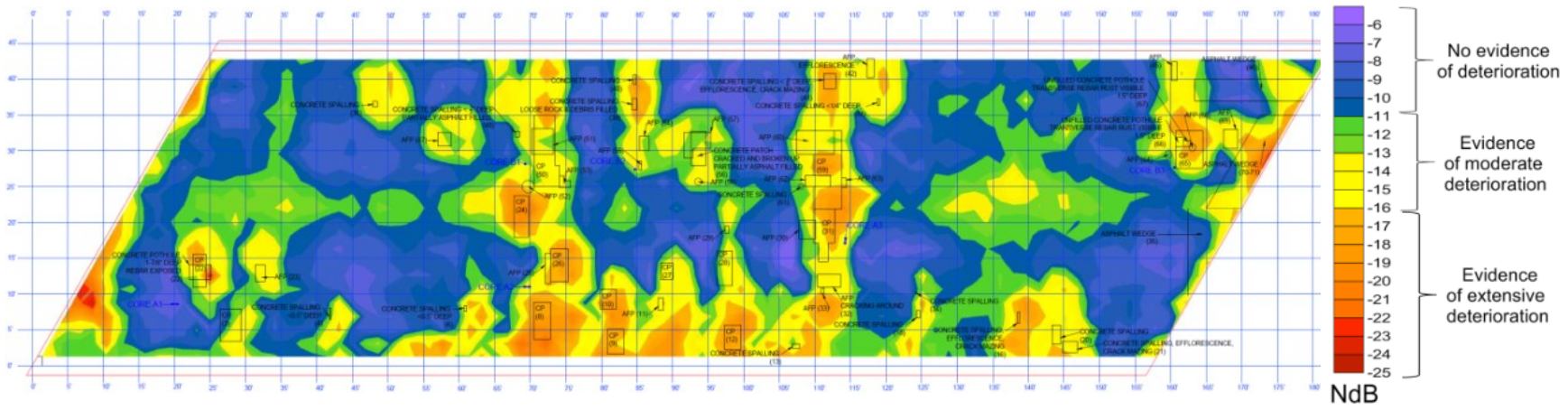

Figure 7-16 GPR Amplitude Map Based on Top Bar Reflection for Bridge Deck A1297 with Superposed Core Locations and Visual Surface Condition Features

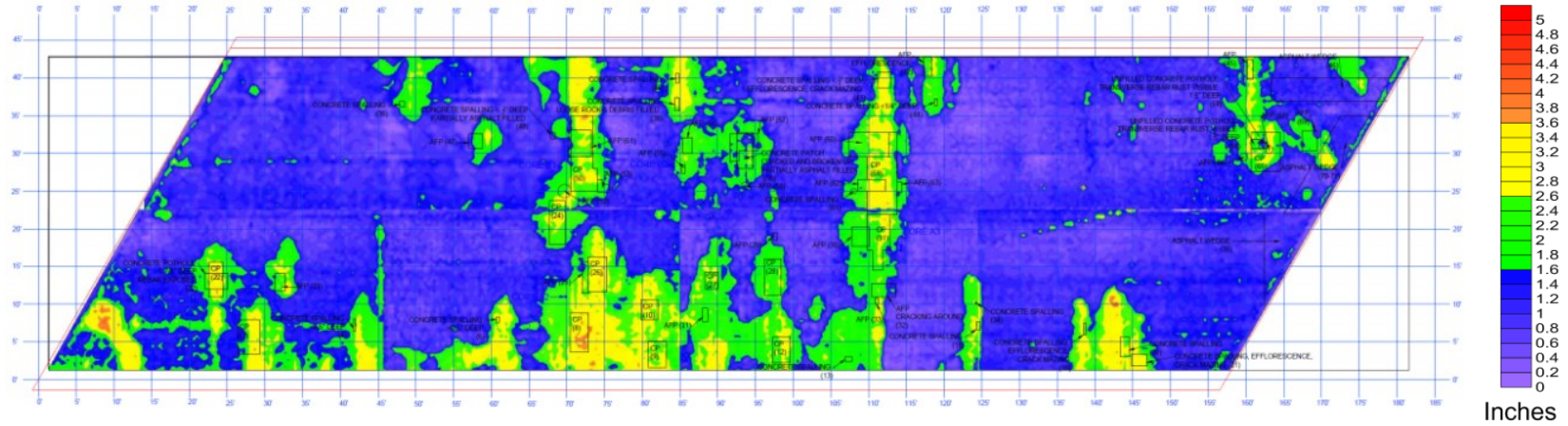

Figure 7-17 Lidar Map Showing Depth of Material Removed After the Hydro Demolition on Bridge Deck A1297. Depth Difference Between Lidar Scan Prior to Hydrodemolition and After Hydrodemolition is Shown in Inches.

.

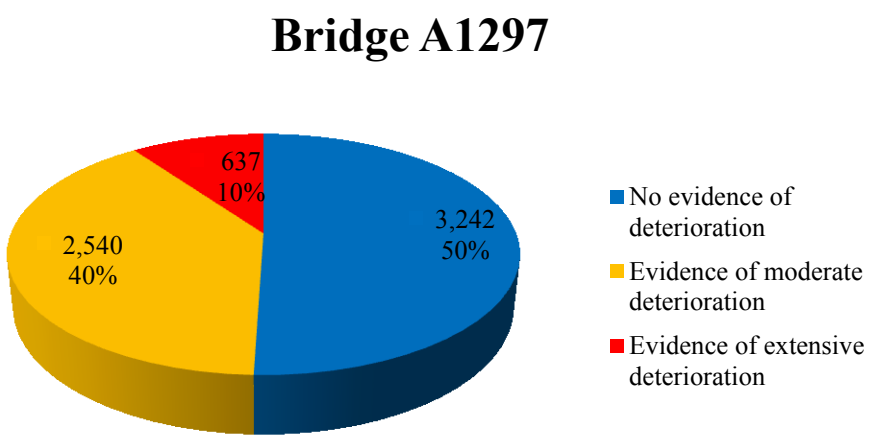

Figure 7-18 Graph Showing Predicted Distribution of Deterioration of the Bridge Deck A1297 in Each Category (Based on the Amplitude of the Reflection from the Top Layer of Rebar). Total Area Investigated - 6,419 ft²; No Evidence of Deterioration – 3,242 ft²; Evidence of Moderate Deterioration - 2,540 ft²; Evidence of Extensive Deterioration 637 ft².

Figure 7-18 shows that 50% of the area investigated on the bridge deck of Bridge A1297 exhibited no evidence of deterioration, 40% exhibited evidence of moderate deterioration, and 10% exhibited evidence of extensive deterioration based on the deterioration categories defined for the GPR amplitude results.

Table 7-5 summarizes the GPR results at the core locations so that the GPR, and visual core evaluation, and chloride ion concentration results can be compared. Results of the visual core evaluations (from Table 4-4) and the chloride ion concentration results (from Section 5) are also included in Table 7-5. The visual core evaluation and GPR estimated deterioration level comparison show a good correlation. Bridge A1297 had 50% of the cores with an ideal match with GPR estimated deterioration levels. If the border line cores are considered to fall into a different GPR estimated deterioration level, Bridge A1297 had 67% of the cores with an ideal match.

Table 7-5 Bridge A1297 GPR Results at Core Locations

Core	Grade Classification Based on GPR Scale	Visual Core Evaluation Results	Chloride Ion Concentration
A1	No evidence of deterioration	Good	<0.15%
A2	Evidence of moderate deterioration	Good	<0.15%
A3	Evidence of moderate deterioration	Fair	Not available
B1	Evidence of moderate deterioration	Poor	Not available
B2	Evidence of moderate deterioration	Fair	Not available
B3	Evidence of moderate deterioration	Good	Not available

Chloride ion concentration test results were determined for two of the six total cores extracted from Bridge A1297, Cores A1 and A2. These cores were rated Good in the visual examination,

however Core A1 showed no evidence of deterioration, and Core A2 showed evidence of moderate deterioration based on the GPR results. Both cores had chloride ion concentrations lower than the threshold of 0.15% by weight of cement.

Comparing Figures 7-16 and 7-17, it can be seen that areas of the bridge deck where the GPR amplitude map indicates evidence of extensive deterioration generally correspond to areas with greater concrete material removal depths based on the lidar survey after hydrodemolition. Similarly, areas where the GPR amplitude map indicates moderate or no evidence of deterioration generally correspond to areas with lesser concrete material removal depths. Figure 7-19 compares the percentage of the bridge deck within each of the three categories defined for the GPR grade classification with three categories defined for depth of concrete material removed. It should be noted that a perfect correlation was not expected because the GPR grade classifications and the material removal depth categories have different meanings; see Section 7.4.2 for further discussion.

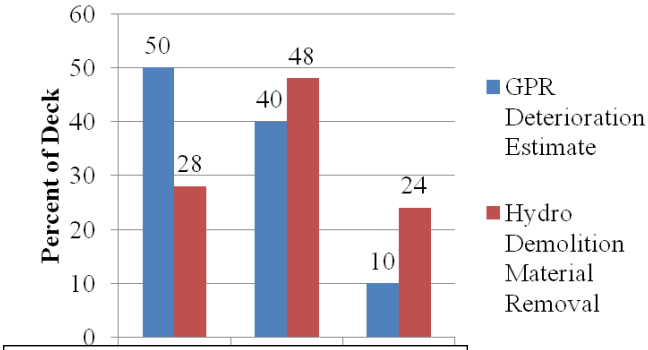

	1	2	3
GPR	No evidence of deterioration	Evidence of moderate deterioration	Evidence of extensive deterioration
Hydro Demolition	Depth < 0.75 in.	0.75 in.< Depth< Top of Rebar	Depth > Top of Rebar

Figure 7-19 Percentage of Bridge Deck Area for Bridge A1297 Categorized by GPR Results and Rehabilitation Lidar Survey

7.3.5 Bridge A1479

The GPR data were acquired along parallel traverses spaced at 2 ft intervals. The acquisition parameters employed were 512 samples/scan, 120 scans/second, and 48 scans/ft (last three GPR profiles were recorded with 512 samples/scan and 36 scans/ft due to the time limitation). The dielectric constant was assumed to be 10.0. A map of reflection amplitudes from the top layer of transverse rebar is shown in Figure 7-20. Amplitude ranges for three deterioration categories shown in Figure 7-20 were defined based on correlation of the GPR data with the visual evaluation of the cores. Bridge A1479 underwent deck rehabilitation after the NDT investigation. The lidar map from Section 6 showing the material removal during the deck rehabilitation is reproduced in Figure 7-21 for comparison with the GPR results. Area and percentage distribution of all three deterioration categories were calculated for the investigated bridge deck area and are shown in Figure 7-22.

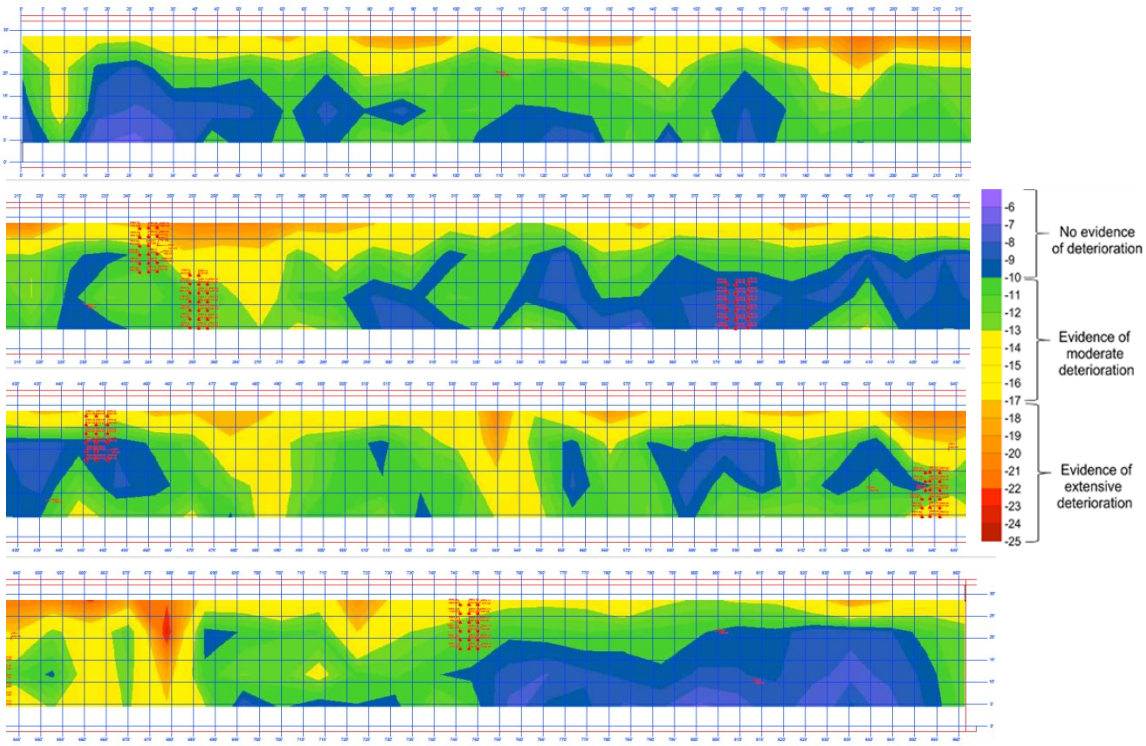

Figure 7-20 GPR Amplitude Map Based on Top Bar Reflection for Bridge Deck A1479 with Superposed Core Locations and Visual Surface Condition Features. Map Sections are Illustrated from Top to Bottom: 0-215 ft., 215-430 ft., 430-645 ft., 645-862 ft.

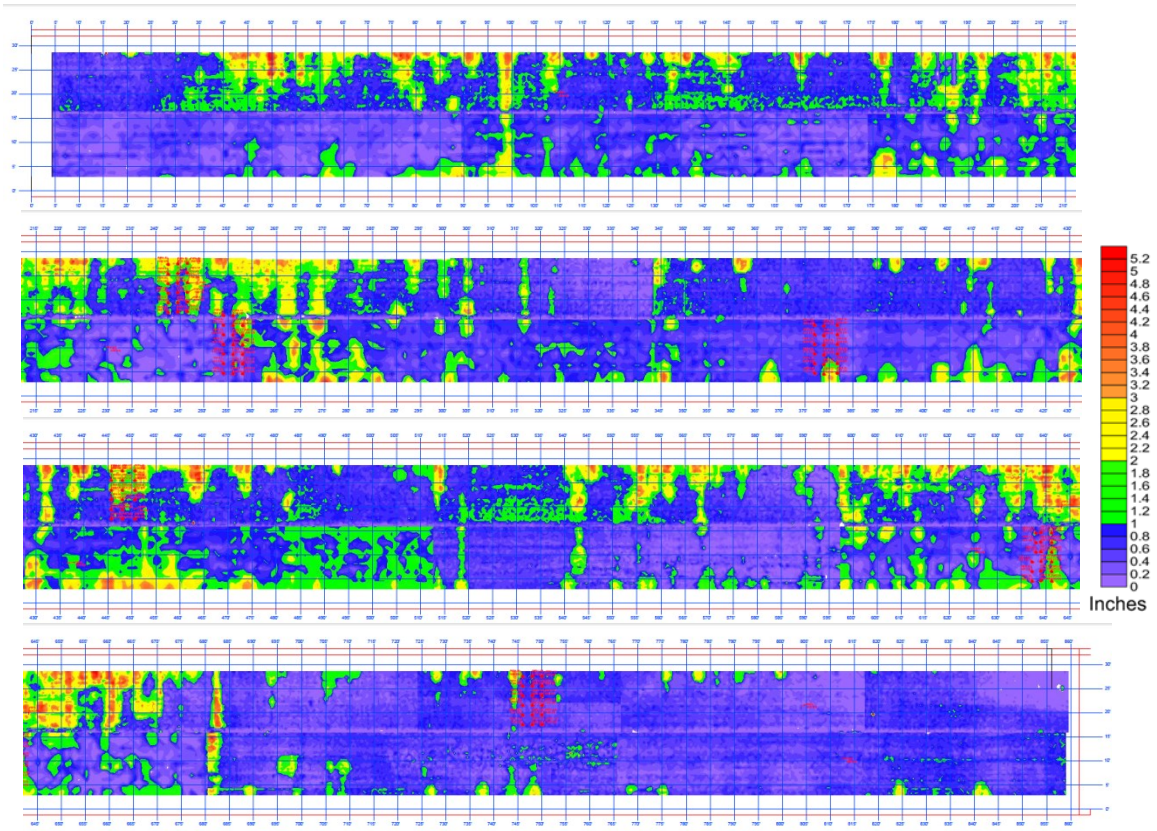

Figure 7-21 Lidar Map Showing Depth of Material Removed After the Hydro Demolition on Bridge Deck A1479. Depth Difference Between Lidar Scan Prior to Hydrodemolition and After Hydrodemolition is Shown in Inches. Map Sections are Illustrated from Top to Bottom: 0-215 ft., 215-430 ft., 430-645 ft., 645-862 ft.

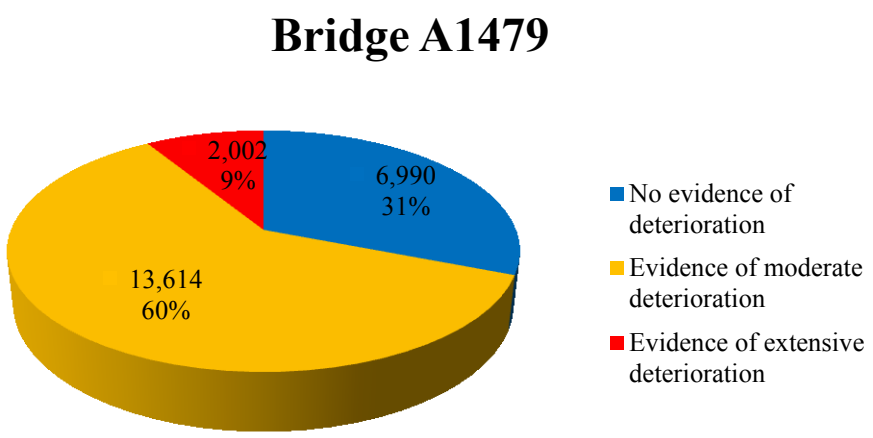

Figure 7-22 Graph Showing Predicted Distribution of Deterioration of the Bridge Deck A1479 in Each Category (Based on the Amplitude of the Reflection from the Top Layer of Rebar). Total Area Investigated - 22,606 ft²; No Evidence of Deterioration – 6,990 ft²; Evidence of Moderate Deterioration - 13,614 ft²; Evidence of Extensive Deterioration 2,002 ft².

Figure 7-22 shows that 31% of the area investigated on the bridge deck of Bridge A1479 exhibited no evidence of deterioration, 60% exhibited evidence of moderate deterioration, and 9% exhibited evidence of extensive deterioration based on the deterioration categories defined for the GPR amplitude results.

Table 7-6 summarizes the GPR results at the core locations so that the GPR, and visual core evaluation, and chloride ion concentration results can be compared. Results of the visual core evaluations (from Table 4-5) and the chloride ion concentration results (from Section 5) are also included in Table 7-6. The visual core evaluation and GPR estimated deterioration level comparison show a good correlation. Bridge A1479 had 56% of the cores with an ideal match with GPR estimated deterioration levels. If the border line cores are considered to fall into a different GPR estimated deterioration level, Bridge A1479 had 78% of the cores with an ideal match.

Table 7-6 Bridge A1479 GPR Results at Core Locations

Core	Grade Classification Based on GPR Scale	Visual Core Evaluation Results	Chloride Ion Concentration
A1	No evidence of deterioration	Fair	Not available
A2	No evidence of deterioration	Good	Not available
A3	Evidence of moderate deterioration	Fair	Not available
A4	No evidence of deterioration	Good	Not available
B1	Evidence of moderate deterioration	Good	<0.15%
B2	Evidence of moderate deterioration	Poor (mostly asphalt)	Not available
B3	No evidence of deterioration	Good	<0.15%
B4	Evidence of moderate deterioration	Fair	Not available
B5	Evidence of moderate deterioration	Good	Not available

Chloride ion concentration test results were determined for two of the nine total cores extracted from Bridge A1479, Cores B1 and B3. Both cores were rated Good in the visual examination, and both cores showed no evidence of deterioration based on the GPR results. Both cores had chloride ion concentrations lower than the threshold of 0.15% by weight of cement.

Comparing Figures 7-20 and 7-21, it can be seen that areas of the bridge deck where the GPR amplitude map indicates evidence of extensive deterioration generally correspond to areas with greater concrete material removal depths based on the lidar survey after hydrodemolition. Similarly, areas where the GPR amplitude map indicates moderate or no evidence of deterioration generally correspond to areas with lesser concrete material removal depths. Figure 7-23 compares the percentage of the bridge deck within each of the three categories defined for the GPR grade classification with three categories defined for depth of concrete material removed. It should be noted that a perfect correlation was not expected because the GPR grade classifications and the material removal depth categories have different meanings; see Section 7.4.2 for further discussion.

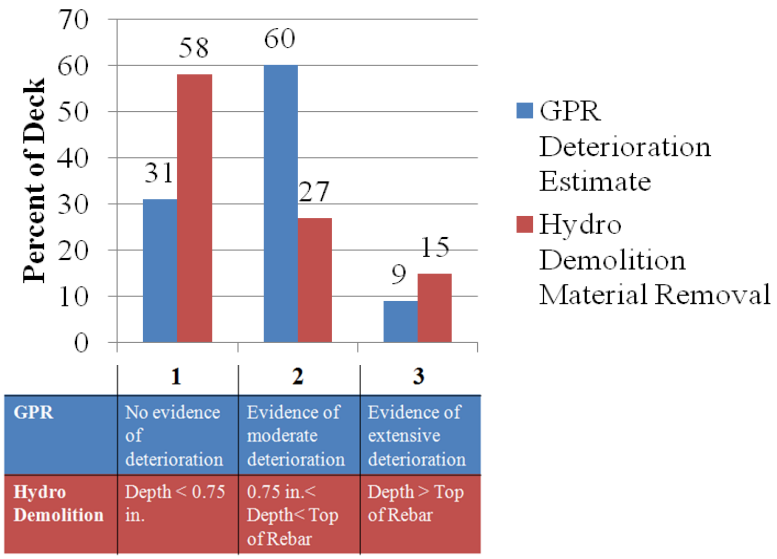

Figure 7-23 Percentage of Bridge Deck Area for Bridge A1479 Categorized by GPR Results and Rehabilitation Lidar Survey

7.3.6 Bridge A2111

The GPR data were acquired along parallel traverses spaced at 1 ft intervals. The acquisition parameters employed were 512 samples/scan, 120 scans/second, and 48 scans/ft. The dielectric constant was assumed to be 10.0. A map of reflection amplitudes from the top layer of transverse rebar is shown in Figure 7-24. Amplitude ranges for three deterioration categories shown in Figure 7-24 were defined based on correlation of the GPR data with the visual evaluation of the cores. Area and percentage distribution of all three deterioration categories were calculated for the investigated bridge deck area and are shown in Figure 7-25.

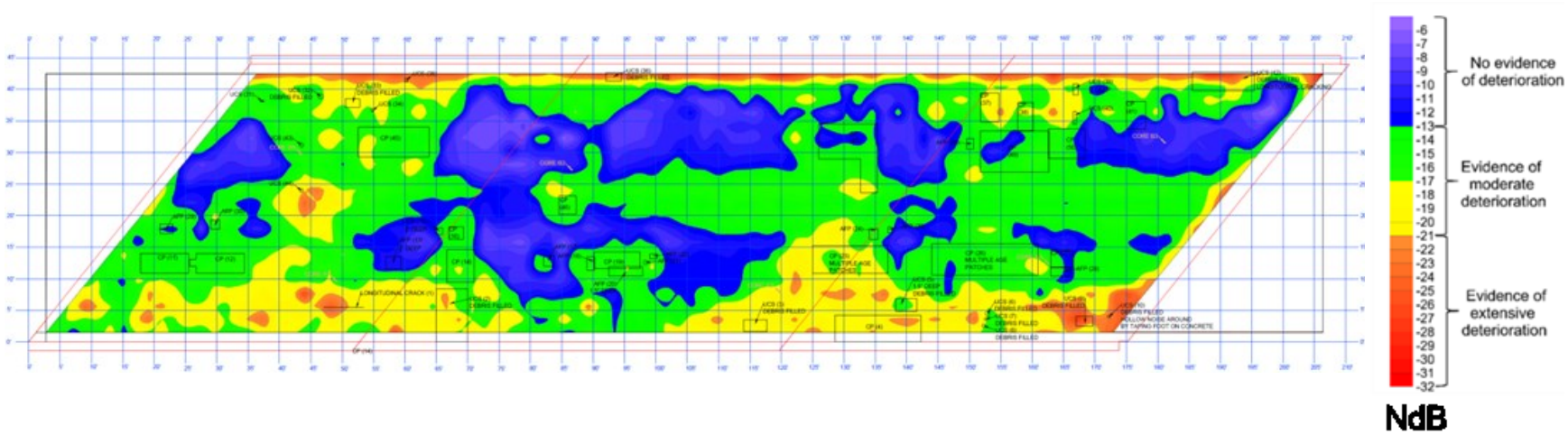

Figure 7-24 GPR Amplitude Map Based on Top Bar Reflection for Bridge Deck A2111 with Superposed Core Locations and Visual Surface Condition Features

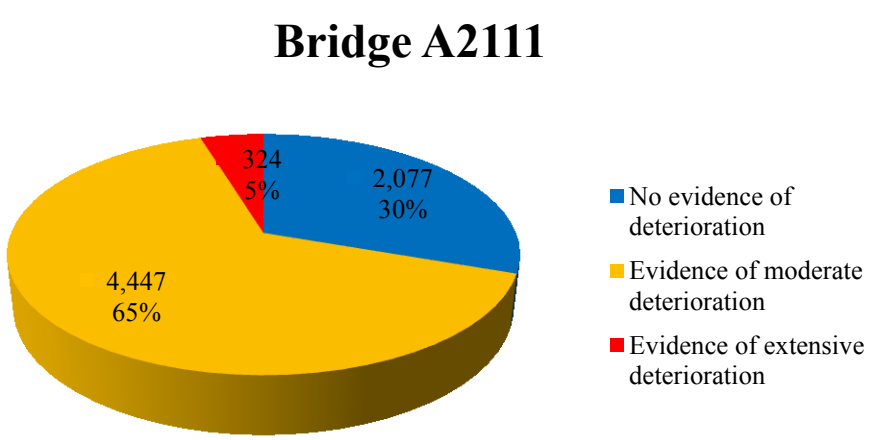

Figure 7-25 Graph Showing Predicted Distribution of Deterioration of the Bridge Deck A2111 in Each Category (Based on the Amplitude of the Reflection from the Top Layer of Rebar). Total Area Investigated - 6,848 ft²; No Evidence of Deterioration – 1,075 ft²; Evidence of Moderate Deterioration - 3,891 ft²; Evidence of Extensive Deterioration 274 ft².

Figure 7-25 shows that 30% of the area investigated on the bridge deck of Bridge A2111 exhibited no evidence of deterioration, 65% exhibited evidence of moderate deterioration, and 5% exhibited evidence of extensive deterioration based on the deterioration categories defined for the GPR amplitude results.

Table 7-7 summarizes the GPR results at the core locations so that the GPR, and visual core evaluation, and chloride ion concentration results can be compared. Results of the visual core evaluations (from Table 4-6) and the chloride ion concentration results (from Section 5) are also included in Table 7-7. The visual core evaluation and GPR estimated deterioration level comparison show a good correlation. Bridge A2111 had 67% of the cores with an ideal match with GPR estimated deterioration levels. If the border line cores are considered to fall into a different GPR estimated deterioration level, Bridge A2111 had 100% of the cores with an ideal match.

Chloride ion concentration test results were determined for each of the cores extracted from Bridge A2111. Cores A1 and B3 were rated Good in the visual examination, and Cores A2, A3, B1, and B2 were rated Fair in the visual examination. Core A1, A2, A3 and B1 showed evidence of moderate deterioration based on the GPR results, and Cores B2 and B3 showed no evidence of deterioration. Results indicate of the chloride ion concentration tests show that levels are less than the threshold limit for each core with the exception of Core B1, which had a measured chloride ion concentration above the threshold limit of 0.15% by weight of cement.

Table 7-7 Bridge A2111 GPR Results at Core Locations

Core	Grade Classification Based on GPR Scale	Visual Core Evaluation Results	Chloride Ion Concentration
A1	Evidence of moderate deterioration	Good	<0.15%
A2	Evidence of moderate deterioration	Fair	<0.15%
A3	Evidence of moderate deterioration	Fair	<0.15%
B1	Evidence of moderate deterioration	Fair	>0.15%
B2	No evidence of deterioration	Fair	<0.15%
B3	No evidence of deterioration	Good	<0.15%

7.3.7 Bridge A2966

The GPR data were acquired along parallel traverses spaced at 1.5 ft intervals. The acquisition parameters employed were 512 samples/scan, 120 scans/second, and 72 scans/ft. The dielectric constant was assumed to be 10.0. A map of reflection amplitudes from the top layer of transverse rebar is shown in Figure 7-26. Amplitude ranges for three deterioration categories shown in Figure 7-26 were defined based on correlation of the GPR data with the visual evaluation of the cores. Area and percentage distribution of all three deterioration categories were calculated for the investigated bridge deck area and are shown in Figure 7-27.

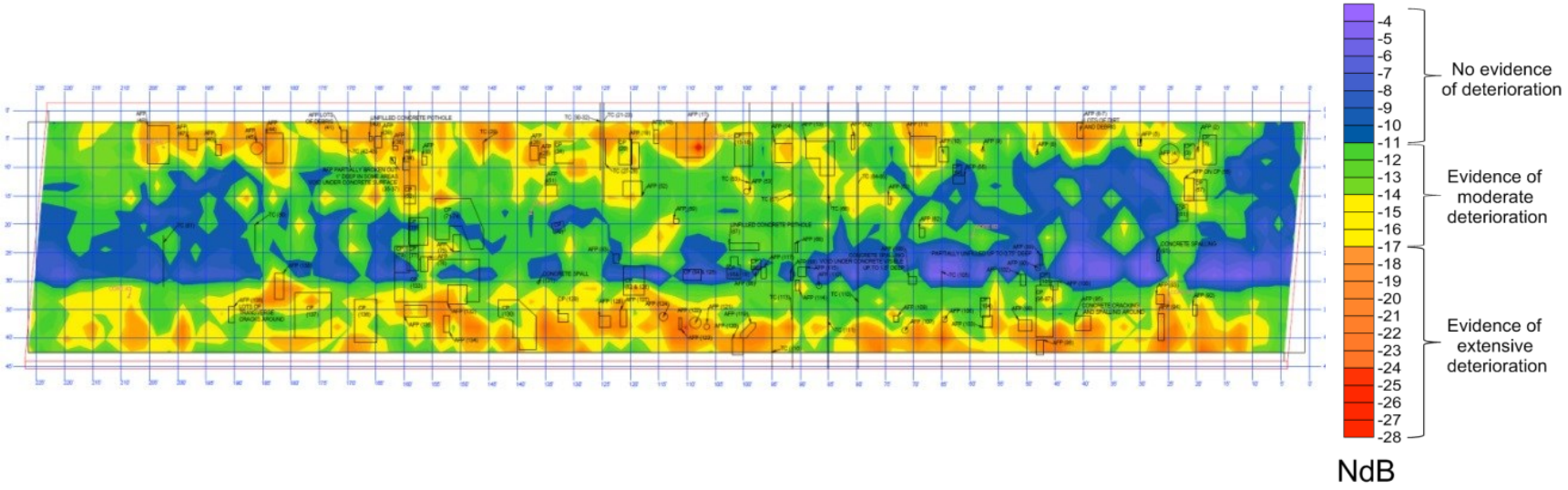

Figure 7-26 GPR Amplitude Map Based on Top Bar Reflection for Bridge Deck A2966 with Superposed Core Locations and Visual Surface Condition Features

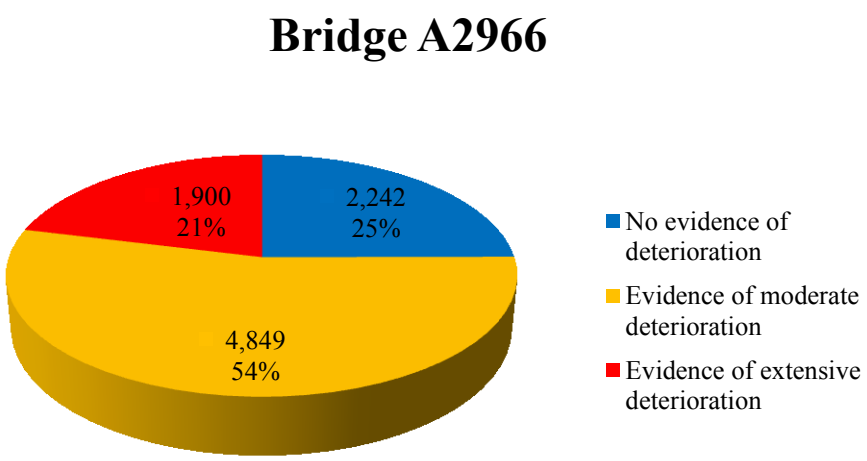

Figure 7-27 Graph Showing Predicted Distribution of Deterioration of the Bridge Deck A2966 in Each Category (Based on the Amplitude of the Reflection from the Top Layer of Rebar). Total Area Investigated - 8,991 ft²; No Evidence of Deterioration – 2,242 ft²; Evidence of Moderate Deterioration - 4,849 ft²; Evidence of Extensive Deterioration 1,900 ft².

Figure 7-27 shows that 25% of the area investigated on the bridge deck of Bridge A2966 exhibited no evidence of deterioration, 54% exhibited evidence of moderate deterioration, and 21% exhibited evidence of extensive deterioration based on the deterioration categories defined for the GPR amplitude results.

Table 7-8 summarizes the GPR results at the core locations so that the GPR, and visual core evaluation, and chloride ion concentration results can be compared. Results of the visual core evaluations (from Table 4-7) and the chloride ion concentration results (from Section 5) are also included in Table 7-8. The visual core evaluation and GPR estimated deterioration level comparison show a good correlation. Bridge A2966 had 67% of the cores with an ideal match with GPR estimated deterioration levels. If the border line cores are considered to fall into a different GPR estimated deterioration level, Bridge A2966 had 83% of the cores with an ideal match.

Table 7-8 Bridge A2966 GPR Results at Core Locations

Core	Grade Classification Based on GPR Scale	Visual Core Evaluation Results	Chloride Ion Concentration
A1	Evidence of moderate deterioration	Fair	Not available
A2	No evidence of deterioration	Good	Not available
A3	No evidence of deterioration	Good	Not available
B1	Evidence of extensive deterioration	Poor	Not available
B2	No evidence of deterioration	Poor	Not available
B3	Evidence of extensive deterioration	Fair	Not available

7.3.8 Bridge A3017

The GPR data were acquired along parallel traverses spaced at 2 ft intervals. The acquisition parameters employed were 512 samples/scan, 120 scans/second, and 48 scans/ft. The dielectric constant was assumed to be 10.0. A map of reflection amplitudes from the top layer of transverse rebar is shown in Figure 7-28. Amplitude ranges for three deterioration categories shown in Figure 7-28 were defined based on correlation of the GPR data with the visual evaluation of the cores. Area and percentage distribution of all three deterioration categories were calculated for the investigated bridge deck area and are shown in Figure 7-29.

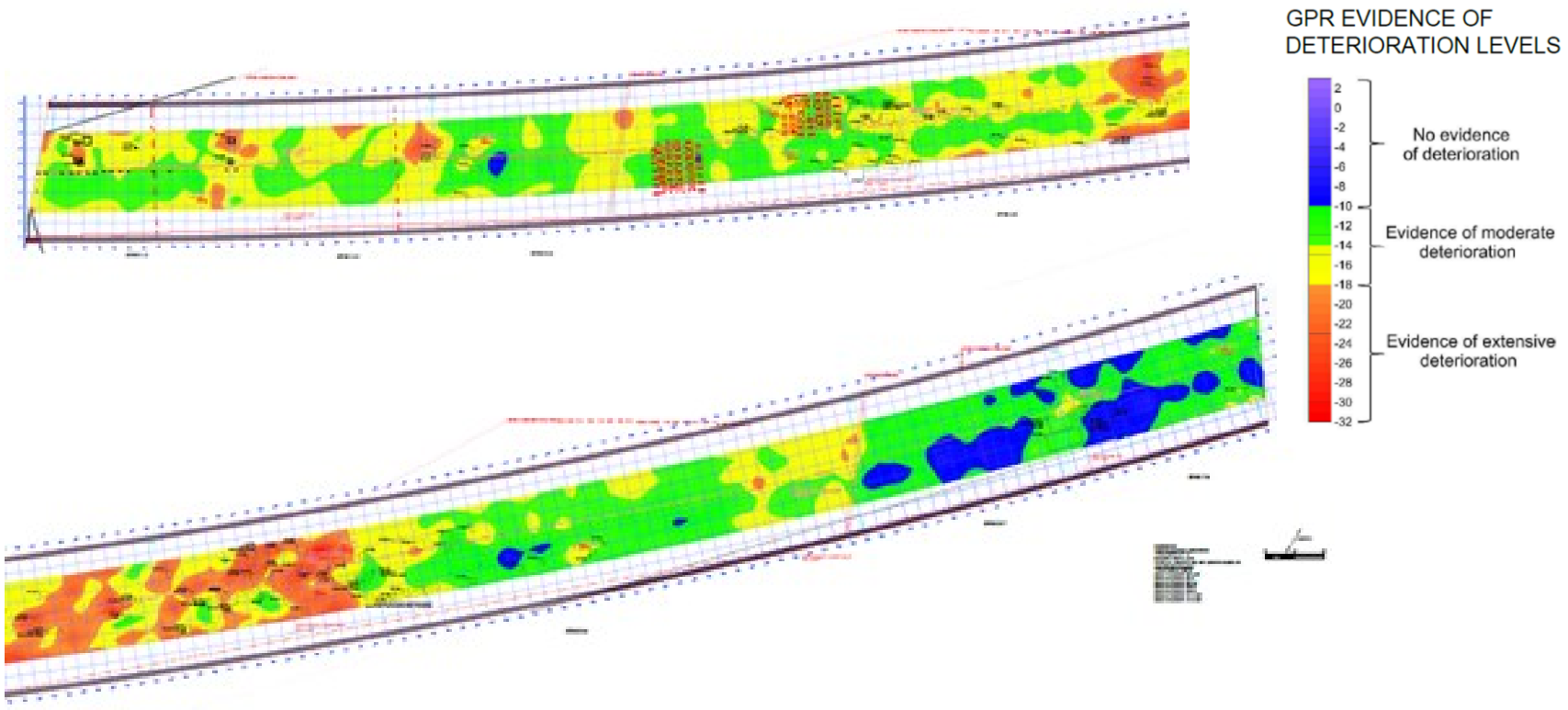

Figure 7-28 GPR Amplitude Map Based on Top Bar Reflection for Bridge Deck A3017 with Superposed Core Locations and Visual Surface Condition Features

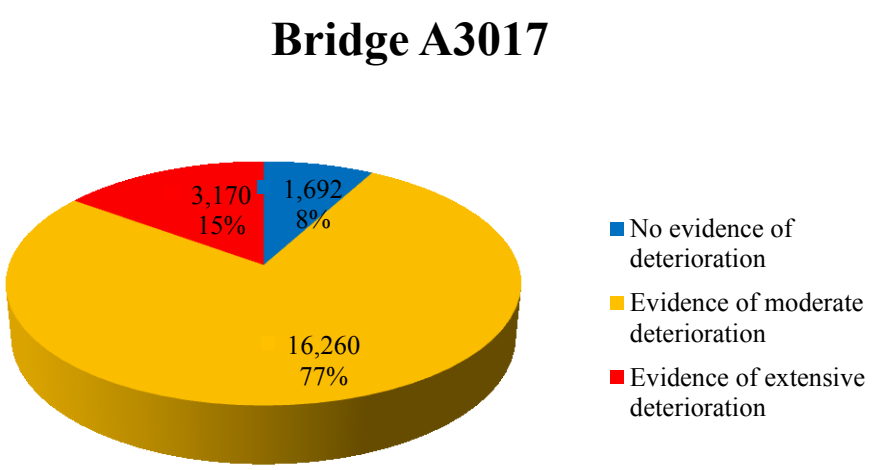

Figure 7-29 Graph Showing Predicted Distribution of Deterioration of the Bridge Deck A3017 in Each Category (Based on the Amplitude of the Reflection from the Top Layer of Rebar). Total Area Investigated - 21,122 ft²; No Evidence of Deterioration – 1,692 ft²; Evidence of Moderate Deterioration - 16,260 ft²; Evidence of Extensive Deterioration 3,170 ft².

Figure 7-29 shows that 8% of the area investigated on the bridge deck of Bridge A3017 exhibited no evidence of deterioration, 77% exhibited evidence of moderate deterioration, and 15% exhibited evidence of extensive deterioration based on the deterioration categories defined for the GPR amplitude results.

Table 7-9 summarizes the GPR results at the core locations so that the GPR, and visual core evaluation, and chloride ion concentration results can be compared. Results of the visual core evaluations (from Table 4-8) and the chloride ion concentration results (from Section 5) are also included in Table 7-9. The visual core evaluation and GPR estimated deterioration level comparison show a fair correlation. Bridge A3017 had 25% of the cores with an ideal match with GPR estimated deterioration levels. If the border line cores are considered to fall into a different GPR estimated deterioration level, Bridge A3017 had 88% of the cores with an ideal match.

Chloride ion concentration test results were determined for each of the cores extracted from Bridge A3017. Cores A1, B1, B2, and B3 were rated Good, Cores A2, A3, and B4 were rated Fair, and Core A4 was rated Poor in the visual examination. Cores A1, A2, A4, B1, B2 and B4 showed evidence of moderate deterioration, and Cores A3 and B3 showed evidence of extensive deterioration based on the GPR results. Chloride ion concentration results were not available at the design depth of top reinforcing bar, but projection of the trends in the figure suggest that chloride ion concentration levels would be below the threshold limit for each core.

Table 7-9 Bridge A3017 GPR Results at Core Locations

Core	Grade Classification Based on GPR Scale	Visual Core Evaluation Results	Chloride Ion Concentration
A1	Evidence of moderate deterioration	Good	Not available
A2	Evidence of moderate deterioration	Fair	Not available
A3	Evidence of extensive deterioration	Fair	Not available
A4	Evidence of moderate deterioration	Poor	Not available
B1	Evidence of moderate deterioration	Good	Not available
B2	Evidence of moderate deterioration	Good	Not available
B3	Evidence of extensive deterioration	Good	Not available
B4	Evidence of moderate deterioration	Fair	Not available

7.3.9 Bridge A3405

The GPR data were acquired along parallel traverses spaced at 0.75 ft intervals. The acquisition parameters employed were 512 samples/scan, 120 scans/second, and 48 scans/ft (GPR profiles 16-56 were recorded with 512 samples/scan and 36 scans/ft due to the time limitation). The dielectric constant was assumed to be 10.0. A map of reflection amplitudes from the top layer of transverse rebar is shown in Figure 7-30. Amplitude ranges for three deterioration categories shown in Figure 7-30 were defined based on correlation of the GPR data with the visual evaluation of the cores. Area and percentage distribution of all three deterioration categories were calculated for the investigated bridge deck area and are shown in Figure 7-31.

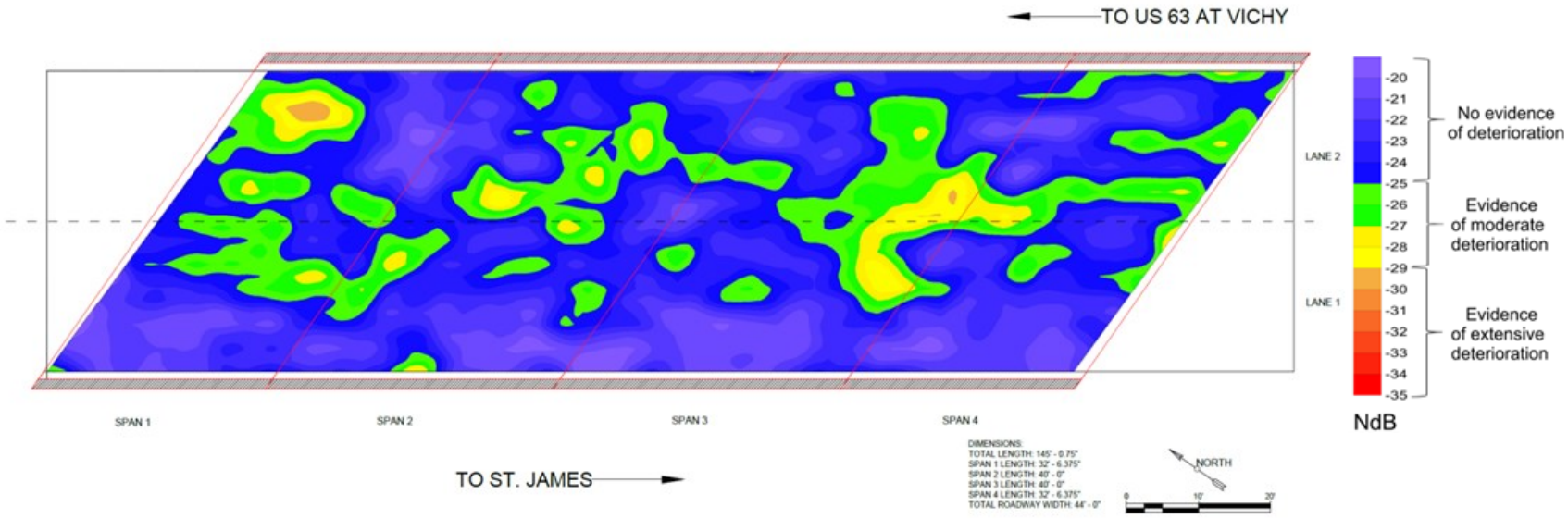

Figure 7-30 GPR Amplitude Map Based on Top Bar Reflection for Bridge Deck A3405 with Superposed Core Locations and Visual Surface Condition Features

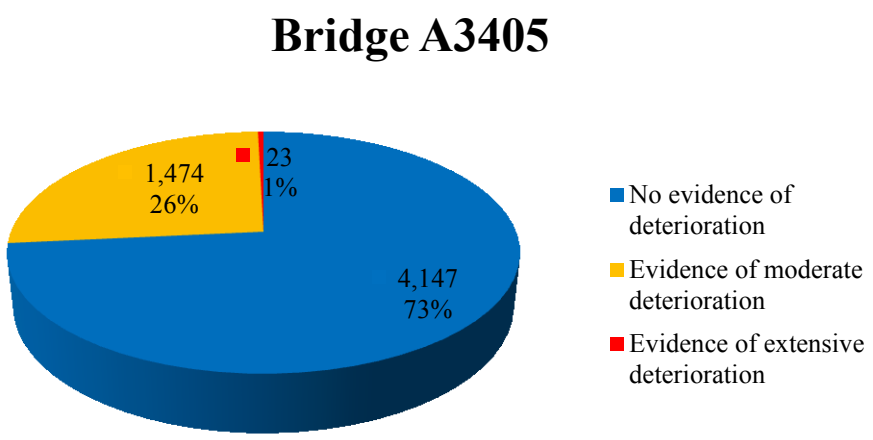

Figure 7-31 Graph Showing Predicted Distribution of Deterioration of the Bridge Deck A3405 in Each Category (Based on the Amplitude of the Reflection from the Top Layer of Rebar). Total Area Investigated - 5,644 ft²; No Evidence of Deterioration – 4,147 ft²; Evidence of Moderate Deterioration - 1,474 ft²; Evidence of Extensive Deterioration 23 ft².

Figure 7-31 shows that 73% of the area investigated on the bridge deck of Bridge A3405 exhibited no evidence of deterioration, 26% exhibited evidence of moderate deterioration, and 1% exhibited evidence of extensive deterioration based on the deterioration categories defined for the GPR amplitude results.

Table 7-10 summarizes the GPR results at the core locations so that the GPR, and visual core evaluation, and chloride ion concentration results can be compared. Results of the visual core evaluations (from Table 4-9) and the chloride ion concentration results (from Section 5) are also included in Table 7-10. The visual core evaluation and GPR estimated deterioration level comparison show a good correlation. Bridge A3405 had 63% of the cores with an ideal match with GPR estimated deterioration levels. If the border line cores are considered to fall into a different GPR estimated deterioration level, Bridge A3405 had 100% of the cores with an ideal match.

Table 7-10 Bridge A3405 GPR Results at Core Locations

Core	Grade Classification Based on GPR Scale	Visual Core Evaluation Results	Chloride Ion Concentration
A1	Evidence of moderate deterioration	Good	Not available
A2	Evidence of moderate deterioration	Fair	Not available
A3	No evidence of deterioration	Good	Not available
A4	No evidence of deterioration	Good	Not available
B1	No evidence of deterioration	Fair	Not available
B2	No evidence of deterioration	Good	Not available
B3	Evidence of extensive deterioration	Good	Not available
B4	No evidence of deterioration	Good	Not available

7.3.10 Bridge A3406

The GPR data were acquired along parallel traverses spaced at 1 ft intervals. The acquisition parameters employed were 512 samples/scan, 120 scans/second, and 48 scans/ft. The dielectric constant was assumed to be 10.0. A map of reflection amplitudes from the top layer of transverse rebar is shown in Figure 7-32. Amplitude ranges for three deterioration categories shown in Figure 7-32 were defined based on correlation of the GPR data with the visual evaluation of the cores. Area and percentage distribution of all three deterioration categories were calculated for the investigated bridge deck area and are shown in Figure 7-33.

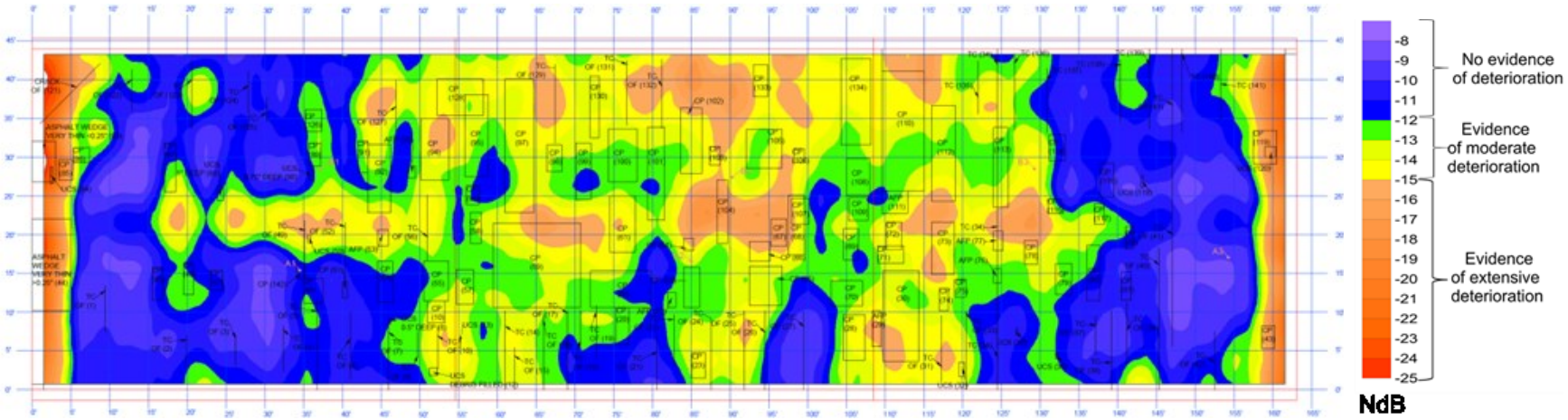

Figure 7-32 GPR Amplitude Map Based on Top Bar Reflection for Bridge Deck A3406 with Superposed Core Locations and Visual Surface Condition Features

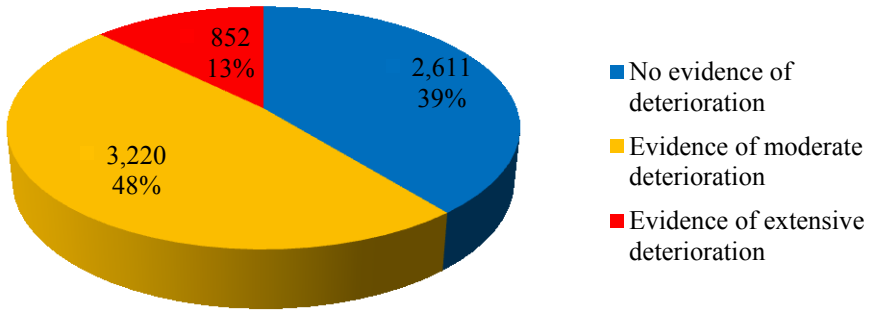

Figure 7-33 Graph Showing Predicted Distribution of Deterioration of the Bridge Deck A3406 in Each Category (Based on the Amplitude of the Reflection from the Top Layer of Rebar). Total Area Investigated - 6,683 ft²; No Evidence of Deterioration – 2,611 ft²; Evidence of Moderate Deterioration - 3,220 ft²; Evidence of Extensive Deterioration 852 ft².

Figure 7-33 shows that 39% of the area investigated on the bridge deck of Bridge A3406 exhibited no evidence of deterioration, 48% exhibited evidence of moderate deterioration, and 13% exhibited evidence of extensive deterioration based on the deterioration categories defined for the GPR amplitude results.

Table 7-11 summarizes the GPR results at the core locations so that the GPR, and visual core evaluation, and chloride ion concentration results can be compared. Results of the visual core evaluations (from Table 4-10) and the chloride ion concentration results (from Section 5) are also included in Table 7-11. The visual core evaluation and GPR estimated deterioration level comparison show a fair correlation. Bridge A3406 had 50% of the cores with an ideal match with GPR estimated deterioration levels. If the border line cores are considered to fall into a different GPR estimated deterioration level, Bridge A3406 had 100% of the cores with an ideal match.

Table 7-11 Bridge A3406 GPR Results at Core Locations

Core	Grade Classification Based on GPR Scale	Visual Core Evaluation Results	Chloride Ion Concentration
A1	No evidence of deterioration	Fair	Not available
A2	Evidence of moderate deterioration	Fair	<0.15%
A3	No evidence of deterioration	Good	<0.15%
B1	Evidence of moderate deterioration	Poor	Not available
B2	Evidence of moderate deterioration	Poor	<0.15%
B3	Evidence of moderate deterioration	Fair	Not available

Chloride ion concentration test results were determined for three of the six cores extracted from Bridge A3406. Core A3 was rated Good, Core A2 was rated Fair, and Core B2 was rated Poor in the visual examination. Core A3 showed no evidence of deterioration, and Cores A2 and B2

showed evidence of moderate deterioration based on the GPR results. Results indicate of the chloride ion concentration tests show that levels are less than the threshold limit for each core.

7.3.11 Bridge K0197

The GPR data were acquired along parallel traverses spaced at 1 ft intervals. The acquisition parameters employed were 512 samples/scan, 120 scans/second, and 48 scans/ft. The dielectric constant was assumed to be 10.0. A map of reflection amplitudes from the top layer of transverse rebar is shown in Figure 7-34. Amplitude ranges for three deterioration categories shown in Figure 7-34 were defined based on correlation of the GPR data with the visual evaluation of the cores. Area and percentage distribution of all three deterioration categories were calculated for the investigated bridge deck area and are shown in Figure 7-35.

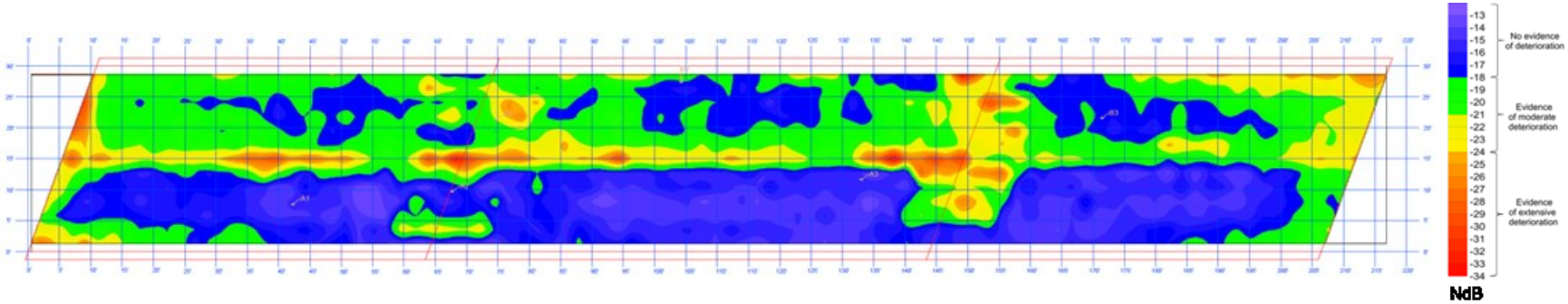

Figure 7-34 GPR Amplitude Map Based on Top Bar Reflection for Bridge Deck K0197 with Superposed Core Locations and Visual Surface Condition Features

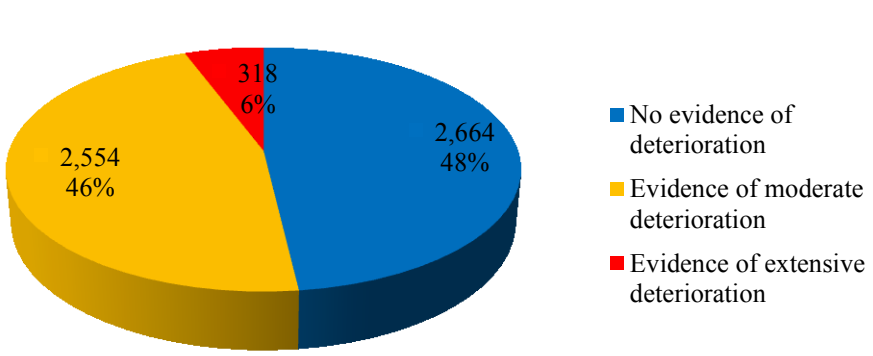

Figure 7-35 Graph Showing Predicted Distribution of Deterioration of the Bridge Deck K0197 in Each Category (Based on the Amplitude of the Reflection from the Top Layer of Rebar). Total Area Investigated - 5,536 ft²; No Evidence of Deterioration – 2,664 ft²; Evidence of Moderate Deterioration - 2,554 ft²; Evidence of Extensive Deterioration 318 ft².

Figure 7-35 shows that 48% of the area investigated on the bridge deck of Bridge K0197 exhibited no evidence of deterioration, 46% exhibited evidence of moderate deterioration, and 6% exhibited evidence of extensive deterioration based on the deterioration categories defined for the GPR amplitude results.

Table 7-12 summarizes the GPR results at the core locations so that the GPR, and visual core evaluation, and chloride ion concentration results can be compared. Results of the visual core evaluations (from Table 4-11) and the chloride ion concentration results (from Section 5) are also included in Table 7-12. The visual core evaluation and GPR estimated deterioration level comparison show a fair correlation. Bridge K0197 had 50% of the cores with an ideal match with GPR estimated deterioration levels. If the border line cores are considered to fall into a different GPR estimated deterioration level, Bridge K0197 had 100% of the cores with an ideal match.

Chloride ion concentration test results were determined for three of the six cores extracted from Bridge K0197. Cores B2 and A3 were rated Good, and Core A1 was rated Poor in the visual examination. Cores A1, B2, and B3 showed no evidence of deterioration based on the GPR results. Results indicate of the chloride ion concentration tests show that levels are less than the threshold limit for each core.

Table 7-12 Bridge K0197 GPR Results at Core Locations

Core	Grade Classification Based on GPR Scale	Visual Core Evaluation Results	Chloride Ion Concentration
A1	No evidence of deterioration	Poor	<0.15%
A2	Evidence of moderate deterioration	Good	Not available
A3	No evidence of deterioration	Good	Not available
B1	Evidence of moderate deterioration	Poor	Not available
B2	No evidence of deterioration	Good	<0.15%
B3	No evidence of deterioration	Good	<0.15%

7.4 Discussion

7.4.1 Correlation of GPR data with visual core analysis

Although fair to good correlation was observed between the GPR data and the visual core evaluation results, a perfect correlation between the visual descriptions of the cores and GPR estimated deterioration levels was not expected. A higher degree of correlation was anticipated in areas where the concrete cores were visibly deteriorated; a lesser degree of correlation was expected in areas where the concrete cores did not exhibit signs of deterioration. The fact that concrete appears to be in good condition visually does not necessarily mean incipient deterioration is not occurring. The visual examination does not take into account the pore structure of the concrete, where incipient degradation of the concrete could be occurring. The visual examination also gives no indication of concrete strength or the concentration of chlorides present in the pore structure. Another important aspect to consider is the somewhat qualitative interpretation of the decibel scale used to estimate GPR-based deterioration levels. The cutoff values for the different GPR levels (no evidence of deterioration, evidence of moderate deterioration, and evidence of extensive deterioration) were developed independently for each bridge deck by researchers. This was necessary because attenuation of the GPR signal is a function of the moisture content of the concrete, and the moisture content of a particular bridge deck varies with weather conditions.

7.4.2 Correlation of GPR data with deck rehabilitation survey

As discussed in Section 6, Bridges A1193, A1297, and A1479 underwent deck rehabilitation after the investigation. Lidar maps showing the location and depth of concrete material removal were compared to the GPR maps to determine the correlation. In general, regions of the deck where the GPR indicates areas with evidence of extensive deterioration correspond to areas with greater material removal depths from the lidar survey. Similarly, regions where the GPR indicate areas of the bridge deck with moderate or no evidence of deterioration correspond to areas with lower material removal depths from the lidar survey. Therefore it can be concluded that, qualitatively, good correlation was observed between the GPR results and the rehabilitation lidar scans.

For a quantitative comparison, Figures 7-15, 7-19, and 7-23 compare the percentage of the bridge deck within each of the three categories defined for the GPR grade classification with the percentage of the deck within the three categories defined for depth of concrete material removed. Although good correlation between the two classifications is observed in Figure 7-15 for Bridge A1193, the correlations in Figures 7-19 and 7-23 for Bridges A1297 and A1479 are

not as strong. It must be noted that perfect correlation between the GPR maps and the lidar maps is not expected. The GPR responds to the presence of saline moisture present in the deck, whereas rehabilitation removes weaker concrete. GPR and rehabilitation results are therefore expected to correlate best in those areas where the pore space within physically degraded concrete is infilled with slightly saline moisture. Apparent discrepancies between the GPR and lidar results could also be caused by the fact that the GPR maps reflect degradation and saline moisture in a section of concrete that was removed by milling prior to hydrodemolition. Furthermore, the GPR results presented in this report are based on the reflection amplitude from the top transverse layer of reinforcement and do not represent the condition of the concrete below the top transverse reinforcement. Therefore category 3 of the depth of concrete material removed (depth > top of rebar) is not reflected directly in the GPR results, because the GPR results used in the interpretations do not extend deeper than the top transverse reinforcement bar. Thus, the two classifications systems do not have a direct physical correlation.

Considering the issues discussed in the previous paragraph, additional study was initiated to investigate the potential for improving the correlation between these two data sets. This process involved reevaluation of the amplitude ranges for defining the three GPR classifications by altering the threshold values, without consideration of other factors used in the initial interpretations of the data (e.g., visual evaluation data). Threshold values were artificially adjusted higher or lower until the best correlation between the GPR and the material removal percentages was achieved for each bridge deck. This work is ongoing at the time of this report, but preliminary results shown in Figures 7-36, 7-37, and 7-38 for Bridges A1193, A1297, and A1479, respectively, suggest that improved correlation is possible. Presently, a statistical approach is being used in an attempt to correlate the amplitude of the reflection with concrete removal depth for each data point for each of the three bridges. The major challenge, however, is to understand how to determine the GPR threshold values a priori, without having the benefit of the control data. Therefore, it should be noted that the results shown in Figures 7-36, 7-37, and 7-38 are not predictive.

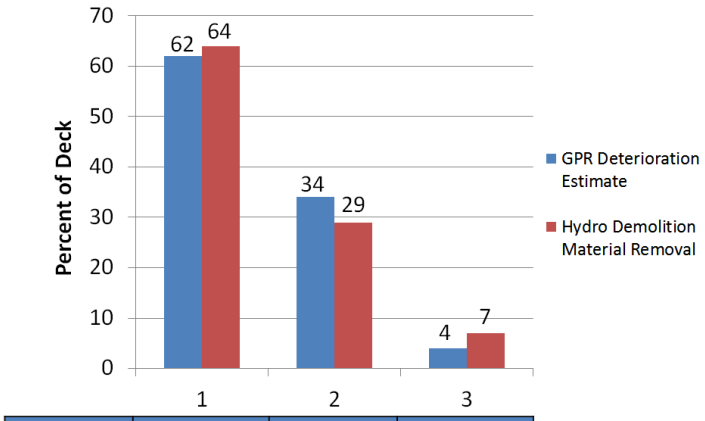

GPR	No evidence of deterioration	Evidence of moderate deterioration	Evidence of extensive deterioration
Hydro Demolition	Depth < 0.75 in.	0.75 in. < Depth< Top of Rebar	Depth > Top of Rebar

Figure 7-36 Percentage of Bridge Deck Area for Bridge A1193 Categorized by GPR Results with adjusted threshold levels and Rehabilitation Lidar Survey

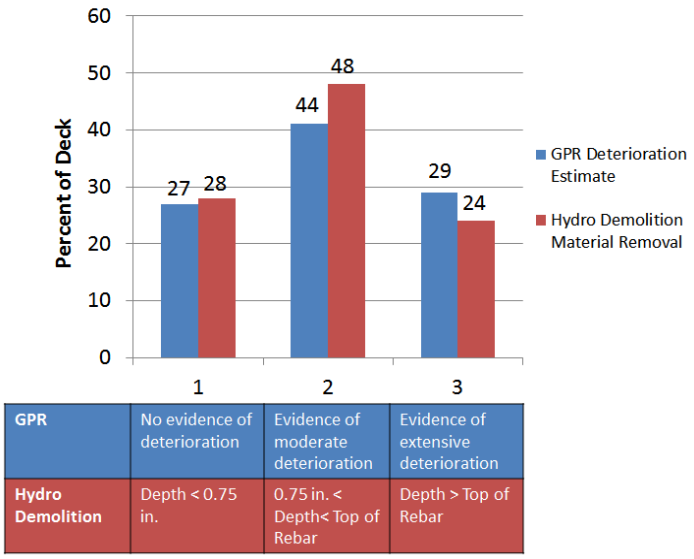

GPR	No evidence of deterioration	Evidence of moderate deterioration	Evidence of extensive deterioration
Hydro Demolition	Depth < 0.75 in.	0.75 in. < Depth< Top of Rebar	Depth > Top of Rebar

Figure 7-37 Percentage of Bridge Deck Area for Bridge A1297 Categorized by GPR Results with adjusted threshold levels and Rehabilitation Lidar Survey

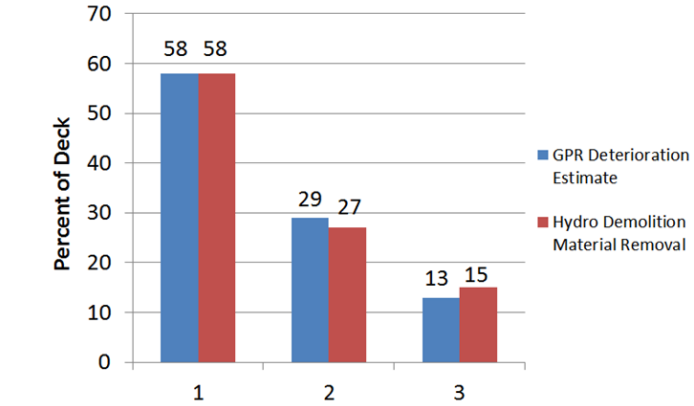

GPR	No evidence of deterioration	Evidence of moderate deterioration	Evidence of extensive deterioration
Hydro Demolition	Depth < 0.75 in.	0.75 in. < Depth< Top of Rebar	Depth > Top of Rebar

Figure 7-38 Percentage of Bridge Deck Area for Bridge A1479 Categorized by GPR Results with adjusted threshold levels and Rehabilitation Lidar Survey

Several factors might affect the amplitude threshold values, including but not limited to variable depth of top rebar layer, and different weather conditions prior and/or during GPR data acquisition. Further data analysis can enhance a data correlation between the concrete material depth removal and GPR amplitudes from top of rebar, and increase reliability of concrete material removal depth prediction based on the GPR data.

7.4.3 Correlation of GPR data with chloride ion concentration data

Chloride ion concentration test results were determined for a limited number of cores extracted from Bridges A1187, A1193, A1297, A1479, A2111, A33406, A3017, and K0197 as discussed in Section 5. Due to the limited amount of chloride ion concentration measurements available, no conclusions can be made on the correlation between chloride ion concentration levels with the GPR results. In general, the chloride ion data available are from cores that showed no deterioration during the visual core evaluations, and no data are available from cores that showed visible signs of deterioration. In order to effectively determine how chloride ion concentrations relate to GPR and visual investigations, data from cores with a variety of deterioration levels are needed.

7.5 Recommended Parameters for GPR Data Acquisition, Processing, and Interpretation

Based on the eleven bridges investigated parameters for GPR data acquisition, processing, and interpretation are recommended and shown in Table 7-13. It should be noted that, in general, the volume and quality of the data acquired on each bridge depends on a bridge design (reinforcing bar spacing, deck width), availability of traffic control and lane closures, survey grid (GPR profiles spacing), equipment settings and weather conditions.

Table 7-13 Recommended Parameters for Ground Coupled GPR Data Acquisition, Processing, and Interpretation

Ground-coupled GPR antenna employed	GSSI 5100 antenna (1.5 GHz)
Parameters measured	Two-way travel time of GPR-pulses, reflection amplitude from reinforcement bars
How these parameters relate to concrete bridge deck	• debonding – electromagnetic reflections from debonded interfaces have lower amplitudes • delaminations – additional layers observed on GPR images • concrete degradation – increasing of apparent depth to the rebar and strong signal attenuation • corrosion of rebar – weak amplitudes of reflected GPR signal • moisture content (concrete and asphalt) – apparent thickness/depth variations
Acquisition parameters recommended	512 samples/scan 120 scans/second 48 scans/ft (or more) 10 dielectric constant (can be adjusted during data processing) 1 point gain amplification 3000 MHz vert IIR LP filter 250 MHz vert IIR HP filter 2 ft traverse spacing
Weather conditions recommended	No precipitation, no condensation. Presence of moisture in the deck (after a rain or watering)
Crew size	4-5 crew members
Equipment costs	At the time of this report, $20,000 (SIR-3000 and GSSI 5100 1.5 GHz antenna kit)
Volume of data acquired; time required	4-7 hours depending on bridge length and width. The survey time includes laying out survey traverses and GPR data acquisition in the alternate mode
Acquisition problems (incl. potential)	• very low temperatures (below 50°F) can decrease the GPR control unit battery life in the field • high humidity in the air can cause condensation on sensitive electronic components inside of the control unit • standing water/dirt/trash/debris on bridge deck slows down investigation process and can cause relative gain jumps (anomalies) • additional time may be required for marking traverses where top layer of reinforcement is oriented in the bridge longitudinal direction (to avoid low quality data)
Ease of acquisition	• procedure is straightforward if traverses are marked • traffic control and lane closure are required • data acquisition easier during day light
Processing parameters	• signal gain amplification • position correction • the dielectric constant adjustment (versus the initial 10 used in the field); dielectric constant of 10 is chosen based on the rebar depth from the drawings provided by MoDOT • migration of data
Time required to process data	0.5-1 day
Ease of processing	• good quality data can be processed automatically, however, procedure requires manual corrections • procedure can be performed by a trained person (operator should have a background related to the GPR and EM theory, and understanding of construction materials)

Table 7-13 Recommended Parameters for Ground Coupled GPR Data Acquisition, Processing, and Interpretation (Cont.)

Ease of processing	• good quality data can be processed automatically, however, procedure requires manual corrections • procedure can be performed by a trained person (operator should have a background related to the GPR and EM theory, and understanding of construction materials)
Potential processing problems	• presence of ringing noise (can be mitigated by filtering and deconvolution) • presence of electromagnetic noise caused by surrounding electromagnetic field variations (can be reduced by vertical/horizontal/spatial filters) • low visibility of reflections from the rebar (can be increased by arithmetic functions and applying of display and range gain) • presence of diffractions and dipping layers (can be enhanced by migration) • profiles length adjustment may be required due to reinforcing steel design • presence of the longitudinal reinforcing bars as the top layer of reinforcement • manual processing control always required
Interpretation parameters	• reflection amplitudes and apparent depth from top and bottom (where visible) layers of rebar are exported to Microsoft Excel • generating of contour maps of amplitude reflections from the rebar, utilizing Golden Software Surfer • analysis of the contour maps for amplitude of reflection values distribution • investigation of relative changes in reflection amplitudes across the bridge deck • correlation of spatial data distribution with observed bridge deck conditions • amount of deteriorated concrete was estimated by careful GPR scans examination, which resulted in amplitude threshold consideration
Time required to interpret data	0.5-1 day
Ease of interpretation	• procedure can be performed by a trained person (requires experience with Radan and Golden Software Surfer software packeges; may require Matlab computational software skills; GIS software skills) • correlation with other available data sets required
Deliverables	A contour map showing estimated distribution of areas of deterioration
Reliability of interpretations	Ground truth data is required to constrain interpretation (core control). Rehabilitation survey data can help improve reliability.
Potential interpretation problems	• moisture presence and chloride ion concentration variations along the bridge deck affect the amplitude of reflections and apparent depth to rebar • variations in reflection amplitude may be caused by other factors such as differences in depth to the rebar, variations in rebar diameter, and variable moisture content of the overlying asphalt, should be taken into account • actual depth/thickness differs from bridge drawings • where the most top layer of reinforcement is oriented in the bridge longitudinal direction, a high-amplitude continuous reflector appears across the profile and affects the reflection amplitude and apparent depth to rebar • automated interpretation needs control and manual corrections • GPR images should be correlated with available visual inspection data, and when available additional data sets such as core and other NDT data sets

8 PORTABLE SEISMIC PROPERTY ANALYZER

8.1 Overview

A portable seismic property analyzer (PSPA) was used to acquire additional data on each of the bridge decks investigated in this study. The objectives of acquiring these data were to 1) evaluate the capabilities of PSPA for identifying and characterizing common defects in concrete bridge decks; and 2) identify sources of error or potential misinterpretation with respect to PSPA data acquisition, processing and interpretation.

PSPA results of three bridges are summarized in this section: Bridges A1193, A1297, and A1479. These bridges underwent rehabilitation during the project duration, which allowed the researchers to compare the data to control data. Section 8-2 briefly discusses background information on the PSPA tool. Section 8-3 discusses the methodology. Section 8-4 presents the PSPA results for Bridges A1193, A1297, and A1479. Finally, Section 8-5 discusses the results.

8.2 Background

The PSPA, shown in Figure 8-1, is an integrated ultrasonic seismic device that can be used to estimate the average elastic modulus and the thickness of asphalt and/or concrete paved surfaces (Baker et al, 1995). The PSPA is a nondestructive device that consists of an acoustic impact source and two receiver transducers packaged into a portable system for performing seismic tests in the field. The device is connected to a laptop computer through a cable that carries commands to the PSPA and stores the signals recorded by the transducers. The impact source is equipped with a transducer for consistency in trigging and for advanced analysis of the source signal (Nazarian et al, 1997). The PSPA generates and records acoustic (strain) waves. PSPA data processing and interpretation are based on the ultrasonic surface wave (USW) and impact-echo (IE) nondestructive testing methods (Gucunski et al, 2008). The basic theory for each method is described briefly in the following sections.

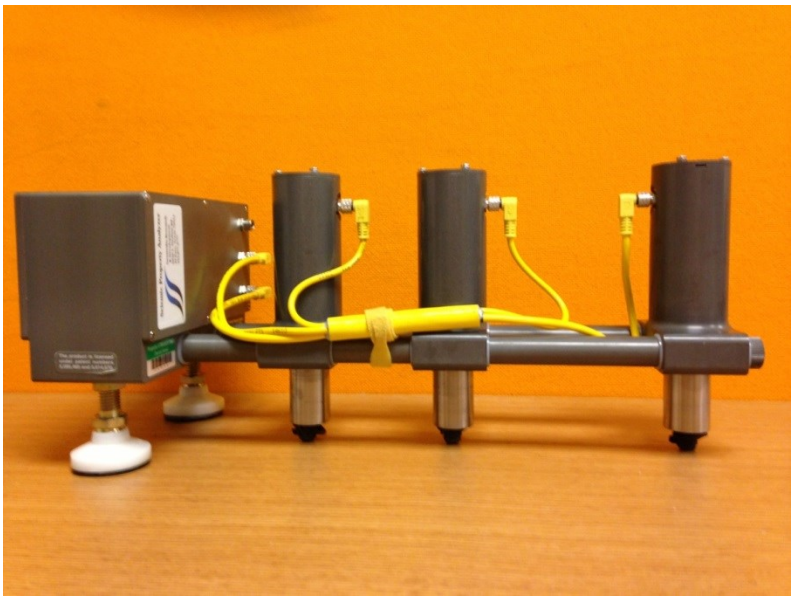

Figure 8-1 Portable Seismic Property Analyzer (PSPA)

8.2.1 Ultrasonic Surface Wave (USW)

The ultrasonic surface (Rayleigh) wave method is used to estimate the elastic modulus (Young's Modulus) of a layered concrete or asphalt. At wavelengths less than or equal to the thickness of the uppermost layer of a relatively uniform media, the velocity of propagation of a surface wave (Rayleigh wave) is independent of wavelength (Baker et al, 1995). Consequently, if the properties of the uppermost layer are assumed to be uniform, the elastic modulus of the upper layer can be determined simply by generating high-frequency (short wavelength) waves.

The general procedure of evaluation the elastic modulus of the material through the ultrasonic surface wave method is shown in Figure 8-2. The surface wave or body wave velocity of a concrete slab can be determined by measuring the travel time difference between two receiver transducers. If the material properties, such as the density and Poisson's ratio, are assumed to be uniform, the elastic modulus can be determined based on the calculations of surface wave velocity. A case study also mentioned that: "the variability of test results with the PSPA on uniform quality test samples of portland cement concrete is less than 3% without moving the device and is around 7% when the device is moved in a small area (Celaya et al, 2007)."

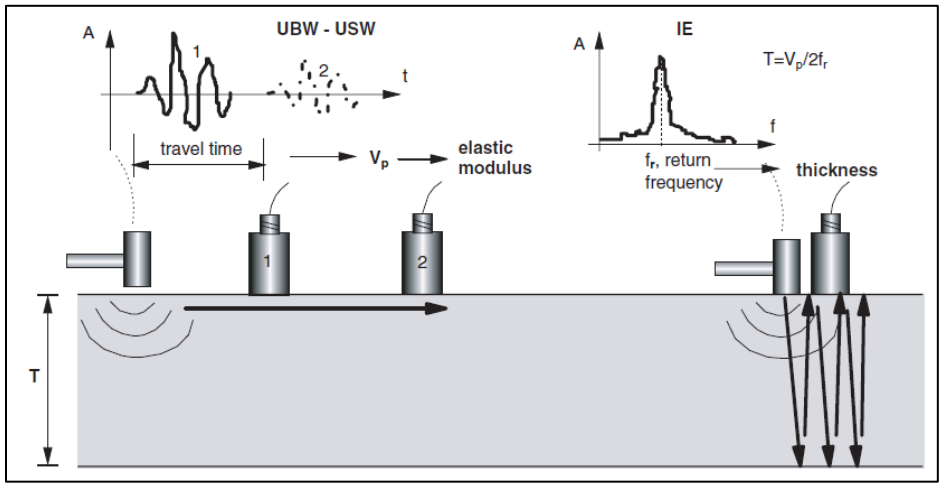

Figure 8-2 Measurement of Concrete Slab Elastic Modulus and Thickness by USW (left) and IE (right) Methods (Gucunski et al 2008)

To collect data with the PSPA, the high-frequency source is activated four to six times. Prerecorded impacts of the source are used to adjust the gains of the amplifiers to optimize the dynamic range of the electronics. The outputs of the three transducers from the final three impacts are saved and stacked (Nazarian et al, 1997). Typical voltage outputs (waveforms) of the three transducers for bridge deck investigations are shown in Figure 8-3. Actual variations in estimated elastic modulus with depth are shown in Figure 8-3 are shown in Figure 8-4. In this manner, the operator of the PSPA can obtain a qualitative feel for the variation in modulus with depth. The modulus is reasonably constant for the first 4 in., below which the modulus tends toward higher values with depth. To obtain the average elastic modulus, the average modulus from a wavelength of about 2 in. to slightly less than the normal thickness of the deck is calculated.

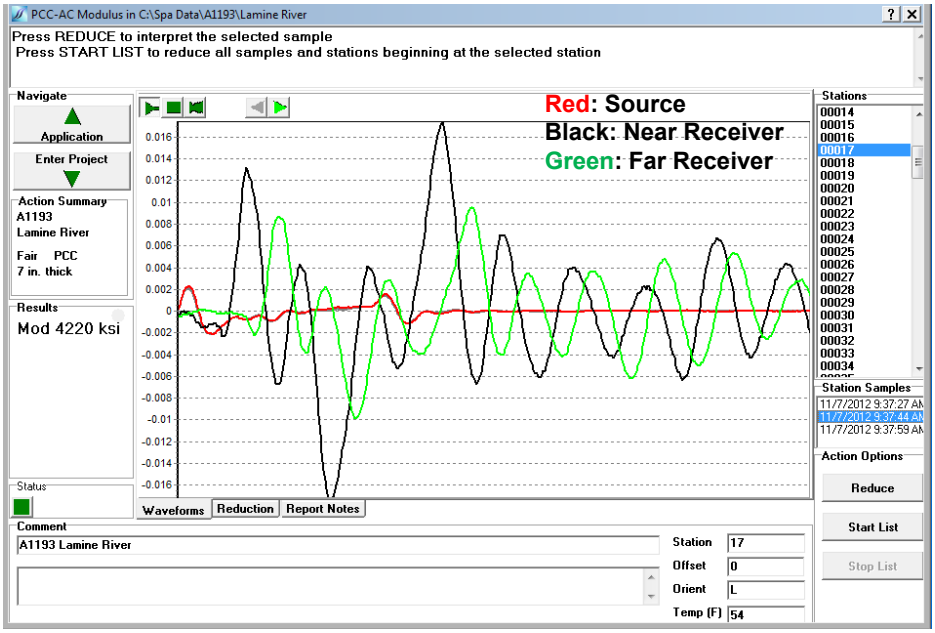

Figure 8-3 Typical Time Records of Three Transducers (Source: Bridge A1193)

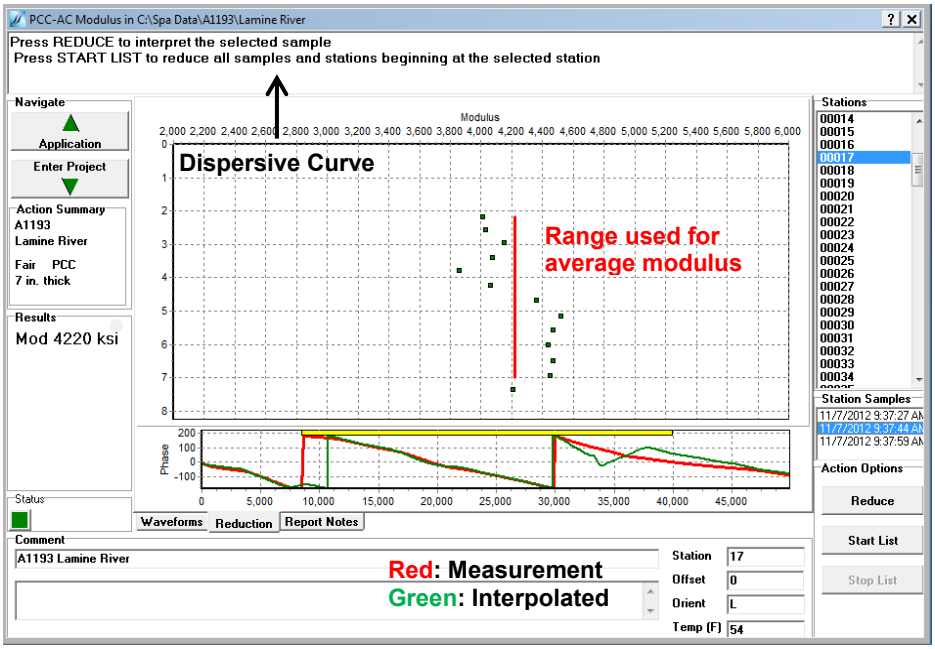

Figure 8-4 Typical Dispersion Curve Obtained from the Time Records (Source: Bridge A1193)

8.2.2 Impact Echo (IE)

The impact echo method is a nondestructive technique (NDT) that can be used to estimate the apparent thickness of a concrete layer and for flaw detection in concrete (Carino et al, 1986). Thus, it can be used with some success to detect defects in concrete structure and can be considered as a diagnostic tool for defect identification. The high-frequency impact source and the nearby transducer of PSPA instrument are used to conduct the impact echo tests in the field.

The configuration of impact echo testing is shown in Figure 8-2. In practice, the estimation of P-wave velocity by measuring the travel time of P-wave between two transducers is often difficult since the P-wave arrivals are difficult to identify on the time records.

An alternative approach is to indirectly estimate the P-wave velocity through the measurement of the surface wave velocity (V_R) from the ultrasonic surface wave test since the relationship between P-wave velocity and surface wave velocity is known if the properties of the uppermost layer are assumed to be uniform. Compressional waves are generated when the mechanical impact is applied on the surface of the material. Because of a significant contrast in rigidity of concrete and air, the elastic wave is mostly or entirely reflected off the bottom of the deck back to the deck surface. The frequency of the reflection, called return frequency, can be identified in the response spectrum of the recorded signal (Carino et al, 1986). Thus, the depth of the reflector, in this case the deck thickness, can be obtained from the return frequency and the previously determined P-wave velocity, as illustrated in Figure 8-5. The relationship between P-wave velocities, return frequency f and deck thickness T can be determined simply by Equation 1:

$$f = \frac{Vp}{2*\mathrm{T}} \quad \text{.....Eq (1)}$$

Figure 8-5 shows an example of an "ideal" amplitude spectrum (frequency spectrum) contrast between intact and debonded concrete slabs. For the case of the intact slab, a large portion of input energy is reflected back from the bottom of the slab or concrete base interface. For the case of the debonded slab, energy will be reflected from the concrete-air interface created by the debonding. Therefore, other than the full slab thickness frequency f_h, the amplitude spectrum will "ideally" show one or more frequency peaks at $f_d = \frac{\mathrm{Vp}}{2\mathrm{d}}$, corresponding to the frequency of reflections from the deboning at a depth of $d < h$. The relative amplitude of the peaks depends on a number of factors, including the extent, depth, continuity, and position of deboning, as well as the frequency content of the impact source (Celaya et al, 2007).

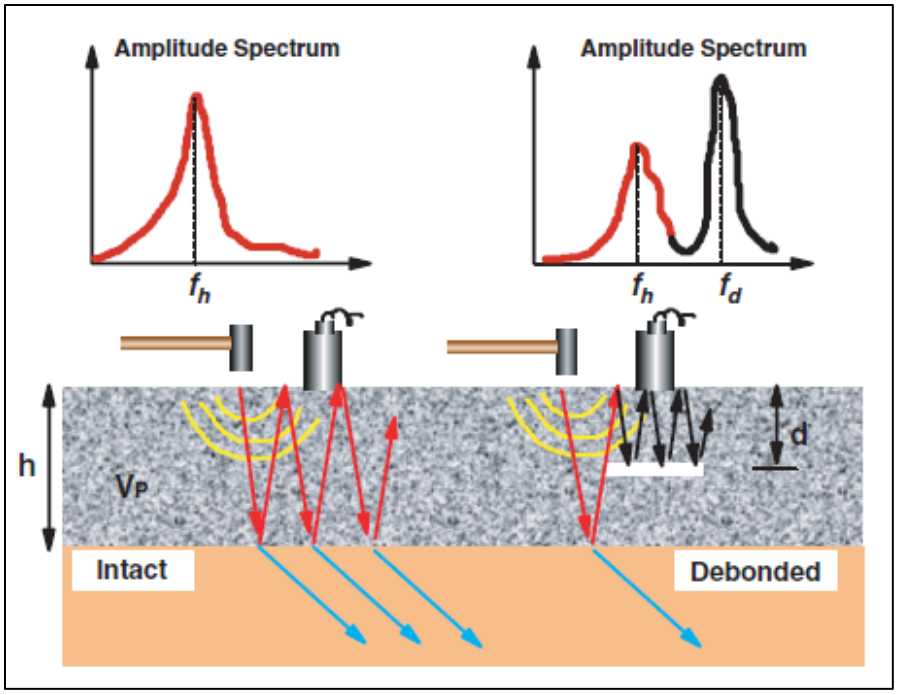

Figure 8-5 The "Ideal" Amplitude Spectrum for Intact and Debonded Concrete Slabs. The Higher Frequency Peaks f_d, Corresponding to the Frequency of Reflections from the Debonding Layers at a Depth of d < h, has been Demonstrated in the Amplitude Spectrum (Celaya at el, 2007).

8.3 Methodology

The sections that follow describe the location and number of PSPA test points on each bridge deck. PSPA data are presented in terms of contour maps showing average elastic (Young's) modulus and apparent thickness at each test section from the USW and IE data, respectively. The contour maps of average elastic modulus values provide the information related to the strength and quality of concrete material by estimating the concrete modulus at the test point locations. It should be noted that the average elastic modulus represents an average value between the depth of 2 in. and the bottom of the deck. It was necessary to interpolate between discrete measurement points. Relatively low values of concrete modulus are an indication of the presence of concrete degradation. Relatively high values of concrete modulus are an indication of good integrity of concrete. In general, moduli greater than 5000 ksi tend to indicate good integrity of concrete, while moduli less than 4000 ksi tend to indicate the presence of concrete degradation (Nazarian 2010). Moduli less than 2000 ksi are indicative of severe concrete degradation and/or the presence of a shallow delamination.

To interpret the PSPA USW results, a rating scale was developed by the researchers by comparing the average elastic modulus values with lidar data and visual evaluation of cores. The scale was developed considering the combined results of the three bridge decks. Test points were then given a rating defined for this project of either "Good", "Fair", "Poor", or "Severe." A rating of "Good" indicates that the average elastic modulus was greater than or equal to 5000 ksi. "Fair" indicates that the average elastic modulus was between 4000 ksi and 5000 ksi. "Poor" indicates that the average elastic modulus was between 2000 ksi and 4000 ksi. "Severe" indicates that the average elastic modulus was less than 2000 ksi.

The contour maps of apparent thickness values provide the information related to the condition assessment of the concrete deck with respect to the presence or absence of delamination. The presence of a delamination in the concrete will result in a lower frequency, which results in larger values of thickness as indicated in Eq. 1. Therefore, values of apparent thickness that are larger than the deck thickness will be an indication of the presence of concrete delamination. Values of apparent thickness that are approaching the actual deck thickness (±1 in.) are an indication of good integrity of concrete.

To interpret the PSPA IE results, a rating scale was developed by the researchers by comparing the apparent thickness values with PSPA modulus maps and visual evaluation of cores. The scale was developed considering the results of all three bridge decks. Test points were then given a rating defined for this project of either "Good", "Fair", "Poor", or "Severe."

8.4 Results

8.4.1 Bridge A1193

A total of 141 test points were acquired on Bridge A1193 in Sections A, B, C, D, E, and F as shown in Figure 8-6. The time to acquire the data was approximately 5 hours with a 2-person crew.

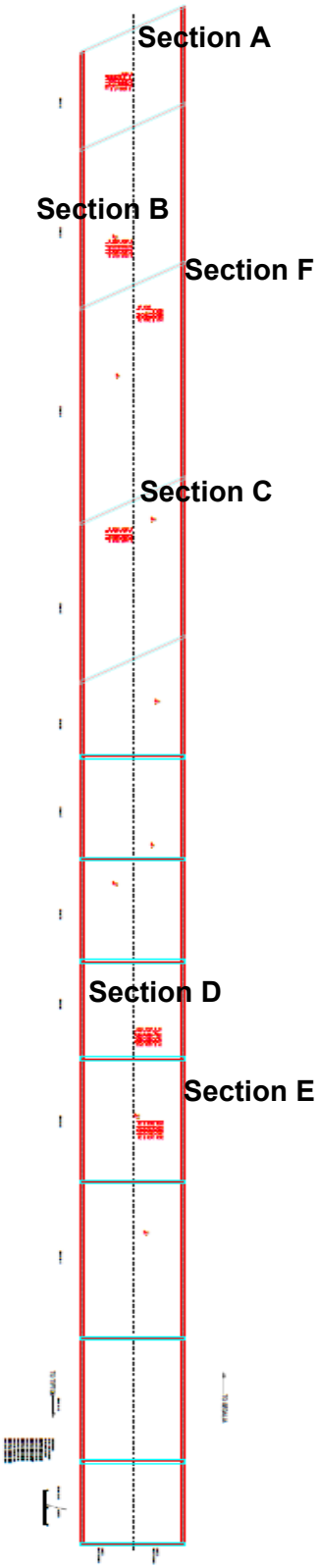

Figure 8-6 Bridge A1193 base map with PSPA test locations

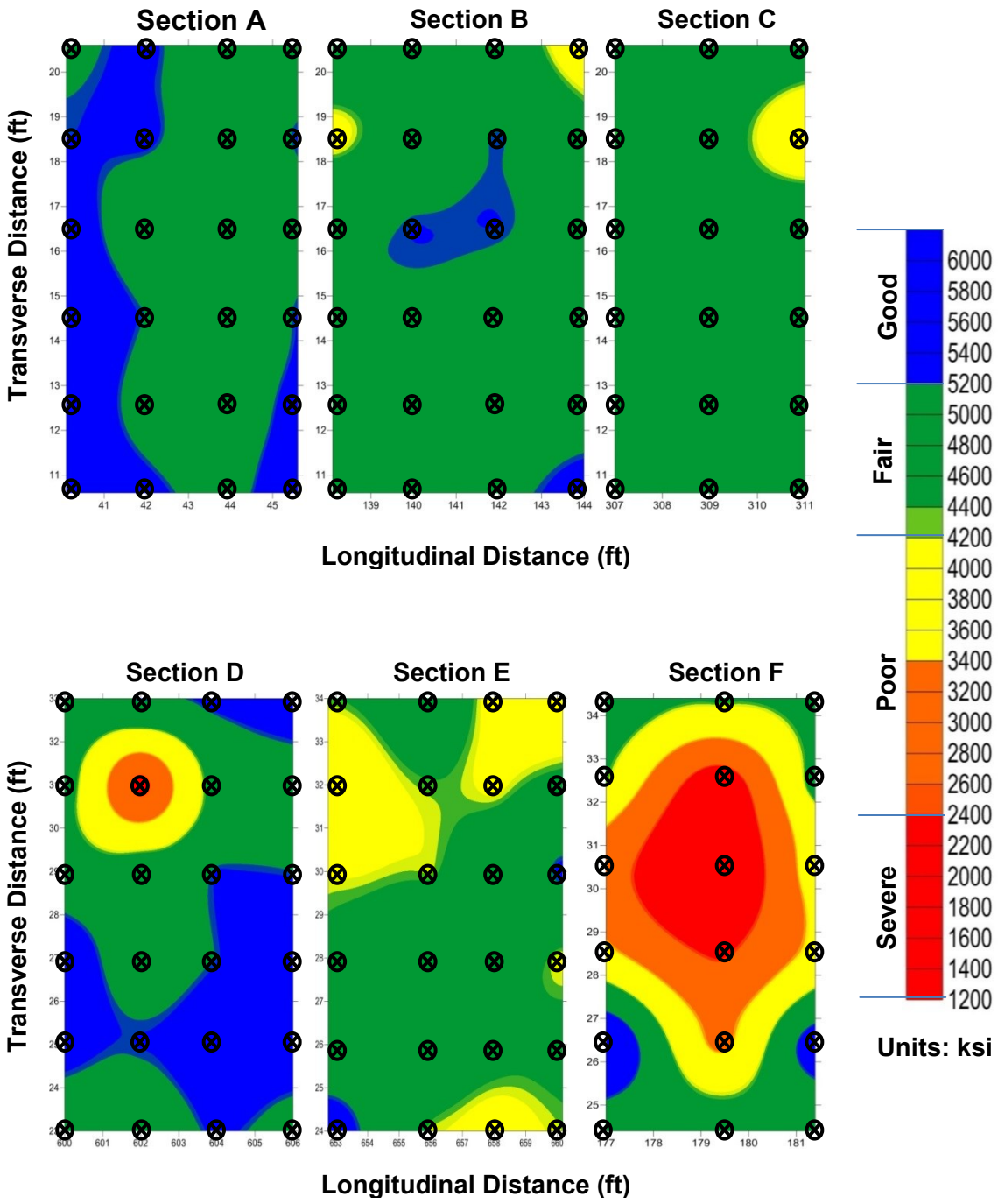

Figure 8-7 Bridge A1193 map of average elastic modulus (Young's Modulus) values for each PSPA section

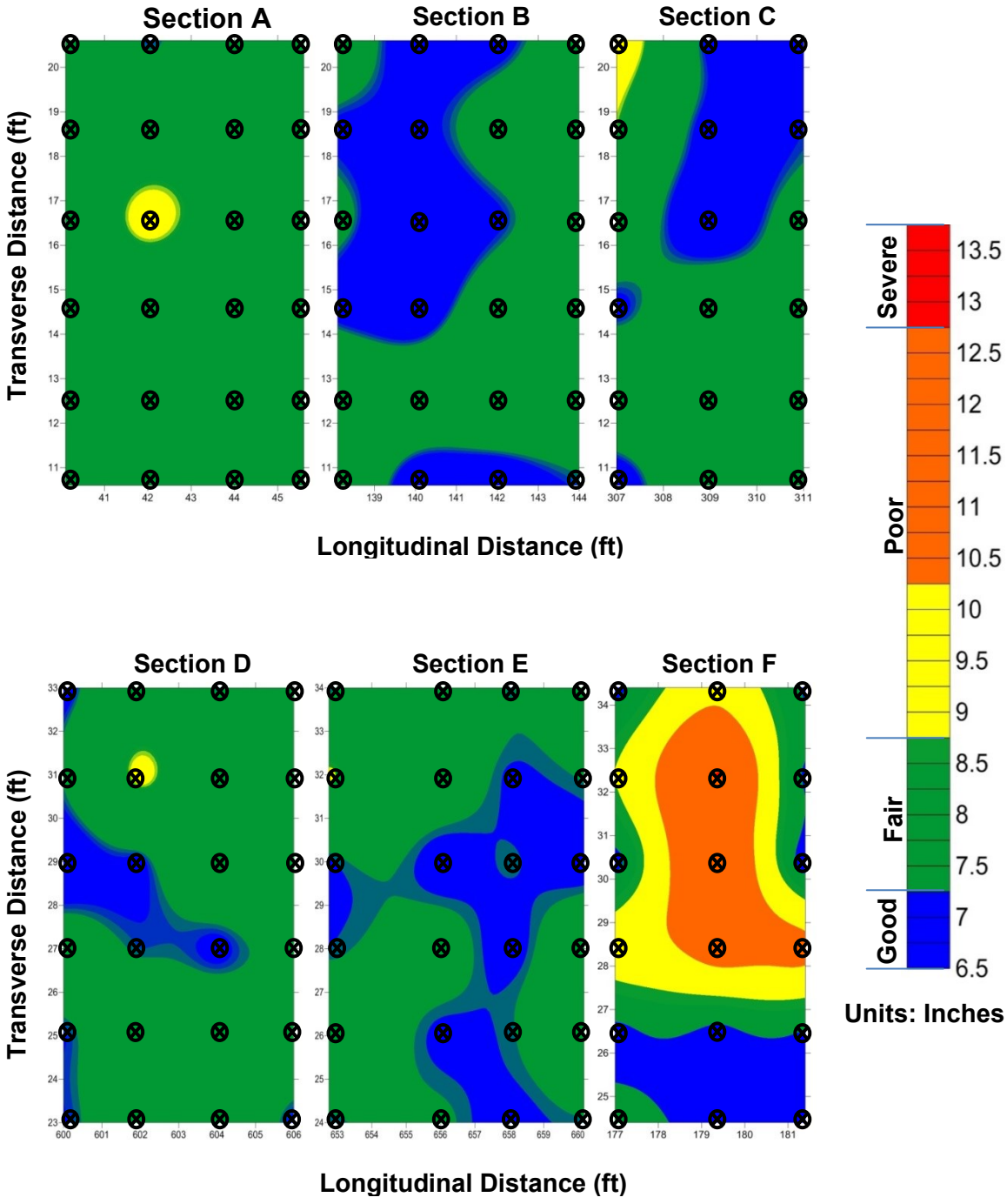

Figure 8-8 Bridge A1193 apparent depth map for each PSPA section

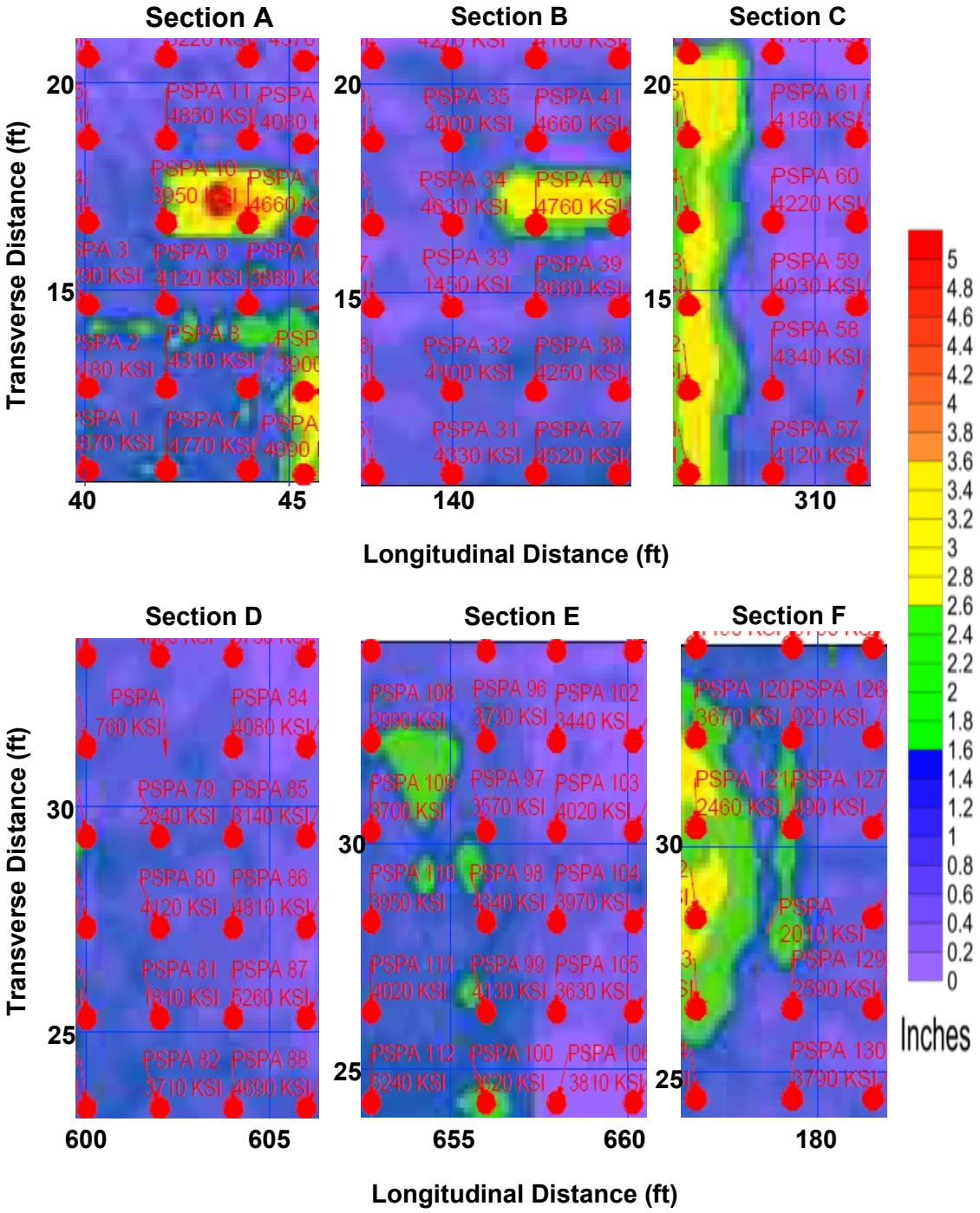

Figure 8-9 Bridge 1193 lidar data superposed with PSPA test points

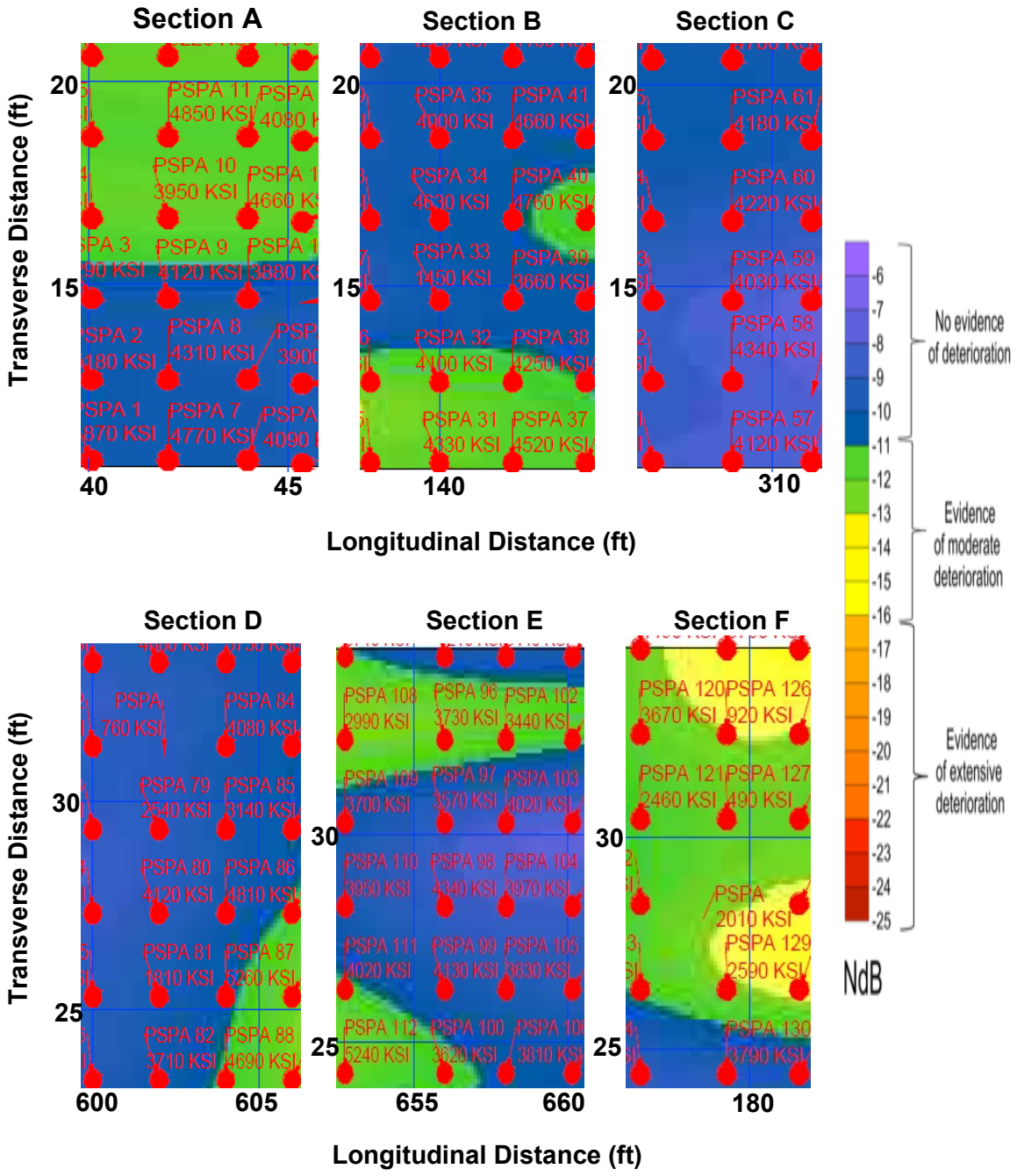

Figure 8-10 Bridge 1193 GPR data superposed with PSPA test points

Of the 141 test points acquired on Bridge A1193, 19% of the PSPA test points located in the USW map (Figure 8-7) indicate concrete deterioration (Poor or Severe condition). 8% of the PSPA test points located in the IE map (Figure 8-8) indicate concrete deterioration (Poor or Severe condition). To determine correlation with other data sets, the PSPA USW results are compared to the hydrodemolition and GPR data sets in Figures 8-9 and 8-10. 15% of the PSPA test points located in lidar map (Figure 8-9) indicate concrete deterioration (warm color). 34% of PSPA test points located in GPR map (Figure 8-10) indicate moderate concrete deterioration (warm color). The correlation of the PSPA results is good between the USW and hydrodemolition results. The correlation of PSPA results is fair between USW and GPR results.

Table 8-1 summarizes the PSPA results at the core locations so that the PSPA and visual core evaluation results can be compared. Results of the visual core evaluations (from Table 4-3) are also included in Table 8-1. 67% of USW data obtained from each coring location indicate concrete deterioration (Poor or Severe condition). 17% of the IE results obtained at the core locations indicate concrete deterioration (Poor or Severe condition). 50% of the cores were classified as Fair or Poor according to the visual evaluation. The PSPA USW results correlated well with the visual core evaluation results, while the PSPA IE results did not correlate well with the visual core evaluation results.

Table 8-1 Bridge A1193 PSPA Results at Core Locations

Core	Average Modulus (ksi) Based on USW Data	Grade Classification Based on USW Scale	Apparent Thickness (in.) Based on IE Data	Grade Classification Based on IE Scale	Visual Core Evaluation Results
A1	5140	Good	8.2	Fair	Good
A2	3540	Poor	7.0	Good	Fair
A3	3900	Poor	7.8	Fair	Good
A4	4910	Fair	8.0	Fair	Good
A5	3800	Poor	8.0	Fair	Good
B1	2010	Severe	11.4	Poor	Poor
B2	5150	Good	7.5	Good	Fair
B3	3790	Poor	7.4	Good	Fair
B4	3340	Poor	7.6	Fair	Poor
B5	1640	Severe	8.9	Poor	Good
B6	3800	Poor	8.0	Fair	Good
B7	4030	Fair	7.3	Good	Fair

8.4.2 Bridge A1297

A total of 56 test points were acquired on Bridge A1297 at Sections A and B as shown in Figure 8-11. The time to acquire the data was approximately 3.5 hours with a 2-person crew.

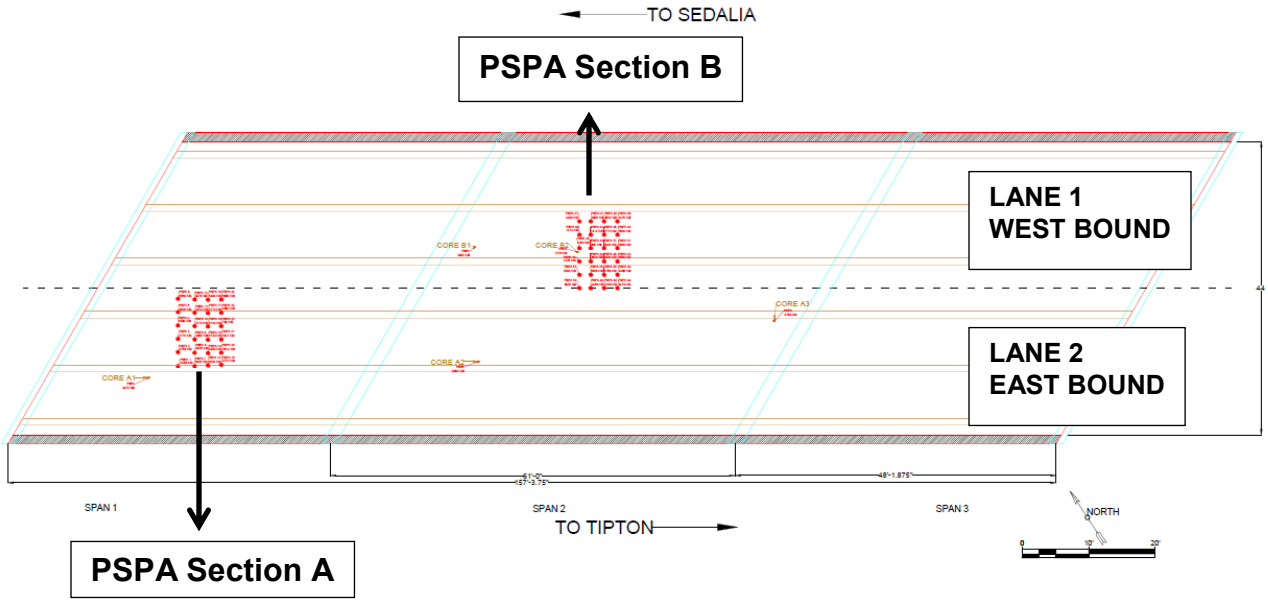

Figure 8-11 Bridge A1297 base map with PSPA test locations

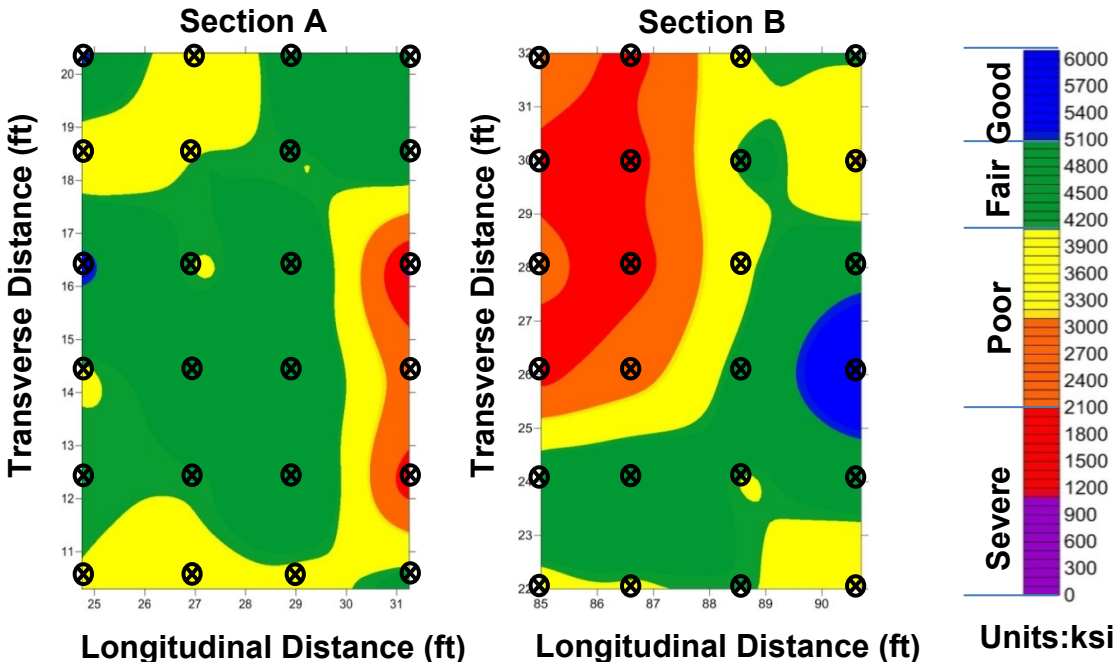

Figure 8-12 Bridge A1297 map of average elastic modulus (Young's Modulus) values for each PSPA section

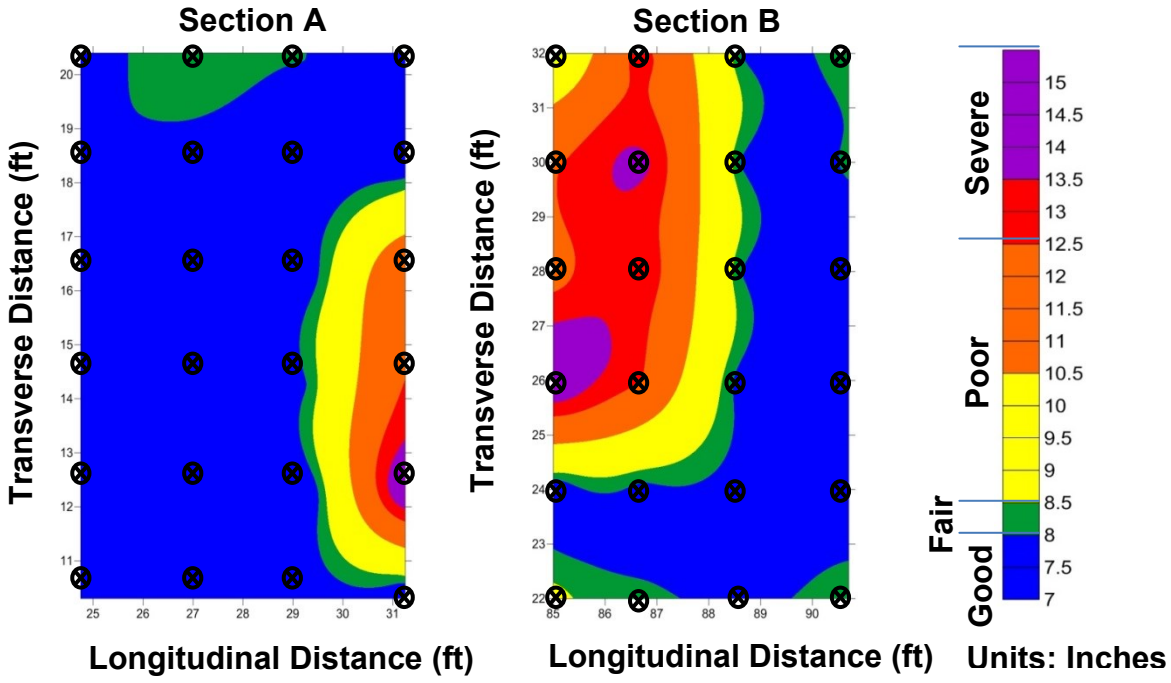

Figure 8-13 Bridge A1297 apparent depth map for each PSPA section

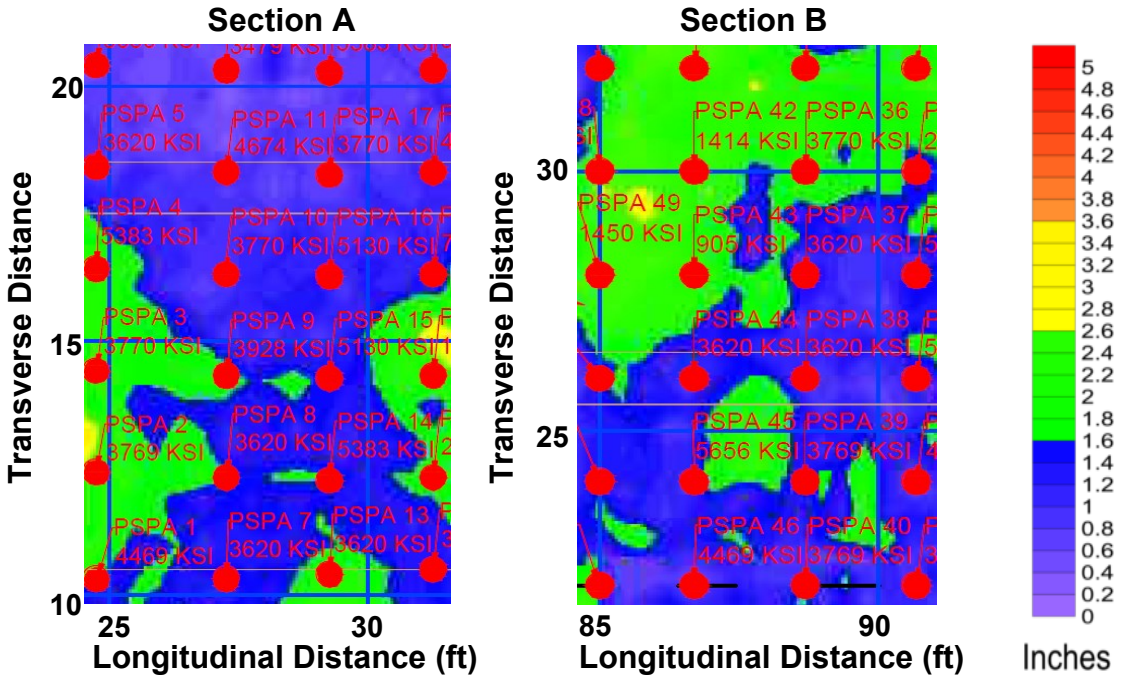

Figure 8-14 Bridge 1297 lidar data superposed with PSPA test points

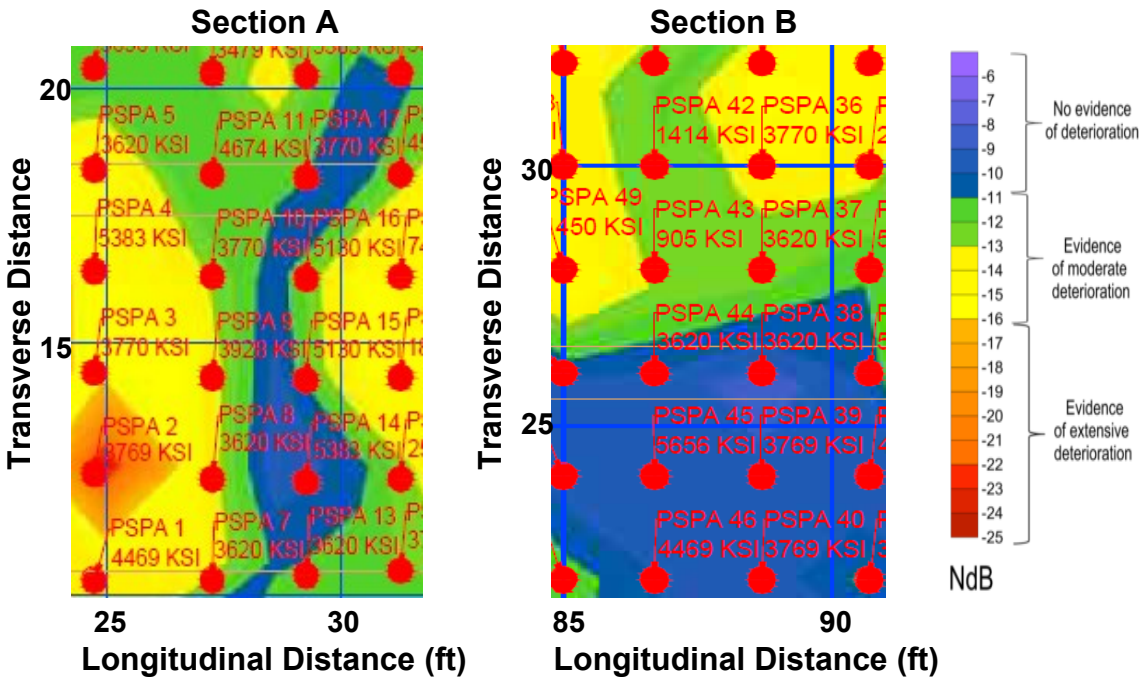

Figure 8-15 Bridge 1297 GPR data superposed with PSPA test points

Of the 56 test points acquired on Bridge A1297, 56% of the PSPA test points located in the USW map (Figure 8-12) indicate concrete deterioration (Poor or Severe condition). 33% of the PSPA test points located in the IE map (Figure 8-13) indicate concrete deterioration (Poor or Severe condition). To determine correlation with other data sets, the PSPA USW results are compared to the hydrodemolition and GPR data sets in Figures 8-14 and 8-15. 48% of the PSPA test points located in lidar map (Figure 8-14) indicate concrete deterioration (warm color). 70% of PSPA test points located in GPR map (Figure 8-15) indicate moderate concrete deterioration (warm color). The correlation of the PSPA results is good between the USW and hydrodemolition results. The correlation of PSPA results is fair between USW and GPR results.

Table 8-2 summarizes the PSPA results at the core locations so that the PSPA and visual core evaluation results can be compared. Results of the visual core evaluations (from Table 4-4) are also included in Table 8-2. 50% of PSPA USW data obtained from each core location indicate concrete deterioration (Poor or Severe condition). 33% of the PSPA IE results obtained at the core locations indicate concrete deterioration (Poor or Severe condition). 50% of the cores were classified as Fair or Poor according to the visual evaluation. The correlation between PSPA USW results and core results is good, while the correlation between PSPA IE results and core results is fair.

Table 8-2 Bridge A1297 PSPA Results at Core Locations

Core	Average Modulus (ksi) Based on USW Data	Grade Classification Based on USW Scale	Apparent Thickness (in.) Based on IE Data	Grade Classification Based on IE Scale	Visual Core Evaluation Results
A1	4470	Fair	6.9	Good	Good
A2	5383	Good	7.5	Good	Good
A3	3769	Poor	7.2	Good	Fair
B1	3620	Poor	8.0	Poor	Poor
B2	1379	Severe	13.4	Severe	Fair
B3	5656	Good	7.5	Good	Good

8.4.3 Bridge A1479

A total of 120 test points were acquired on Bridge A1479 in Sections A, B, C, D, E, and F as shown in Figure 8-16. The time to acquire the data was approximately 5.5 hours with a 2-person crew.

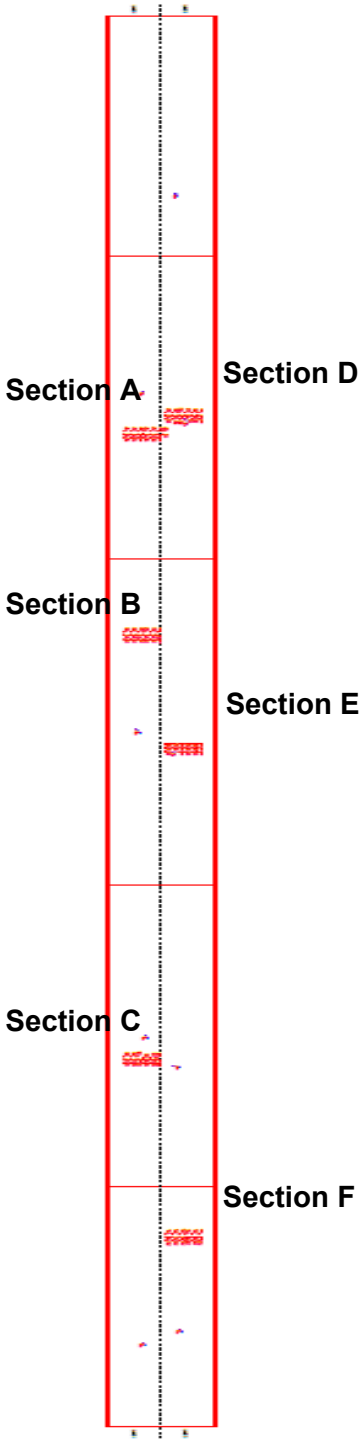

Figure 8-16 Bridge A1479 base map with PSPA test locations

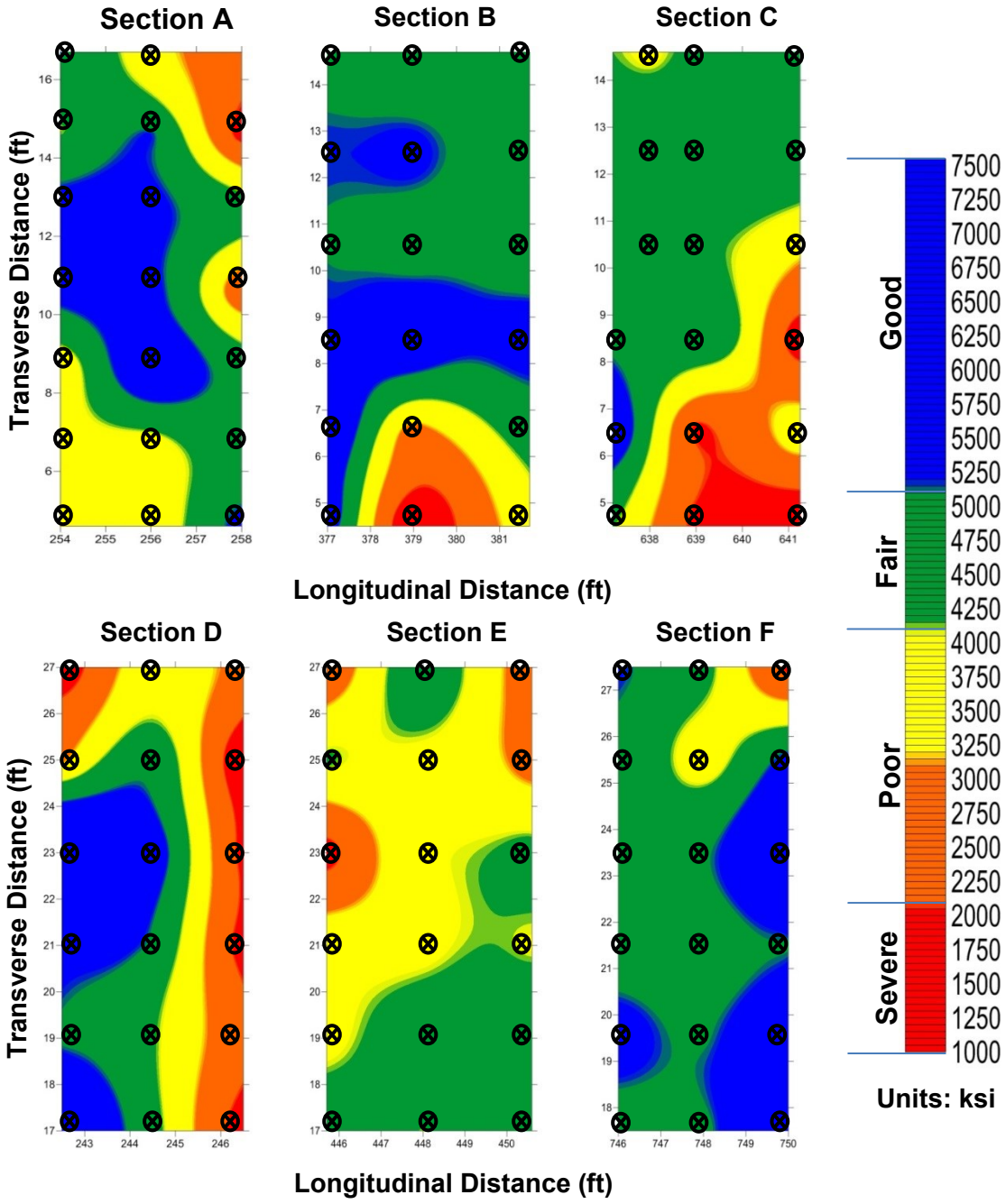

Figure 8-17 Bridge A1479 map of average elastic modulus (Young's Modulus) values for each PSPA section

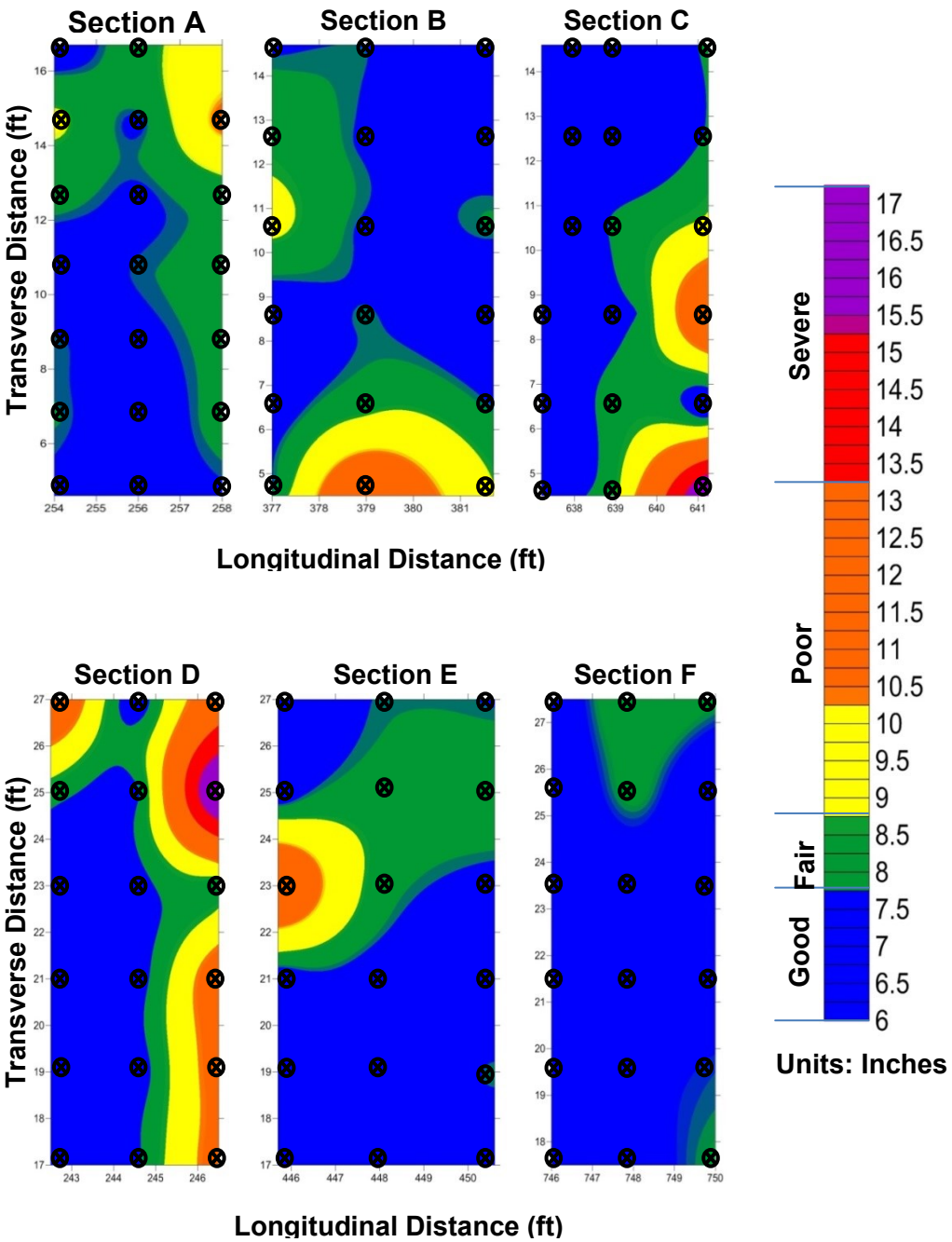

Figure 8-18 Bridge A1479 apparent depth map for each PSPA section

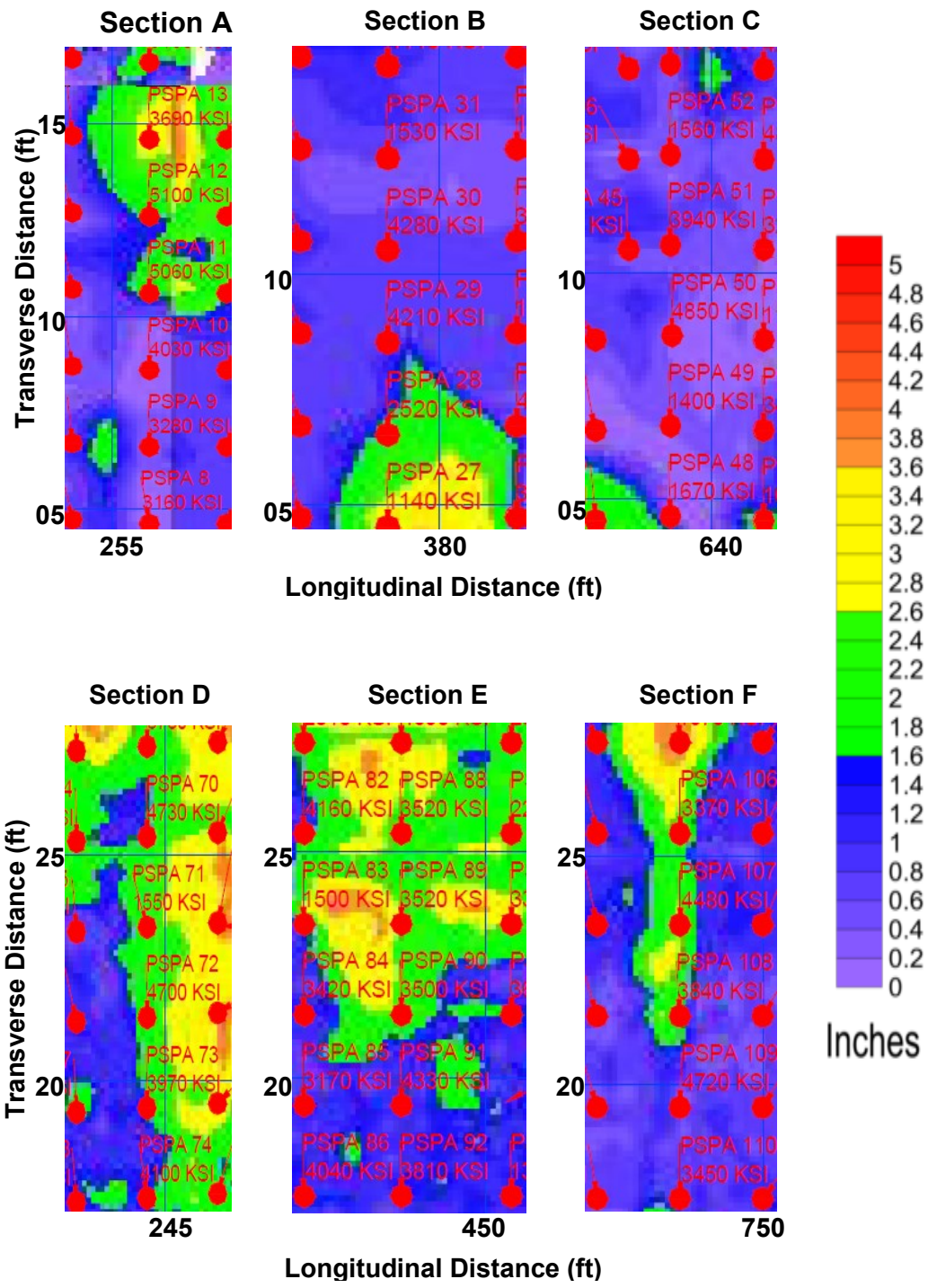

Figure 8-19 Bridge A1479 lidar data superposed with PSPA test points

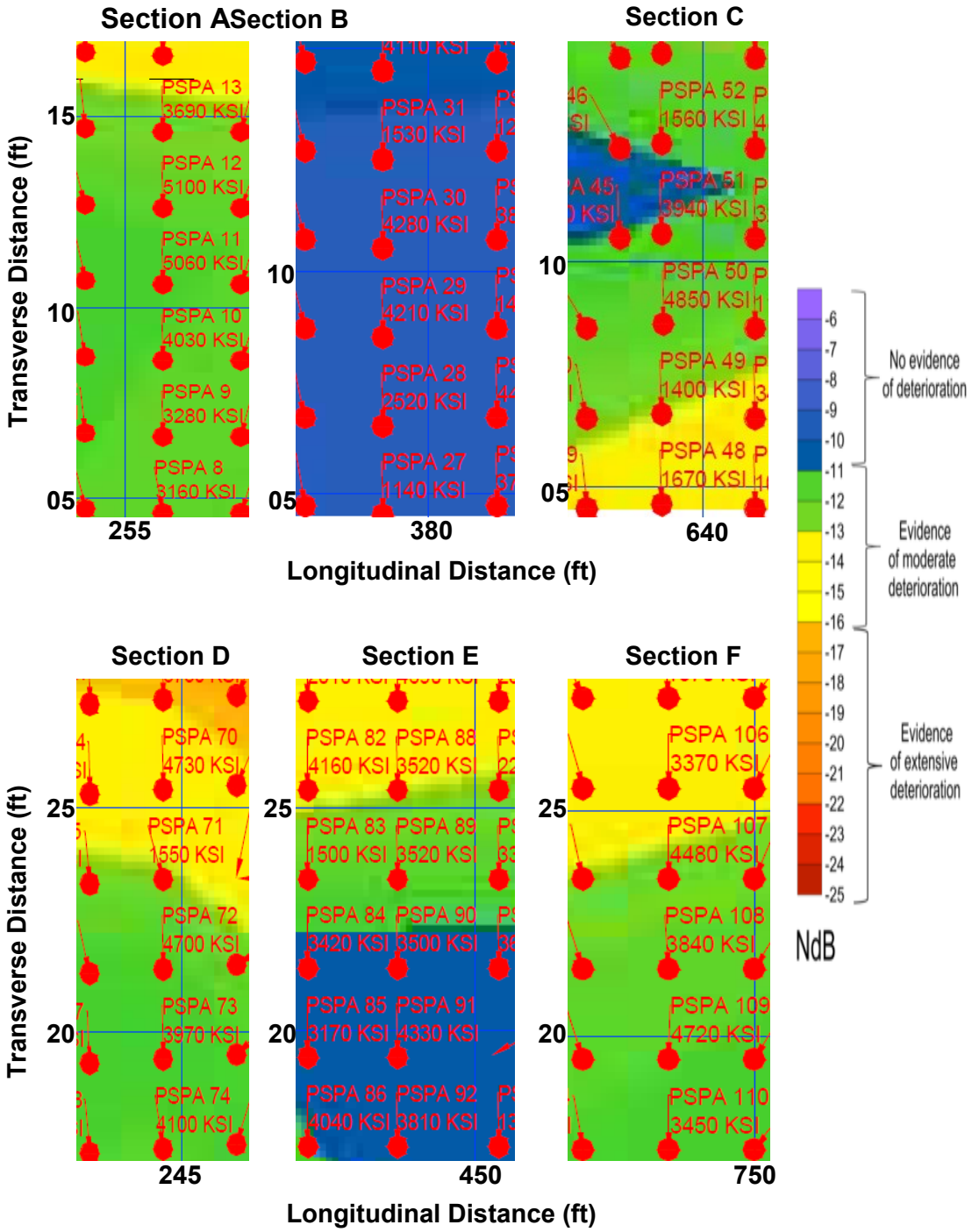

Figure 8-20 Bridge A1479 GPR data superposed with PSPA test points

Of the 120 test points acquired on Bridge A1479, 35% of the PSPA test points located in the USW map (Figure 8-17) indicate concrete deterioration (Poor or Severe condition). 17% of the PSPA test points located in the IE map (Figure 8-18) indicate concrete deterioration (Poor or Severe condition). To determine correlation with other data sets, the PSPA USW results are compared to the hydrodemolition and GPR data sets in Figures 8-19 and 8-20. 38% of the PSPA

test points located in lidar map (Figure 8-19) indicate concrete deterioration (warm color). 72% of PSPA test points located in GPR map (Figure 8-20) indicate moderate concrete deterioration (warm color). The correlation of the PSPA results is good between the USW and hydrodemolition results. The correlation of PSPA results is poor between USW and GPR results.

Table 8-3 summarizes the PSPA results at the core locations so that the PSPA and visual core evaluation results can be compared. Results of the visual core evaluations (from Table 4-5) are also included in Table 8-3. 33% of PSPA USW data obtained from each core location indicate concrete deterioration (Poor or Severe condition). 44% of the PSPA IE results obtained at the core locations indicate concrete deterioration (Poor or Severe condition). 44% of the cores were classified as Fair or Poor according to the visual evaluation. The correlation between PSPA USW and IE results and core results is good.

Table 8-3 Bridge A1479 PSPA Results at Core Locations

Core	Average Modulus (ksi) Based on USW Data	Grade Classification Based on USW Scale	Apparent Thickness (in.) Based on IE Data	Grade Classification Based on IE Scale	Visual Core Evaluation Results
A1	3240	Poor	9.1	Poor	Fair
A2	4090	Fair	7.8	Fair	Good
A3	2720	Poor	10.0	Poor	Fair
A4	4470	Fair	8.5	Poor	Good
B1	4860	Fair	7.2	Good	Good
B2	1490	Severe	17.1	Severe	Poor
B3	4840	Fair	7.7	Fair	Good
B4	4450	Fair	7.0	Good	Fair
B5	4840	Fair	7.0	Good	Good

8.5 Discussion

Results of bridges A1193, A1297, and A1479 indicate that the visual core evaluation results showing the evidence of shallow delaminations (less than 2 in.) tend to correlate well with the PSPA USW scale (Severe condition) with low elastic modulus values (less than 2000 ksi). The lidar results showing evidence of concrete deterioration (warm color) also correlate well with the PSPA USW scale (Poor & Severe condition) with elastic modulus values (less than 4000 ksi). Differences between the GPR interpretations and the PSPA interpretations can be attributed, in part, to the fact that GPR responds to changes in the moisture content (and salinity) of the concrete whereas the PSPA responds to changes in the physical properties of the concrete. Comparable results are achieved only where variations in moisture content are related to changes in physical properties.

Visual core evaluation results showing the evidence of shallow delaminations (less than 2 inches) tend to correlate well with the IE scale (Severe condition) with the large apparent thickness values (more than 13 in). The lidar results showing the evidence of concrete deterioration (warm color) also correlate well with the IE scale (Poor & Severe condition) with large apparent thickness values (more than 8.5 in.).

8.6 Summary of PSPA Tool

Table 8-4 summarizes the use of the PSPA tool based on the researchers' experience during this investigation.

Table 8-4 PSPA Tool Summary Table

Parameters estimated	Modulus of elasticity; apparent thickness of the deck
How these parameters relate to bridge deck conditions	Significant reduction or variation of elastic modulus is indicative of concrete degradation. Apparent thickness that is greater than the actual deck thickness is indicative of concrete degradation.
Acquisition parameters employed	Spacing of receivers; locations of PSPA measurements; placement relative to reinforcing steel.
Weather conditions	Results can be significantly influenced due to the hot weather when the test is conducted on asphalt or asphalt overlays.
Crew size	2-person
Equipment costs	At the time of this report, the operation system cost is approx. $20,000.
Acquisition problems	The surface condition of the bridge deck, such as the presence of cracks or rough surface, can significantly affect the quality of PSPA data. Reinforcing steel or other embedded items in the bridge deck can also significant affect the quality of PSPA data. Improper operation of PSPA instrument, such as poor coupling to the deck surface during the field test or entering incorrect parameters (concrete vs. asphalt) before conducting the field test, can also affect the quality of PSPA data.
Ease of acquisition	Only an experienced operator can collect good quality PSPA data.
Processing parameters	Excel software can be used to export and process the original data for each PSPA test point. Surfer software can be used to generate 2D contour maps for each PSPA test section.
Time required to process data	For each PSPA test point, the time required to process good quality USW data is approximately 10 minutes. The time required to process IE data is approximately 20 minutes. The time required to generate a 2D contour map of elastic modulus or apparent depth of the deck areas depends on the number of PSPA test locations. The time required to generate a 2D contour map for 24 PSPA test points with 2×2 feet spacing is approximately 2 hours.
Ease of processing	Only an experienced operator can collect good quality PSPA data.
Potential processing problems	If the estimated P-wave velocity derived from the surface wave velocity is inaccurate, corresponding thickness estimates will be inaccurate. High level ambient noise induced by reinforcing steel will also significantly affect the accuracy of the apparent depth calculation of the deck.
Interpretation parameters	Modulus of elasticity; apparent depth of the deck
Time required to interpret data	In the case of the bridges considered in this study, the time required to interpret the overall results was approximately 12.5 hours. The post analysis required for anomalous PSPA data is more time consuming. Extensive time is needed for large scale of PSPA data interpretation. Interpretation should be done by a data processor.
Ease of interpretation	Extensive experience and time are needed for PSPA data interpretation. For USW data interpretation, elastic modulus value estimates may not be reliable across deteriorated sections of the bridge deck, such as debonded or delaminated sections. Experience is required for understanding and interpreting test results. For IE data interpretation, the high level ambient noise induced by reinforcing steel in the bridge deck will significantly affect the interpretation of IE spectra. Extensive experience is required to identify and characterize the bottom frequency from the IE spectra with high level ambient noise.
Deliverables	2D contour map of average elastic modulus, 2D contour map of apparent deck thickness.

Table 8-4 PSPA Tool Summary Table (cont.)

Reliability of interpretations	For USW data, the elastic modulus values are reliable for intact sections of the bridge deck. Post-analysis and verification tests are needed in order to confirm the test results. For IE data, the apparent depth of the deck cannot provide accurate depth of deteriorated sections of the bridge deck. However, if the apparent depth of the deck is larger than the deck thickness, this result can provide reliable information about the location and size of deteriorated sections of the bridge deck.
Potential interpretation problems	The automatic interpretation results of IE data are not reliable due to several reasons: the measured P-wave velocity derived from the surface wave velocity is not accurate, and the identification and characterization of the bottom reflection frequency in IE spectra can be significantly affected by the high level ambient noise induced by the reinforcing steel in the bridge deck.
Utility of technology	The PSPA tool was identified as having good capabilities for concrete degradation and vertical cracking detection and characterization in concrete bridge decks. However, extensive labor and time are needed for PSPA data field acquisition and processing. Furthermore, extensive experience is needed to understand and interpret PSPA data results.

9 SUMMARY OF FINDINGS AND RECOMMENDATIONS

9.1 Summary

This study investigated the use of nondestructive evaluation techniques for bridge deck condition assessments. The primary nondestructive testing/evaluation (NDT/NDE) technique utilized in this study was ground-coupled ground penetrating radar (GPR), and the use of a portable seismic property analyzer (PSPA) was also investigated. Eleven bridge decks were investigated in this project using visual inspections, GPR, PSPA, core extraction, and chloride ion concentration measurements. Three of the bridges investigated underwent bridge deck rehabilitation during this project, and material removal was surveyed using lidar in order to evaluate the NDE predictions. The cores underwent a detailed visual evaluation and testing to determine the volume of permeable pore space. Data sets were compared to determine correlations between bridge deck evaluation methods.

9.2 Conclusions

The following conclusions are made based on the results of this project:

1. Refer to Section 7.5 and Table 7-13 for recommended parameters for ground coupled GPR data acquisition, processing, and interpretation.
2. Ground-coupled GPR responds to the presence of saline moisture in a bridge deck and can be used to identify areas of a bridge deck where there is a high probability that incipient to extensive concrete deterioration has occurred.
3. Ground-coupled GPR is a useful tool for estimating areas of a bridge deck that are in good condition, fair condition, and poor condition. In this study, this was achieved by defining reflection amplitude ranges for three deterioration categories: “no evidence of deterioration,” “evidence of moderate deterioration,” and “evidence of extensive deterioration,” corresponding to relatively high reflection amplitude, moderate reflection amplitude, and low reflection amplitude, respectively.
4. For the bridge decks investigated in this project, GPR interpretations of the top reinforcement reflection amplitude showed a strong correlation with visual assessment results in areas where visual deterioration was noted.
5. A fair to good correlation was observed between the GPR data and the visual core evaluation results. A higher degree of correlation can be anticipated in areas where the concrete cores are visibly deteriorated; a lower degree of correlation can be expected in areas where the concrete cores do not exhibit signs of deterioration. In general, cores with higher volume of permeable core space had a lower visual core rating.
6. For the bridges that underwent deck rehabilitation (Bridges A1197, A1297, and A1479), it was shown that areas of the decks where the GPR interpretations indicated extensive deterioration generally corresponded to areas with greater concrete material removal depths after hydrodemolition. Similarly, areas where the GPR interpretations indicated moderate or no evidence of deterioration generally corresponded to areas with lesser material removal depths. Qualitatively, there was a strong correlation between the two data sets. Apparent discrepancies between the GPR interpretations and the concrete removal depths can be attributed to the fact that GPR responds to the presence of saline moisture in the deck, whereas rehabilitation removes weaker concrete. Therefore GPR and rehabilitation results are expected to correlate best in those areas where the pore space within physically degraded concrete is infilled with slightly saline moisture. Also,

GPR interpretations presented in this report are based on the reflection amplitude from the top transverse layer of reinforcement and do not represent the condition of the concrete below the top transverse reinforcement.

7. The GPR classifications and concrete material removal thickness categories defined in Sections 7.2 and 6.1 of this report do not have a direct physical correlation. Although good correlation between the two classifications was observed for Bridge A1193, the correlations for Bridges A1297 and A1479 were not as strong. However, additional study was initiated to investigate the potential for improving the correlation between these two data sets. Preliminary findings suggest that improved correlation is possible by adjusting the threshold values for the GPR classifications, and a statistical approach is currently being used by the researchers in an attempt to improve the correlation between the amplitude of the reflection and concrete removal depth for each data point for each of the three bridges. The major challenge, however, is to understand how to determine the GPR threshold values a priori, without having the benefit of the control data.
8. Acquisition of limited core control is recommended to constrain the interpretation of ground-coupled GPR data when used for concrete removal area estimates.
9. Ground-coupled GPR interpretations do not correlate exactly with degradation estimates based on visual inspection of bridge deck surface, visual assessment of core control, PSPA results (elastic modulus), and hydrodemolition results. This is because GPR responds to the presence of saline moisture, whereas the other approaches are more reflective of the physical condition of the bridge deck. GPR is often said to overestimate areas of degradation because it identifies areas where incipient deterioration (ingress of saline moisture) is occurring.
10. It is the opinion of the authors that the ground-coupled GPR tool is superior to visual assessment, chain dragging, hammer sounding, limited core control, or chloride ion testing for comprehensive bridge deck evaluation. However, these data sets can be used to constrain the interpretation of GPR data.
11. Ground-coupled GPR results can also be used for baseline condition assessments of bridge decks, as well as assessing the relative condition of multiple bridge decks.
12. The interpretation of GPR data is somewhat subjective because GPR responds to the presence of saline moisture. Saline moisture content within a bridge deck will vary with the weather, and thus the GPR signature of a bridge deck will vary as the weather varies. GPR data should be acquired when the bridge deck is slightly moist.
13. The acquisition of ground-coupled GPR data is relatively slow and normally requires lane closures. Air-launched GPR may be a more appropriate tool for rapidly assessing the relative condition of multiple bridges.
14. PSPA is a relatively new tool that can be used to identify and characterize concrete degradation effectively in concrete bridge decks. However, data processing and interpretation requires expertise. If PSPA is to be utilized in routine condition assessment of concrete bridge decks, it should be considered supplemental to other NDT tools because of the localized results and relatively slow data collection speed. A general protocol is needed for PSPA data acquisition, processing, and interpretation in order to assist the user in the rapid condition assessment of concrete bridge decks. Additionally, an automatic scanning system for PSPA data acquisition is needed in order to conduct PSPA testing on the large area of concrete bridge decks.

9.3 Ongoing and Future Work

At the time of this report, additional studies are being conducted by the research team related to the results presented in this report. These studies are aimed at better calibrating GPR results so that it can be used more accurately in the monitoring of bridge decks and planning of rehabilitation. The following is a list of ongoing studies.

1. Estimation of through-thickness deterioration: Analysis of the through-thickness of deterioration of the bridge decks is ongoing. Researchers are using different reflectors, such as the bottom of the slab, to estimate the depth of deterioration. Results from this study could be used to monitor deterioration for the full slab depth as well as better prepare estimates for repair and rehabilitation.
2. Calibration of GPR results to material removal from hydrodemolition results: This analysis could improve the interpretation of GPR results for future bridge scans as well as better calibrate results of the eight bridges investigated in this study that did not undergo rehabilitation.
3. Determination of climate effects on GPR results: Analysis of this study will determine the significance that climate changes have in GPR results, as well as aide in the calibration of GPR results to reflect climate conditions at the time of scanning.
4. Analysis of how reinforcing bar depth influences GPR reflection amplitude: This study is being performed to determine how great of an impact varying depths of reinforcing bars has on GPR results. Results from this study can be used to either further validate that reinforcing bars with varying amounts of clear cover do not significantly impact GPR results, or that the impact on results is significant.
5. Ability of air-launched GPR antenna to detect bridge deck deterioration: This study is a separate project, however some of the bridges evaluated in this study will also be evaluated in the new study so results can be compared. If proven effective, the collection of air-launched GPR data could enable more efficient evaluation of bridge decks.

REFERENCES

American Standard Test Method (ASTM) C 642, 2006. "Standard Test Method for Density, Absorption, and Voids in Hardened Concrete." ASTM International, West Conshohocken, PA.

American Standard Test Method (ASTM) C 1218/ C 1218M, 1999. "Standard Test Method for Water-soluble Chloride in Mortar and Concrete." ASTM International, West Conshohocken, PA.

Baker, M. R., K. Crain, and S. Nazarian., 1995. "Determination of Pavement Thickness with a New Ultrasonic Device," Center for Highway Materials Research, University of Texas, El Paso.

Carino, N.J., Sansalone, M., and Hsu, N.N., 1986. "A Point Source - Point Receiver Technique for Flaw Detection in Concrete," *Journal of the American Concrete Institute*, Vol. 83, No. 2, April, pp. 199-208.

Celaya, M., Nazarian, S., 2007. "Assessment of Debonding in Concrete Slabs Using Seismic Methods," *Transportation Research Record*, No. 2016, pp 65-75.

Gucunski, N., Slabaugh, G., 2008. "Impact Echo Data from Bridge Deck Testing," *Transportation Research Record*, No. 2050, pp 111-121.

Gucunski, N., Nazarian, S., Yuan, D., 2012. "Nondestructive Testing to Identify Concrete Bridge Deck Deterioration," Strategic Highway Research Program (SHRP 2) report, *Transportation Research Board*, Washington D.C.

Maser, K., (2009). "Integration of ground penetrating radar and infrared thermography for bridge deck condition evaluation." *Proceedings*, Non-Destructive Testing in Civil Engineering, Nantes, France.

Missouri Department of Transportation (MoDOT), 2002. "Hydrodemolition and Repair of Bridge Decks." RI97-025, Missouri Department of Transportation. Jefferson City, MO.

Nazarian, S., M. Baker, and K. Crain., 1997, "Assessing Quality of Concrete with Wave Propagation Techniques," *ACI Materials Journal*, Vol. 94, No. 4, pp. 296–306.

Nazarian, S., 1984, "In Situ Determination of Soil Deposits and Pavement Systems by Spectral Analysis of Surface Waves Method*," PhD thesis*, University of Texas at Austin.

Nazarian, S., Alvarado, G., 2006, "Impact of Temperature Gradient on Modulus of Asphaltic Concrete Layers," *Journal of Materials in Civil Engineering, Vol.* 18, No. 4, pp. 492-499.

Portland Cement Association (PCA), 2013. "Corrosion of Embedded Metals." *Portland Cement Association,* <http://www.cement.org/tech/cct_dur_corrosion.asp> accessed November 2013.

Sheriff, R. E., Geldart, L. P., 1995. Exploration Seismology, Second Edition, Cambridge University Press, NY.

APPENDIX A
DIGITAL APPENDIX DESCRIPTION AND FILES

A. DIGITAL APPENDIX DESCRIPTION

A.1 INTRODUCTION

This appendix provides details on the digital bridge investigation drawings that are located on the CD-ROM included with this report. As mentioned in Section 2.1, CAD drawings were generated showing structural bridge elements that were significant to the investigations discussed in this report. Visual inspection, GPR, core locations, and the rehabilitation lidar survey results (where applicable) were inserted into this drawing to create a comprehensive investigation drawing. These CAD drawings were then converted to a PDF file. When viewed using the software Adobe Reader, layers can be changed to be visible or hidden as shown in Figure A.1 below. One ft. and 5 ft. scales have been overlaid on each drawing. For optimal viewing of results, it is recommended to turn off the 1 ft. scale layers, along with all reinforcement layers. The drawing files are large enough to allow the user to zoom in on small details. The GPR Map layer was positioned on top of the Lidar Hydrodemolition Map layer, so to view the lidar map, simply hide the GPR layer.

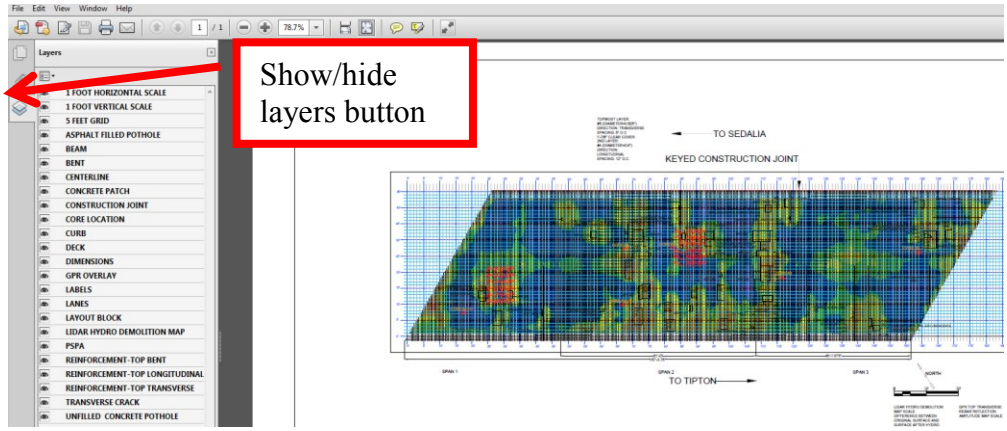

Figure A.1 Layers in Digital Drawing

A.2 CONTENTS

The following files are included in this Digital Appendix:

Bridge A0569 MO S&T 2012-2013 NDE Investigation.pdf
Bridge A1187 MO S&T 2012-2013 NDE Investigation.pdf
Bridge A1193 MO S&T 2012-2013 NDE Investigation.pdf
Bridge A1297 MO S&T 2012-2013 NDE Investigation.pdf
Bridge A1479 MO S&T 2012-2013 NDE Investigation.pdf
Bridge A2111 MO S&T 2012-2013 NDE Investigation.pdf
Bridge A2966 MO S&T 2012-2013 NDE Investigation.pdf
Bridge A3017 MO S&T 2012-2013 NDE Investigation.pdf
Bridge A3405 MO S&T 2012-2013 NDE Investigation.pdf
Bridge A3406 MO S&T 2012-2013 NDE Investigation.pdf
Bridge K0197 MO S&T 2012-2013 NDE Investigation.pdf